Report Prepared by :

A. A. Sagüés
T. Eason
C. Cotrim
J. Lopez-Sabando

Validation and Practical Procedure for Vibrational Evaluation of Tendons

Contract No. BC 353-44

Final Report to Florida Department of Transportation

A. A. Sagüés
Principal Investigator
Department of Civil and Environmental Engineering

March 31, 2008

University of South Florida
Tampa, FL, 33620

Technical Report Documentation Page

1. Report No.	2. Government Accession No.	3. Recipient's Catalog No.
BC353 - 44		

4. Title and Subtitle	5. Report Date
VALIDATION AND PRACTICAL PROCEDURE FOR VIBRATIONAL EVALUATION OF TENDONS	March 31, 2008
	6. Performing Organization Code
7. Author(s) A. A. Sagüés, T. Eason, C. Cotrim, J. Lopez-Sabando	8. Performing Organization Report No.
9. Performing Organization Name and Address Department of Civil and Environmental Engineering University of South Florida Tampa, FL 33620	10. Work Unit No. (TRAIS) 11. Contract or Grant No. BC353 - 44
12. Sponsoring Agency Name and Address Florida Department of Transportation 605 Suwannee St. MS 30 Tallahassee, Florida 32399 (850)414-4615	13. Type of Report and Period Covered Final Report 10/15/02 - 3/31/2008 14. Sponsoring Agency Code

15. Supplementary Notes

Prepared in cooperation with the USDOT and FHWA

16. Abstract

Vibrational testing of tension to identify potentially distressed external tendons of post-tensioned segments and columns has been successfully used in major FDOT bridges. This investigation provided validation of basic assumptions and verification of tension obtained by the vibration method against independent load cell measurements with tendon segments of size, length, and tension levels comparable of those used in actual structures. Measurements were conducted in a specially build tendon test facility with 12-strand tendons up to nearly 10 m (400 in) long, some including a deviation block. Tension estimated from vibration tests was on average within ~6% of load cell measurements, after correction for the effect of metal pipe ends in some cases. Upon simulated strand failures at the anchorage area there was tension loss that was tracked adequately in nearly all cases by the vibration tests. Advanced data processing methods were developed to perform rapid evaluation of data from large populations (thousands) of tendons in actual bridges. Vibration test field equipment was developed for simplified operation and analysis procedures. A portable field equipment prototype was designed and constructed to permit testing by a single-operator. Extensive vibration tests of tendons were conducted in the segmental approaches of the Sunshine Skyway Bridge, revealing generally normal tension levels but flagging specific tendons with fringe performance for subsequent inspection. A user-oriented summary of findings and applications is provided.

17. Key Words	18. Distribution Statement
Vibration Testing, Tendons, Post-Tensioned, Validation, Field Testing, Simplified Procedures	No Restriction This report is available to the public through the NTIS, Springfield, VA 22161

19. Security Classif. (of this report)	20. Security Classif. (of this page)	21. No. of Pages	22. Price
Unclassified	Unclassified	188	

Form DOT F 1700.7 (8-72) Reproduction of completed page authorized

DISCLAIMER

The opinions, findings, and conclusions expressed in this publication are those of the authors and not necessarily those of the State of Florida Department of Transportation.

SI* (MODERN METRIC) CONVERSION FACTORS

APPROXIMATE CONVERSIONS TO SI UNITS

Symbol	When You Know	Multiply By	To Find	Symbol
		LENGTH		
in	inches	25.4	millimeters	mm
ft	feet	0.305	meters	m
yd	yards	0.914	meters	m
mi	miles	1.61	kilometers	km
		AREA		
in^2	square inches	645.2	square millimeters	mm^2
ft^2	square feet	0.093	square meters	m^2
yd^2	square yard	0.836	square meters	m^2
ac	acres	0.405	hectares	ha
mi^2	square miles	2.59	square kilometers	km^2
		VOLUME		
fl oz	fluid ounces	29.57	milliliters	mL
gal	gallons	3.785	liters	L
ft^3	cubic feet	0.028	cubic meters	m^3
yd^3	cubic yards	0.765	cubic meters	m^3
		NOTE: volumes greater than 1000 L shall be shown in m^3		
		MASS		
oz	ounces	28.35	grams	g
lb	pounds	0.454	kilograms	kg
T	short tons (2000 lb)	0.907	megagrams (or "metric ton")	Mg (or "t")
		TEMPERATURE (exact degrees)		
^oF	Fahrenheit	5 (F-32)/9 or (F-32)/1.8	Celsius	^oC
		ILLUMINATION		
fc	foot-candles	10.76	lux	lx
fl	foot-Lamberts	3.426	candela/m^2	cd/m^2
		FORCE and PRESSURE or STRESS		
lbf	poundforce	4.45	newtons	N
lbf/in^2	poundforce per square inch	6.89	kilopascals	kPa

APPROXIMATE CONVERSIONS FROM SI UNITS

Symbol	When You Know	Multiply By	To Find	Symbol
		LENGTH		
mm	millimeters	0.039	inches	in
m	meters	3.28	feet	ft
m	meters	1.09	yards	yd
km	kilometers	0.621	miles	mi
		AREA		
mm^2	square millimeters	0.0016	square inches	in^2
m^2	square meters	10.764	square feet	ft^2
m^2	square meters	1.195	square yards	yd^2
ha	hectares	2.47	acres	ac
km^2	square kilometers	0.386	square miles	mi^2
		VOLUME		
mL	milliliters	0.034	fluid ounces	fl oz
L	liters	0.264	gallons	gal
m^3	cubic meters	35.314	cubic feet	ft^3
m^3	cubic meters	1.307	cubic yards	yd^3
		MASS		
g	grams	0.035	ounces	oz
kg	kilograms	2.202	pounds	lb
Mg (or "t")	megagrams (or "metric ton")	1.103	short tons (2000 lb)	T
		TEMPERATURE (exact degrees)		
^oC	Celsius	1.8C+32	Fahrenheit	^oF
		ILLUMINATION		
lx	lux	0.0929	foot-candles	fc
cd/m^2	candela/m^2	0.2919	foot-Lamberts	fl
		FORCE and PRESSURE or STRESS		
N	newtons	0.225	poundforce	lbf
kPa	kilopascals	0.145	poundforce per square inch	lbf/in^2

*SI is the symbol for the International System of Units. Appropriate rounding should be made to comply with Section 4 of ASTM E380.

EXECUTIVE SUMMARY

Vibrational testing of tension to identify potentially distressed external tendons of post-tensioned segments and columns has been successfully used in several major FDOT bridges. The tests consist of lightly impacting the free length of the tendon, recording the resulting vibration frequencies, and applying the value of those frequencies as well as the tendon dimensions and unit mass length to a computational model that calculates the tendon tension.

This investigation provided resolution of key issues in the applicability of the vibration test method. Those issues include:

1. Validation of the assumptions used to interpret the vibration spectra to obtain a value of the tendon tension, including hypotheses used to account for the presence of double peaks in the field data, and sensitivity of the vibration test response of an external tendon to distress in the anchorage region.

2. Efficient and rapid handling of data from large numbers of tendons in a bridge to obtain accurate tension estimates.

3. Development of a simplified testing and analysis method for rapid screening in the field.

4. Immediate supplemental work in support of testing tendons in the segmental approaches of the Sunshine Skyway Bridge.

Tasks addressing each of those areas were implemented and highlights of the main findings are noted next. Much of the work was conducted in cooperation with the personnel and facilities of the FDOT Structures Research Laboratory in Tallahassee.

The ability of the vibration test to obtain estimates of tendon tension was validated with six independent tendon segments of size, length, and tension levels comparable of those used in actual structures. The tendons had each 12 1/2-inch strands and were up to nearly 10 m (400 in) long. Some of the tendons contained a sloping segment and a horizontal segment, separated by a deviation block. The tendon test facility was fully instrumented with load cells to obtain independent tension measurements. For tendons with relatively short end metal pipes at the points were the tendon emerged from the concrete, deviation between tension estimated from vibration tests (average of multiple measurements) and independent load cell measurements ranged from less than 1% to approximately 6%.

An algorithm was developed and applied to numerically correct force estimates from vibration tests for the effect of metal pipe segments at the tendon ends. The method was found to best apply to cases with total pipe lengths to tendon length ratio above 0.05. Upon correction in those cases, agreement between force estimates from vibration and load cell determinations was better than approximately 6%.

The effect of strand failures in the anchorage and nearby regions was evaluated by controlled cuts of strands with intentionally unbonded segments. Tension losses of as much as ~9% (per load cell measurements) resulted from those strand cuts. The decrease in most cases was comparable in magnitude when measured by both the load cell and vibration tests. One exception took place however, in which a stiffening response took place upon strand cutting, resulting in a false indication of tension increase.

Analysis of the vibration response and measurements of strand positions in autopsied tendon cross supported the hypothesis that dual vibration spectrum peaks stem largely from asymmetric distribution of strands in the tendon cross section.

Supplemental static deflection tests showed good promise as a means to obtain accurate vibration tension determinations in the absence of reliable linear mass information. Linear mass recovered from combined deflection-vibration tests closely matched independently determined reference values. Tension determinations based on static deflection tests as the primary measurement method may be a good practical alternative to a vibration test -based approach given development of practical instrumentation.

An efficient numerical procedure was constructed to evaluate tendon tension and stiffness from mode frequencies revealed by analysis of the time domain response of the tendon during a vibration test. The procedure was implemented with commercially available software including a refined doublet sequence identification and automatic operation of large data sets. Ordinary desktop computers typically processed data from hundreds of tendons in times in the order of 1 hour.

Vibration test field equipment was developed for simplified operation and analysis procedures. A compact and easily portable field equipment prototype was designed and constructed, with a wireless remote actuator to permit testing by a single-operator thus minimizing personnel needs. A step-by-step operating procedure was prepared suitable for training of technical non-specialist FDOT personnel and consultants.

Early on in the project the segmental approaches of the Sunshine Skyway Bridge were evaluated with procedures and guidance provided by this project. Tension estimates from vibration testing were successfully conducted using the detailed analysis in all but one of the 864 tendon segments tested. Estimated tension patterns were in agreement with the presence of friction at deviation blocks. The end-to-end tension disparity increased with the number of intermediate deviation blocks. Vibration testing did not reveal any indications of dramatically reduced tension in any of the tendons segments evaluated. Tendon segments having estimated tensions lower than ~7% below their peer group average, and a tendon with unusual end-to-end tension disparity, were flagged for proposed special attention during subsequent inspections.

A user-oriented summary of principles and findings is provided.

TABLE OF CONTENTS

EXECUTIVE SUMMARY iv
INTRODUCTION AND PROBLEM STATEMENT 1
OBJECTIVES 4
TASK 1: MODEL VALIDATION 5
1.1 Approach 5
1.2 Methodology 5
1.2.1 General 5
1.2.2 Lateral Deflection Tests. 8
1.2.3 Impact and response recording 12
1.2.4 Load Cell Tension Determination 13
1.2.5 Dimension Records and Tendon Autopsy 13
1.2.6 Analysis of vibration response 14
1.2.7 Refined calculations for effect of protruding metal pipe at tendon ends 14
1.2.8 Supplementary Tests 18
1.3 Results 21
1.3.1 Data record and processing 21
1.3.2 Lateral Deflection tests 23
1.3.3 Tendon cross sections 23
1.4 Correlations and Findings 27
1.4.1 Load cell force determination 27
1.4.2 Vibration force determination and ability to detect tendon distress 27
1.4.3 Origin of double peaks 34
1.4.4 Lateral Deflection Tests 36
1.5 Task 1 Conclusions 41
TASK 2: IMPROVED DATA PROCESSING 42
2.1 Basic Treatment 42
2.2 Improved Data Processing 45
2.2.1 Efficient estimation of stiffness and forc 45

2.2.2 Improved identification of peak doublet components 47
2.2.3 Implementation 48
2.2.4 Detailed Example 48
2.3 Task 2 Conclusions 49
TASK 3: SIMPLIFIED TESTING AND ANALYSIS METHOD 51
3.1 Products 51
3.2 Equipment and Software 51
3.3 Data Processing 52
3.4 Procedure Details 52
3.5 Task 3 Conclusions 53
TASK 4: TESTING AT THE SUNSHINE SKYWAY BRIDGE 54
4.1 Scope 54
4.2 Execution and Findings 54
4.3 Task 4 Conclusions 54
LIST OF SYMBOLS 55
REFERENCES 58
APPENDIX 1 - DATA TABLES FOR TASK 1: MODEL VALIDATION 60
APPENDIX 2 - SIMPLIFIED TESTING AND ANALYSIS METHOD 105
APPENDIX 3 - TESTING AT THE SUNSHINE SKYWAY BRIDGE 129
APPENDIX 4 - USER-ORIENTED SUMMARY OF PRINCIPLES AND FINDINGS 156
APPENDIX 5 - DETAILED TABLE OF NONDIMENSIONAL MODE FREQUENCIES AS FUNCTION OF NONDIMENSIONAL STIFFNESS 171

ACKNOWLEDGMENT

The extensive collaborative technical support, facility design, construction and operation by the personnel of the FDOT State Structures Laboratory in Tallahassee, under the direction of Marc Ansley, was essential to the execution of the Task 1 experiments and it is gratefully acknowledged.

INTRODUCTION AND PROBLEM STATEMENT

Incidents of severe corrosion of strands have occurred in grouted tendons of marine segmental bridges in Florida (Corven Engineering 2001, Parsons B.Q.&D. 2002, Sagüés et al 2000). The bridges had been in service from as little as 7 years to 18 years. In most cases the corrosion was associated with the presence of voids from bleed water formation during grouting, often with chloride ion contamination as an aggravating factor (Sagüés et al 2003a). In some instances, the corrosion led to fracture of strands and complete tendon failure, usually at or near the anchorage region. All affected tendons had from 19 to 24 7-wire strands conforming to ASTM A-416. The strands were No. 13 Grade 270 (nominal diameter 0.5 in) and No. 15 Grade 270 (nominal diameter 0.6 in), 1.86 GPa (270 klbf) Guaranteed Ultimate Tensile Strength (GUTS). All affected tendons had a majority of their length external to the concrete (usually in a readily accessible position within the segmental box or in a hollow column) with the strands encased within polyethylene ducts filled with grout.

After the first incidents were discovered, extensive inspections of the bridges affected and similar structures were conducted to determine whether corrosion was in progress elsewhere. Unfortunately, direct corrosion detection is complicated, as the potentially damaged regions are not easily accessible. Thus, supplemental methods based on indirect manifestations of tendon distress were attempted. One such approach is detecting tendon tension loss, which may occur after one or more strands have failed if the transfer of force to the remaining strands through grout friction is less than ideal. This condition may not always be satisfied, but observation of a reduction in tension is a clear indication that detailed examination of the affected tendon is in order. Because the tendons of interest have portions of significant length external to the concrete, a tension measurement method based on the tendon vibration behavior was developed for the special conditions present in this application.

Vibration-based tension measurements are based on an extension of the observation that a plucked stretched string vibrates faster as the tension acting on the string increases. For strings with negligible flexural stiffness effects and with known length L and mass per unit length (linear mass) m, the tension T can be obtained as function of the fundamental lateral vibration frequency f by application of the well known relationship (Morse 1948):

$$T = 4\, f^2\, L^2\, m \qquad \text{(Eq. I.1)}$$

(a list of symbols is provided starting in page 55)

For stretched beams where the effects of a finite flexural stiffness S cannot be neglected (as is the case of most external tendons in segmental box construction) the relationship between vibration behavior and tension is more complicated than in Eq.(I.1). In those cases the relationship involves not only the frequency of the fundamental Mode but also that of at least one of the overtones, which are now inharmonic (Morse 1948). Despite the complexity the problem is tractable (Sagüés et al

2006) and measurement of those frequencies allows for recovery of the value of T as well as that of S when both L and m are known.

Thus, measurement of the vibration spectrum of a tendon excited by a small lateral impact or disturbance can provide quantitative indication of the tension acting on the tendon. Such measurements are routinely conducted on bridge cable stays. Vibration excitation can be provided by wind action, and motion sensing can be conducted remotely by a laser system (Ciolcko et al 1999, Mehrabi et al 1998). Obtaining a tension estimate in those cases may involve considering factors such as gravitational sag (Zui et al 1996), but the complicating effects of flexural stiffness tend to become less important as stay cables are relatively long. The total number of stays in a typical bridge is also relatively small. In contrast, for external post-tensioned tendon segments gravitational sag may not be a concern but flexural stiffness effects are enhanced by the relatively short vibrating length of the tendons and cannot be ignored. Furthermore, post-tensioned bridges may contain thousands of external tendon segments needing assessment. This report addresses challenges of the vibrational method when applied to large inventories of tendons in post tensioned segmental bridges such as those that experienced severe early corrosion.

Vibrational testing of tension to identify potentially distressed external tendons of post-tensioned segments and columns has been successfully used in several major FDOT bridges [Sagüés et al 2000, 2003b, 2004a, 2004b, 2005, 2006; Corven 2005). The tests consist of lightly impacting the free length of the tendon, recording the resulting vibration frequencies, and applying the value of those frequencies as well as the tendon dimensions and unit mass length to a computational model that calculates the tendon tension. The procedure is very useful but several key issues not adequately resolved at the beginning of this investigation limited applicability and were resolved here. Those issues are the following, with need areas identified in italics at the end of each item.

1. Vibration spectra of actual tendons in the field are, on first approximation, a series of peaks corresponding to a fundamental mode plus inharmonic overtone modes. However, upon close examination each mode is often found to consist of doublets with two closely spaced but still different frequencies. It has been assumed for tension calculation (Sagüés et al 2006) that asymmetry of strand arrangement is responsible for that behavior, causing different values of S depending on the orientation of the lateral displacement during vibration. Based on that assumption, independent tension calculations have been made using one series of frequencies corresponding to the low-frequency component of each doublet, and another for the high frequency component. Both series yield comparable values of T but different values of S, consistent with the initial assumption. However, before the present study the validity of the assumption was never directly validated. Thus, uncertainty remained as to whether alternative causes for the presence of dual peaks may be at work, potentially leading to a different quantitative outcome of the vibration measurements. Other working assumptions in the stretched-beam model used for interpretation of the results included clamped end conditions, and an effective tendon length

given by distance between the tendon exit points at the concrete surface, neglecting the effect of protruding steel collars at those exit points. The validity of those assumptions and the corresponding tension evaluation procedure had not been assessed, as no direct comparison existed between independently known tendon tension and the value estimated from the vibrational measurements. In addition, the sensitivity of the vibration test results to one or more strands having experienced detensioning at the anchorage ends upon corrosion had not yet been established. *Validation of the vibration test method by implementation in a well-characterized realistic tendon system was needed.*

2. Aside from validation, processing of the vibration test method data needed improvement. The spectrum peaks were determined manually or with partially reliable automatic procedures. These procedures were inadequate for accurate evaluation of data sets from large bridges. *A practical and accurate processing procedure for automatic peak identification and tension estimation from large data sets was needed.*

3. There was need also for rapid and economical preliminary screening of structures, prior to detailed analysis. Field tests were being conducted on a custom basis for each bridge, requiring custom equipment and specialists to analyze results for even preliminary estimates of tendon tension. *A simplified testing and analysis method for rapid screening was needed.*

4. There was need for immediate supplemental work in support of testing tendons in the segmental approaches of the Sunshine Skyway Bridge. *Activities were required to prepare for testing, provide equipment, train personnel, and interpret results of vibrational tests in the segmental sections of the North and South elevated approaches of the Sunshine Skyway Bridge.*

OBJECTIVES

Based on the above needs the following objectives were established for the present investigation:

1. **Model Validation:** Resolve issues per need area 1 above needed for validation of the vibrational model and data processing method to detect tension loss.

2. **Improved Data Processing:** Establish a practical and accurate processing procedure for automatic peak identification and tension estimation from large data sets.

3. **Simplified testing and analysis method:** Establish a simplified and rapid testing and analysis method for screening tendons with possible failed strands in existing structures.

4. **Testing at the Sunshine Skyway Bridge:** Support activities and interpret results of vibrational tests to be conducted in the Sunshine Skyway Bridge High Level Approach segmental boxes.

The following sections describe the effort under Tasks keyed to addressing each of the objectives and the corresponding findings.

TASK 1: MODEL VALIDATION

Note: The treatment presented in the Task 1 and Task 2 sections is oriented to readers already familiar with the specific problems addressed in this investigation. A summary of principles, findings and applications dealing with these tasks and intended for broader use is provided as Appendix 5, starting on page 158.

1.1 Approach

The general approach was to conduct vibration tests on nearly full-scale tendons constructed at the FDOT Structures Laboratory. The tendons were tensioned to precisely known forces under well-characterized conditions. The tension evaluation models available at the beginning of the investigation were applied to the data and the model force estimate was contrasted with the actual value. Based on that comparison, the model assumptions and interpretation method of vibration results were modified to improve the accuracy of force estimates.

1.2 Methodology

1.2.1 General

A Tendon Test Facility (TTF) was constructed at the FDOT Structures Laboratory (FSL) in Tallahassee, FL. for the large-scale model validation tests. The PI cooperated with FDOT Structures Laboratory personnel under the direction of Marc Ansley in establishing the test parameters; the detailed facility design and construction was conducted by the FSL.

The TTF had one fixed reinforced concrete anchor block (South end) and one movable anchor block (North end) with horizontal anchors approximately 10 m (400 in) away (Figure 1.1). The anchor assemblies were Type E manufactured by VSL. The fixed block had provisions for horizontal anchors at the same elevation as those in the movable block, allowing for straight horizontal tendons with a free length of ~10m (~400 in). The fixed block had also sloping anchors at higher elevation for an ~ 5 m (~200 in) long sloping tendon extending to a deviation block placed approximately halfway to the movable block. That tendon became horizontal in the remaining ~4m (~160 in) long free length between the deviation block and the movable block. A stiff steel frame extended from the fixed block to the movable block. Tension was applied by displacing the movable block by the required amount with hydraulic jacks and than placing stops between the block and the end of the frame. Load cells monitored the tensioning force at the movable block end and the reactions at the deviation block allowing for precise computation of the force in both horizontal and sloping sections of the tendon. The anchor at the fixed block end had an extension fixture (Figure 1.2) that allowed torch-cutting individual strands thus simulating consecutive failures (maximum of two for safety reasons) of single strands. The force on the extension fixture was monitored by a load cell as shown in Figure 1.2. Selected strands, usually including those to be cut, were individually surrounded by a separating sleeve for some length from the extension fixture. The sleeve was intended to prevent bond to the grout over the sleeve length, thus simulating a condition where the strand is not surrounded by grout in a voided anchorage or nearby duct with consequent greater strength loss upon strand failure at the anchor.

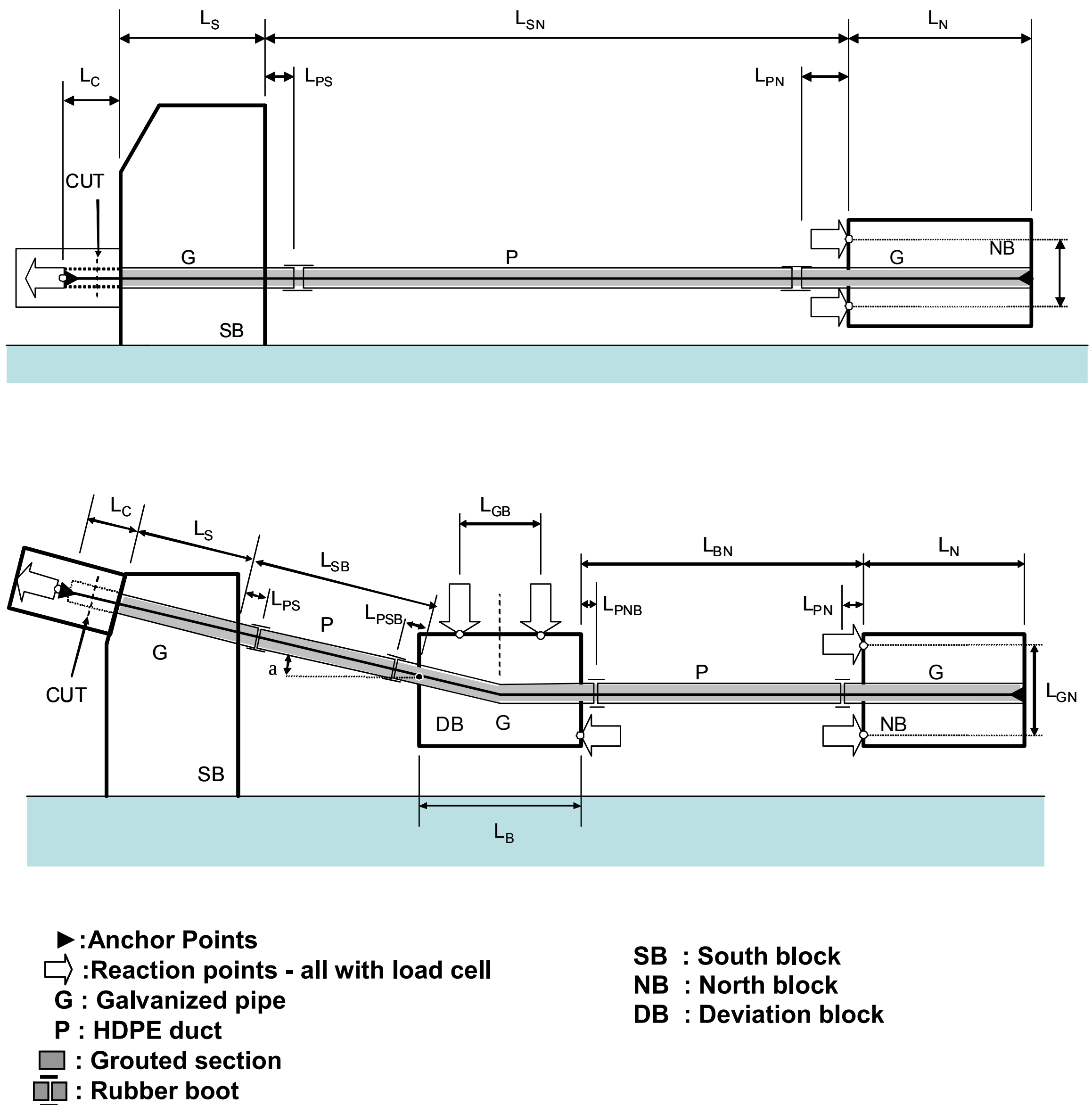

Figure 1.1 - Main features of the Tendon Test Facility for Tendons 0A and 0B (top) and 13A and 13B (bottom).

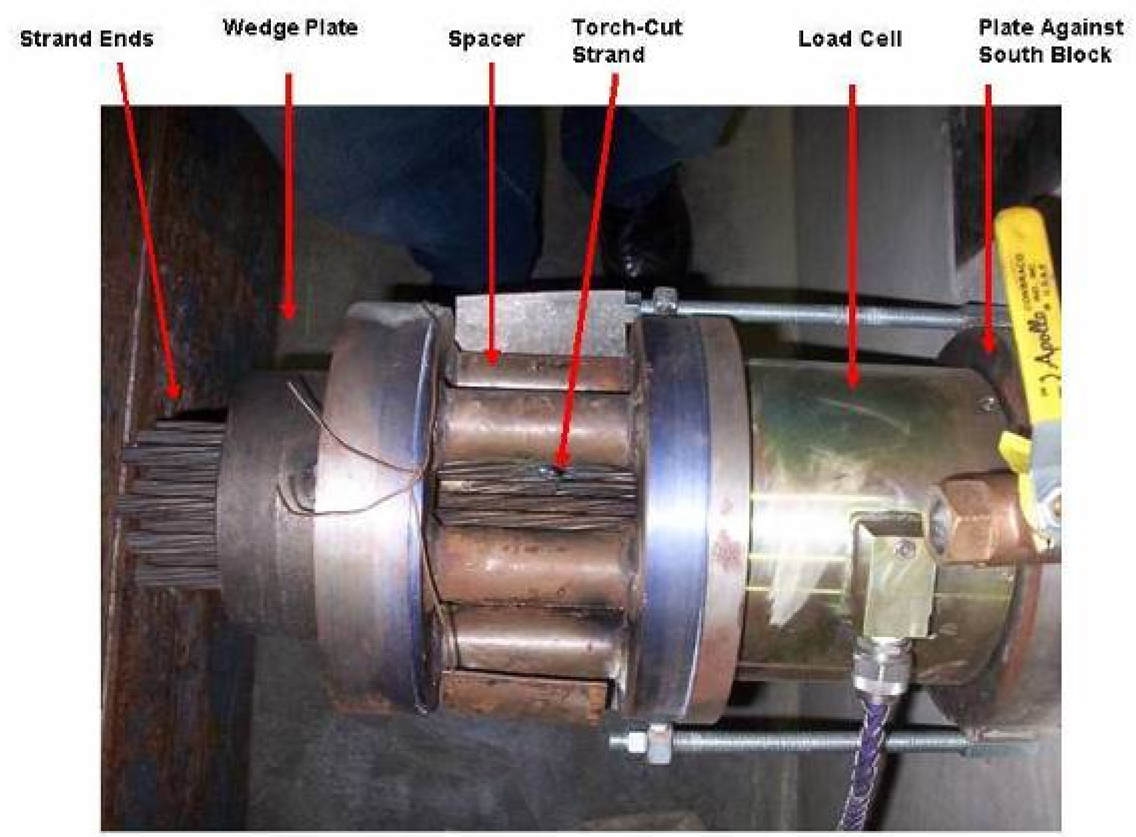

Figure 1.2 - Bottom: South Block tendon termination setup for controlled strand cuts.

The research schedule consisted of sequentially constructing and evaluating two duplicate full length horizontal tendons (0A and 0B) and two duplicate sloping tendons (13A and 13 B). All tendons had twelve ½-inch, low-relaxation, seven-wire strands per ASTM A416 grade 270 supplied by VSL. The design stretching stress capability was 400000 lbf, corresponding to 80 % of the Guaranteed Ultimate Tensile Strength (GUTS) but actual stretching stresses were typically 1.51 MN (340 klbf), (67 % GUTS). The strands were contained in a high density polyethylene (HDPE) duct type DR17 3 in NPS (76 mm (3 in) internal diameter with a wall thickness of 5.71mm (0.225 in)). Galvanized steel pipes 76 mm (3 in) internal diameter, 4.76 mm (3/16) in wall thickness emerged from the end and deviation blocks and served as attachment points for the polymer duct by means of an 89 mm (3.5 in) inner diameter 150 mm (6 in) long Neoprene duct coupler. After stretching the tendons, they were grouted with QPL-938 Masterflow. ™ grout manufactured by Masters Builders using a colloidal pump. There was no indication of grout voids in any of the tendons constructed. Relevant dimensions for all the tendons and accessories in each experiment are detailed in Table 1.1 and corresponding sketches.

After a grout setting period of 7 days minimum, vibration testing was conducted on the free length(s) of the tendon. In the vibration tests the tendon was impacted at a point 1/6 of the free length away from one of the blocks at either end of the free length of the tendon, and the accelerometer was placed at 1/3 of the distance from the same or opposite end of the tendon. Table 1.2 and ancillary sketches summarize the arrangements used in the tests conducted in each tendon. Table 1.3 details the strand cut schedule and sleeve length/type used for each tendon.

1.2.2 Lateral Deflection Tests.

Lateral stiffness measurements were conducted in selected cases by applying a deflection force near the center of the tendon and measuring the resulting displacement. Ideally, the resulting lateral stiffness can be used in conjunction with vibration measurements to obtain the value of the tension without need of knowing or assuming the value of the linear mass (Sagüés et al 2006). The results of the deflection measurements were used to ascertain the accuracy to which such determination can be made. Lateral deflection tests were made for forces applied in the vertical and in the horizontal direction as illustrated in Figure 1.3.

Table 1.1 - Relevant Dimensions [m (in)] Keyed to Figure 1

	Tendon			
	0A	0B	13A	13B
L_{SN}	9.319 (366.9)	9.279 (365.3)		
L_{SB}			4.905 (193.1)	4.956 (195.1)
L_{BN}			3.289 (129.5)	3.292 (129.6)
L_{PS}	0.12 (4.7)	0.12 (4.7)	0.13 (5.1)	0.065 (2.6)
L_{PSB}			0.12 (4.7)	0.065 (2.6)
L_{PNB}			0.151 (5.9)	0.08 (3.1)
L_{PN}	0.118 (4.6)	0.12 (4.7)	0.102 (4.0)	0.08 (3.1)
L_S	1.22 (48.0)		1.15 (45.3)	
L_N	1.22 (48.0)			
L_B			1.221 (48.1)	
L_C*	0.43 (16.9)			
L_{GB}			0.856 (33.7)	
L_{GN}*			0.415 (16.3)	
Sloping Angle*			12.5 deg.	

* Approximate

Table 1.2 - Vibration Test Configurations: Accelerometer and Impact Positions. Accelerometer and impact orientations in each configuration are noted in Table A1.1

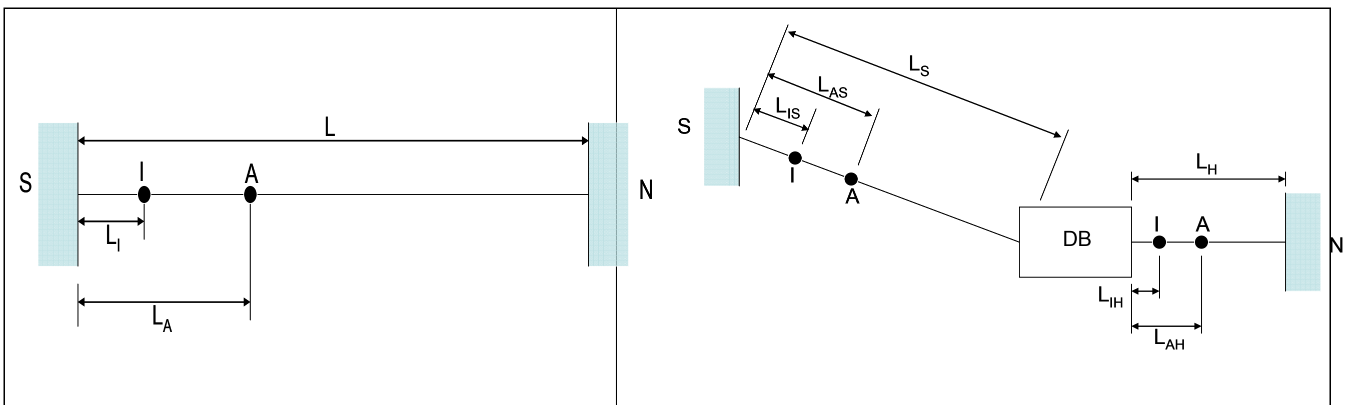

0A, 0B				13A, 13B					
Tendon	Conf.	L_I/L	L_A/L	Tendon	Conf	L_{IS}/L_S	L_{AS}/L_S	L_{IH}/L_H	L_{AH}/L_H
0A	1	1/6	1/3	13A	1	1/6	1/3	-	-
0A	11	1-1/6	1-1/3	13A	4	-	-	1/6	1/3
0B	1	1/6	1/3	13B	1	1-1/3	1-1/6	-	-
0B	3	1/6	1/2	13B	2	-	-	1/6	1/3
0B	5	1-1/6	1-1/3						

Table 1.2D Deflection Test Configurations. Key to entries is same as in Table 1.2.1 except that L_l corresponds to lateral force load cell position and L_A to deflection gage position. Load and deflection orientations are noted in Table A1.3.

Tendon	Conf.	L_l/L	L_A/L
0A	D1	1/2	1/2
0B	D1	1/2	1/2
0B	D2	1/2	½+4.8e-3

Table 1.3 - Strand Cut Arrangement and Schedule - Strand pattern as seen on south anchorage facing north

Tendon	Sleeved Strands # in cutting order	Sleeved Length / ft	Time since Casting / days
0A	1	2*	27
	11	5*	
0B	1	10	15
	2	6	
13A	1	2	91
	11	4	
13B	1	2	11
	5	2	

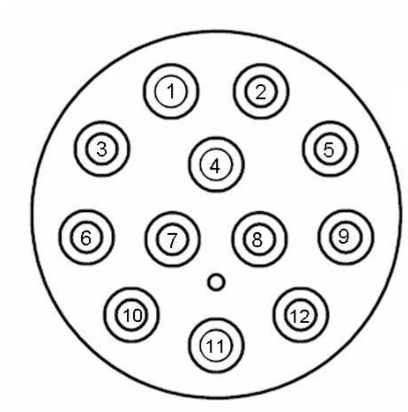

*Sleeved with PVC pipe found subsequently to be filled with hardened grout effectively retaining bond.

Lateral forces were applied by a V-shaped yoke pushing against a threaded rod and reaction nut attached to the tendon frame. Force was measured by a Model JP 200 load cell by Data Instruments, Inc. calibrated against known mass weights. Deflections were made with dial/digital deflection gages) with 25 μm (0.0001 in) resolution mounted against a stiff tripod resting on the floor. Force-deflection was recorded starting at zero force, through and apex value (up to ~800 N (~180 lbf)) and returning to zero force, at intervals ~ 1/10 of the total force. The forward and return sequence data were fit to a straight line to determine the average slope of the load line during the test.

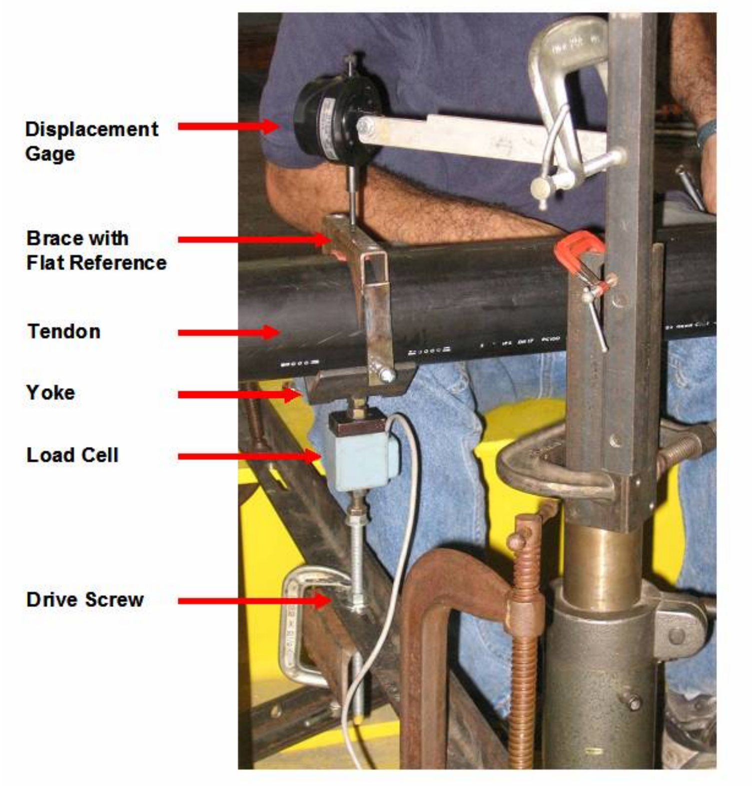

Figure 1.3 - Deflection test setup

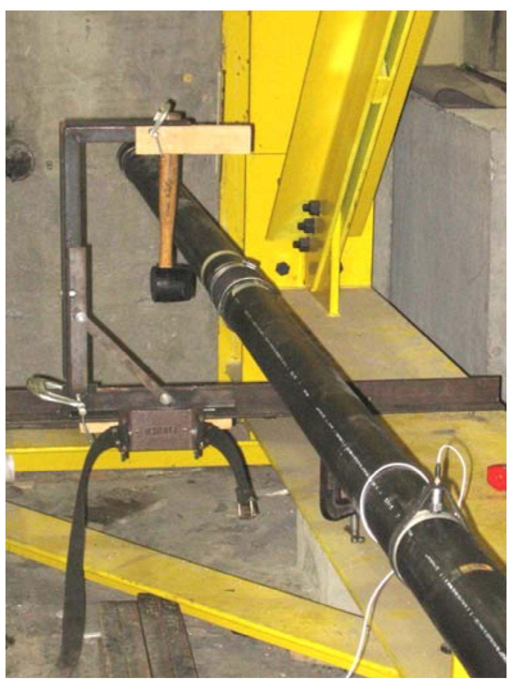

Figure 1.4 - Hammer arrangement.

1.2.3 Impact and response recording

All impacts were conducted with a rubber hammer (Figure 1.4) with a total mass of 611 grams, operated with a hammer holder device (Figure 1.4) and manually preventing the hammer from hitting the tendon again after rebounding. The holder allowed for precise impact angles at 0° from the vertical (Top impact), 90° (Side impact) and 45° (Angle impact) with kinetic energies of ~0.32, ~0.39 and ~0.39 J (~2.8, ~3.5 and ~3.5 in-lbf) respectively, of which about half remained in the rebounded hammer. The resulting vibration data files were designated by T, S or A respectively in the place reserved for impact type. Tests in tendons 13A and 13B were conducted manually retaining approximately the corresponding angles and energies resulting when using the holder.

The accelerometer was a Model 338B34 by PCB Piezotronics with 10 mV/*g* sensitivity, normally attached to the tendon duct with adhesive wax and further retained by a Velcro ™ strap. The accelerometer was placed with its sensing axis on a vertical plane and attached to the top of the tendon (Top sensing), or with axis on a horizontal plane and attached to the side of the tendon (Side sensing), or with axis at 45° from horizontal and attached at a halfway position (Angle sensing). The resulting vibration data files were designated by T, S or A respectively in the place reserved for accelerometer sensing direction. A flexible coaxial wire ~2.5mm (~0.1 in) diameter connected the accelerometer to a Model 480E09 signal conditioning unit by PCB Piezotronics, with a voltage gain set to 10x, resulting in a signal amplitude upon impact typically < 0.6 V . The signal was acquired for a period of 11.89 seconds starting ~ 2 seconds before impact, at an acquisition rate of 11,025 samples per second, using the Sound Card line input of a Model Latitude C840 computer by Dell configured as a Monaural recorder with 16-bit resolution and controlled by Labview™ version 7.1 program. The resulting array was stored as a 256 KB long .wav file. After completion of the recording sequence the hammer was repositioned and the test was repeated to obtain a duplicate. In tendon 13B an alternative accelerometer arrangement was used where two accelerometers and conditioning units were used simultaneously for the T and S positions. The accelerometers were placed in a mounting ring shown in Figure1.5. The results were recorded in a 512 KB long stereo .wav file with each channel recorded with 16-bit resolution. In these tests no Angle accelerometer orientation was used.

The .wav file designation is exemplified by **13ATSXXB.YYY** where 13A is the tendon name, T and S designate accelerometer and impact orientation respectively, XX is an additional optional descriptor, B indicates it is the second (duplicate) test while A would have indicated the first, and .YYY is an additional identifier replacing the .wav extension for further identification of the test conditions if desired. Stereo files were named in the same fashion except that since there was no accelerometer orientation variation the single character C (for combined) would replace the TS characters in the above example, thus **13ACSXXB.YYY**.

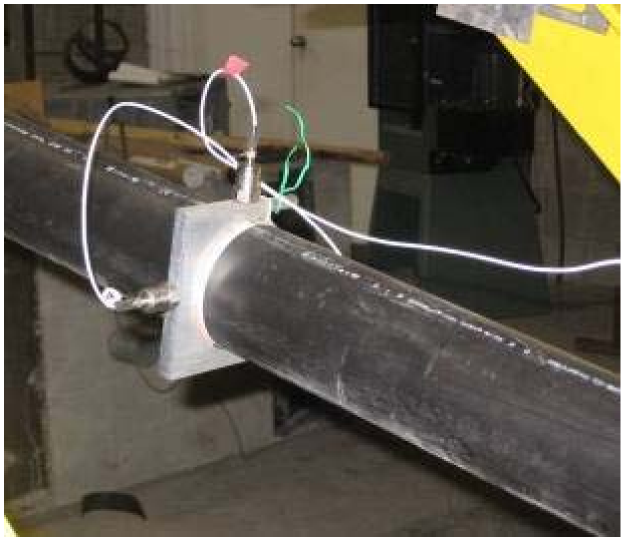

Figure 1.5 - Special accelerometer configuration for Tendon 13B.

1.2.4 Load Cell Tension Determination

Load cell forces were recorded by FSL at data acquisition rates typically ranging from one per hour to one per second (faster during strand cut tests) and stored as a text file. Recorded time was conciliated with actual time whenever needed by tagging to known time events. Load cell calibrations were on file at the FSL and reported values are deemed to be accurate in the order of 1%. Internal consistency was further verified during tendon stretching at the time of grouting by noting the reported force at the South end gage and the sum of the four reactions at the North block cells in tendons 0A and 0B. Those values agreed with each other to within 0.8% when stretching Tendon 0A and 1.6% for Tendon 0B.

1.2.5 Dimension Records and Tendon Autopsy

Tendon lengths of the stretched tendons were determined with laser sights and further verified by metallic tape measurements. After completion of the vibration tests and detensioning the tendon ends were cut off with a torch and the stubs cut again ~0.1 m (~ 4 in) from the end with an abrasive wheel to obtain a flat cross section. An additional cut was made near the center of the tendon. Electric continuity tests were made to identify individual strands at both ends of each cut length. Photographs of the exposed cross sections were used to document the strand pattern for subsequent determination of nominal moment of inertia and stiffness. The cut tendon lengths were weighed to 0.11 kg (1/4 lb) resolution with a Chatillon™ model HB1000 balance to determine detensioned linear mass. It was subsequently converted to linear mass under tension by assuming simple elastic extension of the steel and not crediting the grout or duct for any significant elastic resistance. The resulting values are listed in Table 1.4.

Table 1.4 - Tendon Linear Mass [$Kg\text{-}m^{-1}$ ($lb\text{-}in^{-1}$)]

Tendon	Sloping Section Linear Mass	Horizontal Section Linear Mass
0A		17.46 (0.978)
0B		17.13 (0.959)
13A	17.78 (0.996)	17.66 (0.989)
13B	17.27 (0.967)	17.51 (0.981)

1.2.6 Analysis of vibration response

The section on Task 2: Improved Data Processing describes in detail the tools used in analyzing the vibration response. In summary, the .wav files generated by the response recording were first processed with a Matlab™ program that made a preliminary determination of the peak frequencies and the amplitude of the corresponding peaks. Because of the small size of the data set (compared with that of a bridge survey) and only one tendon being analyzed at a time, peak identification and position within individual doublets were typically determined manually as well automatically. Once peaks were identified, the nondimensional stiffness for each of the dual components of each peak was determined by the procedure detailed by Sagüés et al (2006) and implemented in a spreadsheet program named FF. Tension was then determined for each component of the doublet using the nondimensional stiffness and the linear mass obtained from the tendon autopsy. The tension values thus obtained were then compared with the load cell values. Similar procedures were conducted for the after-strand cut results. For short tendons where end pipe effects may become important (see next section) the analysis was conducted with a reduced set of peak frequencies and the results were applied a correction factor as appropriate before comparison with the load cell results.

1.2.7 Refined calculations for effect of protruding metal pipe at tendon ends

Galvanized pipe segments emerge from the concrete at tendon ends, creating a short length where the tendon sheath is much stiffer than the normal HDPE sheath or rubber booth. The non-uniform stiffness distribution changes mode frequencies relative to those of a tendon with uniform sheathing. Calculations using the normal procedure (FF) based on the actual frequencies but assuming uniform sheathing will therefore yield a tension value erroneous to same extent. In the extreme case of fully stiff pipe segments, the effect is equivalent to having a shortened tendon but analyzed as if the length were the full length. The effect is however expected to be limited, to be best compensated by use of a small correction factor. This section addresses calculation of that factor as function of dimensions of pipe and tendon, and of tendon tension and stiffness of the regular portion of the tendon.

The approach consists of first using finite element modeling to find the mode frequencies of an idealized tendon of total concrete-to-concrete length L with pipe-sheathed ends of effective stiffness Sp, stiffness Sm in the part of the tendon between the pipe ends, and tension Ta'. The resulting mode frequencies are processed by FF to obtain a tension estimate Te'. The correction factor k'=Ta'/Te' is then calculated for a variety of cases that bracket commonly expected situations. An interpolating function is then obtained by multiple regression to obtain k for any case of interest as defined by pipe type and length, tendon length, etc.

Given a tension estimate Te obtained from vibration data for a given tendon but ignoring the presence of the pipes, an improved estimate T_{IMPR} is then obtained by multiplying Te by the value of k that corresponds to the conditions of the case:

$$T_{IMPR} = k\,Te \qquad \text{Eq. (1.0)}$$

In the following it will be assumed that the pipe segments are of the same length Lp/2 at each end of the tendon, and that the segments are fully clamped at the concrete end. The presence and effect of the rubber boot will be ignored, and the HDPE sheath will be assumed to start where the pipe ends.

The calculations addressed the combinations shown in Table 1.5, all with Ta'=1.44 MN (323.7 lbf) and linear mass 17 kg/m (0.952 lb/in) but with Lp/L ranging from 0.01 to 0.1, central portion stiffness values representative of those observed in the test tendons, and pipe sheathed end stiffness values covering a wide range centered on the approximate expected value of a galvanized pipe of the dimensions used combined with the portion of the tendon inside the pipe. The validity of that condition is discussed later on.

The effect of the metal pipes is greatest when Sp>>Sm and Lp is an appreciably large fraction of L, as in the case of the short free tendon lengths in configuration 13 or 13 B. In those cases the smooth progression of f_n/n as function of n^2 (Sagüés et al, 2006) is altered noticeably especially at the higher overtones. Thus the computed apparent tendon force based on the simple assumption of uniform stiffness (and the resulting value of k) tends to become an increasingly complicated function of system variables as an increasingly large number of overtones is used in the calculations. In addition, as shown in Items 1.3 and 1.4 below, Mode 1 tended to be affected by spurious deviation block support vibrations in the 13 degree assemblies. Experimentation to obtain an optimal compromise between number of overtones and simplicity of the interpolating function for a wide range of conditions showed best results when using only the two or three Modes higher than Mode 1. The resulting k' values are listed in Table 1.5.

Table 1.5 - Metal Pipe Effect Calculations - All with Fa'=1.44 MN (323.7 klbf)

L m (in)	Lp m (in)	Stiffness Main Section Sm $N\text{-}m^2$ ($lbf\text{-}in^2$)	Stiffness Pipe End Sp $N\text{-}m^2$ ($lbf\text{-}in^2$)	k' Using Modes 2-3	k' Using Modes 2-4
10 (393.7)	0.1 (3.94)	70000 (2.439E7)	305800 (1.066E8)	0.985	0.985
5 (196.9)	0.05 (1.97)			0.983	0.981
3 (118.1)	0.03 (1.18)			0.969	0.960
10 (393.7)	0.5 (19.7)			0.943	0.943
5 (196.9)	0.25 (9.84)			0.931	0.929
3 (118.1)	0.15 (5.91)			0.912	0.902
10 (393.7)	1 (39.4)			0.915	0.915
5 (196.9)	0.5 (19.7)			0.881	0.878
3 (118.1)	0.3 (11.8)			0.846	0.833
5 (196.9)	0.25 (9.84)	70000 (2.439E7)	150000 (5.227E7)	0.956	0.954
3 (118.1)	0.15 (5.91)			0.936	0.927
5 (196.9)	0.5 (19.7)			0.931	0.929
3 (118.1)	0.3 (11.8)			0.897	0.885
5 (196.9)	0.25 (9.84)	105000 (3.659E7)	600000 (2.091E8)	0.921	0.918
3 (118.1)	0.15 (5.91)			0.895	0.882
5 (196.9)	0.5 (19.7)			0.858	0.853
3 (118.1)	0.3 (11.8)			0.817	0.800
5 (196.9)	0.25 (9.84)	70000 (2.439E7)	105000 (3.659E7)	0.974	0.972
3 (118.1)	0.15 (5.91)			0.956	0.946
5 (196.9)	0.5 (19.7)			0.961	0.960
3 (118.1)	0.3 (11.8)			0.933	0.923

Table 1.6 - Power law parameters for estimating k

Modes Used	k_0	q
2-3	2.0815	0.7843
2-4	2.0848	0.767

The results were processed by a power-law regression to obtain an interpolating function yielding k as function of a non-dimensional system parameter P where

$$k=1- k_0 P^q \qquad \text{(Eq. 1.1)}$$

where

$$P= (1-k_{INF}) (1-Sm/Sp)^{1.5} (\sigma_m/(1+\sigma_m))^{0.25} \qquad \text{(Eq. 1.2)}$$

k_{INF}= ((L-Lp)/L)^2 (Eq. 1.3)

(value of k for the limit case of infinitely stiff metal pipes)

σ_m = Sm/ Ta' L^2 (Eq. 1.4)

(non-dimensional stiffness of the tendon if Lp=0)

and k_0 and q are non-dimensional parameters that depend on whether Modes 2-3 or 2-4 are used , per Table 1.6 .

The goodness of fit of the interpolating function for the range of conditions examined is illustrated in Figures 1.6 and 1.7 which show good correlation factors and an interpolation accuracy better than ~1% when using Modes 2-3 and better than ~2% when using Modes 2-4. It is noted that if the determinations of mode frequencies were ideally accurate, using the lower number of modes would on average provide the most accurate estimate of k. However, experimental scatter is always present which introduces uncertainty that would be lowered by using a larger number of modes in computing the apparent force. Thus, calculations using Modes 2-4 are likely to represent the best compromise for obtaining more accurate overall results. A quantitative analysis of propagation of both modeling and experimental errors should be conducted in future research to better evaluate the optimal choice of number of modes under various error structure scenarios.

For practical application of the correction factor, dimensional information on the steel pipes is obtained by direct measurement or from construction plans, yielding Lp, pipe diameter D, and wall thickness d. D and d allow for calculation of the pipe segment stiffness Spp assuming a nominal value of E= 202.0 GPa (2.93 10^7 psi) for the elastic modulus of steel and multiplying by the moment of inertia of the annular pipe section. Sp may be estimated on first approximation by adding Spp to Sm . Vibration data are then processed first ignoring the presence of the metal pipes, assuming that the tendon stiffness is uniform along its length. That procedure yields apparent force and apparent stiffness estimates Te and Sme respectively. From the above and tendon length L an estimated non dimensional stiffness σ_{me} = Sme/Te L^2 is obtained, as well as k_{INF} per Eq. (1.3).

The above values are then inserted in Eq.(1.2), using Sme and σ_{me} instead of Sm and σ_m respectively to obtain the value of P, which then is inserted in Eq.(1.1) to determine an approximate value of k, named k_{APPR} . The improved tension estimate T_{IMPR} accounting for steel pipe effects is then obtained with Eq. (1.0) using k_{APPR} instead of k.

It is noted that the estimate Sp= Sm + Spp assumes that there is completely efficient elastic coupling between the tendon strands, the intervening roughly annular grout section, and the short open ended outer steel pipe. That assumption is not likely to be justified as the elastic modulus of the grout is typically one order of magnitude lower than that of steel (Mirza et al 2002) and the shape of the system does not promote uniform bending. Therefore, the effective stiffness of the pipe-sheathed end is expected to be less than that given by the above simple addition, and may be expressed instead as $S_p = S_m + \beta S_{pp}$ with and adjustment factor $\beta < 1$. Application of this concept and the above procedure is illustrated in the subsection on Correlation and Findings of this section of the report.

1.2.8 Supplementary Tests

Supplementary tests were performed during the investigation which may be analyzed in the future pending availability of resources. Supplementary tests included vibration behavior with a fret placed at an intermediate position in the tendon, resulting in a temporarily reduced vibrating length (and a near pinned, non-clamped condition at the fret end). Future analysis of fret tests may assist in improving accuracy of similar configurations in the field used when obstructions that prevent free tendon vibration are circumvented with a temporary fret. Additional supplementary tests used an added known mass at the center of the vibrating length which lowered the frequency of the tendon in a controlled manner. Contrasting results with the same tendon without the added mass may provide an additional means of evaluating tendon linear mass when accurate values for it are not otherwise available. Data from these tests have been archived.

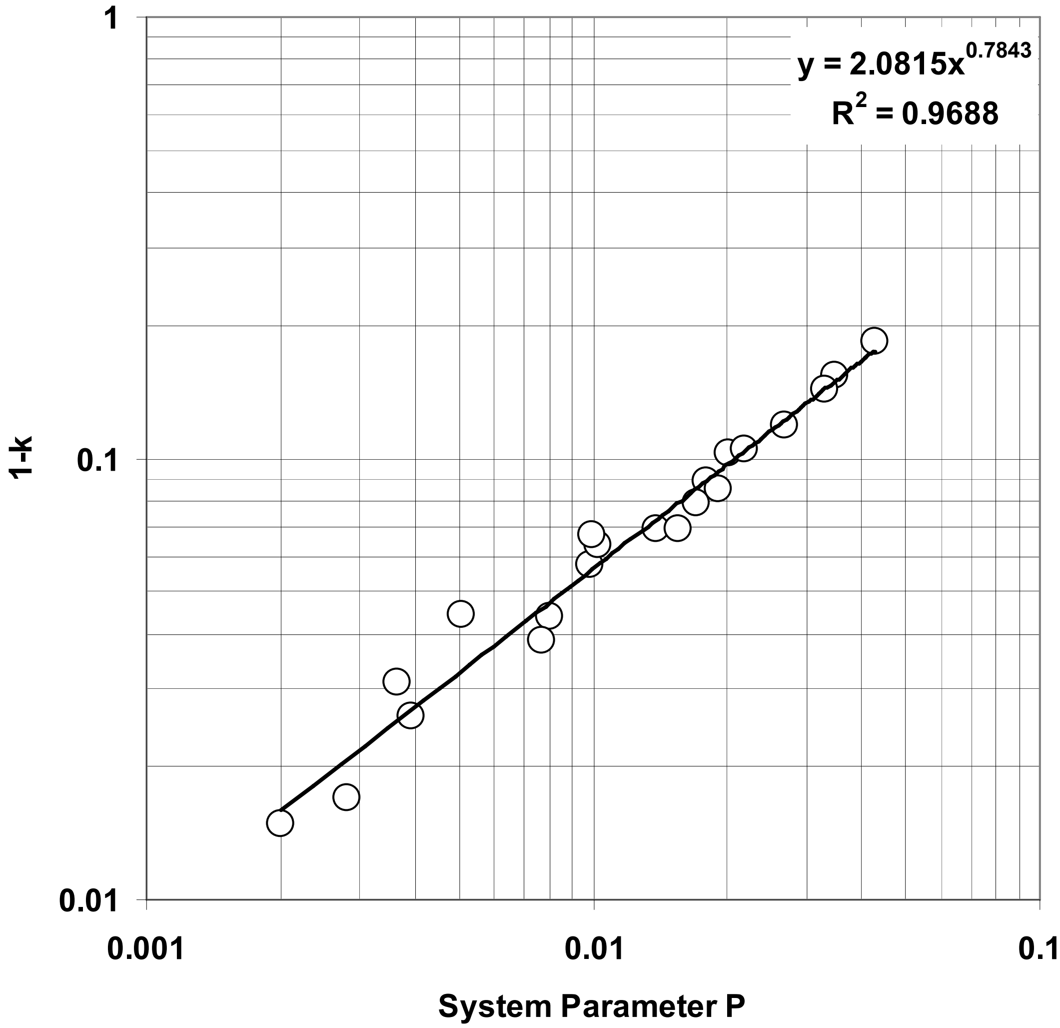

Figure 1.6 Correction factor k' (circles) and interpolating function k (solid line, parameters in legend) as function of system parameter P for calculations using Modes 2 and 3. For clarity the results are displayed as 1-k.

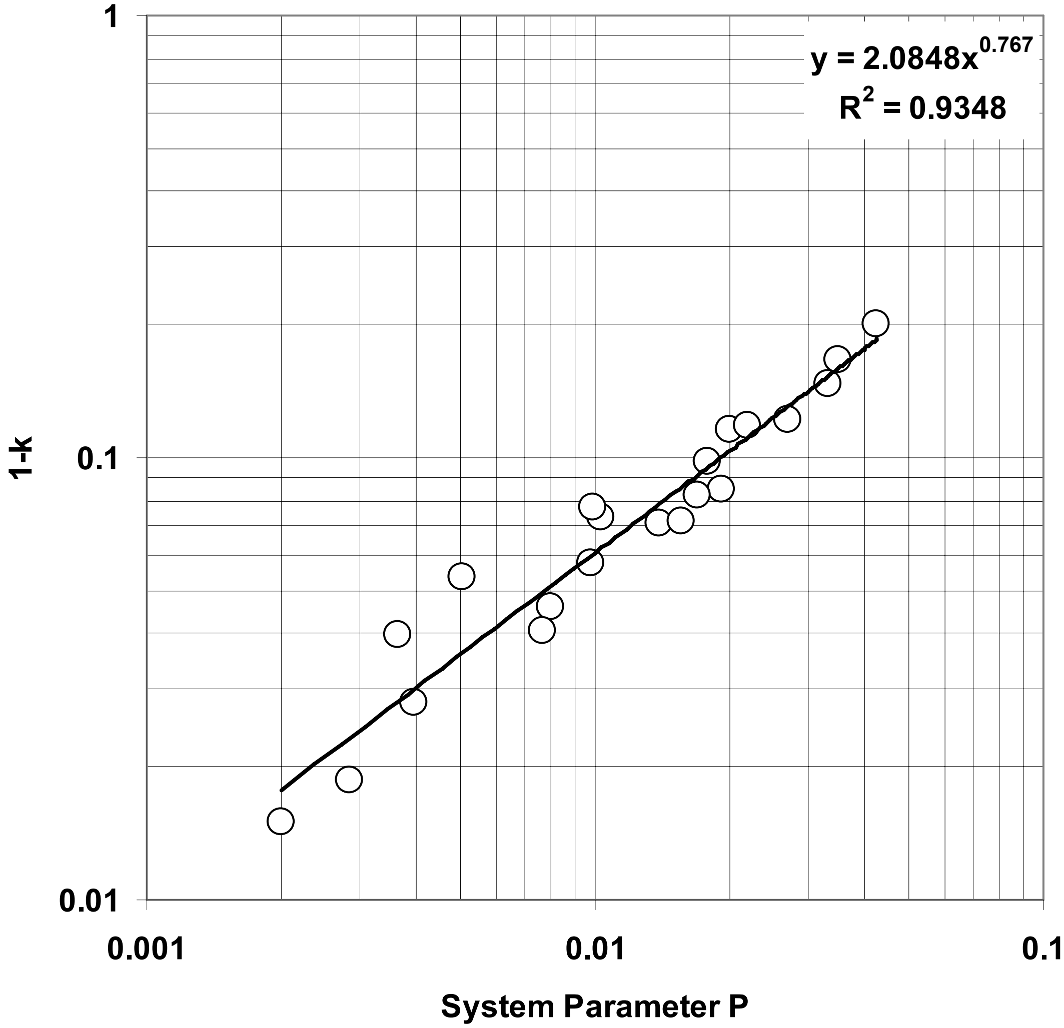

Figure 1.7 Correction factor k' (circles) and interpolating function k (solid line, parameters in legend) as function of system parameter P for calculations using Modes 2 to 4 For clarity the results are displayed as 1-k.

1.3 Results

1.3.1 Data record and processing

Figure 1.8 shows the vibration spectral response obtained in a typical case (13BCTZA for tendon 13B, tested after strand Cut 2; Tables A1.1 and A1.2 Appendix 1). The spectrum is as output by the initial peak identification program, with the components of each doublet identified for the lowest 7 vibration modes. The proper identification of those components was verified manually and the corresponding frequencies and amplitudes were then recorded as a 28 -element vector which included 7 dual frequencies and 7 dual amplitudes. Some of those may be blank if either or both of the components of a doublet were too weak or uncertain for adequate identification. For Tendons 13A and 13B spurious vibrations tended to affect Mode 1, and because of the short free lengths the metal pipe end effects were relatively strong. Thus for those tendons analysis was restricted to modes 2 to 4 with consequently limited vectors. Table A1.1 in Appendix 1 lists the frequency portion of the result vectors after sorting out whenever applicable, for all the tests conducted, keyed to the test conditions in Table 1.2. The full set of all possible nine T, A and S combinations for accelerometer and impact orientation in duplicate (a total of 18 .wav files) was conducted for many but not all of the conditions listed in Table 1.2. In the remaining cases abbreviated test sequences were used with only selected impact angle/accelerometer position combinations. For tendon 13 B where dual accelerometers were used, no angle-orientation accelerometer data were present.

The analysis results for each vibration test are listed in Table A1.2 in Appendix 1. Most tests yielded a force and a stiffness estimate from each the series of low frequency (LF) components of the doublets, and the series of high frequency (HF) components. The two forces were averaged and reported as an end-pipe effect uncorrected average. An end-pipe correction factor was computed by the procedure described earlier, using the average of the LF and HF stiffness values for Sme. The factor was then applied to produce a corrected force estimate and so reported. If the peaks could not be resolved into doublets or a given series was incomplete, the values reported were for the single available series and not an average. Table A1.2 lists also for comparison the force acting on the tendon, obtained from load cell measurements, (see Table A1.5 description next) at the time of the vibration test.

Table A1.5 in Appendix 1 shows the direct load cell measurements and calculated tendon tensions obtained for each tendon condition relevant to each group of vibration tests. Tension TF on the single free tendon segment for 0A and 0B, or TH on the horizontal segment for 13A and 13B, was calculated by addition of the four North Block horizontal reactions. Tension on the sloping tendon segment of 13A and 13B was calculated by first subtracting the sum of the deviation block horizontal reactions from the horizontal segment tension TH, thus obtaining the horizontal force TBH acting on the North end of the deviation block. The vertical force TBV acting on the deviation block was then computed by adding the four Deviation Block Vertical Reactions to a nominal block weight of 24,465 N (5,500 lb).

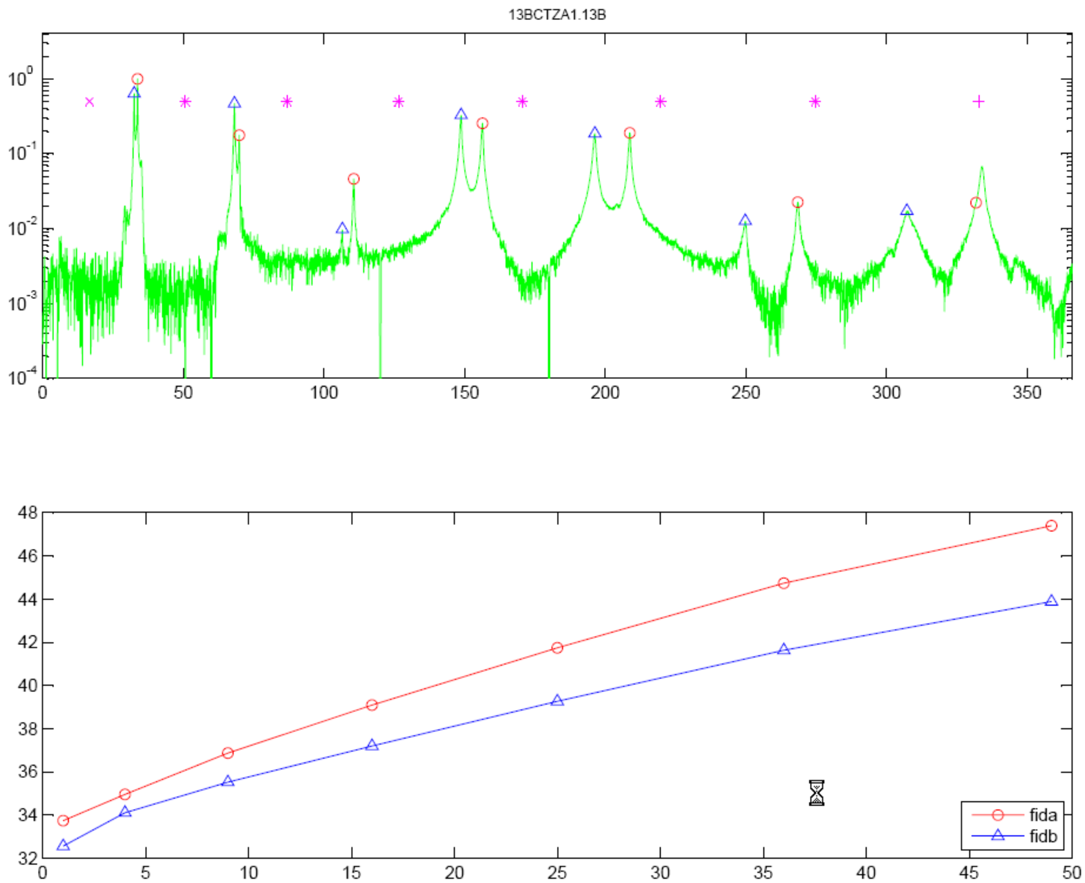

Figure 1.8 - Top: Vibration spectral response obtained in a typical case (13BCTZA for tendon 13B, tested after strand Cut 2; Tables A1.1 and A1.2 Appendix 1). For clarity of display, a logarithmic scale was used for the amplitude axis. The automatically identified peaks are highlighted with triangles (low frequency component of doubled) and circles (high). Bottom: Peaks of both the high and low frequency sequences represented using an f/n vs. n^2 graph (Sagüés et al 2006).

Both horizontal and vertical components were then added by Pythagorean combination to obtain a calculated Sloping Segment Tension TS, which was used in subsequent comparisons with the results from vibration measurements of that segment. The force at the load cell in the South Block anchor was not used for calculating the free tendon segment force in the after-grouting condition as then the South reaction includes the effect of force transfer between strands and block through hardened grout. However, in the pre- or fluid-grout condition the South block reaction TSB provides a direct reading of the force on the tendon segment in 0A and 0B (or of the sloping tendon segment in 13A and 13B) with minimal friction error. Ideally, in that condition for 0A and 0B the tendon force TF calculated as above from the North Block reactions should match the value of TSB. Likewise, for 13A and 13B the calculated value of TS should match TSB.

The extent to which that balance existed was computed as a percentage with Table A1.5 headings listed as "SB Anchor-Free"=100*(TSB-TF)/TSB or "SB Anchor-Sloping" =100*(TSB-TS)/TSB for 0A,0B and 13A,13B respectively. Those values are listed in bold italics for the fluid grouting condition. For illustration, the balance was computed also for the post-grouting conditions but listed in plain font.

Additional checks on the suitability of the estimation of tension in the sloping segment of 13A and 13B were made by comparing TBH with the horizontal component of TS by means of the percentage 100*(TBH-TS*cos α)/TBH, and by the percentage 100*(TBV-TS* sin α)/TBV for the vertical component. These balances, listed as "Horizontal" and "Vertical" respectively in Table A1.5, measure the consistency between the Pythagorean approach used to compute TS and an alternative trigonometric calculation that would rely on the known tendon slope (12.5 deg, Table 1.1) instead.

1.3.2 Lateral Deflection tests

Results for deflection tests are listed in Tables A1.3 and A1.4 of Appendix 1.

1.3.3 Tendon cross sections

Figures 1.9 to 1.14 show cross sections of each of the tendons near the S and N ends of each tendon segment.

Figure 1.9 - Tendon 0A. L: Near S end. R: Near N end. PVC pipe outline visible at S end. Mark denotes top of tendon. in this and subsequent pictures.

Figure 1.10 - Tendon 0B. L: Near S end. R: Near N end. Outlines of disbonding foam visible on two strands at S end.

Figure 1.11 - Tendon 13A, Sloping Section. L: Near S end. R: Near N end.

Figure 1.12 - Tendon 13 A, Horizontal Section. L: Near S end; R: Near N end.

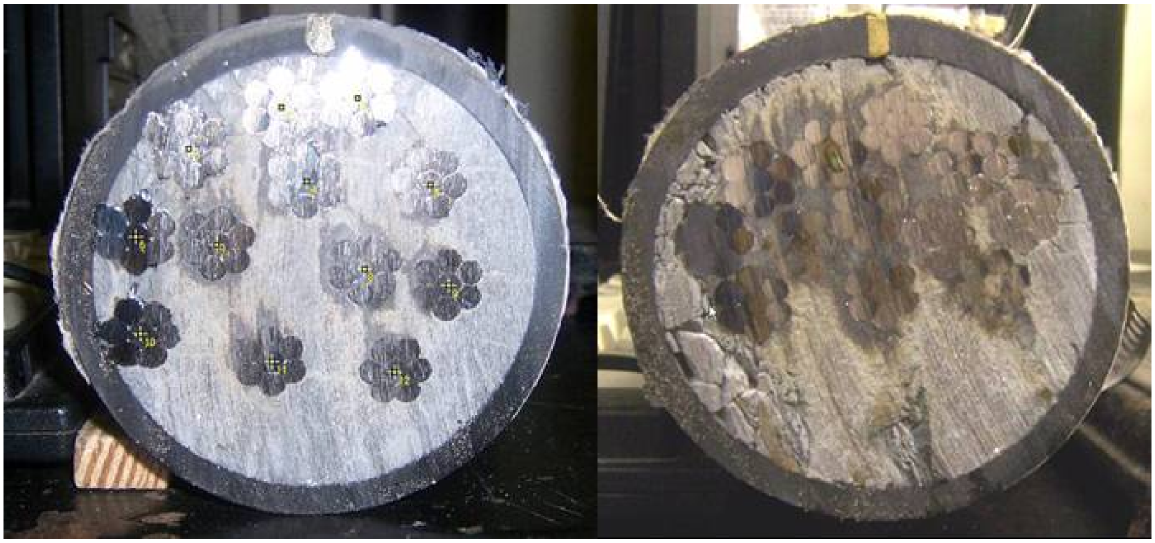

Figure 1.13 - Tendon 13B, Sloping Section. L: Near S end. R: Near N end.

Figure 1.14 - Tendon 13 B, Horizontal Section. L: Near S end; R: Near N end

1.4 Correlations and Findings

1.4.1 Load cell force determination

The results listed in Table A1.5 for the (fluid) grouting condition of Tendons 0A and 0B showed very small (-0.8%) to moderate (-1.6%) difference of readings of the load cell at the South Block minus the sum of those of the four North Block cells (SB Anchor-Free listing). Since the North Block did not rest on any supports under that condition and the grout was still fluid, frictional forces should have played no important role. Thus, in that condition the calculated imbalances are expected to reflect the intrinsic uncertainty in load cell force determinations by the methods and equipment used.

The values listed in Table A1.5 for the "SB Anchor-Sloping" balance in the (fluid) grouting condition of Tendons 13A and 13B show appreciably greater disparities (2.5% for 13A, -6.1% for 13B) than for the comparable listing in the straight tendons. The greater disparity likely reflects a combination of several factors. These include the presence of horizontal frictional forces at the Teflon™ bearing pads at the Deviation Block vertical reaction load cells, and of bending moment at the strands in the sloping tendon segment. Additionally, at least for the case of 13B, there is the possibility of malfunction of one of the horizontal Deviation Block reaction gages (DB NW) as manifested by a moderate negative reaction (indicative of tension, not possible in that configuration) during tensioning and grouting as listed in Table A1.5. Examination of that load cell records showed a maximum negative reaction of 10.8 kN suggesting that the error was at least by that amount. Adjusting the DB NW load cell readings by that amount would reduce the 13B SB Anchor-Sloping disparity during grouting to 5.4 %. These observations suggest that the values of TS listed for the sloping portion of Tendon 13 in Table A1.5 for the grouting and subsequent conditions should be considered as an upper bound, with actual values likely being a few percent lower than indicated there.

The Horizontal force balance entry in Table A1.5 for 13A and 13 B indicates good agreement (better than 1%) between the projection (assuming a 12.5^{o} slope angle) of the sloping tendon force calculated using Pythagorean composition, and the horizontal force calculated from the horizontal reactions on the South side of the block. That result is not surprising given the low value of the slope angle and corresponding high cosine value. Agreement for the Vertical balance is only modest (~5%) to poor (~18%) for 13A and 13B respectively, suggesting the presence of some bending moment in the strand or less than ideal alignment of the tendon. That discrepancy by itself however is of secondary concern to the accuracy of sloping segment force determination, given the shallow angle involved and the consequent sensitivity of the balance to minor variability in the value of the angle.

1.4.2 Vibration force determination and ability to detect tendon distress.

Figures 1.15 to 1.17 summarize the findings relevant to validation of the vibrational test method and its ability to detect tendon distress. Each figure contrasts the tendon force estimated from vibration data (T_e, vertical axis) with force determined from load cell measurements (T_{LC}, horizontal axis) for the system in its initial condition, and after the first and second strand cuts. For simplicity, only the average values for each condition are shown. The top part of each figure shows the Te results as calculated, while the lower part shows the T_{IMPR} values corrected for pipe end effect as detailed further below. The thick solid 45^o line denotes the locus that the data would have occupied under ideal agreement between both vibrational and load cell determinations. The thin solid lines and dashed lines delimit bands containing cases of ideal deviations of <1%, <5% and <10% respectively between both determinations, with deviation defined as

% deviation = 100 (Te [or T_{IMPR}] - T_{LC})/ [(Te [or T_{IMPR}]+T_{LC})/2] (Eq. 1.5)

Without any correction for pipe end effects, 18 out of 22 averages (the exceptions being those for the horizontal segment of 13A) fell within the 10% agreement bounds. All the 14 averages for 0A, 0B and 13B fell within an ~6% band of deviation from the load cell readings with, 11 within ~4% and 3 within ~1%.

As shown in Table 1.1, both the horizontal and the sloping sections of Tendon 13A had the longest galvanized end pipe lengths relative to the free length (largest Lp/Lo ratios 0.077 and 0.051 respectively) of the group tested. Thus, the observation of the greatest deviation (and in the excess direction) of Te with respect to T_{LC} in those cases was not surprising. Pipe-end correction factors were therefore calculated using Eqs. 1.1 to 1.4 based on the approach described earlier. The equations used the average Sme from the group of vibration measurements for the tendon condition that had produced the Te value to be corrected, with one global correction for each tendon condition. Calculations were based on estimating Sp= Spp+βSme also as indicated earlier. The pipe stiffness Spp was assigned a nominal value Spp=200 kN-m^2 (69.7 klbf-in^2) based on the pipe cross sectional dimensions (7.62 10^{-2} m (3 in) ID, 4.76 10^{-3} m (3/16 in) wall thickness) and a nominal value of the elastic modulus of medium-carbon steel (E=2 10^{11} Pa (29.01 10^7 psi)). The set of k factors thus obtained with β=1 resulted, as anticipated earlier, in significant overcorrection so that most of the corrected values of Te fell markedly below the 1:1 line. Ranging calculations showed that the value β=0.25 yielded tentatively corrected values of Te that fell within the 5% bounds for most of the test conditions examined. The results for that choice are given for comparison with the uncorrected data in the lower part of Figures 1.15 to 1.17.

For tendons 0A and 0B, which combined low Lp/L ratios (0.026) with low non-dimensional stiffness, the uncorrected tension values from vibration measurement were close to or lower (notably in the case of 0B, by ~6% consistently before and after strand cuts) than the load cell tension values. Agreement between both load cell and vibration tension determinations did not improve upon pipe end correction even with the small value of α used, suggesting that the vibration determination may have already have underestimated tension by some small percentage. A portion of that shortage may be ascribed to intrinsic uncertainty in the load cell values. The load cell values used to compare with the vibration estimates are obtained from the North Block cells, which in the case of 0B where found to be 1.6% below the value given by the South Block cell during the fluid stage of grouting. If the South Block cell was the more accurate, then the ~ 6% 0B difference between the load cell and uncorrected vibration results would have been reduced accordingly.

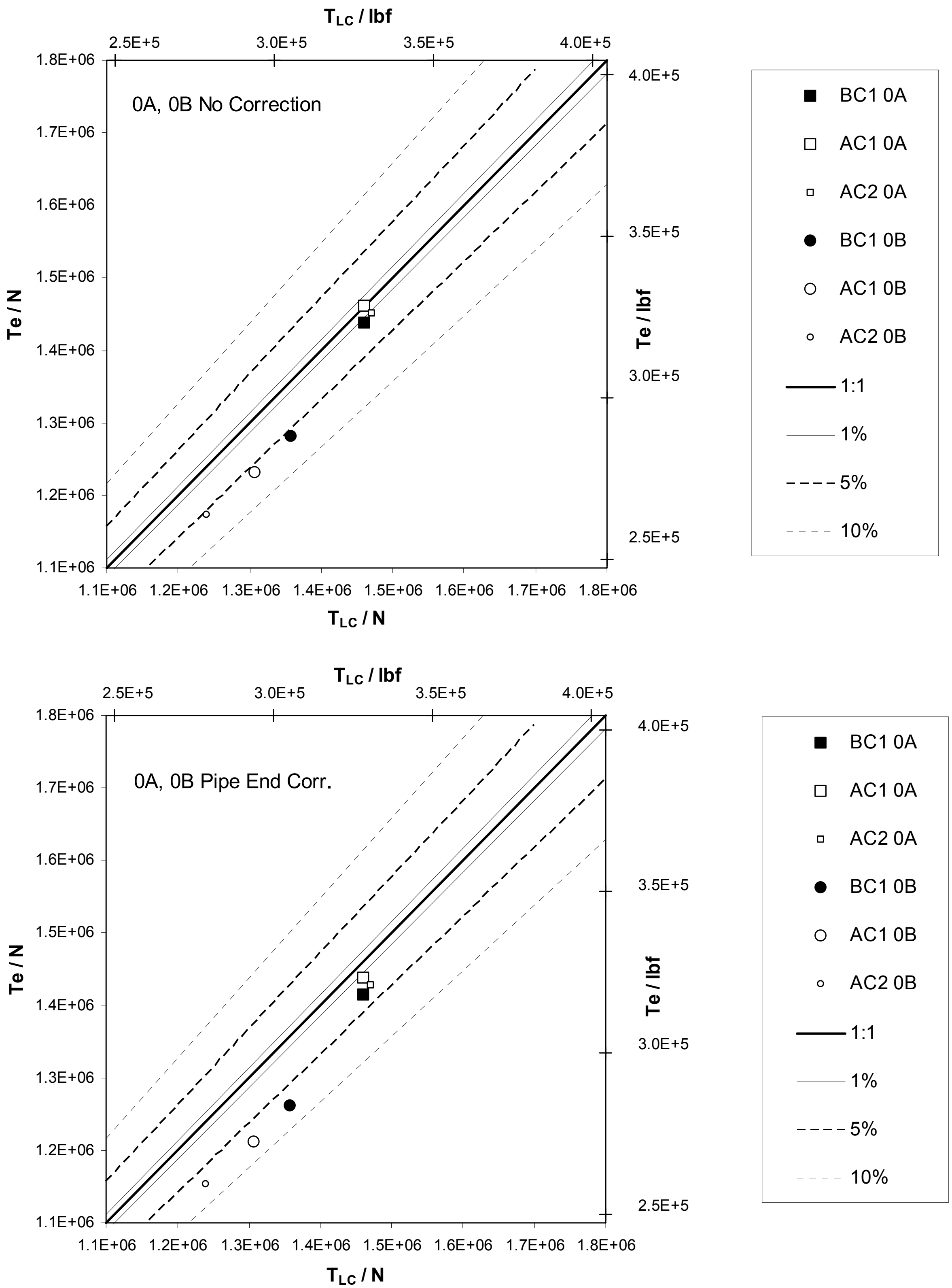

Figure 1.15 - Summary of results of tendons 0A (circles) and 0B (squares).
BC1: Before Cut 1. AC1,2: After Cut 1,2. The diagonal line represents ideal 1:1 match; the other lines represent deviations by the indicated percent. Top: Te values not corrected for pipe end effects. Bottom: Tentative pipe end correction with α=0.25 as explained in text.

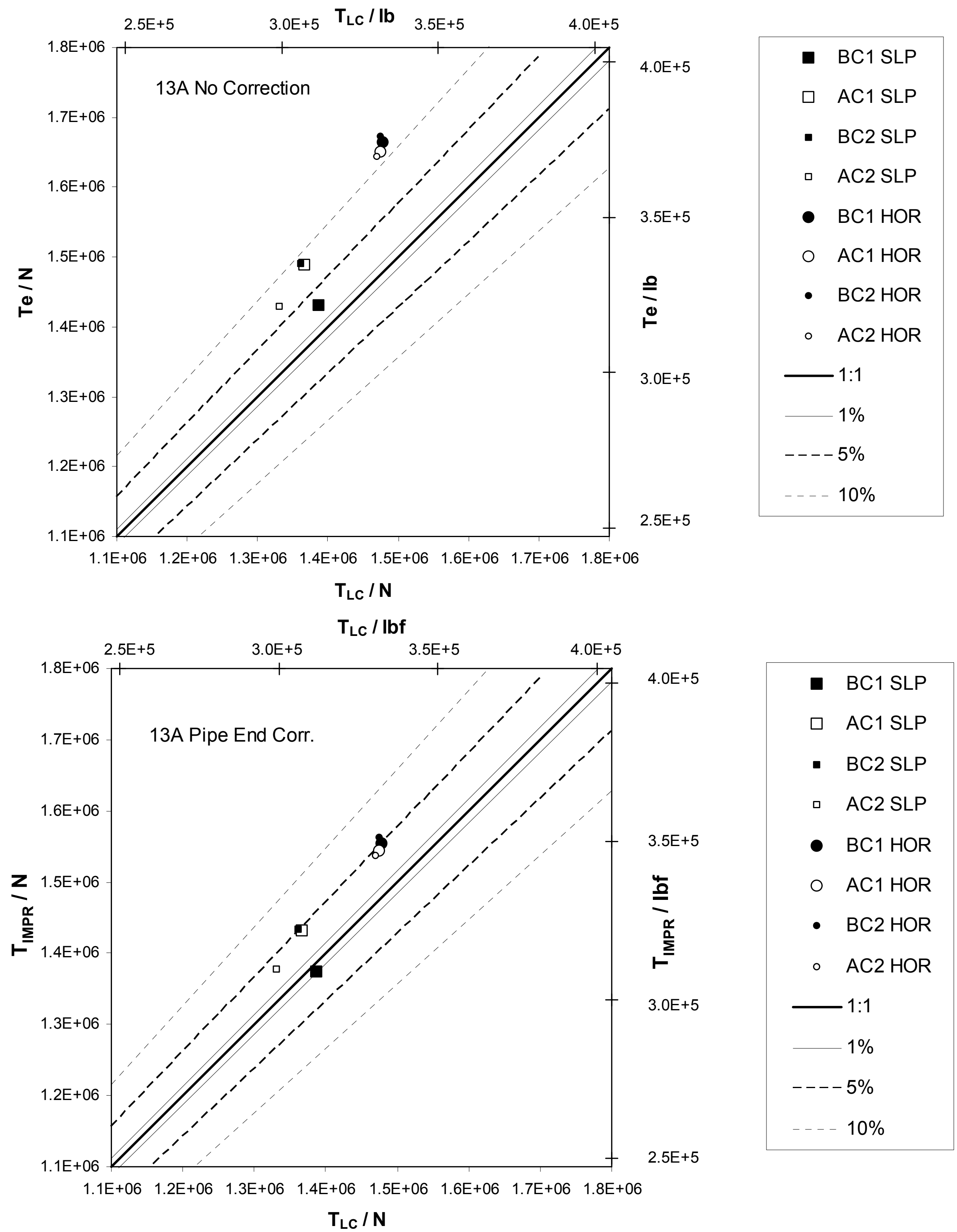

Figure 1.16 - Summary of results of tendon 13A. See Fig. 1.16 caption for explanation of symbols and conditions represented.

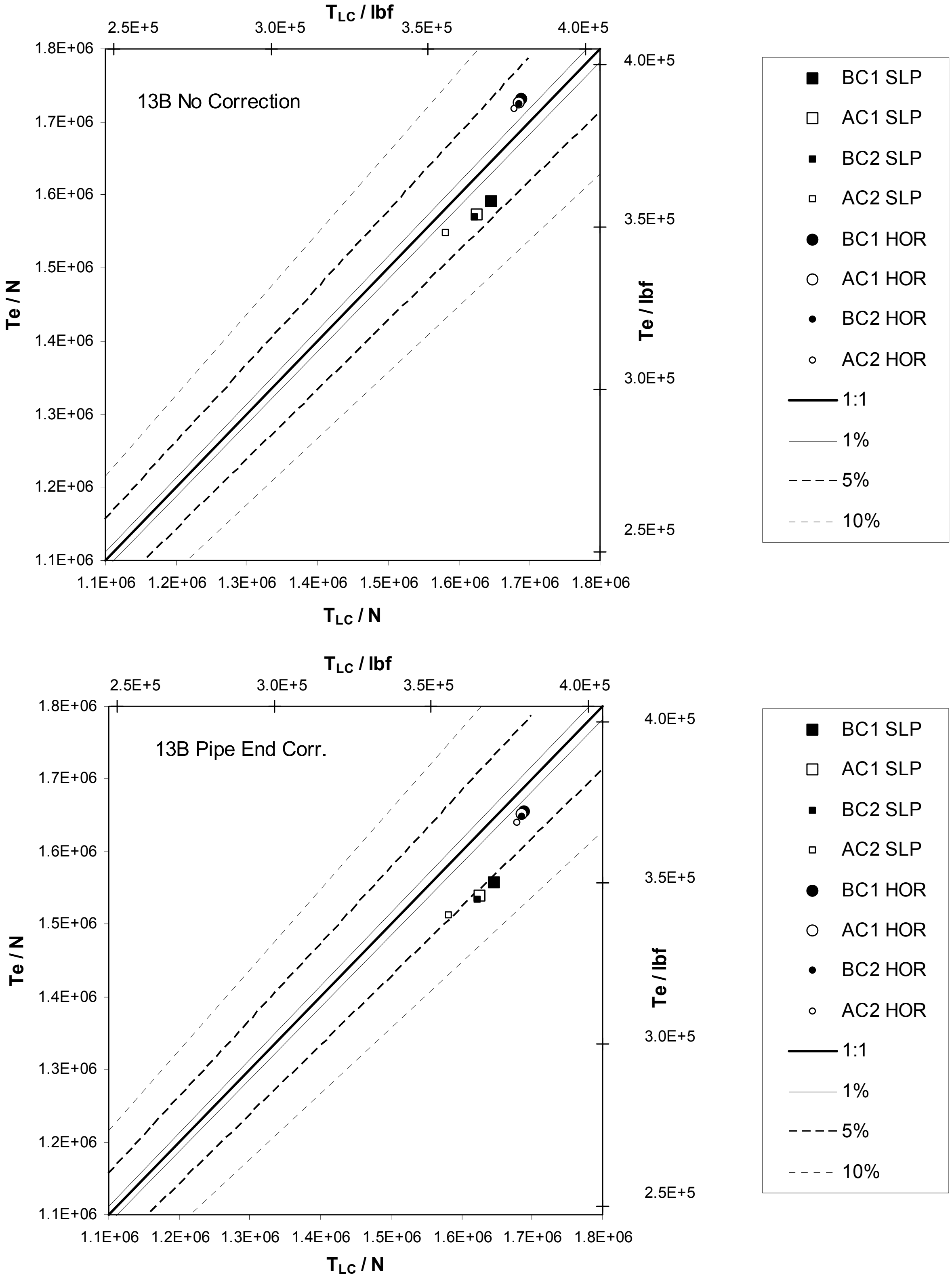

Figure 1.17 - Summary of results of tendon 13B. See Fig. 1.16 caption for explanation of symbols and conditions represented..

The remaining offset in 0B and comparable cases may be the result of less than ideal end fixity instead of the fully clamped condition assumed in the vibration calculations. The reduced fixity would stem from the same cause considered earlier for the pipe end case, namely compliant elastic coupling between the stiff strand bundle and the embedded part of the metal duct, due to the much lower elastic modulus of the grout (Mirza et al 2002) in the annulus surrounding the strand steel, compared to the steel modulus. In the absence of protruding metal pipe, such effect would lower somewhat the frequencies of the vibration modes and the corresponding tension estimate, respective to a fully clamped tendon. A protruding metal pipe would act in the opposite direction, as discussed earlier. Thus it is likely that for small Lp/L ratios and moderate nondimensional stiffness cases both effects may approximately compensate each other, and correcting for pipe end effects is not warranted. Consequently, correction for pipe end effects would appear to be productive only for cases with relatively large Lp/L values (e.g. >0.05) as in both the horizontal and sloping segments of 13A, and the horizontal segment of 13B. It is further noted that the correction parameter values used for 0A and 0B were developed for tensions computed with modes 2 to 4 only, while the tensions for these tendons were calculated with up seven modes. However, given the relatively small amount of correction involved for these tendons the above conclusions are expected to remain generally adequate.

Figures 1.15 to 1.17 show also that cuts in strands intentionally disbonded from the grout in the anchorage area (and sometimes beyond) resulted in instances of distinct tension reduction manifested by load cell measurements, and paralleled in most cases by the vibration tension estimates. The cumulative % relaxation of tendon segment forces following each strand cut is displayed in Table 1.7. In tendon 0A the strands that were cut had been placed in PVC pipes that, unlike what was originally intended, still allowed effective grout ingress. Thus there was little bond degradation, and when the strands were cut the transfer of force from the cut strands to the rest of the system was quite efficient. That was evidenced by post-cut forces that were not smaller than those before the cuts. The post-cut values evaluated from the vibration tests were actually modestly higher (~1.5%) than before, but the difference was well within the range of uncertainty noted earlier. The strand cuts in the other tendons, which had significant disbondment between the cut strand and the grout, did result in appreciable decrease in tendon force in the tendon segment adjacent to the South block. The decrease in most cases was comparable in magnitude when measured by both the load cell and vibration tests, as it is clearly visible in Figure 1.15 for Tendon 0B and the corresponding numeric data in Table 1.7.

A notable exception was the case of the first cut of the strands in the sloping segment of Tendon 13A. For that case there was a marked 4.2% increase in the value of the segment tension as evaluated from the vibration measurements, while the load cell determinations indicated, as expected, a decrease (1.5%). Careful examination of the individual cases in the corresponding data set failed to reveal any data identification or processing artifacts, and direct examination of the spectral data confirms qualitatively that a vibration frequency increase consistent with the computed change took place. The anomaly was not repeated in the subsequent strand cut in the same tendon segment. There differential tension changes took place in the expected direction and by roughly comparable amounts when evaluated by both load cell and vibration determinations.

Table 1.7 - Tension degradation resulting from strand cuts, from average values used for Figures 2.2-2.4.

Tendon	After Cut No.	Cumulative % Reduction in Tension from Condition Before First Cut			
		Sloping Segment (13A, 13B) Single Segment (0A, 0B)		Horizontal Segment (13A, 13B)	
		Per Vibration Test	Per Load Cells	Per Vibration Test	Per Load Cells
0A	1	-1.7	0.0		
	2	-1.0	-0.7		
0B	1	3.9	3.8		
	2	8.5	8.8		
13A	1*	-4.2	1.5	0.7	0.2
	2	-0.2	4.0	1.1	0.6
13B	1*	1.1	1.3	0.2	0.2
	2	2.8	3.9	0.9	0.6

*Condition just before Cut No. 2. Negative values indicate an increase.

The causes for the initial discrepancy in 13A are not clear, but may be related to less than optimal rigidity in the placement of the deviation block of both deviated tendons 13A and 13B. In those tendons, but especially for 13A, the fundamental vibration mode of the sloping tendon showed a strongly separated doublet indicative of coupling with lateral motion of the deviation block, possibly aggravated by uneven seating against the block reaction points. The block was temporarily braced to minimize those effects, and vibration analysis was limited to modes 2-4 to minimize spurious indications from near-mode 1 resonances. However, residual artifacts might have remained in the before-cut-1 condition, that were reduced upon strand cut and subsequent more rigid seating against the reaction points. Another possible factor may have been improved rigidity at the tendon end after the first strand cut, with the cut strand setting more firmly against crushed grout and insulation. However, it is noted that similar effects could have taken place at tendon 0B, which did not exhibit anomalous behavior.

The combined results from vibration and load cell tests show that in the tendons with deviation blocks the cut-induced decrease in tension of the horizontal segment (separated from the South block by the deviation block) was typically smaller than in the sloping segment. This is to be expected since substantial force transfer should have occurred between strands and grout in the pipe embedded in the deviation block, and it rested against fixed reaction points. The decrease in horizontal segment force as measured by the vibration tests (about 3%) was roughly twice that calculated from the load cell measurements, but this difference is of limited significance as it approaches the range of relative uncertainty in the vibration measurements noted above.

1.4.3 Origin of double peaks

Prior to this investigation it was hypothesized (Sagüés 2006) that the double peaks in the frequency spectrum were due to non uniform strand arrangement within the tendon cross section. As indicated in Sagüés 2006, the strands tend to crowd against the inside curvature of the tendon path as it is altered at end span and deviation blocks. A strand arrangement such as that shown schematically in Figure. 1.18 then occurs along much of the length of the external tendon segment. As the steel strands contribute the most to the composite flexural stiffness, their nonisotropic distribution provides greater flexure stiffness in the horizontal than in the vertical direction. Thus different sets of vibration frequencies may be expected for vibration deflection along those two directions, with individual frequencies reflecting the corresponding differences in flexural stiffness. Unless the impact and measured response directions are along the same principal axis of the cross section, both modes would be excited simultaneously and reflected in the measured response as corresponding to the same tension, but with different stiffness.

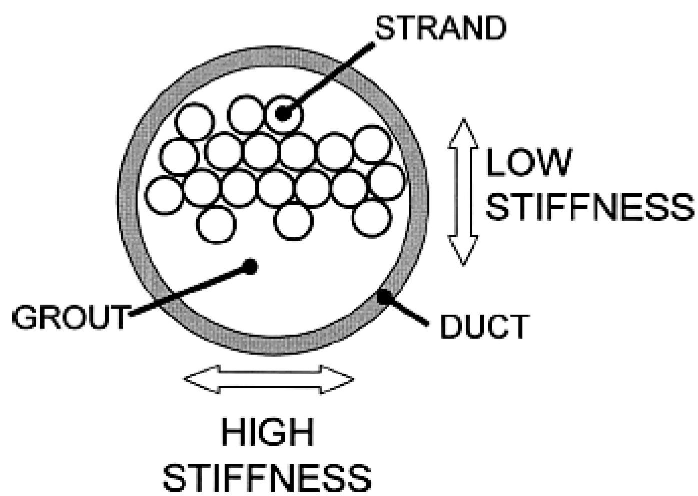

Figure 1.18 - Likely cause for the appearance of vibration frequency doublets (from Sagüés et al 2006, paper produced under this project).

The tendon cross sections shown in Figures 1.9 to 1.14 conformed in most cases to the schematic arrangement in Figure 1.18. This was notably so in the N end of the sloping section, and the S end of the horizontal section (that is, on either side of the deviation block) in 13B, and in the S end of the horizontal section in 13A. The N end of the sloping section in 13A did not show much preferential crowding toward the top, possibly because of a particular alignment of the the metal duct in that section. There was some crowding of strands to one side of the section of the N end of 0A, consistent with observation at the time of slight sideways misalignment of the N block when tensioning that tendon.

A simplified quantitative test of the above hypothesis on cause of dual peaks was made by computing the relative difference in principal moments of inertia of each of the strand arrangements in Figures 1.9 to 1.14, and comparing those with the relative differences in tendon stiffness calculated from the vibration tests in each of those tendon segments. To that end, the coordinates of the centroid of each strand cross section were first determined manually by clicking on a digitized version of each picture. The nominal second order moments I_X and I_Y of the array of points were then calculated with respect to the X and Y axes respectively, as well as the central moment I_{XY}. The principal moments I_1 and I_2 were then obtained by

$$I_1 = (I_X+I_Y)/^2 + \{ [(I_X-I_Y)/2]^2 + I_{XY}^2\}^{1/2} \qquad \text{(Eq. 1.6)}$$

$$I_2 = (I_X+I_Y)/^2 - \{ [(I_X-I_Y)/2]^2 + I_{XY}^2\}^{1/2} \qquad \text{(Eq. 1.7)}$$

A moment asymmetry factor Fm indicative of how much the principal moments differed from each other was then computed by

$$Fm = |(I_1-I_2)/ [(I_1+I_2)/2]| \qquad \text{(Eq. 1.8)}$$

It is noted that Fm is a relative dimensionless measurement, independent of the scale used in the picture of the tendon cross section. The values of Fm computed for each tendon segment end are listed in Table 1.8.

Table 1.8 - Moment and Stiffness (Approximate) Asymmetry Factors

Tendon Segment	Fs	Fm (S end)	Fm (N end)	Fm average
0A	0.49	0.16	0.69	0.42
0B	0.09	0.01	0.25	0.13
13A (Sloping)	0.28	0.29	1.03	0.66
13A (Horiz.)	0.63	1.04	0.82	0.92
13B (Sloping)	0.02	0.04	0.36	0.20
13B (Horiz)	0.06	0.33	0.06	0.19

Similarly, a stiffness asymmetry factor Fs was defined to measure how much the tendon stiffness evaluated from the HF and LF doublet components in the vibration evaluation of a tendon differed from each other:

$Fs = | (S_{HF}-S_{LF})/ [(S_{HF}+S_{LF})/2] |$ (Eq. 1.9)

As Fm, Fs is also a relative dimensionless magnitude. The values of Fs were computed for each tendon segment, for the condition before the first strand cut, using the stiffness data in Table A2.1 . There is significant dispersion in the values of S_{HF} and S_{LF}, in some cases with clear overlap of their respective ranges and consequent uncertainty in the value to be assigned to each. The uncertainty becomes especially important when the two values are close to each other. Thus, a formal device was implemented to assign values to S_{HF} and S_{LF}, consisting in plotting a cumulative distribution of the entire set of S_{HF} and S_{LF} values for a given tendon segment, and visually identifying a breakpoint in the distribution. The average of values below and above the breakpoint (after clearing any grossly evident outlier) was assigned to S_{HF} and S_{LF} respectively. The resulting approximate values of Fs are listed in Table 1.8.

If a tendon segment would have uniform constitution and strand arrangement through its entire external length, then Fs would be the same as the comparable ratio of the effective tendon stiffnesses aligned with the principal axes of the cross section. Those stiffnesses are expected to be approximately proportional to the corresponding I1 and I_2 values since the steel strands are main contributors the tendon flexural stiffness, so on first approximation it would be expected that Fm ~ Fs.

As it can be seen from the tendon cross sections in Figures 1.9 to 1.14 , the strand arrangement is not uniform along the tendon free length so the effect of stiffness asymmetry on the vibration spectrum is likely to be a convolution of the local dominant configurations as they vary along the tendon. For the purposes of comparison with Fs, that convolution may be roughly approximated by averaging the values of Fm for each end of the external segment.

The Fm values in Table 1.8 range from very small for the evenly distributed strand patterns e.g. the S ends of 0B and 13B, to near 1:2 asymmetry as in most sections of 13A. The values of Fs span a comparable range, and generally follow the pattern of the Fm average values. This is shown in the cross-plot in Figure 1.19, where the three tendon segment with low vibrational stiffness asymmetry also have low values of average moment asymmetry, while the three high value vibrational stiffness cases have comparably high moment asymmetry. Moreover, the Fm - Fs pairs on the whole did not deviate dramatically from an ideal 1:1 relationship (dashed line), confirming the above expectation that Fm ~ Fs. These observations, while reflecting only approximate values, are quantitatively supportive of the initial hypothesis that dual peaks stem largely from asymmetric distribution of strands in the tendon cross section.

1.4.4 Lateral Deflection Tests

The results of the tests are given in Table A1.3 as δ = lateral deflection per applied lateral force. The theoretical relationship between lateral force and deflection for a uniform stressed stiff beam of non-dimensional stiffness σ and length L is can be easily adapted from solutions listed in standard handbooks (Young 1989). Numerical evaluation of that relationship readily shows that for forces and deflections taking place

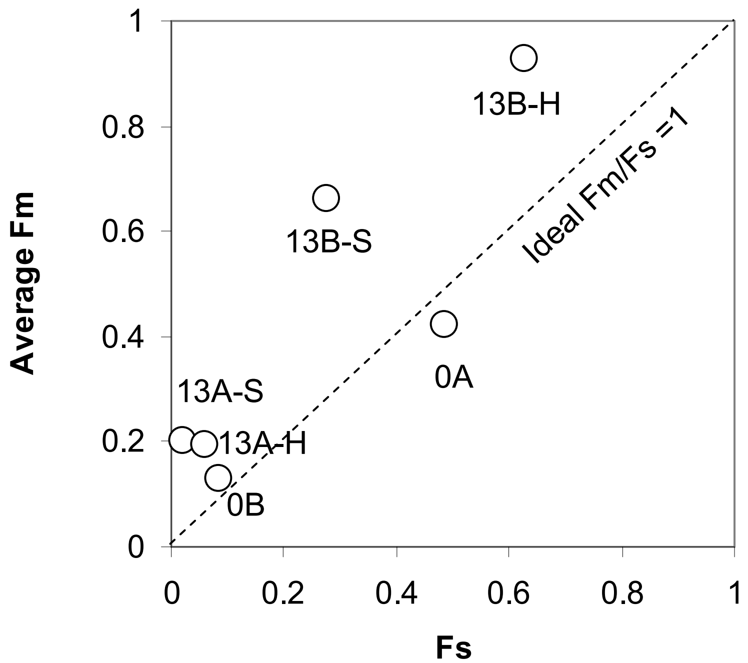

Figure 1.19 - Correlation between asymmetry of moments of inertia of strands in tendon cross sections (average of both ends of the tendon segment) and asymmetry of HF and LF stiffness as approximately determined from vibration tests.

at the exact center of the beam and small values of σ (e.g. $\sigma < \sim 0.1$) the value of the tension is well approximated by

$$T = \delta^{-1} L \, (1/4 - \sigma^{1/2}) \qquad \text{(Eq. 1.10)}$$

which for $\sigma=0$ reduces, as expected, to the formula for the lateral deflection of an ideal elastic string on a rigid bow.

As it will be shown in the Task 2 section Item 2.2, the vibration test yields an estimated value of the nondimensional stiffness, σ_e, without needing knowledge of the tendon linear mass m. If the value of m is not known or subject to large uncertainty, but accurate lateral deflection data for the tendon center are available instead to give δ, then an estimate T_D of the tendon tension can be obtained using the value σ_e from the vibration test and Eq. 1.10 [A] , without need of knowing m beforehand. Indeed, once T_D is obtained a value of m (designated as m_D) can be determined from the value of R_{avm} that is obtained simultaneously with σ_e during the data analysis procedure, by rewriting Eq. (2.12) (see subsequent Item 2.2) as:

$$m_D = T_D R_{avm}^{-2} L^{-2} \qquad \text{(Eq. 1.11)}$$

Table 1.9 shows the result of applying the above concepts to the deflection tests listed in Table A1.3 performed in the straight tendons 0A and 0B in the "Before Cut 1" condition[B]. The data from the individual deflection tests was used in conjunction with the average results for σ_e and R_{avm} from the analyzed set of vibration tests closest to the time of the deflection test. For Tendon 0A that set corresponded to Test Serial Numbers) 0A100-117 and -118 to -135; for 0B 0B0100-124, 125-148 and 149-170. The corresponding tensions determined from load cell readings (T_{LC}) and tensions estimated from vibration tests in the usual manner (Te) as listed in Table A1.2 were averaged for each test group and used for comparison with the values. The value of m from direct mass measurement, from Table 1.4, is also used for comparison.

Comparison with independently determined values is expressed as exemplified by $\%(T_{LC}\text{-}T_D)= 100\ (T_{LC}\text{-}T_D) / [(T_{LC}+T_D)/2]$, so the value listed is the difference as a percentage of the average of the values being compared.

The results show excellent agreement (deviation always <= 2.3 %, average absolute deviation 0.9%) between tension determined by the usual vibration procedure using a known value of m, and the tension determined solely by deflection and vibration tests. Equally good agreement was found between the value of linear mass recovered from combined deflection and vibration tests, and the linear mass independently determined.

Agreement between tensions determined solely by deflection-vibration tests or load cell measurements was also very good for the 0A tendon (deviation <= 2.6%, average absolute deviation 1.5%). For 0B the deviation was <=5.4% and the absolute average deviation was ~5%, replicating the significant bias with respect to the load cell measurements noted earlier for this tendon when discussing the conventional vibration test analysis. Such bias remains unexplained, but the remarkable agreement between T_D and Te indicates that the bias is not due to using an inaccurate value of m in the conventional vibration analysis. Detailed analysis of load cell data will continue in the future to glean possible load cell calibration issues that may have resulted in the observed offset for this tendon. Future work will also address the tendon end fixity condition mentioned earlier as a possible contributor to the observed discrepancy, as well as further examination of the possible effect of extended disbonded strands in this tendon in lowering the frequency of the relevant vibration modes.

[A] Appropriately subscripted as $T_D = \delta^{-1} L\ (1/4 - \sigma_e^{1/2})$

[B] The results from test DOB003 were not used as the force-displacement diagram for that test showed pronounced hysteresis and slope grossly different from peer tests, indicative of malfunction.

Table 1.9 - Results of combined deflection-vibration tests and comparison with independent determinations.

Tendon	Test Serial Number	Orientation	δ µm/N (µin/lbf)	Avg. σ_e	T_D MN (Mlbf)	Avg. T_{LC} MN (Mlbf)	$\%(T_{LC}-T_D)$	Avg. Te MN (Mlbf)	$\%(Te-T_D)$	Avg. R_{avm} Hz	m_D kg-m^{-1} (lb-in^{-1})	m kg-m^{-1} (lb-in^{-1})	$\%(m-m_D)$
0A	D0A 001	V	1.456 (255.0)	7.322 E-4	1.427 (320.9)	1.465 (329.3)	2.6	1.437 (323.0)	0.6	30.77	17.36 (0.972)	17.46 (0.978)	0.6
	D0A 002	V	1.443 (252.8)		1.440 (323.7)		1.7		-0.2		17.51 (0.980)		-0.3
	D0A 003	H	1.437 (251.7)		1.446 (325.1)		1.3		-0.7		17.58 (0.985)		-0.7
	D0A 004	V	1.414 (247.7)		1.470 (330.4)		-0.4		-2.3		17.87 (1.001)		-2.3
	D0A 005	H	1.456 (254.9)		1.428 (321.0)		2.5		0.6		17.36 (0.972)		0.6
	D0A 006	A	1.429 (250.2)		1.455 (327.1)		0.7		-1.3		17.69 (0.991)		-1.3
0B	D0B 001	V	1.581 (276.8)	9.505 E-4	1.287 (289.3)	1.358 (305.4)	5.4	1.277 (287.0)	-0.8	29.42	17.27 (0.967)	17.13 (0.959)	-0.8
	D0B 002	H	1.587 (277.9)		1.281 (288.1)		5.8		-0.4		17.19 (0.963)		-0.3
	D0B 004	V	1.581 (276.8)		1.287 (289.2)		5.4		-0.8		17.26 (0.967)		-0.7
	D0B 005	H	1.580 (276.6)		1.287 (289.4)		5.4		-0.8		17.27 (0.967)		-0.8
	D0B 006	A	1.572 (275.3)		1.294 (290.8)		4.9		-1.3		17.35 (0.972)		-1.3

T_D: tension determined solely from combined deflection-vibration tests with no information on tendon linear mass i.e. from values of δ per Eq. 1.10.
T_{LC}: tension determined solely from load cell readings.
Te: tension determined from vibration tests and previously known value of tendon linear mass (m) i.e. using σ_e , R_{avm}, m and L per procedure described in Section 2. Not corrected for pipe end effects.
R_{avm}: Average R parameter value obtained solely from vibration spectrum analysis and value of L.
m: value of tendon linear mass determined by direct weighing and elasticity corrections as listed in Table 1.4.
m_D: tendon linear mass obtained solely from combined deflection-vibration tests e.g. from values of T_D, R_{avm} and L per Eq. 1.11.
%(*x*-*y*): difference between values of *x* and *y* as a percentage of their average.

It is noted that in the above analysis an average value of σ for both doublet peak modes was used for the calculations. The result was not highly sensitive to the presence of doublets in part because for tendons 0A and 0B the non dimensional stiffness was of moderate value ($<10^{-3}$, not unlike values encountered in bridge tests(Sagüés et al 2000,2003a, 2003b,)), so the correction with respect to the no-stiffness case was only in the order of ~10%. Moreover, the correction varies only with the square root of the stiffness, so even differences in effective moment of inertia for principal axes of as much as 2:1 would affect the final result by not much more than about 2%.

The results, especially those demonstrating successful recovery of linear mass values, are highly encouraging of the use of deflection measurements to resolve uncertainty in the value of m when, for example, the density of grout may have varied significantly from design values. Such situation was encountered during vibration tests of the vertical tendons in columns of the Sunshine Skyway Bridge (Sagüés et al 2004b) where an effective global grout density value of only 1,650 Kg/m^3 (0.0596 lb in^{-3}) (as opposed to values ~10% greater in most other bridges evaluated to date) was adopted due to indications of unusually high expansion of grout during curing. The value was inferred from a small number of samples extracted from autopsied tendons but may not have been representative of the bulk of the tendons tested. Static deflection tests performed in selected tendons could have assisted in significantly reducing uncertainty in assumed value of m and improved accuracy accordingly.

Static deflection tests, as implemented here, were much more time consuming than vibration tests (e.g. 30 minutes vs less than 1 minute). Furthermore, in a field situation traffic induced vibrations can introduce added scatter in the individual data and consequently greater uncertainty in the value of δ. However, the test procedure and instrumentation could be optimized substantially for speed and automatic operation, including cancellation of vibration related noise effects.

Under proper optimization, static deflection tests could have the potential for replacing vibration tests if a suitable database is available relating tendon properties (number and size of strands, duct diameter, type of grout) to dimensional tendon stiffness S. In such case, having obtained δ and solving the system of Eqs. 1.10 and 2.13 (see next Section) yields the tension T. Alternatively, a limited number of vibration tests could be conducted to obtain representative S values for the structure of interest. It is noted that the use of approximate S values is already part of the basis of the simplified testing procedure introduced in the Task 3 section of this report.

With the present vibration testing approach, even without further optimization static deflection tests would be worthwhile conducting, in a typical bridge evaluation, on a small percentage (e.g. 1%) of the evaluated tendons to confirm that the value of m used for the calculations is reasonably accurate.

1.5 Task 1 Conclusions

1. The ability of the vibration test to obtain estimates of tendon tension was validated with six independent external tendon segments of size, length, and tension levels comparable to those used in actual structures. For tendons with relatively short end metal pipes at the points were the tendon emerged from the concrete, deviation between tension estimated from vibration tests (average of multiple measurements) and independent load cell measurements ranged from less than 1% to approximately 6%.

2. An algorithm was developed and applied to numerically correct force estimates from vibration tests for the effect of metal pipe segments at the tendon ends. The method was found to best apply to cases with total pipe lengths to tendon length ratio above 0.05. Upon correction in those cases, agreement between force estimates from vibration and load cell determinations was better than approximately 6%.

3. The effect of strand failures in the anchorage and nearby regions was evaluated by controlled cuts of strands with intentionally unbonded segments. Tension losses of as much as ~9% (per load cell measurements) resulted from those strand cuts. The decrease in most cases was comparable in magnitude when measured by both the load cell and vibration tests. One exception took place however, in which a stiffening response took place upon strand cutting, resulting in a false indication of tension increase.

4. Load cell and vibration experiments confirmed expectations that the effect of strand failures on one side of a deviation block will be minimized on the other side due to force transfer between strands and grout in the pipe embedded in the deviation block, and validate the ability of the vibration test to assess that condition.

5. Autopsy measurements of strand positions in tendon cross sections confirmed that strands crowded against one side of the cross section at deviation block entry and exit points and also upon cases of otherwise minor misalignment of end blocks.

6. Measured strand positions in tendon cross sections were used to compute an approximate indicator of asymmetry in the average flexural moment of inertia of each tendon segment. The indicator, Fm, was computed from the principal moments of the nominal array of strand centroids in the cross section. Fm was comparable in value and trends to a similar indicator computed from the dual flexural stiffness obtained from dual peaks in the vibration spectrum. This observation supports the hypothesis that dual vibration spectrum peaks stem largely from asymmetric distribution of strands in the tendon cross section.

7. Supplemental static deflection tests showed good promise as a means to obtain accurate vibration tension determinations in the absence of reliable linear mass information. Linear mass recovered from combined deflection-vibration tests closely matched independently determined reference values. Tension determinations based on static deflection tests as the primary measurement method may be a good practical alternative to a vibration test -based approach given development of practical instrumentation.

TASK 2: IMPROVED DATA PROCESSING

2.1 Basic Treatment

This section addresses basic aspects of the vibration tension determination approach used here. Those aspects were employed to develop a peak identification and force calculation system suitable for processing data from a large number of tendons, subsequently used in the tension calculations for the Sunshine Skyway Bridge under Task 4.

The treatment described next is abstracted from the detailed description in Sagüés et al 2006, which was published in the open literature as a product of the present contract.

The analysis uses a non-dimensional version of the derivation by Morse (1948). The vibrating tendon was abstracted a vibrating stiff string of length L, uniform cross section with a composite flexural stiffness [C] , S, mass per unit length m, stretched along the x (longitudinal) direction by a force T, and clamped at both ends. The governing differential equation was formulated and expressed in non-dimensional terms (except for the transverse deflection y) by defining the non-dimensional variables for distance, stiffness and time as:

$$\chi = x / L \qquad \text{(Eq. 2.1)}$$

$$\sigma = S / T L^2 \qquad \text{(Eq. 2.2)}$$

$$\tau = t / (L(m T^{-1})^{1/2}) \qquad \text{(Eq. 2.3)}$$

Thus the vibrating stiff string equation is:

$$\partial^2 y / \partial\chi^2 - \sigma\, \partial^4 y / \partial\chi^4 = \partial^2 y / \partial\tau^2 \qquad \text{(Eq. 2.4)}$$

Clamping at both ends means that the following spatial boundary conditions apply:

$$y = 0 \text{ and } \partial y/\partial\chi = 0 \text{ at both } \chi = 0 \text{ and } \chi = 1 \qquad \text{(Eq. 2.5)}$$

The temporal initial conditions are determined by the condition at t=0. Separation into spatial and temporal variables yields the string vibration modes non-dimensional frequencies, ν_n:

[C] Flexural stiffness in a non-composite beam reduces to the product of moment of inertia times the elastic modulus.

$$\nu_n = 2\,\pi\, u_n\, (\, (u_n^2 + 1/\,4\pi^2\sigma)\sigma)^{1/2} \qquad \text{(Eq. 2.6)}$$

where u_n satisfies, for the even spatial modes (n=1, 3, 5...) :

$$\tan(\pi\, u_n) = -\,[(\,1+ 1/(4\,\pi^2\, u_n^2\,\sigma)\,)^{1/2}]\,\tanh(\,\pi\,(\,u_n^2 + 1/(4\,\pi^2\, u_n^2\,\sigma)\,)^{1/2}\,) \qquad \text{(Eq. 2.7)}$$

and for the odd spatial modes (n = 2, 4, 6 ....) :

$$[(\,1+ 1/(4\,\pi^2\, u_n^2\,\sigma)\,)^{1/2}]\,\tan(\pi u_n) = \tanh(\,\pi\,(\,u_n^2 + 1/(4\,\pi^2\, u_n^2\,\sigma)\,)^{1/2}\,) \qquad \text{(Eq. 2.8)}$$

The values of u_n can be obtained by numerical solution of Eqs. (2.7) and (2.8). Note that the only parameter in the non-dimensional problem is σ, typically in the range ~ 10^{-4} to ~ 10^{-2} in tendon segments of recently examined bridges (Sagüés et al 2000).

Figure 2.1 summarizes the results of calculations over the range. The fundamental frequency corresponds to an n =1. For better visualization the non-dimensional mode frequencies are represented as ν_n /n and plotted as a function of n^2. The corresponding dimensional mode frequencies f_n are given by:

$$f_n = \nu_n\, \tau\, /\, t = \nu_n\, (T\, m^{-1})^{1/2} / L \qquad \text{(Eq. 2.9)}$$

In Figure 2.1 the ν_n /n values for each constant value of σ can be joined by line segments to graphically reveal an overall trend as function of n^2 (recognizing that only integer values of n have physical meaning). Linear trends are observed at low mode numbers and low stiffness, coinciding with the approximate solution obtained by Morse (1948) which is equivalent in non-dimensional terms to:

$$\nu_n / n \sim \tfrac{1}{2} + \sigma^{1/2} + (2 + n^2\, \pi^2 / 4)\, \sigma \qquad \text{(Eq. 2.10)}$$

For the ideal string case (σ=0) the modes are harmonic (ν_n = n ν_1) and the trend line becomes horizontal. The dimensional frequencies for that case follow the familiar relationship (Young 1962):

$$f_n = n\, (T\, m^{-1})^{1/2} / 2\, L \qquad \text{(Eq. 2.11)}$$

It is noted that the effect of stiffness is to increase the fundamental (n=1) frequency by up to several percent compared to that of a string with no stiffness, over the stiffness range of interest. The effect becomes more marked at the higher overtones, and the inharmonic sequence of modes is evident in Figure 2.1 for the higher values of the non-dimensional parameter σ. These results indicate that the effect of stiffness must not be neglected if an accurate estimate tension value is desired from vibrational test data of typical tendon configurations.

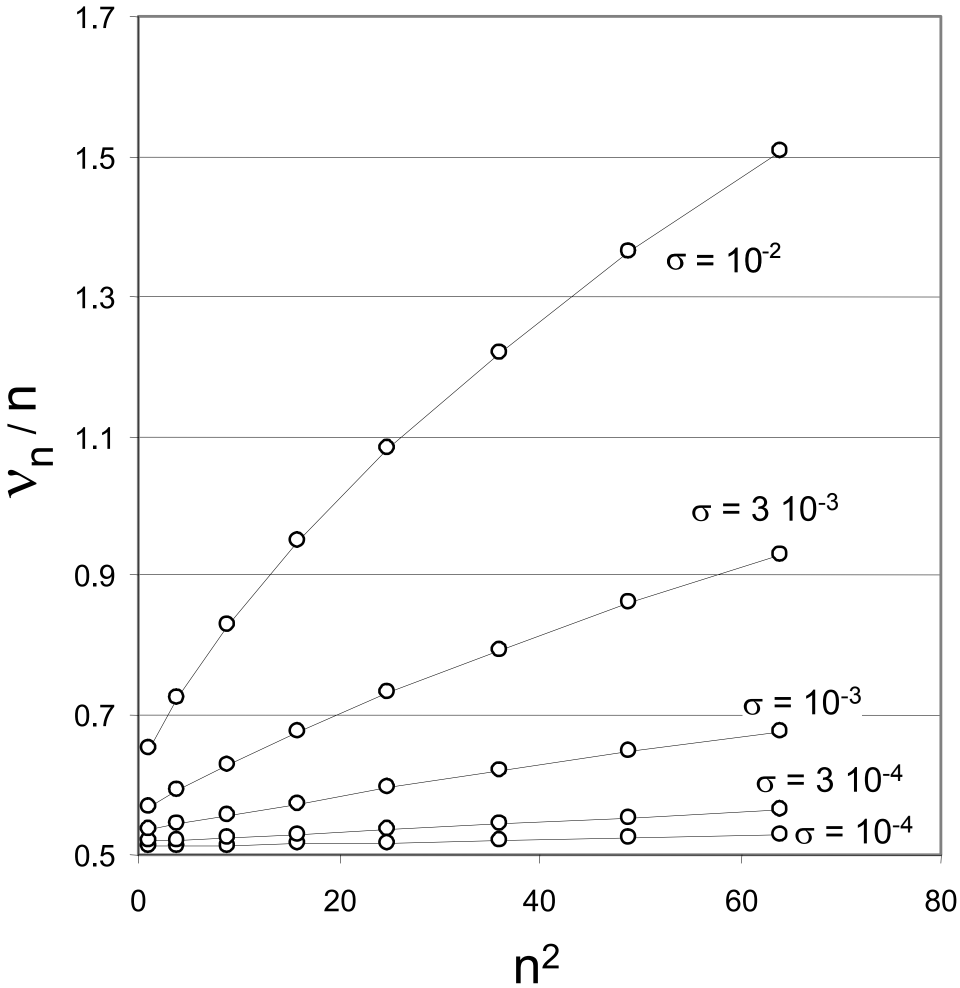

Figure 2.1 - Non-dimensional frequency ν_n (divided by n) as function of n^2 for cases with σ ranging from 10^{-4} to 10^{-2}. Lines shown for clarity only, function valid only for n=integer.

2.2 Improved Data Processing

2.2.1 Efficient estimation of stiffness and force

The relationships derived above served to construct an efficient procedure to evaluate tendon tension (and stiffness) from the mode frequencies revealed by Fourier analysis of the time domain response of the tendon to the hammer impact. The frequency spectrum was analyzed automatically to identify the peaks corresponding to the lowest (usually seven) vibration modes of the external tendon segment being evaluated. The frequency values of the identified modes are designated f_n^m with the superscript indicating they are the result of measurement and not ideally predicted. To minimize false peak identification, peak search was initiated in frequency windows centered on guessed dimensional frequencies obtained from Eq. (2.9), the numerical solutions to Eqs. (2.7) and (2.8), and using the expected values of tension and stiffness calculated from tendon design parameter records.

After frequency identification, the estimated tension and flexural stiffness for the tendon segments were obtained by determining which combination of both values best predicts the observed spectrum. An efficient procedure to achieve this was implemented by referring the f_n^m values against a master table of ν_n values (n=1 to n_{max}, with n_{max} usually = 7) as function of σ. The master table entries were made for closely spaced σ values in the range $10^{-4} < \sigma < 10^{-2}$, by solving Eqs. (2.7) and (2.8) numerically to within a tolerance of 10^{-12} using a simplex search method. The first lines of the master table are reproduced in Table 2.1, and a complete listing is provided in Appendix 5.

According to Eq. (2.9), the ratio $R_n = f_n / \nu_n$ is independent of n and equal to a single value $R = (T/m)^{1/2} /L$. Figure 2.1 shows that the variation of ν_n/n with n^2 (and consequently ν_n with n) is unique for each value of σ. For a given σ, the f_n values have to vary with n in the same proportion as ν_n since the factor R is the same for all n. Thus if the ratios $R_n(\sigma_i)= f_n^m /\nu_n(\sigma_i)$ are calculated for n = 1 to n_{max} for each tabulated value of σ (the subscript i indicates calculation for the ith entry in the table), the value of σ that yields ratios least dependent [D] on n can be regarded as representing the best approximation to the measured behavior. This value is then the estimated non-dimensional stiffness, named σ_e, and it is the key result of the evaluating procedure.

It is noted that σ_e is obtained without needing to know the value of the tendon linear mass. That circumstance can be used to advantage to obtain an estimate of the tendon tension if the tendon linear mass is unknown or highly uncertain, but accurate static lateral deflection data are available instead. That is done following the procedure indicated in the Task 1 section, items 1.3.2 and 1.4.4.

[D] For each tabulated value σ_i the variability of $R_n(\sigma_i)$ with n was measured by a parameter $Er(\sigma_i)$ $= \sum_{n=1}^{n=n_{max}} (((R_n(\sigma_i) - R_{avg}(\sigma_i))/ R_{avg}(\sigma_i))^2$, where $R_{avg}(\sigma_i)$ is the average of the $R_n(\sigma_i)$ values. The minimum value of $Er(\sigma_i)$ was used to flag the σ entry that yielded the condition of least dependence of R on n.

Table 2.1 - Initial portion of the master table of non-dimensional frequencies as function of non-dimensional stiffness σ for Modes 1-7. The entire table for σ ranging from 10^{-4} to 10^{-2} is given in Appendix 5.

σ	ν_1	ν_2	ν_3	ν_4	ν_5	ν_6	ν_7
0.0001	0.510457	1.022432	1.537433	2.056954	2.582463	3.1154	3.657165
0.00012	0.511494	1.02481	1.541758	2.064123	2.593658	3.132071	3.681018
0.00014	0.512456	1.027039	1.545859	2.070995	2.604479	3.148284	3.70431
0.000159	0.513359	1.02915	1.549785	2.077633	2.615004	3.164128	3.727145
0.000179	0.514212	1.031164	1.553566	2.084079	2.625284	3.179666	3.749597
0.000199	0.515025	1.033097	1.557227	2.090364	2.635358	3.194945	3.771718
0.000219	0.515803	1.034961	1.560785	2.09651	2.645256	3.209997	3.793547
0.000239	0.516551	1.036765	1.564254	2.102538	2.654999	3.224851	3.815116
0.000258	0.517273	1.038516	1.567645	2.10846	2.664605	3.239526	3.836448
0.000278	0.517971	1.040222	1.570967	2.114289	2.674089	3.254041	3.857565
0.000298	0.518648	1.041886	1.574226	2.120034	2.683462	3.268408	3.878481
0.000318	0.519306	1.043512	1.57743	2.125703	2.692735	3.28264	3.899211
0.000338	0.519947	1.045104	1.580584	2.131303	2.701915	3.296746	3.919767
0.000357	0.520572	1.046666	1.583691	2.13684	2.71101	3.310736	3.940158
0.000377	0.521183	1.048199	1.586755	2.142319	2.720026	3.324615	3.960394
0.000397	0.521781	1.049706	1.589781	2.147744	2.728968	3.338392	3.980481
0.000417	0.522366	1.051189	1.59277	2.153118	2.737841	3.35207	4.000427
0.000437	0.52294	1.052649	1.595726	2.158446	2.746649	3.365656	4.020237
0.000456	0.523504	1.054089	1.59865	2.16373	2.755395	3.379153	4.039917
0.000476	0.524057	1.055509	1.601544	2.168972	2.764083	3.392565	4.059472
0.000496	0.524601	1.05691	1.604411	2.174176	2.772715	3.405896	4.078906
0.000516	0.525137	1.058294	1.607252	2.179342	2.781295	3.419149	4.098223
0.000536	0.525664	1.059662	1.610069	2.184474	2.789824	3.432327	4.117427
0.000555	0.526184	1.061015	1.612862	2.189573	2.798305	3.445433	4.13652
0.000575	0.526696	1.062353	1.615633	2.194639	2.80674	3.458469	4.155507
0.000595	0.527201	1.063677	1.618383	2.199676	2.81513	3.471437	4.17439
0.000615	0.527699	1.064989	1.621113	2.204684	2.823477	3.484339	4.193172
0.000635	0.528191	1.066288	1.623825	2.209664	2.831782	3.497177	4.211855
0.000654	0.528677	1.067574	1.626518	2.214617	2.840048	3.509953	4.230442
0.000674	0.529158	1.06885	1.629194	2.219545	2.848274	3.522669	4.248934
0.000694	0.529633	1.070115	1.631853	2.224448	2.856463	3.535325	4.267334
0.000714	0.530102	1.071369	1.634496	2.229328	2.864616	3.547924	4.285645
0.000734	0.530567	1.072614	1.637124	2.234184	2.872733	3.560467	4.303866
0.000753	0.531027	1.073849	1.639737	2.239019	2.880816	3.572955	4.322002

In the following it was assumed that a reliable value of m is available with reasonable accuracy. In such case, once σ_e is known, and calling R_{avm} the average of the R ratios over n=1 to n_{max} for σ_e, the corresponding estimated tension T_e is then calculated from:

$$T_e = R_{avm}^2 L^2 m \qquad \text{(Eq. 2.12)}$$

and the corresponding estimated dimensional flexural stiffness is given by:

$$S_e = \sigma_e T_e L^2 \qquad \text{(Eq. 2.13)}$$

The calculation was further refined by interpolating between master table entries as appropriate. It is noted that while this procedure was found to be convenient for rapid processing of data from large tendon inventories, equally valid alternative data processing schemes exist.

2.2.2 Improved identification of peak doublet components

In early versions of the force estimation method, the above procedure was applied separately to the mode frequencies set corresponding to the low frequency (LF), and to the high frequency (HF), components of each doublet respectively. Thus force and stiffness estimates resulted for each the HF and LF components set. Usually both force estimates differed little (e.g. 1%-5%) from each other and the average value of both was reported as the estimated tendon force. However, instances of appreciable uncertainty remained especially in cases where the amplitude of one of the doublet components of one or more of the modes was so low as to be undetectable. The peak search program used for the first data processing step labels the only remaining component by default as belonging with the LF sequence. That formal assignment, when wrong, can result in appreciable error of the estimated force. Other errors could result from improper identification of noise features in the spectrum as mode frequencies instead of an actual mode frequency that may be of lower amplitude, again resulting in force estimation error. To minimize errors of these types, an additional processing step was introduced as follows.

Call f_{nha} and f_{nla} respectively the apparent high and low frequency component mode frequencies for the doublet peak for mode n, as identified by the first peak search program. If for a given mode g (n=g) only one component was identified, then it was labeled as f_{gha} and f_{gla} was declared blank. The improved procedure, implemented for data sets with frequency measurements for modes 1 to 7, consisted of first creating all 128 possible permutations of the apparent mode frequencies. Some of those permutations contained one or more blanks depending on how many doublets had only one identified component. The procedure indicated in the previous section was then applied to each permutation to obtain the value of P_{min}, (see footnote in previous subsection) normalized to account for the number of blanks if any. The permutation yielding the minimum value of normalized P_{min} (or a comparable descriptor of goodness of fit) was declared as the best representation of a consistent set of frequencies for one of the doublet component sequences. It is noted that such choice may correspond to either an HF or a LF set. The frequencies not included in that permutation were not automatically labeled as the other doublet sequence, because they could incorporate grossly spurious peaks. Instead, the remaining set was again permutated this time against a set of all blanks and the permutation yielding the lowest P_{min} was declared as that corresponding to the remaining doublet sequence unless a quality criterion was not met. The quality criterion was conservatively placed to exclude any final selection with more than 3 blank frequencies; in such cases the remaining doublet set was declared not found and force estimation was based only on the first set choice.

2.2.3 Implementation

The above procedures were implemented with commercially available software: Matlab® for the initial peak identification, and Excel® spreadsheets for the stiffness and force estimates including permutations for refined doublet sequence identification. Ordinary desktop computers typically processed data from hundreds of tendons in times in the order of 1 hour.

Results yielding force estimates for the HF and LF sequences of the same tendon that differed by more than a threshold criterion (e.g. 5%) were flagged for human inspection. Human inspection of results was also conducted with aid of graphic display of the data to flag possible outliers resulting from sources ranging from tendons obstructed from free vibration, to data entry errors or improper identification of tendon parameters such as length. Data for tendons so flagged were examined in detail, reprocessed manually if that was deemed necessary, and a determination was made as to whether to declare force estimation unfeasible or to report force with a caveat.

The above procedures, as they became available from execution if this task, were implemented in ongoing tests of the FDOT bridge inventory (e.g Corven 2005 and the investigation reported in Appendix 3).

2.2.4 Detailed Example

As an illustration of the procedure, following is an example of how the data from Tendon 0A (L=9.319m, m=17.462 kg/m), Test Serial No. 0A0100 (Filename 0ABTTSC) was processed. Fourier analysis of the time domain data for this tendon segment resulted in the following f_{nha} and f_{nla} frequency sequences as shown in Table 2.2.

Table 2.2 - Apparent Mode frequency sequences from analysis of *.wav* file.

Mode	1	2	3	4	5	6	7
f_{nha} (Hz)	16.4233	33.3512	51.2886	70.4666	90.4647	113.575	137.8419
f_{nla} (Hz)	-	32.9096	50.0689	68.1955	87.037	107.2875	128.7576

After identifying repeats (e.g. data for Modes 1 and 2) with only one defined doublet component, and conducting permutation analysis to conservatively eliminate possible outliers (resulting in blanks), the sorted out data consisted of sets 1 and 2 as shown in Table 2.3.

Table 2.3 - Refined mode frequency identification after automatic sorting.

Mode	1	2	3	4	5	6	7
f_{set1} (Hz)	-	32.9096	50.0689	68.1955	87.037	107.2875	128.7576
f_{set2} (Hz)	16.4233	33.3512	51.2886	-	-	113.575	137.8419

For each mode and for each candidate value of σ, the values of f_{set1} and f_{set2} were divided by the corresponding value of n, resulting in a series of trial values of the parameter $R_n=f_n/\nu_n$. The resulting table of R_n values is illustrated for Set 2[E] in Table 2.4 for the values of σ corresponding to the portion of the master table shown in Table 2.1, leading to an estimate of σ_e by identifying the values of σ yielding the lowest error sum and subsequent interpolation. A similar procedure was applied to Set 1.

The resulting values were σ_{e1} = 5.76E-4 and σ_{e2}=9.42E-4, with R_{avm1}= 31.007 Hz and R_{avm2}= 31.744Hz. The corresponding tensions ($T_e = R_{avm}^2 L^2 m$) were T_{e1}= 1.458 MN (328 klbf) and T_{e2}=1.433 MN (322 klbf) , with average value of 1.446 MN (325 klbf) and differing from each other by only 2%. The corresponding dimensional values of $S_e = \sigma_e T_e L^2$ were S_{e1}=0.73 E5 N-m^2 (25 Mlbf-in^2) and S_{e2}=1.17E5 N-m^2 (41 Mlbf-in^2).

2.3 Task 2 Conclusions

1. A non-dimensional treatment of the stretched stiff beam problem was formulated in terms suitable for automatic solution of the vibrating tendon segment system.

2. An efficient procedure was constructed to evaluate tendon tension and stiffness from mode frequencies revealed by Fourier analysis of the time domain response of the tendon to the hammer impact. The procedure featured a table lookup to identify the best parameters that fit experimental results and a permutation procedure to perform refined doublet peak identification.

3. The procedure was implemented with commercially available software including a refined doublet sequence identification and automatic operation of large data sets. Ordinary desktop computers typically processed data from hundreds of tendons in times in the order of 1 hour.

[E] Set 2 was chosen for clarity as the error minimum fell within the σ range covered by Table 2.1.

Table 2.4 - Example for Set 1 of Test serial 0A0159 of values of ratio R= f_n/ν_n (Hz) for each available mode and error sum. Highlighted is the case with σ yielding minimum error sum. Weighted interpolation of surrounding cases gives σ_e=0.000576 as best estimate of σ and R_{avm2}= 31.007Hz.

σ	R_1	R_2	R_3	R_4	R_5	R_6	R_7	$R_{average}$	Error Sum
0.0001	-	32.188	32.567	33.154	33.703	34.438	35.207	33.543	0.0325
0.00012	-	32.113	32.475	33.038	33.558	34.254	34.979	33.403	0.0294
0.00014	-	32.043	32.389	32.929	33.418	34.078	34.759	33.269	0.0265
0.000159	-	31.977	32.307	32.824	33.284	33.907	34.546	33.141	0.0238
0.000179	-	31.915	32.228	32.722	33.153	33.742	34.339	33.017	0.0213
0.000199	-	31.855	32.153	32.624	33.027	33.580	34.138	32.896	0.0189
0.000219	-	31.798	32.079	32.528	32.903	33.423	33.941	32.779	0.0168
0.000239	-	31.743	32.008	32.435	32.782	33.269	33.749	32.664	0.0147
0.000258	-	31.689	31.939	32.344	32.664	33.118	33.562	32.553	0.0129
0.000278	-	31.637	31.871	32.255	32.548	32.971	33.378	32.443	0.0112
0.000298	-	31.587	31.805	32.167	32.435	32.826	33.198	32.336	0.0096
0.000318	-	31.537	31.741	32.081	32.323	32.683	33.021	32.231	0.0082
0.000338	-	31.489	31.677	31.997	32.213	32.543	32.848	32.128	0.0069
0.000357	-	31.442	31.615	31.914	32.105	32.406	32.678	32.027	0.0057
0.000377	-	31.396	31.554	31.833	31.999	32.271	32.511	31.927	0.0047
0.000397	-	31.351	31.494	31.752	31.894	32.137	32.347	31.829	0.0037
0.000417	-	31.307	31.435	31.673	31.790	32.006	32.186	31.733	0.0029
0.000437	-	31.264	31.377	31.595	31.688	31.877	32.027	31.638	0.0022
0.000456	-	31.221	31.319	31.518	31.588	31.750	31.871	31.544	0.0016
0.000476	-	31.179	31.263	31.441	31.489	31.624	31.718	31.452	0.0011
0.000496	-	31.138	31.207	31.366	31.391	31.501	31.567	31.361	0.0007
0.000516	-	31.097	31.152	31.292	31.294	31.378	31.418	31.272	0.0004
0.000536	-	31.057	31.097	31.218	31.198	31.258	31.271	31.183	0.0002
0.000555	-	31.017	31.044	31.146	31.103	31.139	31.127	31.096	8E-05
0.000575	-	30.978	30.990	31.074	31.010	31.022	30.985	31.01	3E-05
0.000595	-	30.939	30.938	31.003	30.918	30.906	30.845	30.925	7E-05
0.000615	-	30.901	30.886	30.932	30.826	30.791	30.706	30.84	0.0002
0.000635	-	30.864	30.834	30.862	30.736	30.678	30.570	30.757	0.0004
0.000654	-	30.827	30.783	30.793	30.646	30.567	30.436	30.675	0.0006
0.000674	-	30.790	30.732	30.725	30.558	30.456	30.304	30.594	0.001
0.000694	-	30.753	30.682	30.657	30.470	30.347	30.173	30.514	0.0014
0.000714	-	30.717	30.633	30.590	30.383	30.240	30.044	30.435	0.0018
0.000734	-	30.682	30.583	30.524	30.298	30.133	29.917	30.356	0.0024
0.000753	-	30.646	30.535	30.458	30.213	30.028	29.791	30.278	0.003

TASK 3: SIMPLIFIED TESTING AND ANALYSIS METHOD.

3.1 Products

This task developed vibration testing field equipment and simplified test and analysis procedures for rapid screening of structures with commonly encountered tendon configurations. The intended users are non-specialist technical FDOT or consultant personnel.

A compact and easily portable working field equipment prototype was designed and constructed. The prototype included a laptop computer with customized data acquisition software, an accelerometer and signal conditioner, a calibration tuning fork, cabling, and a wireless remote actuator to permit testing by a single-operator thus minimizing personnel needs.

A step-by-step operating procedure was prepared suitable for training of technical non-specialist FDOT personnel and consultants in a one-day seminar. The procedure was prepared for a generic FDOT bridge tendon configuration, but it can be easily adapted by the user to specific span tendon configurations.

Software was also prepared and incorporated in the unit for rapid analysis of the test results to obtain an immediate estimate of tendon force, plus graphic display of tensions in peer tendons to facilitate flagging potentially deficient tendons. The equipment and software also automatically logged all primary data for later accurate analysis by specialists as needed per the procedures developed under Tasks 1 and 2 of this project.

All the acquired data and results are intended to remain in archive also for comparison with results from previous data sets on the same structure

3.2 Equipment and Software

The unit was based on a Dell Latitude 840 computer operating Windows XP. The audio Line In port of the computer sound card acquired the processed accelerometer output with 16-bit resolution, with data acquisition settings similar to those described in the Task 1 section of this report for the Tendon Test Facility tests. Data acquisition was managed through the Labview-based program Analyzer-M, which is operated per the step-by-step instructions contained in the Testing Procedure detailed further below. The Analyzer-M program was prepared for this project and is contained in the unit as an executable file. That electronic version of the program is functional in the indicated computer and, together with the data processing spreadsheet (next section) is provided under the terms of this the project as a deliverable separate from this final report.

The accelerometer was a Model PCB 338B34, connected to the Line-In computer input through an ICP-Model 480E09 signal conditioner. A wireless presentation remote control Targus Model PAUM30 served to actuate the computer be the operator impacting the tendon, thus permitting single-person operation.

3.3 Data Processing

As part of the operating procedure, the equipment operator obtains a full record of each vibration experiment in electronic form, and also manually records the frequencies of vibration Modes 1 and 2 in a Data Form. Those values are entered manually in the Excel data processing spreadsheet *Tension.xls*, together with additional specific tendon information, to obtain an immediate estimate of tendon tension.

Additional specific tendon information needed by *Tension.xls* to compute tension are tendon length L, estimated linear mass m, and estimated stiffness S. The value of L is measured directly by the operator. Estimates of m and S are obtained from lookup tables included in the operating procedure, using as input the number and type of strands in the tendon (from construction data). Tension is calculated as force per strand, to permit comparison between tendons of same type but not necessarily same number of strands. Tension is calculated for modes n=1 and 2 using Eq. 2.14, which is a dimensional version of Eq. 2.10 cleared for the value of T:

$$T = \left[L^2 \frac{f_n}{n} - \sqrt{\frac{S}{m}} + \frac{1}{n\sqrt{2}} \cdot \left(\frac{2f_n^2 \cdot L^4 \cdot m \cdot \sqrt{\frac{S}{m}} - 6S \cdot n^2 \cdot \sqrt{\frac{S}{m}} - n^4 \cdot \sqrt{\frac{S}{m}} \cdot \pi^2 \cdot S - 4L^2 \cdot f_n \cdot S \cdot n}{m \cdot \sqrt{\frac{S}{m}}} \right)^{\frac{1}{2}} \right]^2 \cdot \frac{m}{L^2}$$

(Eq. 2.14)

The Output field lists an average value of the T values calculated using modes 1 and 2, and a Quality parameter equal to the percentage difference between both calculated values. That difference is usually < 4%; instances where it is > 4% are indicative of possible irregularities in the test data, and a repeat test may be in order before the results are subject to specialized examination.

The spreadsheet *Tension.xls* was prepared assuming that data are obtained for a set of 6 tendons, three on each side of a symmetrical bridge span, each tendon having external segments terminating at the diaphragm at each end of the span. A bar graph is automatically prepared that compares the estimated tensions of peer segments in the group. Display layouts for other bridge configurations can be prepared by the user necessitating only basic spreadsheet skills.

3.4 Procedure Details

Appendix 2 includes the Step by Step Procedure to operate equipment and software, a sample Data Form, a tendon linear mass and stiffness Estimation Table, and illustration of the *Tension.xls* spreadsheet input and output fields and graphic output.

3.5 Task 3 Conclusions

1. Vibration test field equipment was developed for simplified operation and analysis procedures. A compact and easily portable field equipment prototype was designed and constructed.

2. The prototype included a laptop computer with customized data acquisition software, an accelerometer and signal conditioner, a calibration tuning fork, cabling, and a wireless remote actuator to permit testing by a single-operator thus minimizing personnel needs

3. A step-by-step operating procedure was prepared suitable for training of technical non-specialist FDOT personnel and consultants in a short seminar. The procedure was prepared for a generic FDOT bridge tendon configuration, but it can be easily adapted by the user to specific span tendon configurations.

TASK 4: TESTING AT THE SUNSHINE SKYWAY BRIDGE

4.1 Scope

This supplemental task addressed an immediate need to support testing of external post tensioned tendons in the Sunshine Skyway bridge. The task was conducted early in the project (starting September 2002). Some of the data interpretation was completed as findings from Task 2 became available. The tendons to be evaluated are in the segmental spans of the Sunshine Skyway Bridge between piers 88 and 105 (south approach) and 107 and 135 (north approach). There are 18 northbound (NB) and 18 southbound (SB) spans on each approach, for a total of 72 spans. Each span contains 6 tendons (3 on each side) for a total of 432 tendons. The tendons on each side were designated Top, Middle and Bottom according to the relative position of their anchorages at the bulkhead adjacent to the next contiguous bridge segment.

Each tendon has external tendon segments that extend from anchorage to deviation saddles, or between deviation saddles. The Top tendon is divided into only two external segments by a single intermediate deviation. Middle and Bottom tendons are divided into three segments. The total of tendon segments is 1152, and all were to be evaluated unless insurmountable physical obstructions to vibration existed.

4.2 Execution and Findings

The activity was successfully conducted and a Final Task 4 report was submitted after revision and approval on December 22, 2003. That report is reproduced in its entirety in Appendix 3 where the findings are described in detail. Conclusions are reproduced below for consistency with the other sections of the main report.

4.3 Task 4 Conclusions

1. Tension estimates from vibration testing were successfully conducted using the detailed analysis in all but one of the 864 tendon segments tested.

2. Estimated tension patterns were in agreement with the presence of friction at deviation blocks. The end-to-end tension disparity increased with the number of intermediate deviation blocks.

3. Vibration testing did not reveal any indications of dramatically reduced tension in any of the tendons segments evaluated. The average estimated tension standard deviation within tendon segment peer groups was on the order of 3%. No estimated tension (with one exception where vibration was obstructed) was lower than 11% below the average of its tendon segment peer group.

4. Tendon segments having estimated tensions lower than ~7% below their peer group average, and a tendon with unusual end-to-end tension disparity, were flagged for proposed special attention during upcoming inspections.

LIST OF SYMBOLS

Regular Letter Symbols

D Steel pipe diameter, internal.

d Steel pipe wall thickness.

E Elastic modulus of steel.

Er Sum of squares of differences between R and the average of R values, divided by that average.

f Frequency (generic term).

f_n Frequency of vibration mode n.

f_n^m Measured value of fn (when it needs to be distinguished from a calculated value)

f_{nha} Apparent mode frequency of the high frequency component of the doublet peak at mode n, as identified by the first peak search program.

f_{nla} Apparent mode frequency of the low frequency component of the doublet peak at mode n, as identified by the first peak search program.

$f_{set1,2}$ Mode frequencies sorted out by doublet identification program.

FF Name of program to process vibration data.

Fm Moment asymmetry factor.

F_S Stiffness asymmetry factor.

GUTS Guaranteed Ultimate Tensile Strength.

HF High frequency.

i_i Principal second order moment i.

I_X Second order moment with respect to horizontal axis (through centroid) of strand arrangement in tendon cross section.

I_Y Second order moment with respect to vertical axis (through centroid) of strand arrangement in tendon cross section.

I_{XY} Second order moment with respect to centroid of strand arrangement in tendon cross section.

k Ratio T_{IMPR} / Te.

k' Value of k in model calculations.

k_{APPR} Approximate value of k.

k_0 1st. power law parameter to calculate k from tendon and pipe data.

k_{INF} Ideal value of k for the limiting case of infinitely stiff metal pipes.

L Tendon vibrating length.

LF Low frequency.

Lp Sum of both pipe end lengths.

m Tendon mass per unit length or linear mass (generic term).

m_D Value of m calculated from a combination of deflection and vibration test results, with no need of knowing m beforehand.

n Mode number. Fundamental vibration frequency corresponds to n=1.

n_{max} Highest mode number identified for processing.

q 2nd power law parameter to calculate k from tendon and pipe data.

R_n Ratio $R_n = f_n / \nu_n$ (generic term).

R_{avg} Value of R, averaged for n=1 to $n_{max.}$

R_{avm} Value of R, averaged for n=1 to n_{max}, for the ν_i set yielding $\sigma=\sigma_e$.

S Flexural stiffness (generic term).

S_{HF} Stiffness corresponding to the high frequency doublet component series

S_{LF} Stiffness corresponding to the low frequency doublet component series

Sm Flexural stiffness of part of tendon between pipe ends.

Sme Flexural stiffness estimated from vibration tests (not corrected for pipe end effects).

Sp Flexural stiffness of part of tendon containing pipe ends.

Spp Flexural stiffness of the pipe itself.

T Tendon tension (generic term).

Ta' Tension of idealized tendon in configuration used to calculate correction factors for end pipe effects..

T_D Tendon tension estimate calculated from a combination of deflection and vibration test results, with no need of knowing m beforehand.

Te Tendon tension estimated from vibration tests (not corrected for pipe end effects).

T_{IMPR} Tendon tension estimate improved by accounting for pipe end effects.

T_{LC} Tendon tension determined from load cell measurements.

TF Tension on tendons 0A and 0B.

TH Tension on horizontal portion of tendons 13A and 13B.

TS Tension on sloping portion of tendons 13A and 13B.

TBH Horizontal force acting on N end of deviation block.

TBV Vertical force acting on top of deviation block.

TSB South block reaction force.

u_n Intermediate parameter in the solution of Eq. 2.4 for mode n.

x,y Longitudinal distance along tendon and transverse deflection during vibration.

X,Y Flexion axes to define moments of inertia of strand arrays.

Greek letter symbols

α Sloping tendon angle with the horizontal.

β Adjustment factor applied to pipe stiffness when added to tendon stiffness in pipe end section.

χ Non-dimensional distance $\chi = x / L$.

δ Ratio of lateral deflection to lateral force

ν_n Non-dimensional mode frequency.

σ Non-dimensional stiffness $\sigma = S / T L^2$ (generic term).

σ_e Non-dimensional stiffness estimated from vibration tests.

τ Non-dimensional time $\tau = t / (L(m T^{-1})^{1/2})$.

REFERENCES

Ciolko, A. T. and Yen, W. P. (1999) “An Immediate Payoff From FHWA's NDE Initiative.” *Public Roads*, 62 (6) 10-17.

Corven Engineering, Inc. (2001). “Mid-Bay Bridge Post-Tensioning Evaluation Final Report”, Final Report to Florida Department of Transportation District 3 (available through the Florida Department of Transportation at <http://www.dot.state.fl.us/>).

Corven Engineering, Inc. (2005)Assessment of Florida Keys Bridges. Final Report to FDOT.

Fletcher, H. (1964), “Normal Vibration Frequencies of a Stiff Piano String.” *J. Acoustical Soc. of Am*. 36(1), 203-209.

Mehrabi, A. and Tabatabai, H. (1998). "Unified Finite Difference Formulation for Free Vibration of Cables." *J. Struct. Eng*. 124, (11) 1313-1322.

Mirza, J., Mirza, M., Roy, V. and Saleh, K. (2002) "Basic rheological and mechanical properties of high-volume fly ash grout", Construction and Building Materials, Vol. 16, p. 353

Morse, P.M. (1948). *Vibration and Sound*, Mc.Graw Hill, New York.

Naaman. A. and Bren, J. Eds. (1990). *External Prestressing in Bridges*, ACI SP-120, American Concrete Institute, Detroit, 1990.

Parsons Brinckerhoff Quade & Douglas, Inc. in association with Concorr Florida, Inc. and Kisinger Campo & Associates Corp. (2002), “Sunshine Skyway Bridge Post Tensioned Tendon Investigation”, FPN: 411135 1 32 01, Report to Florida Department of Transportation District Seven.

Sagüés, A. A., Kranc, S.C. and Hoehne, R.H. (2000). “Initial Development of Methods for Assessing Condition of Post-Tensioned Tendons of Segmental Bridges”, Final Report to Florida Department of Transportation, Contract No. BC374 (available through the Florida Department of Transportation at <http://www.dot.state.fl.us/>).

Sagüés, A.A., Powers, R.G. and Wang, H. (2003a). “Mechanism of Corrosion of Steel Strands in Post Tensioned Grouted Assemblies”, Paper No. 03312, Corrosion/2003, NACE International, Houston.

Sagüés, A.A., Eason, T.G., Cotrim, C. and Saradhi, A. (2003b). “Results of Detailed Analysis of Vibration Testing of External Tendons in the High Approaches of the

Sunshine Skyway Bridge," Final Report to Florida Department of Transportation, Task 4, Project BC353-44.

Sagüés, A. A., Kranc, S.C., Balakrishna, V. and Saradhi. A. (2004a) "Test Preparation and Data Analysis for Vibrational Testing of Mid Bay Bridge Tendons." Final Report to Florida Department of Transportation, Contract No. BC353-17. (available through the Florida Department of Transportation at <http://www.dot.state.fl.us/>).

Sagüés, A. A., Kranc, S.C., Balakrishna, V. (2004b), "Column Tendon Vibrational Test Preparation and Data Analysis", Final Report, FDOT Project BC353-23, , (available through the Florida Department of Transportation at <http://www.dot.state.fl.us/>).

Sagüés, A. A., Cotrim, C., Balakrishna, V. (2005), "Vibrational Evaluation of Tendons in Segmental Sections of Sunshine Skyway Bridge Main Spans", Final Report, FDOT Project BD544-3, , (available through the Florida Department of Transportation at <http://www.dot.state.fl.us/>).

Sagüés, A. A., Kranc, S.C. and Eason, T.G. (2006), "Vibrational Tension Measurement of External Tendons in Segmental Posttensioned Bridges", ASCE J. Bridge Engineering, Vol. 11, p.582

Young, R. W. (1962). "Frequencies of Simple Vibrators." *American Institute of Physics Handbook*, McGraw-Hill, New York, 3 -110.

Young, W.C. (1989). *Roark's Formulas for Stress and Strain*, 6th edition, McGraw-Hill, Inc., New York.

Zui, H., Shinke, T. and Namita, Y. (1996). " Practical Formulas for Estimation of Cable Tension by Vibration Method." *J. Struct. Eng*., 122(6) 651-656.

APPENDIX 1

DATA TABLES FOR TASK 1: MODEL VALIDATION

Notes for Table A1.1:

1) Frequencies for 0A and 0B are shown as produced by the peak identification program, with the exception of automatic discarding the lower amplitude component of Mode 1, for which doublet resolution tended to be uncertain. Frequency entries for unidentified mode components are indicated by zeroes.

2) Frequencies for 13A and 13B are given only for Modes 2-4 due to spurious coupling affecting Mode 1 for those tendons, and wide doublet splits at Mode numbers >4 which obscured identification. Analysis was based on those modes only.

3) All frequencies are presented in 1 mHz precision only to minimize roundoff error in future processing of the results using the text version of the document. Reporting precision does not imply corresponding accuracy.

Table A1.1- Doublet peak frequencies per analysis of each reported vibration test.

Test Serial Number	Filename	Mode Frequencies / Hz													
		Set 1 for Mode number:							Set 2 for Mode number:						
		1	2	3	4	5	6	7	1	2	3	4	5	6	7
0A 0100	0ABTTSC	16.339	33.225	50.889	69.962	90.233	112.692	136.643	0.000	32.784	49.838	67.859	86.427	106.678	127.959
0A 0101	0ABTTSD	16.339	33.225	50.889	69.962	90.254	112.692	136.643	0.000	32.784	49.838	67.859	86.427	106.699	127.959
0A 0102	0ABTASC	0.000	32.784	49.817	67.859	86.427	106.636	127.938	16.360	33.225	50.931	69.983	90.275	112.755	136.706
0A 0103	0ABTASD	0.000	32.784	49.817	67.859	86.406	106.636	127.917	16.360	33.246	50.931	69.983	90.275	112.734	136.706
0A 0104	0ABTSSC	16.339	33.204	50.889	69.962	90.254	112.713	136.685	0.000	32.784	49.817	67.880	86.427	106.636	127.938
0A 0105	0ABTSSD	16.339	33.204	50.889	69.962	90.254	112.713	136.685	0.000	32.784	49.817	67.880	86.427	106.636	127.959
0A 0106	0ABASSA	16.129	32.784	49.838	67.880	86.427	106.657	127.959	0.000	33.162	50.826	69.941	90.233	124.783	0.000
0A 0107	0ABASSB	16.129	32.784	49.838	67.880	86.427	106.636	127.959	0.000	33.162	50.847	69.941	90.233	124.825	0.000
0A 0108	0ABATSA	0.000	32.784	49.817	67.880	86.406	106.657	127.959	16.360	33.246	50.910	69.962	90.233	124.426	149.113
0A 0109	0ABATSB	0.000	32.784	49.817	67.859	86.406	106.657	127.959	16.360	33.246	50.910	69.962	90.233	124.846	148.651
0A 0110	0ABAASA	16.108	32.784	49.817	66.787	86.406	106.636	127.917	0.000	33.057	0.000	67.859	0.000	124.804	0.000
0A 0111	0ABAASB	16.129	32.784	49.817	67.859	86.406	106.636	127.938	0.000	0.000	0.000	70.004	90.297	124.678	0.000
0A 0112	0ABSASC	16.129	32.784	49.817	67.859	86.385	106.615	127.917	0.000	33.183	50.868	69.941	90.233	124.867	148.209
0A 0113	0ABSASD	16.129	32.784	49.817	67.859	86.385	106.615	127.917	0.000	33.204	50.868	69.962	90.254	112.713	136.706
0A 0114	0ABSSSC	16.129	32.784	49.817	67.859	86.406	106.657	127.959	0.000	33.225	50.931	69.983	90.275	112.755	136.685
0A 0115	0ABSSSD	16.129	32.784	49.817	67.859	86.406	106.636	127.959	0.000	33.225	50.931	69.983	90.275	112.755	136.685
0A 0116	0ABSTSC	16.339	33.204	50.889	69.941	90.233	112.692	136.643	0.000	32.784	49.817	67.880	86.406	106.636	127.959
0A 0117	0ABSTSD	16.339	33.204	50.889	69.962	90.233	112.692	136.643	0.000	32.784	49.817	67.880	86.406	106.636	127.959
0A 0118	0ABNTTA	16.381	33.267	50.910	69.731	90.191	112.397	136.349	0.000	32.784	49.838	67.375	86.301	106.446	127.748
0A 0119	0ABNTTB	16.381	33.267	50.931	69.731	90.191	112.376	136.370	0.000	32.762	49.838	67.375	86.301	106.446	127.748
0A 0120	0ABNTAA	16.213	32.805	49.817	67.375	86.301	106.404	127.727	0.000	33.288	50.952	69.752	90.212	112.461	136.412
0A 0121	0ABNTAB	16.213	32.805	49.817	67.375	86.301	106.404	127.727	0.000	33.288	50.952	69.752	90.212	112.524	136.391
0A 0122	0ABNTSA	16.234	32.868	49.838	67.396	86.322	106.446	127.748	0.000	33.267	50.931	69.731	90.212	112.461	136.412
0A 0123	0ABNTSB	16.234	32.847	49.838	67.396	86.322	106.425	127.748	0.000	33.267	50.931	69.731	90.212	112.482	136.433
0A 0124	0ABNASA	16.213	32.805	49.838	67.417	86.322	106.425	127.769	0.000	33.267	50.931	69.752	90.212	112.461	148.461
0A 0125	0ABNASB	16.213	32.805	49.838	67.417	86.322	106.425	127.769	0.000	33.246	50.931	69.752	90.212	124.321	148.567
0A 0126	0ABNATA	16.213	32.784	49.838	67.417	86.322	106.467	127.790	0.000	33.288	50.952	69.731	90.212	112.461	136.391
0A 0127	0ABNATB	16.213	32.805	49.838	67.396	86.322	106.446	127.769	0.000	33.288	50.952	69.731	90.212	112.292	136.391
0A 0128	0ABNAAA	16.213	32.784	49.838	67.396	86.301	106.404	127.748	0.000	33.330	0.000	69.773	90.233	124.678	0.000
0A 0129	0ABNAAB	16.213	32.805	49.838	67.396	86.301	106.425	127.748	0.000	33.330	50.973	69.773	90.254	124.194	0.000
0A 0130	0ABNSAA	16.213	32.868	49.838	67.396	86.301	106.425	127.748	0.000	33.267	50.931	69.752	90.233	124.720	148.840
0A 0131	0ABNSAB	16.213	32.910	49.838	67.396	86.301	106.404	127.748	0.000	33.267	50.931	69.752	90.233	124.552	148.398
0A 0132	0ABNSSA	16.213	32.868	49.838	67.417	86.301	106.425	127.769	0.000	33.288	50.952	69.752	90.233	112.440	136.454
0A 0133	0ABNSSB	16.213	32.868	49.838	67.417	86.301	106.425	127.769	0.000	33.288	50.952	69.752	90.233	112.419	136.454
0A 0134	0ABNSTA	16.234	32.931	49.838	67.396	86.301	106.425	127.769	0.000	33.267	50.931	69.731	90.191	112.376	136.412
0A 0135	0ABNSTB	16.234	32.931	49.838	67.417	86.301	106.446	127.769	0.000	33.267	50.931	69.731	90.212	112.376	136.412

Table A1.1 Continued

Test Serial Number	Filename	Mode Frequencies / Hz													
		Set 1 for Mode number:							Set 2 for Mode number:						
		1	2	3	4	5	6	7	1	2	3	4	5	6	7
0A 0136	0ACNTTA	16.486	33.498	51.310	70.446	90.990	113.470	128.863	0.000	33.141	50.195	68.322	87.079	100.285	0.000
0A 0137	0ACNTTB	16.507	33.520	51.310	70.446	90.990	113.512	137.737	0.000	33.120	50.195	68.301	87.079	107.414	128.863
0A 0138	0ACNTAA	16.318	33.120	50.195	68.322	87.058	107.309	128.821	0.000	33.520	51.310	70.467	91.011	113.512	137.758
0A 0139	0ACNTAB	16.318	33.120	50.195	68.322	87.058	107.309	128.821	0.000	33.520	51.310	70.467	91.011	113.512	137.779
0A 0140	0ACNTSA	16.339	33.141	50.195	68.364	87.079	107.267	128.842	0.000	33.520	51.310	70.467	91.011	113.491	137.758
0A 0141	0ACNTSB	0.000	33.520	51.310	70.467	91.011	113.575	137.758	16.339	33.141	50.195	68.343	87.079	107.267	128.842
0A 0142	0ACNASA	16.318	33.120	50.195	68.364	87.058	100.432	128.821	0.000	33.498	51.310	70.446	90.990	107.288	0.000
0A 0143	0ACNASB	16.318	33.141	50.195	68.364	87.079	107.330	128.842	0.000	33.498	51.310	70.467	91.011	113.533	0.000
0A 0144	0ACNATA	16.318	33.141	50.195	68.364	87.079	107.309	128.863	0.000	33.520	51.310	70.467	90.990	113.701	137.716
0A 0145	0ACNATB	16.318	33.141	50.195	68.364	87.079	107.330	128.842	0.000	33.520	51.310	70.446	90.990	113.638	137.716
0A 0146	0ACNAAA	0.000	33.562	0.000	68.301	0.000	107.267	0.000	16.318	33.120	50.174	67.165	87.016	100.348	128.758
0A 0147	0ACNAAB	16.318	33.120	50.174	68.343	87.037	100.327	128.779	0.000	33.562	51.331	70.467	0.000	107.288	0.000
0A 0148	0ACNSAA	16.318	33.120	50.174	68.343	87.037	100.727	128.779	0.000	33.477	51.289	70.488	90.990	107.267	0.000
0A 0149	0ACNSAB	16.318	33.120	50.174	68.364	87.037	100.264	128.779	0.000	33.498	51.289	70.488	90.990	107.267	137.695
0A 0150	0ACNSSA	16.318	33.120	50.174	68.406	87.037	100.348	128.800	0.000	33.498	51.310	70.530	90.990	107.267	137.716
0A 0151	0ACNSSB	16.318	33.120	50.174	68.427	87.058	107.267	128.800	0.000	33.498	51.310	70.530	90.990	113.470	137.716
0A 0152	0ACNSTA	16.339	33.141	50.195	68.364	87.058	107.330	128.821	0.000	33.498	51.289	70.467	90.969	113.470	137.695
0A 0153	0ACNSTB	16.318	33.141	50.195	68.406	87.058	107.330	128.842	0.000	33.498	51.310	70.488	90.969	113.554	137.695
0A 0154	0ATNTTA	16.402	32.910	50.090	68.196	87.037	107.288	128.737	0.000	33.351	51.289	70.446	90.486	113.554	137.779
0A 0155	0ATNTTB	16.402	32.910	50.069	68.196	87.037	107.309	128.737	0.000	33.351	51.289	70.446	90.486	113.554	137.779
0A 0156	0ATNTAA	0.000	32.910	50.069	68.196	87.016	107.267	128.716	16.423	33.372	51.289	70.467	0.000	113.575	137.821
0A 0157	0ATNTAB	0.000	32.910	50.048	68.196	87.016	107.267	128.716	16.423	33.351	51.289	70.467	0.000	113.575	137.842
0A 0158	0ATNTSA	0.000	32.910	50.048	68.217	87.016	107.309	128.779	16.423	33.351	51.310	70.446	90.486	113.575	137.842
0A 0159	0ATNTSB	0.000	32.910	50.069	68.196	87.037	107.288	128.758	16.423	33.351	51.289	70.467	90.465	113.575	137.842
0A 0160	0ATNASA	16.129	32.910	50.048	68.196	87.016	107.267	128.737	0.000	0.000	51.289	0.000	0.000	113.575	137.821
0A 0161	0ATNASC	16.129	32.910	50.048	68.196	87.037	107.288	128.758	0.000	0.000	51.310	0.000	0.000	113.575	137.821
0A 0162	0ATNATA	0.000	32.910	50.048	68.217	87.037	107.288	128.758	16.402	0.000	51.289	70.467	0.000	113.554	137.800
0A 0163	0ATNATB	0.000	32.910	50.069	68.196	87.037	107.309	128.758	16.402	0.000	51.289	70.467	0.000	113.554	137.800
0A 0164	0ATNAAA	0.000	32.910	50.048	68.196	87.016	107.245	128.716	16.423	0.000	51.310	0.000	87.310	113.575	0.000
0A 0165	0ATNASB	0.000	32.910	50.048	68.196	87.016	107.245	128.716	16.423	0.000	51.310	0.000	87.310	113.575	0.000
0A 0166	0ATNSAA	16.129	32.910	50.048	68.196	87.016	107.267	128.737	0.000	33.351	51.289	0.000	0.000	113.575	137.842
0A 0167	0ATNSAB	16.129	32.910	50.048	68.196	86.995	107.267	128.716	0.000	33.351	51.268	0.000	0.000	113.575	137.821
0A 0168	0ATNSSA	16.129	32.910	50.048	68.196	87.016	107.267	128.758	0.000	33.351	51.310	70.488	90.528	113.575	137.821
0A 0169	0ATNSSB	16.129	32.910	50.048	68.196	87.037	107.267	128.758	0.000	33.351	51.310	70.488	90.570	113.575	137.842
0A 0170	0ATNSTA	0.000	32.910	50.048	68.196	87.037	107.267	128.758	16.402	33.351	51.289	70.467	90.507	113.554	137.800
0A 0171	0ATNSTB	0.000	32.910	50.048	68.196	87.016	107.267	128.758	16.402	33.351	51.289	70.467	90.507	113.554	137.800

Table A1.1 Continued

Test Serial Number	Filename	Mode Frequencies / Hz													
		Set 1 for Mode number:							Set 2 for Mode number:						
		1	2	3	4	5	6	7	1	2	3	4	5	6	7
0B 0100	0BBTTSA	15.687	31.879	48.807	67.333	86.722	108.381	131.050	0.000	31.879	49.060	67.670	87.668	125.603	0.000
0B 0101	0BBTTSB	15.687	31.900	48.807	67.333	86.743	108.444	131.050	0.000	32.132	59.553	0.000	87.647	125.330	0.000
0B 0102	0BBTASA	0.000	0.000	0.000	0.000	86.785	125.477	0.000	15.687	31.879	48.807	67.354	85.649	108.423	131.050
0B 0103	0BBTASB	0.000	0.000	0.000	0.000	86.785	125.330	0.000	15.687	31.879	48.786	67.354	85.712	108.423	131.050
0B 0104	0BBTSSA	0.000	0.000	49.018	0.000	87.142	108.486	0.000	15.729	32.069	48.849	67.649	86.890	102.682	132.248
0B 0105	0BBTSSB	0.000	0.000	48.975	0.000	0.000	123.038	0.000	15.708	32.048	47.419	67.544	87.121	108.423	132.122
0B 0106	0BBTSSC	0.000	0.000	49.186	0.000	88.215	108.423	0.000	15.729	32.048	48.954	67.607	87.163	101.925	132.164
0B 0107	0BBTSSD	0.000	0.000	58.922	0.000	0.000	109.180	132.059	15.708	32.026	48.954	67.439	87.079	108.339	131.029
0B 0108	0BBTSSE	0.000	0.000	58.123	0.000	0.000	109.138	132.059	15.708	32.026	48.954	67.439	87.079	108.339	131.029
0B 0109	0BBASSA	15.687	31.795	48.975	67.354	87.142	108.444	130.040	0.000	32.069	0.000	67.649	0.000	109.264	131.092
0B 0110	0BBASSB	15.687	31.795	48.975	67.354	87.142	108.444	130.040	0.000	32.069	0.000	67.649	0.000	109.243	131.092
0B 0111	0BBASSC	0.000	32.048	0.000	0.000	0.000	109.180	130.987	15.687	31.774	48.954	67.312	87.079	108.360	129.935
0B 0112	0BBASSD	0.000	32.048	0.000	0.000	0.000	109.180	130.987	15.687	31.774	48.954	67.312	87.079	108.360	129.935
0B 0113	0BBATSA	0.000	0.000	0.000	67.817	0.000	109.201	132.122	15.687	31.900	48.807	67.354	86.785	108.423	131.050
0B 0114	0BBATSB	0.000	0.000	0.000	0.000	87.899	124.825	0.000	15.687	31.900	48.807	67.354	86.806	108.423	131.071
0B 0115	0BBAASA	15.687	31.879	48.765	67.333	86.806	108.402	130.082	0.000	32.132	49.018	0.000	87.142	109.306	131.050
0B 0116	0BBAASB	15.687	31.879	48.765	67.333	86.764	108.423	129.914	0.000	32.132	49.018	0.000	87.142	109.285	131.050
0B 0117	0BBSASA	15.708	32.069	48.702	67.333	87.163	108.402	131.050	0.000	32.069	48.996	67.649	0.000	109.285	132.164
0B 0118	0BBSASB	15.708	31.837	48.702	67.333	87.163	108.423	131.050	0.000	32.069	48.996	67.649	0.000	109.306	132.143
0B 0119	0BBSSSA	0.000	0.000	0.000	67.628	0.000	109.264	132.185	15.729	32.069	48.975	67.333	87.142	108.444	131.008
0B 0120	0BBSSSB	0.000	0.000	0.000	67.628	0.000	109.264	132.185	15.729	32.069	48.975	67.354	87.142	108.423	131.029
0B 0121	0BBSTSA	0.000	0.000	0.000	67.628	0.000	109.285	132.227	15.729	32.069	48.975	67.417	87.163	108.444	131.092
0B 0122	0BBSTSB	0.000	0.000	0.000	67.628	0.000	109.243	132.227	15.729	32.069	48.975	67.396	87.205	108.423	131.071
0B 0123	0BBSTSC	15.708	31.900	48.954	67.375	87.163	108.381	131.029	0.000	32.048	0.000	67.586	0.000	109.243	132.185
0B 0124	0BBSTSD	0.000	0.000	0.000	67.565	0.000	109.222	132.164	15.708	32.048	48.954	67.375	87.163	108.360	131.029
0B 0125	0BBTTCA	15.687	31.900	48.786	67.333	86.701	108.381	131.050	0.000	31.900	49.039	67.670	87.647	109.285	132.248
0B 0126	0BBTTCB	15.687	31.900	48.786	67.354	86.722	108.402	131.050	0.000	31.900	49.060	67.691	87.710	109.306	132.269
0B 0127	0BBTACA	0.000	0.000	49.123	0.000	0.000	109.222	0.000	15.708	31.942	48.786	67.354	86.827	108.423	131.008
0B 0128	0BBTACB	0.000	0.000	0.000	0.000	86.806	125.603	0.000	15.687	31.900	48.786	67.354	85.712	108.402	131.029
0B 0129	0BBTSCA	0.000	0.000	0.000	0.000	0.000	109.243	132.164	15.729	32.069	48.954	67.607	87.142	108.465	131.113
0B 0130	0BBTSCB	0.000	0.000	0.000	0.000	0.000	109.243	132.164	15.729	32.048	48.954	67.586	87.163	108.465	131.113
0B 0131	0BBTSCC	0.000	0.000	0.000	0.000	87.521	109.159	132.059	15.708	32.048	48.933	67.502	87.079	108.402	131.029
0B 0132	0BBTSCD	0.000	0.000	0.000	0.000	87.521	109.159	132.059	15.708	32.048	48.933	67.502	87.079	108.402	131.029
0B 0133	0BBASCA	15.687	31.879	48.681	67.396	87.142	108.423	131.071	0.000	32.069	48.975	79.656	0.000	109.264	132.227
0B 0134	0BBASCB	15.687	31.837	48.681	67.396	87.142	108.444	131.071	0.000	32.069	48.975	0.000	0.000	109.264	132.206
0B 0135	0BBASCC	0.000	32.048	0.000	0.000	0.000	109.180	132.122	15.687	31.795	48.933	67.354	87.079	108.381	130.987
0B 0136	0BBASCD	0.000	32.048	0.000	0.000	0.000	109.159	132.122	15.687	31.795	48.933	67.354	87.079	108.381	130.987
0B 0137	0BBATCA	15.687	31.900	48.786	67.354	85.733	108.402	131.050	0.000	31.900	48.786	67.712	86.743	109.264	131.912
0B 0138	0BBATCB	15.687	31.900	48.786	66.955	85.902	108.381	131.050	0.000	31.900	48.786	67.354	86.743	109.264	132.080
0B 0139	0BBAACA	15.687	31.900	48.765	67.375	86.806	108.423	131.071	0.000	32.132	49.018	0.000	87.184	109.243	0.000
0B 0140	0BBAACB	15.687	31.900	48.765	67.354	86.785	108.402	130.061	0.000	32.132	48.996	0.000	87.142	109.264	131.029
0B 0141	0BBSACA	0.000	0.000	48.975	67.628	0.000	109.201	0.000	15.687	32.069	48.681	67.312	87.142	103.229	131.029
0B 0142	0BBSACB	0.000	41.763	0.000	67.628	0.000	109.201	0.000	15.687	32.069	48.975	67.333	87.163	103.271	131.029
0B 0143	0BBSSCA	0.000	0.000	0.000	67.628	0.000	109.243	0.000	15.729	32.069	48.954	67.375	87.142	102.367	132.185
0B 0144	0BBSSCB	0.000	0.000	0.000	0.000	0.000	109.201	0.000	15.729	32.069	48.954	67.607	87.142	102.388	132.185
0B 0145	0BBSTCA	15.708	25.739	48.954	67.649	87.163	108.381	131.071	0.000	32.069	0.000	71.960	0.000	109.201	132.227
0B 0146	0BBSTCB	15.708	32.090	48.954	67.628	87.163	108.297	131.071	0.000	32.868	0.000	68.111	0.000	109.306	132.206
0B 0147	0BBSTCC	0.000	0.000	0.000	79.383	0.000	111.956	0.000	15.687	32.069	48.933	67.607	87.163	109.243	132.164
0B 0148	0BBSTCD	0.000	0.000	0.000	0.000	0.000	109.958	132.164	15.687	32.069	48.933	67.607	87.163	109.159	131.008

Table A1.1 Continued

Test Serial Number	Filename	Mode Frequencies / Hz													
		Set 1 for Mode number:							Set 2 for Mode number:						
		1	2	3	4	5	6	7	1	2	3	4	5	6	7
0B 0149	0BBTTNA	15.666	31.858	48.723	67.228	86.595	109.096	130.797	0.000	32.132	48.954	67.565	87.647	0.000	132.038
0B 0150	0BBTTNB	15.666	31.858	48.723	67.228	86.595	109.096	130.797	0.000	32.132	48.954	67.565	87.794	0.000	132.038
0B 0151	0BBTANA	0.000	0.000	49.081	0.000	0.000	108.844	131.912	15.666	31.858	48.744	67.249	86.617	108.234	130.797
0B 0152	0BBTANB	0.000	0.000	49.060	0.000	0.000	108.760	131.933	15.666	31.858	48.744	67.249	86.595	108.234	130.797
0B 0153	0BBTSNA	0.000	0.000	0.000	0.000	87.794	109.033	131.933	15.687	31.984	48.870	67.396	86.974	108.276	130.861
0B 0154	0BBTSNB	15.687	31.984	48.891	67.354	86.974	108.255	130.861	0.000	31.984	48.891	67.417	87.310	109.054	131.933
0B 0155	0BBTSNC	0.000	0.000	0.000	0.000	87.479	108.970	131.828	15.687	31.963	48.870	67.291	86.911	108.213	130.776
0B 0156	0BBTSND	0.000	0.000	0.000	0.000	87.353	108.970	131.828	15.687	31.963	48.870	67.291	86.890	108.213	130.776
0B 0157	0BBASNA	15.666	31.774	48.618	67.249	86.995	108.234	130.818	0.000	32.005	48.912	67.544	0.000	108.991	131.954
0B 0158	0BBASNB	15.666	31.774	48.912	67.249	86.995	108.255	130.839	0.000	32.026	0.000	67.544	0.000	108.970	131.975
0B 0159	0BBATNA	15.666	31.858	48.744	67.249	86.595	108.234	130.797	0.000	31.858	49.102	67.712	0.000	109.138	131.891
0B 0160	0BBATNB	0.000	0.000	0.000	0.000	86.953	108.654	131.891	15.666	31.858	48.744	67.249	86.595	108.234	130.797
0B 0161	0BBAANA	15.666	31.837	48.702	67.228	86.574	108.213	130.797	0.000	32.069	48.954	0.000	87.016	109.054	132.038
0B 0162	0BBAANB	15.666	31.837	48.702	67.249	86.574	108.213	130.797	0.000	32.048	48.954	0.000	87.016	109.138	132.017
0B 0163	0BBSANA	15.666	31.795	48.618	67.249	86.595	108.234	130.797	0.000	32.026	48.912	67.523	87.037	109.138	131.996
0B 0164	0BBSANB	15.666	31.795	48.597	67.249	87.037	108.234	130.797	0.000	32.026	48.912	67.523	0.000	108.591	132.017
0B 0165	0BBSSNA	0.000	0.000	0.000	67.523	0.000	109.054	131.954	15.708	32.005	48.912	67.228	87.016	108.234	130.797
0B 0166	0BBSSNB	15.708	32.005	48.912	67.228	87.016	108.213	130.797	0.000	32.005	48.912	67.523	87.878	109.054	131.933
0B 0167	0BBSTNA	15.687	32.005	48.912	67.312	87.037	108.234	130.797	0.000	32.005	48.912	67.481	87.731	109.075	131.975
0B 0168	0BBSTNB	0.000	0.000	0.000	0.000	87.479	109.075	131.954	15.687	32.005	48.912	67.460	87.037	108.234	130.797
0B 0169	0BBSTNC	15.687	32.005	48.891	67.291	87.016	108.192	130.734	0.000	32.005	48.891	67.417	87.647	109.033	131.912
0B 0170	0BBSTND	15.687	32.005	48.891	67.291	87.016	108.213	130.734	0.000	32.005	48.891	67.417	87.584	109.033	131.912
0B 0171	0BCTTNA	15.393	31.312	47.966	66.009	85.292	106.678	128.884	0.000	31.312	48.218	66.534	85.986	107.540	130.167
0B 0172	0BCTTNB	15.393	31.312	47.945	66.030	85.271	106.678	128.884	0.000	31.312	48.218	66.745	85.986	107.561	130.167
0B 0173	0BCTANA	15.393	31.312	47.945	66.030	85.271	106.678	128.884	0.000	31.312	48.282	66.787	0.000	107.309	129.893
0B 0174	0BCTANB	15.414	31.312	47.945	66.030	85.271	106.678	128.884	0.000	31.312	48.282	0.000	85.817	107.351	129.914
0B 0175	0BCTSNA	15.414	31.333	48.134	66.030	85.859	106.720	128.947	0.000	31.522	0.000	66.387	0.000	107.456	129.998
0B 0176	0BCTSNB	15.435	31.333	48.134	66.555	85.859	106.741	128.989	0.000	31.522	57.534	0.000	0.000	107.435	129.998
0B 0177	0BCTSNC	0.000	0.000	48.387	0.000	0.000	107.330	129.872	15.414	31.312	48.113	66.366	85.775	106.657	128.863
0B 0178	0BCTSND	0.000	0.000	48.387	0.000	0.000	107.330	129.851	15.414	31.312	48.113	66.366	85.775	106.657	128.863
0B 0179	0BCASNA	0.000	0.000	0.000	0.000	85.859	107.561	129.977	15.477	31.522	48.176	66.471	85.292	106.699	128.884
0B 0180	0BCASNB	15.477	31.522	48.176	66.471	85.271	106.699	128.905	0.000	31.522	48.176	66.850	85.859	107.519	129.998
0B 0181	0BCATNA	15.393	31.312	47.945	66.009	85.313	106.678	128.884	0.000	31.543	0.000	66.471	85.838	107.224	130.019
0B 0182	0BCATNB	15.393	31.312	47.945	66.009	85.334	106.678	128.884	0.000	31.312	48.282	66.450	85.838	107.245	129.956
0B 0183	0BCAANA	15.393	31.312	47.924	65.988	85.250	106.678	128.863	0.000	31.522	48.197	66.492	85.881	107.498	130.040
0B 0184	0BCAANB	15.393	31.312	47.924	65.988	85.229	106.678	128.884	0.000	31.543	48.197	66.492	85.881	107.330	130.040
0B 0185	0BCAANC	15.393	31.312	47.945	65.988	85.271	106.699	128.926	0.000	31.543	48.197	66.555	85.923	107.561	130.146
0B 0186	0BCAAND	15.393	31.312	47.966	66.009	85.292	106.699	128.926	0.000	31.543	48.197	66.555	85.923	107.435	130.146
0B 0187	0BCSANA	15.477	31.269	48.176	66.471	85.208	106.678	128.863	0.000	31.522	48.471	0.000	85.902	107.540	130.061
0B 0188	0BCSANB	15.477	31.290	48.176	66.471	85.271	106.678	128.863	0.000	31.522	0.000	0.000	85.881	107.540	130.040
0B 0189	0BCSSNA	0.000	0.000	0.000	66.850	0.000	107.477	130.019	15.477	31.522	48.176	66.492	85.881	106.678	128.842
0B 0190	0BCSSNB	0.000	0.000	0.000	66.850	0.000	107.477	130.019	15.477	31.522	48.176	66.492	85.881	106.678	128.863
0B 0191	0BCSTNA	15.435	31.312	47.966	65.967	85.460	106.699	128.926	0.000	31.543	48.197	66.513	85.902	107.498	130.061
0B 0192	0BCSTNB	15.414	31.312	48.176	65.945	85.902	106.699	128.926	0.000	31.543	0.000	66.513	0.000	107.477	130.061
0B 0193	0BCSTNC	15.414	31.312	48.176	65.967	85.397	106.678	128.863	0.000	31.543	0.000	66.471	85.881	107.435	130.061
0B 0194	0BCSTND	15.414	31.312	48.176	66.492	85.460	106.657	128.863	0.000	31.543	0.000	0.000	85.881	107.456	130.040

Table A1.1 Continued

Test Serial Number	Filename	Mode Frequencies / Hz													
		Set 1 for Mode number:							Set 2 for Mode number:						
		1	2	3	4	5	6	7	1	2	3	4	5	6	7
0B 0195	0BETTNA	15.056	30.618	46.936	64.747	83.757	104.701	126.508	0.000	30.618	47.188	0.000	84.366	105.689	146.464
0B 0196	0BETTNB	15.056	30.618	46.936	64.747	83.588	104.680	126.592	0.000	30.618	47.188	65.462	84.345	105.689	146.569
0B 0197	0BETANA	0.000	0.000	47.272	0.000	84.198	0.000	146.527	15.056	30.618	46.936	64.726	83.504	104.680	126.529
0B 0198	0BETANB	15.056	30.618	46.936	64.726	83.546	104.680	126.529	0.000	30.870	47.251	0.000	84.198	105.479	146.590
0B 0199	0BETSNA	15.056	30.597	47.083	64.705	83.736	104.659	126.613	0.000	30.786	0.000	65.041	84.198	105.521	127.832
0B 0200	0BETSNB	0.000	0.000	0.000	65.020	84.177	0.000	127.811	15.056	30.597	47.083	64.726	82.873	104.659	126.634
0B 0201	0BEASNA	15.120	30.786	47.104	65.083	84.198	105.395	127.896	0.000	30.554	46.810	64.663	83.357	104.638	126.571
0B 0202	0BEASNB	15.120	30.554	47.104	64.663	83.357	104.638	126.508	0.000	30.786	0.000	65.083	84.177	0.000	127.853
0B 0203	0BEATNA	0.000	0.000	0.000	0.000	84.135	105.668	146.527	15.035	30.576	46.852	64.663	83.231	104.596	126.381
0B 0204	0BEATNB	15.035	30.576	46.852	64.663	83.273	104.596	126.466	0.000	30.576	47.083	0.000	84.135	105.647	146.548
0B 0205	0BEAANA	15.014	30.576	46.852	64.642	83.252	104.575	126.381	0.000	30.786	47.125	65.083	84.198	105.521	127.811
0B 0206	0BEAANB	15.014	30.576	46.831	64.642	83.147	104.575	126.360	0.000	30.786	47.125	65.083	84.198	105.605	127.874
0B 0207	0BESANA	15.141	30.786	47.104	65.062	84.514	104.596	127.811	0.000	30.533	0.000	64.621	84.198	104.175	126.424
0B 0208	0BESANB	15.120	30.786	47.104	65.041	84.198	106.194	127.874	0.000	30.533	0.000	64.621	82.789	104.575	126.339
0B 0209	0BESSNA	0.000	0.000	0.000	65.041	0.000	105.500	127.832	15.120	30.786	47.083	64.600	84.177	104.575	126.360
0B 0210	0BESSNB	0.000	0.000	0.000	65.041	0.000	105.521	127.832	15.120	30.765	47.083	64.600	84.177	104.554	126.445
0B 0211	0BESTNA	15.077	30.786	47.083	65.041	84.177	105.500	127.917	0.000	30.533	46.831	64.663	0.000	104.596	126.339
0B 0212	0BESTNB	15.077	30.786	47.083	65.041	84.177	105.500	127.938	0.000	30.533	46.831	64.663	83.336	104.575	126.255

Table A1.1 Continued

Test Serial Number	Filename	Mode Frequencies / Hz													
		Set 1 for Mode number:							Set 2 for Mode number:						
		1	2	3	4	5	6	7	1	2	3	4	5	6	7
13A 0100	13ATTCDA	-	65.294	103.439	144.130	-	-	-	-	66.345	104.533	146.169	-	-	-
13A 0101	13ATTCDB	-	66.324	104.491	146.169	-	-	-	-	65.294	103.418	144.130	-	-	-
13A 0102	13ATACDA	-	65.315	103.481	144.277	-	-	-	-	-	-	-	-	-	-
13A 0103	13ATACDB	-	65.294	103.460	144.256	-	-	-	-	-	-	-	-	-	-
13A 0104	13ATSCDA	-	65.420	103.397	144.277	-	-	-	-	-	-	-	-	-	-
13A 0105	13ATSCDB	-	65.378	103.334	144.214	-	-	-	-	66.534	104.470	145.623	-	-	-
13A 0106	13AASCDA	-	66.219	104.302	145.791	-	-	-	-	-	-	-	-	-	-
13A 0107	13AASCDB	-	66.219	104.280	145.770	-	-	-	-	-	-	-	-	-	-
13A 0108	13AATCDA	-	65.315	103.376	144.108	-	-	-	-	66.240	104.196	145.391	-	-	-
13A 0109	13AATCDB	-	65.315	103.376	144.108	-	-	-	-	-	-	-	-	-	-
13A 0110	13AAACDA	-	65.315	103.376	144.130	-	-	-	-	66.282	104.449	146.043	-	-	-
13A 0111	13AAACDB	-	65.315	103.418	144.151	-	-	-	-	66.282	104.470	146.127	-	-	-
13A 0112	13ASACDA	-	65.315	103.397	144.066	-	-	-	-	66.177	104.470	146.085	-	-	-
13A 0113	13ASACDB	-	65.294	103.397	144.066	-	-	-	-	66.219	104.449	146.085	-	-	-
13A 0114	13ASSCDA	-	66.240	104.323	145.833	-	-	-	-	-	-	-	-	-	-
13A 0115	13ASSCDB	-	66.198	104.259	145.749	-	-	-	-	-	-	-	-	-	-
13A 0116	13ASTCDA	-	65.357	103.313	144.066	-	-	-	-	-	-	-	-	-	-
13A 0117	13ASTCDB	-	65.357	103.292	144.045	-	-	-	-	66.366	104.259	145.812	-	-	-
13A 0118	13ATTCDSA	-	111.430	178.827	257.053	-	-	-	-	112.419	181.665	260.354	-	-	-
13A 0119	13ATTCDSB	-	111.514	178.911	257.263	-	-	-	-	112.440	181.729	260.543	-	-	-
13A 0120	13ATACDSA	-	111.136	177.523	257.221	-	-	-	-	111.683	178.911	258.903	-	-	-
13A 0121	13ATACDSB	-	111.661	177.060	257.116	-	-	-	-	112.503	178.827	258.777	-	-	-
13A 0122	13ATSCDSA	-	111.788	178.785	257.263	-	-	-	-	112.292	179.731	258.693	-	-	-
13A 0123	13ATSCDSB	-	111.893	178.995	257.494	-	-	-	-	112.650	179.731	259.618	-	-	-
13A 0124	13AASCDSA	-	111.556	178.553	256.758	-	-	-	-	112.229	180.299	258.504	-	-	-
13A 0125	13AASCDSB	-	111.451	178.427	256.548	-	-	-	-	112.229	180.299	258.272	-	-	-
13A 0126	13AATCDSA	-	111.136	178.785	256.905	-	-	-	-	111.430	179.710	258.609	-	-	-
13A 0127	13AATCDSB	-	111.388	178.658	256.737	-	-	-	-	112.082	179.499	258.504	-	-	-
13A 0128	13AAACDSA	-	111.409	178.469	256.485	-	-	-	-	111.998	180.299	258.272	-	-	-
13A 0129	13AAACDSB	-	111.619	178.721	252.532	-	-	-	-	112.145	180.845	257.137	-	-	-
13A 0130	13ASACDSA	-	111.472	178.532	256.506	-	-	-	-	112.019	180.299	258.335	-	-	-
13A 0131	13ASACDSB	-	111.472	178.553	253.373	-	-	-	-	111.998	180.299	256.569	-	-	-
13A 0132	13ASSCDSA	-	111.598	178.490	256.611	-	-	-	-	112.040	180.299	259.892	-	-	-
13A 0133	13ASSCDSB	-	111.451	178.343	256.317	-	-	-	-	111.956	180.299	259.681	-	-	-
13A 0134	13ASTCDSA	-	111.683	178.763	257.074	-	-	-	-	112.040	180.278	259.071	-	-	-
13A 0135	13ASTCDSB	-	111.598	178.595	256.884	-	-	-	-	111.977	179.710	258.483	-	-	-

Table A1.1 Continued

Test Serial Number	Filename	Mode Frequencies / Hz													
		Set 1 for Mode number:							Set 2 for Mode number:						
		1	2	3	4	5	6	7	1	2	3	4	5	6	7
13A 0136	13ATTCA	-	67.144	105.626	147.578	-	-	-	-	67.733	106.488	150.186	-	-	-
13A 0137	13ATTCB	-	67.123	105.605	147.599	-	-	-	-	67.733	106.467	150.165	-	-	-
13A 0138	13ATACA	-	67.186	105.731	147.831	-	-	-	-	-	-	-	-	-	-
13A 0139	13ATACB	-	67.144	105.731	147.767	-	-	-	-	67.796	0.000	149.029	-	-	-
13A 0140	13ATSCA	-	67.607	106.194	149.260	-	-	-	-	67.039	105.710	147.978	-	-	-
13A 0141	13ATSCB	-	-	-	-	-	-	-	-	66.997	105.689	147.957	-	-	-
13A 0142	13AASCA	-	67.396	106.678	148.903	-	-	-	-	66.513	105.605	147.683	-	-	-
13A 0143	13AASCB	-	67.481	106.657	148.882	-	-	-	-	66.534	105.563	147.725	-	-	-
13A 0144	13AATCA	-	67.081	105.563	147.599	-	-	-	-	-	-	-	-	-	-
13A 0145	13AATCB	-	67.102	105.626	146.085	-	-	-	-	-	-	-	-	-	-
13A 0146	13AAACA	-	-	-	-	-	-	-	-	67.102	105.647	147.767	-	-	-
13A 0147	13AAACB	-	67.102	105.647	147.725	-	-	-	-	67.691	106.425	148.693	-	-	-
13A 0148	13ASACA	-	67.060	105.647	147.641	-	-	-	-	67.544	106.425	149.870	-	-	-
13A 0149	13ASACB	-	66.534	105.668	147.767	-	-	-	-	67.523	106.804	149.870	-	-	-
13A 0150	13ASSCA	-	67.460	106.278	149.702	-	-	-	-	-	-	-	-	-	-
13A 0151	13ASSCB	-	67.460	106.236	149.660	-	-	-	-	66.724	105.479	148.945	-	-	-
13A 0152	13ASTCA	-	67.102	105.563	147.683	-	-	-	-	67.964	0.000	149.282	-	-	-
13A 0153	13ASTCB	-	67.144	105.584	147.662	-	-	-	-	-	-	-	-	-	-
13A 0154	13ATTCSA	-	111.367	178.532	257.011	-	-	-	-	112.292	181.413	260.438	-	-	-
13A 0155	13ATTCSB	-	111.430	178.616	257.263	-	-	-	-	112.313	181.413	260.417	-	-	-
13A 0156	13ATACSA	-	111.577	178.637	257.389	-	-	-	-	-	-	-	-	-	-
13A 0157	13ATACSB	-	111.577	178.553	257.242	-	-	-	-	112.440	179.710	258.819	-	-	-
13A 0158	13ATSCSA	-	111.704	178.511	257.137	-	-	-	-	-	-	-	-	-	-
13A 0159	13ATSCSB	-	109.811	178.637	257.494	-	-	-	-	111.725	180.404	259.219	-	-	-
13A 0160	13AASCSA	-	111.640	178.553	257.305	-	-	-	-	-	-	-	-	-	-
13A 0161	13AASCSB	-	111.619	178.490	257.221	-	-	-	-	-	-	-	-	-	-
13A 0162	13AATCSA	-	111.472	178.595	257.242	-	-	-	-	112.397	179.710	258.798	-	-	-
13A 0163	13AATCSB	-	111.493	178.595	257.158	-	-	-	-	112.019	179.710	258.777	-	-	-
13A 0164	13AAACSA	-	111.451	178.385	256.842	-	-	-	-	-	-	-	-	-	-
13A 0165	13AAACSB	-	111.598	178.616	257.242	-	-	-	-	-	-	-	-	-	-
13A 0166	13ASACSA	-	111.577	178.469	257.221	-	-	-	-	-	-	-	-	-	-
13A 0167	13ASACSB	-	111.535	178.448	256.990	-	-	-	-	-	-	-	-	-	-
13A 0168	13ASSCSA	-	112.208	180.299	260.249	-	-	-	-	111.619	179.731	257.074	-	-	-
13A 0169	13ASSCSB	-	112.166	180.299	260.102	-	-	-	-	111.598	179.731	256.990	-	-	-
13A 0170	13ASTCSA	-	111.746	178.763	257.789	-	-	-	-	112.187	180.299	259.702	-	-	-
13A 0171	13ASTCSB	-	111.704	178.637	257.410	-	-	-	-	112.103	180.278	259.492	-	-	-

Table A1.1 Continued

Test Serial Number	Filename	Mode Frequencies / Hz													
		Set 1 for Mode number:							Set 2 for Mode number:						
		1	2	3	4	5	6	7	1	2	3	4	5	6	7
13A 0172	13ATTCC	-	67.081	105.563	147.620	-	-	-	-	-	-	-	-	-	-
13A 0173	13ATTCD	-	67.081	105.584	147.641	-	-	-	-	-	-	-	-	-	-
13A 0174	13AAACC	-	67.102	105.563	147.662	-	-	-	-	-	-	-	-	-	-
13A 0175	13AAACD	-	67.102	105.563	147.683	-	-	-	-	-	-	-	-	-	-
13A 0176	13ASSCC	-	67.396	106.131	148.903	-	-	-	-	-	-	-	-	-	-
13A 0177	13ASSCD	-	67.375	106.110	148.882	-	-	-	-	-	-	-	-	-	-
13A 0178	13ATTCSC	-	111.346	178.490	256.842	-	-	-	-	112.250	181.119	260.501	-	-	-
13A 0179	13ATTCSD	-	111.409	178.469	257.053	-	-	-	-	112.271	181.245	260.585	-	-	-
13A 0180	13AAACSC	-	111.514	178.406	257.011	-	-	-	-	112.587	180.299	258.756	-	-	-
13A 0181	13AAACSD	-	111.514	178.469	252.300	-	-	-	-	112.061	180.614	257.032	-	-	-
13A 0182	13ASSCSC	-	112.566	181.308	259.828	-	-	-	-	111.704	180.299	256.653	-	-	-
13A 0183	13ASSCSD	-	112.566	180.299	259.849	-	-	-	-	111.577	178.259	256.527	-	-	-
13A 0184	13ATTUA	-	67.018	105.837	149.134	-	-	-	-	67.502	106.383	150.669	-	-	-
13A 0185	13ATTUB	-	67.018	105.795	149.071	-	-	-	-	67.481	106.341	150.648	-	-	-
13A 0186	13ATAUA	-	66.492	105.858	149.155	-	-	-	-	-	-	-	-	-	-
13A 0187	13ATAUB	-	67.060	105.837	149.134	-	-	-	-	-	-	-	-	-	-
13A 0188	13ATSUA	-	66.808	105.752	149.071	-	-	-	-	67.207	106.131	150.396	-	-	-
13A 0189	13ATSUB	-	66.808	105.731	149.050	-	-	-	-	67.186	106.110	150.438	-	-	-
13A 0190	13AASUA	-	66.345	105.668	148.924	-	-	-	-	67.060	106.404	149.723	-	-	-
13A 0191	13AASUB	-	67.081	106.404	149.702	-	-	-	-	66.429	105.668	148.924	-	-	-
13A 0192	13AATUA	-	66.934	105.731	149.092	-	-	-	-	-	-	-	-	-	-
13A 0193	13AATUB	-	66.892	105.710	149.050	-	-	-	-	-	-	-	-	-	-
13A 0194	13AAAUA	-	66.955	106.173	149.870	-	-	-	-	66.387	105.752	149.092	-	-	-
13A 0195	13AAAUB	-	66.976	106.173	149.870	-	-	-	-	66.513	105.752	149.092	-	-	-
13A 0196	13ASAUA	-	66.429	105.752	149.071	-	-	-	-	67.249	106.636	149.891	-	-	-
13A 0197	13ASAUB	-	66.913	106.194	149.933	-	-	-	-	66.450	105.773	149.113	-	-	-
13A 0198	13ASSUA	-	66.408	105.668	148.987	-	-	-	-	67.081	106.194	149.765	-	-	-
13A 0199	13ASSUB	-	66.387	105.605	148.861	-	-	-	-	67.060	106.131	149.681	-	-	-
13A 0200	13ASTUA	-	66.534	105.752	149.176	-	-	-	-	-	-	-	-	-	-
13A 0201	13ASTUB	-	66.597	105.710	149.155	-	-	-	-	-	-	-	-	-	-
13A 0202	13ATTUSA	-	111.893	178.742	258.567	-	-	-	-	112.713	182.107	262.793	-	-	-
13A 0203	13ATTUSB	-	111.914	178.742	258.756	-	-	-	-	112.692	182.086	262.857	-	-	-
13A 0204	13ATAUSA	-	111.872	178.658	258.398	-	-	-	-	-	-	-	-	-	-
13A 0205	13ATAUSB	-	111.935	178.721	258.588	-	-	-	-	-	-	-	-	-	-
13A 0206	13ATSUSA	-	112.271	178.995	259.408	-	-	-	-	112.923	181.392	261.679	-	-	-
13A 0207	13ATSUSB	-	112.229	181.350	263.635	-	-	-	-	110.316	178.806	259.345	-	-	-
13A 0208	13AASUSA	-	-	-	-	-	-	-	-	112.019	179.731	258.798	-	-	-
13A 0209	13AASUSB	-	111.851	180.299	258.504	-	-	-	-	112.503	180.908	260.354	-	-	-
13A 0210	13AATUSA	-	111.809	178.742	258.525	-	-	-	-	-	-	-	-	-	-
13A 0211	13AATUSB	-	111.746	178.658	258.251	-	-	-	-	-	-	-	-	-	-
13A 0212	13AAAUSA	-	111.788	178.574	258.188	-	-	-	-	-	-	-	-	-	-
13A 0213	13AAAUSB	-	-	-	-	-	-	-	-	111.809	178.595	258.335	-	-	-
13A 0214	13ASAUSA	-	-	-	-	-	-	-	-	111.767	180.299	258.125	-	-	-
13A 0215	13ASAUSB	-	111.725	178.427	258.125	-	-	-	-	112.419	180.824	262.226	-	-	-
13A 0216	13ASSUSA	-	112.461	180.887	261.700	-	-	-	-	111.893	180.299	258.146	-	-	-
13A 0217	13ASSUSB	-	112.482	180.908	261.826	-	-	-	-	111.998	180.299	258.167	-	-	-
13A 0218	13ASTUSA	-	112.881	181.119	261.258	-	-	-	-	112.082	178.827	258.987	-	-	-
13A 0219	13ASTUSB	-	110.379	178.742	258.903	-	-	-	-	112.061	181.266	261.364	-	-	-

Table A1.1 Continued

Test Serial Number	Filename	Mode Frequencies / Hz													
		Set 1 for Mode number:							Set 2 for Mode number:						
		1	2	3	4	5	6	7	1	2	3	4	5	6	7
13B 0100	13BCTBE	-	68.868	107.771	150.669	-	-	-	-	-	-	-	-	-	-
13B 0101	13BCTBF	-	68.911	107.813	150.775	-	-	-	-	-	-	-	-	-	-
13B 0102	13BCABE	-	68.932	107.834	150.817	-	-	-	-	71.076	112.355	158.828	-	-	-
13B 0103	13BCABF	-	68.889	107.813	150.754	-	-	-	-	71.055	112.292	158.744	-	-	-
13B 0104	13BCSBF	-	68.932	0.000	150.943	-	-	-	-	71.034	112.271	158.744	-	-	-
13B 0105	13BCSBG	-	68.953	107.834	150.922	-	-	-	-	71.034	112.271	158.744	-	-	-
13B 0106	13BCTBE	-	68.868	0.000	150.711	-	-	-	-	71.076	112.355	158.892	-	-	-
13B 0107	13BCTBF	-	-	-	-	-	-	-	-	71.076	112.355	158.934	-	-	-
13B 0108	13BCABE	-	-	-	-	-	-	-	-	71.055	112.313	158.807	-	-	-
13B 0109	13BCABF	-	-	-	-	-	-	-	-	71.034	112.271	158.723	-	-	-
13B 0110	13BCSBF	-	-	-	-	-	-	-	-	71.034	112.271	158.744	-	-	-
13B 0111	13BCSBG	-	-	-	-	-	-	-	-	71.034	112.271	158.744	-	-	-
13B 0112	13BCTBSF	-	110.147	173.780	245.760	-	-	-	-	-	-	-	-	-	-
13B 0113	13BCTBSG	-	110.147	173.759	245.739	-	-	-	-	-	-	-	-	-	-
13B 0114	13BCABSE	-	110.232	173.906	246.055	-	-	-	-	-	-	-	-	-	-
13B 0115	13BCABSF	-	110.253	173.969	246.202	-	-	-	-	-	-	-	-	-	-
13B 0116	13BCSBSE	-	119.106	173.885	246.328	-	-	-	-	120.304	186.397	283.359	-	-	-
13B 0117	13BCSBSF	-	-	-	-	-	-	-	-	119.148	194.976	283.549	-	-	-
13B 0118	13BCSBSG	-	110.295	174.011	246.370	-	-	-	-	119.148	194.682	283.507	-	-	-
13B 0119	13BCTBSH	-	110.232	173.864	245.971	-	-	-	-	-	-	-	-	-	-
13B 0120	13BCABSG	-	110.274	174.011	246.307	-	-	-	-	-	-	-	-	-	-
13B 0121	13BCTBSF	-	110.189	173.696	245.781	-	-	-	-	119.169	194.976	283.612	-	-	-
13B 0122	13BCTBSG	-	110.168	173.696	245.760	-	-	-	-	119.169	194.976	283.591	-	-	-
13B 0123	13BCABSE	-	-	-	-	-	-	-	-	119.148	194.913	283.570	-	-	-
13B 0124	13BCABSF	-	-	-	-	-	-	-	-	119.148	194.955	283.633	-	-	-
13B 0125	13BCSBSE	-	-	-	-	-	-	-	-	119.106	194.808	283.380	-	-	-
13B 0126	13BCSBSF	-	-	-	-	-	-	-	-	119.148	194.913	283.549	-	-	-
13B 0127	13BCSBSG	-	-	-	-	-	-	-	-	119.148	194.892	283.528	-	-	-
13B 0128	13BCTBSH	-	110.295	173.780	245.992	-	-	-	-	119.190	195.019	283.591	-	-	-
13B 0129	13BCABSG	-	-	-	-	-	-	-	-	119.169	194.955	283.570	-	-	-
13B 0130	13BCTCA	-	68.763	107.414	150.207	-	-	-	-	-	-	-	-	-	-
13B 0131	13BCTCB	-	68.700	107.372	150.144	-	-	-	-	-	-	-	-	-	-
13B 0132	13BCACA	-	68.679	107.330	150.102	-	-	-	-	-	-	-	-	-	-
13B 0133	13BCACB	-	68.679	107.351	150.102	-	-	-	-	-	-	-	-	-	-
13B 0134	13BCSCA	-	68.763	107.456	150.312	-	-	-	-	70.572	111.598	157.840	-	-	-
13B 0135	13BCSCB	-	68.742	107.435	150.270	-	-	-	-	70.551	111.577	157.798	-	-	-
13B 0136	13BCTCA	-	68.700	107.372	150.207	-	-	-	-	70.656	111.704	158.071	-	-	-
13B 0137	13BCTCB	-	68.679	107.309	150.144	-	-	-	-	70.614	111.704	157.987	-	-	-
13B 0138	13BCACA	-	-	-	-	-	-	-	-	70.551	111.577	157.777	-	-	-
13B 0139	13BCACB	-	-	-	-	-	-	-	-	70.551	111.577	157.777	-	-	-
13B 0140	13BCSCA	-	-	-	-	-	-	-	-	70.572	111.619	157.840	-	-	-
13B 0141	13BCSCB	-	-	-	-	-	-	-	-	70.551	111.598	157.798	-	-	-

Table A1.1 Continued

Test Serial Number	Filename	Mode Frequencies / Hz													
		Set 1 for Mode number:							Set 2 for Mode number:						
		1	2	3	4	5	6	7	1	2	3	4	5	6	7
13B 0142	13BCTCSA	-	110.000	173.359	245.193	-	-	-	-	-	-	-	-	-	-
13B 0143	13BCTCSB	-	109.958	173.275	245.024	-	-	-	-	-	-	-	-	-	-
13B 0144	13BCACSA	-	110.084	173.569	245.613	-	-	-	-	119.085	194.955	283.528	-	-	-
13B 0145	13BCACSB	-	110.063	173.485	245.697	-	-	-	-	119.064	194.682	283.464	-	-	-
13B 0146	13BCSCSA	-	110.021	173.422	245.403	-	-	-	-	119.000	194.451	283.254	-	-	-
13B 0147	13BCSCSB	-	110.000	173.380	245.529	-	-	-	-	118.979	194.598	283.170	-	-	-
13B 0148	13BCTCSA	-	110.021	173.296	245.235	-	-	-	-	119.106	194.871	283.570	-	-	-
13B 0149	13BCTCSB	-	109.958	173.212	245.024	-	-	-	-	119.085	194.829	283.528	-	-	-
13B 0150	13BCACSA	-	-	-	-	-	-	-	-	119.085	194.850	283.549	-	-	-
13B 0151	13BCACSB	-	-	-	-	-	-	-	-	119.064	194.808	283.464	-	-	-
13B 0152	13BCSCSA	-	-	-	-	-	-	-	-	119.000	194.703	283.254	-	-	-
13B 0153	13BCSCSB	-	-	-	-	-	-	-	-	118.979	194.640	283.170	-	-	-
13B 0154	13BCTCAC	-	68.637	107.267	149.954	-	-	-	-	-	-	-	-	-	-
13B 0155	13BCTCD	-	68.595	107.182	149.828	-	-	-	-	-	-	-	-	-	-
13B 0156	13BCACC	-	68.595	107.161	149.786	-	-	-	-	-	-	-	-	-	-
13B 0157	13BCACD	-	68.595	107.140	149.786	-	-	-	-	-	-	-	-	-	-
13B 0158	13BCSCC	-	68.658	107.267	149.975	-	-	-	-	70.446	111.430	157.567	-	-	-
13B 0159	13BCSCD	-	68.574	107.182	150.018	-	-	-	-	70.446	111.430	157.567	-	-	-
13B 0160	13BCSCE	-	68.637	107.224	149.954	-	-	-	-	70.467	111.409	157.525	-	-	-
13B 0161	13BCTCAC	-	68.637	107.203	149.954	-	-	-	-	70.572	111.598	157.819	-	-	-
13B 0162	13BCTCD	-	68.574	107.119	149.828	-	-	-	-	-	-	-	-	-	-
13B 0163	13BCACC	-	-	-	-	-	-	-	-	70.467	111.472	157.588	-	-	-
13B 0164	13BCACD	-	-	-	-	-	-	-	-	70.446	111.430	157.546	-	-	-
13B 0165	13BCSCC	-	-	-	-	-	-	-	-	70.446	111.451	157.567	-	-	-
13B 0166	13BCSCD	-	-	-	-	-	-	-	-	70.446	111.430	157.567	-	-	-
13B 0167	13BCSCE	-	-	-	-	-	-	-	-	70.425	111.430	157.525	-	-	-
13B 0168	13BCTCSC	-	109.937	173.296	245.087	-	-	-	-	-	-	-	-	-	-
13B 0169	13BCTCSD	-	109.937	173.254	245.024	-	-	-	-	-	-	-	-	-	-
13B 0170	13BCACSC	-	110.000	173.422	245.382	-	-	-	-	-	-	-	-	-	-
13B 0171	13BCACSD	-	109.979	173.359	245.277	-	-	-	-	-	-	-	-	-	-
13B 0172	13BCSCSC	-	109.979	173.359	245.508	-	-	-	-	118.979	194.577	283.275	-	-	-
13B 0173	13BCSCSD	-	110.000	173.401	245.487	-	-	-	-	118.979	194.493	283.254	-	-	-
13B 0174	13BCTCSC	-	109.958	173.233	245.108	-	-	-	-	119.042	194.808	283.486	-	-	-
13B 0175	13BCTCSD	-	109.958	173.170	245.045	-	-	-	-	119.042	194.787	283.443	-	-	-
13B 0176	13BCACSC	-	-	-	-	-	-	-	-	119.021	194.745	283.380	-	-	-
13B 0177	13BCACSD	-	-	-	-	-	-	-	-	119.000	194.703	283.275	-	-	-
13B 0178	13BCSCSC	-	-	-	-	-	-	-	-	119.000	194.703	283.275	-	-	-
13B 0179	13BCSCSD	-	-	-	-	-	-	-	-	119.000	194.682	283.254	-	-	-

Table A1.1 Continued

Test Serial Number	Filename	Mode Frequencies / Hz													
		Set 1 for Mode number:							Set 2 for Mode number:						
		1	2	3	4	5	6	7	1	2	3	4	5	6	7
13B 0180	13BCTZA	-	68.196	106.488	148.735	-	-	-	-	-	-	-	-	-	-
13B 0181	13BCTZB	-	68.196	106.467	148.672	-	-	-	-	-	-	-	-	-	-
13B 0182	13BCAZA	-	68.196	106.488	148.693	-	-	-	-	-	-	-	-	-	-
13B 0183	13BCAZB	-	68.175	106.446	148.630	-	-	-	-	-	-	-	-	-	-
13B 0184	13BCSZA	-	68.217	106.552	148.798	-	-	-	-	69.857	110.505	156.200	-	-	-
13B 0185	13BCSZB	-	68.217	106.467	148.714	-	-	-	-	69.815	110.421	156.053	-	-	-
13B 0186	13BCSZC	-	68.175	106.467	148.735	-	-	-	-	69.815	110.463	156.095	-	-	-
13B 0187	13BCTZA	-	68.196	106.552	148.756	-	-	-	-	69.899	110.589	156.347	-	-	-
13B 0188	13BCTZB	-	-	-	-	-	-	-	-	69.899	110.610	156.347	-	-	-
13B 0189	13BCAZA	-	-	-	-	-	-	-	-	69.857	110.526	156.263	-	-	-
13B 0190	13BCAZB	-	-	-	-	-	-	-	-	69.836	110.484	156.116	-	-	-
13B 0191	13BCSZA	-	-	-	-	-	-	-	-	69.857	110.526	156.200	-	-	-
13B 0192	13BCSZB	-	-	-	-	-	-	-	-	69.815	110.442	156.053	-	-	-
13B 0193	13BCSZC	-	-	-	-	-	-	-	-	69.815	110.463	156.095	-	-	-
13B 0194	13BCTZSA	-	109.769	172.812	244.499	-	-	-	-	-	-	-	-	-	-
13B 0195	13BCTZSB	-	109.790	172.854	244.646	-	-	-	-	-	-	-	-	-	-
13B 0196	13BCAZSA	-	109.832	172.960	244.877	-	-	-	-	-	-	-	-	-	-
13B 0197	13BCAZSB	-	109.790	172.897	244.730	-	-	-	-	-	-	-	-	-	-
13B 0198	13BCSZSA	-	109.916	173.065	245.235	-	-	-	-	-	-	-	-	-	-
13B 0199	13BCSZSB	-	109.937	173.044	245.256	-	-	-	-	118.811	183.053	283.065	-	-	-
13B 0200	13BCTZSA	-	109.790	172.728	244.541	-	-	-	-	118.895	194.556	283.233	-	-	-
13B 0201	13BCTZSB	-	109.811	172.791	244.667	-	-	-	-	118.895	194.598	283.317	-	-	-
13B 0202	13BCAZSA	-	-	-	-	-	-	-	-	118.853	194.493	283.128	-	-	-
13B 0203	13BCAZSB	-	-	-	-	-	-	-	-	118.811	194.367	282.897	-	-	-
13B 0204	13BCSZSA	-	-	-	-	-	-	-	-	118.832	194.451	283.065	-	-	-
13B 0205	13BCSZSB	-	-	-	-	-	-	-	-	118.811	194.451	283.065	-	-	-

Table A1.2- Analysis results for each reported vibration test.

Test Serial Number	Date	Condition	Configuration Per Table 1.2	Orientation (I,A)	Replication	Modes Used for Analysis	Set 1 Estimated Tension (Uncorrected)		Set 1 Stiffness		Set 2 Estimated Tension (Uncorrected)		Set 2 Stiffness		Set 1-2 Average Tension (Uncorrected)	
							kN	klbf	kN-m^2	Mlbf-in^2	kN	klbf	kN-m^2	Mlbf-in^2	kN	klbf
0A 0100	8/2/2005	Before first cut	0A 1	TT	C	1-7	1429	321	112	39	1446	325	71	25	1437	323
0A 0101				TT	D		1429	321	112	39	1445	325	71	25	1437	323
0A 0102				TA	C		1430	321	112	39	1445	325	71	25	1437	323
0A 0103				TA	D		1431	322	112	39	1445	325	71	25	1438	323
0A 0104				TS	C		1427	321	113	39	1445	325	71	25	1436	323
0A 0105				TS	D		1427	321	113	39	1445	325	71	25	1436	323
0A 0106				AS	A		1447	325	71	25	1386	312	126	44	1417	318
0A 0107				AS	B		1448	325	71	25	1386	312	126	44	1417	319
0A 0108				AT	A		1448	325	71	25	1423	320	114	40	1435	323
0A 0109				AT	B		1447	325	71	25	1423	320	114	40	1435	323
0A 0110				AA	A		1448	326	71	25					1448	326
0A 0111				AA	B		1450	326	70	24					1450	326
0A 0112				SA	C		1448	326	70	25					1448	326
0A 0113				SA	D		1426	321	113	39	1445	325	71	25	1436	323
0A 0114				SS	C		1430	321	112	39	1445	325	71	25	1437	323
0A 0115				SS	D		1430	321	112	39	1445	325	71	25	1437	323
0A 0116				ST	C		1427	321	112	39	1445	325	71	25	1436	323
0A 0117				ST	D		1428	321	112	39	1445	325	71	25	1436	323

Table A1.2 Continued

Test Serial Number	Date	Condition	Configuration Per Table 1.2	Orientation (I,A)	Replication	Modes Used for Analysis	Set 1 Estimated Tension (Uncorrected)		Set 1 Stiffness		Set 2 Estimated Tension (Uncorrected)		Set 2 Stiffness		Set 1-2 Average Tension (Uncorrected)	
							kN	klbf	kN-m^2	Mlbf-in^2	kN	klbf	kN-m^2	Mlbf-in^2	kN	klbf
0A 0118	8/4/2005	Before first cut	0A 11	TT	A	1-7	1434	322	110	38	1448	325	69	24	1441	324
0A 0119				TT	B		1434	322	110	38	1446	325	70	24	1440	324
0A 0120				TA	A		1436	323	110	38	1449	326	69	24	1442	324
0A 0121				TA	B		1435	323	110	38	1449	326	69	24	1442	324
0A 0122				TS	A		1433	322	110	38	1444	325	70	24	1439	323
0A 0123				TS	B		1433	322	110	38	1445	325	70	24	1439	323
0A 0124				AS	A		1446	325	70	24	1432	322	111	39	1439	323
0A 0125				AS	B		1446	325	70	24	1405	316	119	42	1425	320
0A 0126				AT	A		1435	323	110	38	1447	325	70	24	1441	324
0A 0127				AT	B		1436	323	109	38	1449	326	69	24	1443	324
0A 0128				AA	A		1442	324	70	24					1442	324
0A 0129				AA	B		1448	326	69	24	1409	317	119	41	1428	321
0A 0130				SA	A		1450	326	69	24	1405	316	119	42	1428	321
0A 0131				SA	B		1453	327	68	24	1405	316	119	42	1429	321
0A 0132				SS	A		1435	323	110	38	1435	323	71	25	1435	323
0A 0133				SS	B		1435	323	110	38	1435	323	71	25	1435	323
0A 0134				ST	A		1434	322	110	38	1444	325	70	24	1439	323
0A 0135				ST	B		1434	322	110	38	1444	325	70	24	1439	323

Table A1.2 Continued

Test Serial Number	Date	Condition	Configuration Per Table 1.2	Orientation (I,A)	Replication	Modes Used for Analysis	Set 1 Estimated Tension (Uncorrected)		Set 1 Stiffness		Set 2 Estimated Tension (Uncorrected)		Set 2 Stiffness		Set 1-2 Average Tension (Uncorrected)	
							kN	klbf	kN-m^2	Mlbf-in^2	kN	klbf	kN-m^2	Mlbf-in^2	kN	klbf
0A 0136	8/4/2005	After first cut	0A 11	TT	A	1-7	1450	326	115	40	1487	334	68	24	1469	330
0A 0137				TT	B		1454	327	113	40	1479	332	70	24	1466	330
0A 0138				TA	A		1454	327	114	40	1480	333	69	24	1467	330
0A 0139				TA	B		1454	327	114	40	1480	333	69	24	1467	330
0A 0140				TS	A		1454	327	113	40	1463	329	72	25	1458	328
0A 0141				TS	B		1454	327	114	40	1463	329	72	25	1458	328
0A 0142				AS	A		1478	332	69	24	1421	319	124	43	1450	326
0A 0143				AS	B		1449	326	115	40	1459	328	73	25	1454	327
0A 0144				AT	A		1453	327	114	40	1459	328	73	25	1456	327
0A 0145				AT	B		1453	327	114	40	1459	328	73	25	1456	327
0A 0146				AA	A		1480	333	69	24					1480	333
0A 0147				AA	B		1477	332	70	24					1477	332
0A 0148				SA	A		1478	332	69	24	1419	319	125	43	1449	326
0A 0149				SA	B		1477	332	70	24	1453	327	113	39	1465	329
0A 0150				SS	A		1477	332	70	24	1454	327	113	39	1466	330
0A 0151				SS	B		1454	327	113	40	1459	328	73	25	1457	327
0A 0152				ST	A		1453	327	113	40	1463	329	72	25	1458	328
0A 0153				ST	B		1453	327	114	40	1459	328	73	25	1456	327

Table A1.2 Continued

Test Serial Number	Date	Condition	Configuration Per Table 1.2	Orientation (I,A)	Replication	Modes Used for Analysis	Set 1 Estimated Tension (Uncorrected)		Set 1 Stiffness		Set 2 Estimated Tension (Uncorrected)		Set 2 Stiffness		Set 1-2 Average Tension (Uncorrected)	
							kN	klbf	kN-m^2	Mlbf-in^2	kN	klbf	kN-m^2	Mlbf-in^2	kN	klbf
0A 0154	8/4/2005	After second cut	0A 11	TT	A	1-7	1459	328	73	25	1442	324	116	40	1450	326
0A 0155				TT	B		1458	328	73	25	1442	324	116	40	1450	326
0A 0156				TA	A		1459	328	73	25	1443	324	116	40	1451	326
0A 0157				TA	B		1458	328	73	25	1433	322	117	41	1446	325
0A 0158				TS	A		1457	328	73	25	1442	324	116	40	1450	326
0A 0159				TS	B		1458	328	73	25	1433	322	117	41	1446	325
0A 0160				AS	A		1455	327	73	25					1455	327
0A 0161				AS	C		1455	327	73	26					1455	327
0A 0162				AT	A		1461	328	72	25	1435	323	117	41	1448	326
0A 0163				AT	B		1462	329	72	25	1435	323	117	41	1448	326
0A 0164				AA	A		1455	327	73	25					1455	327
0A 0165				AS	B		1455	327	73	25					1455	327
0A 0166				SA	A		1455	327	73	25					1455	327
0A 0167				SA	B		1455	327	73	25					1455	327
0A 0168				SS	A		1457	328	73	25	1443	324	116	40	1450	326
0A 0169				SS	B		1458	328	73	25	1442	324	116	40	1450	326
0A 0170				ST	A		1458	328	73	25	1442	324	116	40	1450	326
0A 0171				ST	B		1457	328	73	25	1442	324	116	40	1450	326

Table A1.2 Continued

Test Serial Number	Date	Condition	Configuration Per Table 1.2	Orientation (I,A)	Replication	Modes Used for Analysis	Set 1 Estimated Tension (Uncorrected)		Set 1 Stiffness		Set 2 Estimated Tension (Uncorrected)		Set 2 Stiffness		Set 1-2 Average Tension (Uncorrected)	
							kN	klbf	$kN\text{-}m^2$	$Mlbf\text{-}in^2$	kN	klbf	$kN\text{-}m^2$	$Mlbf\text{-}in^2$	kN	klbf
0B 0100	9/27/2005	Before first cut	0B 1	TT	A	1-7	1273	286	103	36	1256	282	116	41	1264	284
0B 0101				TT	B		1269	285	104	36					1269	285
0B 0102				TA	A		1268	285	104	36					1268	285
0B 0103				TA	B		1267	285	104	36					1267	285
0B 0104				TS	A		1270	286	105	36					1270	286
0B 0105				TS	B		1286	289	102	35					1286	289
0B 0106				TS	C		1293	291	101	35					1293	291
0B 0107				TS	D		1285	289	102	35					1285	289
0B 0108				TS	E		1285	289	102	35					1285	289
0B 0109				AS	A		1303	293	97	34	1258	283	113	39	1281	288
0B 0110				AS	B		1303	293	97	34	1259	283	112	39	1281	288
0B 0111				AS	C		1301	293	97	34					1301	293
0B 0112				AS	D		1301	293	97	34					1301	293
0B 0113				AT	A		1277	287	103	36					1277	287
0B 0114				AT	B		1269	285	104	36					1269	285
0B 0115				AA	A		1272	286	101	35	1283	288	105	37	1278	287
0B 0116				AA	B		1272	286	101	35	1284	289	105	37	1278	287
0B 0117				SA	A		1288	290	102	35	1274	287	108	38	1281	288
0B 0118				SA	B		1288	290	101	35	1257	283	111	39	1273	286
0B 0119				SS	A		1291	290	101	35	1285	289	102	35	1288	290
0B 0120				SS	B		1292	290	101	35	1285	289	102	36	1288	290
0B 0121				ST	A		1293	291	101	35	1285	289	102	36	1289	290
0B 0122				ST	B		1293	291	101	35	1285	289	102	36	1289	290
0B 0123				ST	C		1291	290	101	35	1265	284	111	39	1278	287
0B 0124				ST	D		1291	290	101	35					1286	289

Table A1.2 Continued

Test Serial Number	Date	Condition	Configuration Per Table 1.2	Orientation (I,A)	Replication	Modes Used for Analysis	Set 1 Estimated Tension (Uncorrected)		Set 1 Stiffness		Set 2 Estimated Tension (Uncorrected)		Set 2 Stiffness		Set 1-2 Average Tension (Uncorrected)	
							kN	klbf	$kN\text{-}m^2$	$Mlbf\text{-}in^2$	kN	klbf	$kN\text{-}m^2$	$Mlbf\text{-}in^2$	kN	klbf
0B 0125	9/27/2005	Before first cut	0B 3	TT	A	1-7	1278	287	103	36	1262	284	112	39	1270	286
0B 0126				TT	B		1279	287	103	36	1257	283	113	39	1268	285
0B 0127				TA	A		1305	293	96	33					1305	293
0B 0128				TA	B		1268	285	104	36					1268	285
0B 0129				TS	A		1275	287	104	36					1275	287
0B 0130				TS	B		1275	287	104	36					1275	287
0B 0131				TS	C		1272	286	104	36	1303	293	99	34	1288	289
0B 0132				TS	D		1272	286	104	36	1303	293	99	34	1288	289
0B 0133				AS	A		1288	289	102	35	1257	283	111	39	1272	286
0B 0134				AS	B		1263	284	106	37	1278	287	106	37	1271	286
0B 0135				AS	C		1291	290	101	35	1270	286	103	36	1280	288
0B 0136				AS	D		1291	290	101	35	1270	286	103	36	1280	288
0B 0137				AT	A		1274	286	103	36	1260	283	112	39	1267	285
0B 0138				AT	B		1268	285	104	36	1259	283	111	39	1264	284
0B 0139				AA	A		1268	285	109	38	1270	286	102	36	1269	285
0B 0140				AA	B		1285	289	99	35	1256	282	111	39	1271	286
0B 0141				SA	A		1262	284	110	38					1262	284
0B 0142				SA	B		1279	287	106	37					1279	287
0B 0143				SS	A		1267	285	109	38					1267	285
0B 0144				SS	B		1273	286	106	37					1273	286
0B 0145				ST	A		1294	291	103	36					1294	291
0B 0146				ST	B		1299	292	100	35					1299	292
0B 0147				ST	C		1294	291	103	36					1294	291
0B 0148				ST	D		1267	285	107	37					1267	285

Table A1.2 Continued

Test Serial Number	Date	Condition	Configuration Per Table 1.2	Orientation (I,A)	Replication	Modes Used for Analysis	Set 1 Estimated Tension (Uncorrected)		Set 1 Stiffness		Set 2 Estimated Tension (Uncorrected)		Set 2 Stiffness		Set 1-2 Average Tension (Uncorrected)	
							kN	klbf	kN-m^2	Mlbf-in^2	kN	klbf	kN-m^2	Mlbf-in^2	kN	klbf
0B 0149	9/27/2005	Before first cut	0B 5	TT	A	1-7	1304	293	94	33	1261	284	107	37	1282	288
0B 0150				TT	B		1304	293	94	33	1261	284	107	37	1282	288
0B 0151				TA	A		1261	284	105	36	1287	289	100	35	1274	286
0B 0152				TA	B		1261	284	105	36	1287	289	99	35	1274	286
0B 0153				TS	A		1269	285	104	36	1299	292	99	35	1284	289
0B 0154				TS	B		1283	288	102	35	1261	284	110	38	1272	286
0B 0155				TS	C		1285	289	101	35	1276	287	103	36	1281	288
0B 0156				TS	D		1285	289	101	35	1275	287	103	36	1280	288
0B 0157				AS	A		1283	289	101	35	1252	281	110	38	1268	285
0B 0158				AS	B		1288	290	101	35	1258	283	111	39	1273	286
0B 0159				AT	A		1270	286	103	36	1262	284	112	39	1266	285
0B 0160				AT	B		1261	284	104	36	1284	289	100	35	1273	286
0B 0161				AA	A		1262	284	104	36	1300	292	96	33	1281	288
0B 0162				AA	B		1263	284	104	36	1299	292	96	33	1281	288
0B 0163				SA	A		1284	289	101	35	1268	285	100	35	1276	287
0B 0164				SA	B		1283	288	102	36	1266	285	101	35	1274	286
0B 0165				SS	A		1287	289	101	35	1282	288	101	35	1284	289
0B 0166				SS	B		1284	289	101	35	1270	286	108	38	1277	287
0B 0167				ST	A		1284	289	101	35	1259	283	114	40	1272	286
0B 0168				ST	B		1283	288	102	35	1282	288	102	36	1283	288
0B 0169				ST	C		1284	289	101	35	1260	283	111	39	1272	286
0B 0170				ST	D		1284	289	101	35	1261	283	111	39	1272	286

Table A1.2 Continued

Test Serial Number	Date	Condition	Configuration Per Table 1.2	Orientation (I,A)	Replication	Modes Used for Analysis	Set 1 Estimated Tension (Uncorrected)		Set 1 Stiffness		Set 2 Estimated Tension (Uncorrected)		Set 2 Stiffness		Set 1-2 Average Tension (Uncorrected)	
							kN	klbf	kN-m^2	Mlbf-in^2	kN	klbf	kN-m^2	Mlbf-in^2	kN	klbf
0B 0171	9/30/2005	After first cut	0B 5	TT	A	1-7	1222	275	102	36	1222	275	102	36	1222	275
0B 0172				TT	B		1221	275	102	36	1221	275	102	36	1221	275
0B 0173				TA	A		1224	275	102	35	1224	275	102	35	1224	275
0B 0174				TA	B		1222	275	102	35	1222	275	102	35	1222	275
0B 0175				TS	A		1229	276	101	35	1229	276	101	35	1229	276
0B 0176				TS	B		1227	276	102	35	1227	276	102	35	1227	276
0B 0177				TS	C		1258	283	96	34	1258	283	96	34	1258	283
0B 0178				TS	D		1258	283	96	34	1258	283	96	34	1258	283
0B 0179				AS	A		1234	277	100	35	1234	277	100	35	1234	277
0B 0180				AS	B		1244	280	101	35	1244	280	101	35	1244	280
0B 0181				AT	A		1225	275	102	35	1225	275	102	35	1225	275
0B 0182				AT	B		1223	275	102	35	1223	275	102	35	1223	275
0B 0183				AA	A		1221	275	102	36	1221	275	102	36	1221	275
0B 0184				AA	B		1221	275	102	36	1221	275	102	36	1221	275
0B 0185				AA	C		1221	274	102	36	1221	274	102	36	1221	274
0B 0186				AA	D		1222	275	102	36	1222	275	102	36	1222	275
0B 0187				SA	A		1251	281	100	35	1251	281	100	35	1251	281
0B 0188				SA	B		1228	276	101	35	1228	276	101	35	1228	276
0B 0189				SS	A		1250	281	100	35	1250	281	100	35	1250	281
0B 0190				SS	B		1250	281	100	35	1250	281	100	35	1250	281
0B 0191				ST	A		1222	275	102	36	1222	275	102	36	1222	275
0B 0192				ST	B		1222	275	102	36	1222	275	102	36	1222	275
0B 0193				ST	C		1224	275	102	36	1224	275	102	36	1224	275
0B 0194				ST	D		1222	275	102	36	1222	275	102	36	1222	275

Table A1.2 Continued

Test Serial Number	Date	Condition	Configuration Per Table 1.2	Orientation (I,A)	Replication	Modes Used for Analysis	Set 1 Estimated Tension (Uncorrected)		Set 1 Stiffness		Set 2 Estimated Tension (Uncorrected)		Set 2 Stiffness		Set 1-2 Average Tension (Uncorrected)	
							kN	klbf	kN-m^2	Mlbf-in^2	kN	klbf	kN-m^2	Mlbf-in^2	kN	klbf
0B 0195	9/30/2005	After second cut	0B 5	TT	A	1-7	1170	263	97	34	1170	263	97	34	1170	263
0B 0196				TT	B		1176	264	96	34	1176	264	96	34	1176	264
0B 0197				TA	A		1171	263	96	33	1171	263	96	33	1171	263
0B 0198				TA	B		1173	264	96	34	1173	264	96	34	1173	264
0B 0199				TS	A		1166	262	101	35	1166	262	101	35	1166	262
0B 0200				TS	B		1168	263	102	35	1168	263	102	35	1168	263
0B 0201				AS	A		1163	261	103	36	1163	261	103	36	1163	261
0B 0202				AS	B		1192	268	92	32	1192	268	92	32	1192	268
0B 0203				AT	A		1163	262	97	34	1163	262	97	34	1163	262
0B 0204				AT	B		1165	262	97	34	1165	262	97	34	1165	262
0B 0205				AA	A		1181	266	100	35	1181	266	100	35	1181	266
0B 0206				AA	B		1180	265	101	35	1180	265	101	35	1180	265
0B 0207				SA	A		1190	267	97	34	1190	267	97	34	1190	267
0B 0208				SA	B		1189	267	98	34	1189	267	98	34	1189	267
0B 0209				SS	A		1172	263	99	35	1172	263	99	35	1172	263
0B 0210				SS	B		1172	263	99	35	1172	263	99	35	1172	263
0B 0211				ST	A		1157	260	102	36	1157	260	102	36	1157	260
0B 0212				ST	B		1160	261	104	36	1160	261	104	36	1160	261

Table A1.2 Continued

Test Serial Number	Date	Condition	Configuration Per Table 1.2	Orientation (I,A)	Replication	Modes Used for Analysis	Set 1 Estimated Tension (Uncorrected)		Set 1 Stiffness		Set 2 Estimated Tension (Uncorrected)		Set 2 Stiffness		Set 1-2 Average Tension (Uncorrected)	
							kN	klbf	kN-m^2	Mlbf-in^2	kN	klbf	kN-m^2	Mlbf-in^2	kN	klbf
13A 0100	4/7/2006	Before first cut Sloping End	13A 1	TT	A	2-4	1408	317	69	24	1455	327	69	24	1432	322
13A 0101				TT	B		1453	327	70	24	1408	317	69	24	1431	322
13A 0102				TA	A		1407	316	69	24					1407	316
13A 0103				TA	B		1405	316	69	24					1405	316
13A 0104				TS	A		1415	318	68	24					1415	318
13A 0105				TS	B		1412	317	68	24	1484	334	65	23	1448	326
13A 0106				AS	A		1452	326	69	24					1452	326
13A 0107				AS	B		1452	326	68	24					1452	326
13A 0108				AT	A		1410	317	68	24	1463	329	66	23	1436	323
13A 0109				AT	B		1410	317	68	24					1410	317
13A 0110				AA	A		1409	317	68	24	1452	326	69	24	1431	322
13A 0111				AA	B		1409	317	69	24	1450	326	70	24	1430	321
13A 0112				SA	A		1411	317	68	24	1443	324	70	25	1427	321
13A 0113				SA	B		1409	317	68	24	1446	325	70	24	1428	321
13A 0114				SS	A		1453	327	69	24					1453	327
13A 0115				SS	B		1451	326	69	24					1451	326
13A 0116				ST	A		1414	318	68	24					1414	318
13A 0117				ST	B		1414	318	68	24	1463	329	67	23	1439	323

Table A1.2 Continued

Test Serial Number	Date	Condition	Configuration Per Table 1.2	Orientation (I,A)	Replication	Modes Used for Analysis	Set 1 Estimated Tension (Uncorrected)		Set 1 Stiffness		Set 2 Estimated Tension (Uncorrected)		Set 2 Stiffness		Set 1-2 Average Tension (Uncorrected)	
							kN	klbf	kN-m^2	Mlbf-in^2	kN	klbf	kN-m^2	Mlbf-in^2	kN	klbf
13A 0118	4/7/2006	Before first cut, Horizontal End	13A 4	TT	A	2-4	1647	370	59	21	1666	374	62	22	1656	372
13A 0119				TT	B		1649	371	59	21	1664	374	62	22	1656	372
13A 0120				TA	A		1618	364	60	21	1630	367	61	21	1624	365
13A 0121				TA	B		1648	371	58	20	1681	378	59	20	1665	374
13A 0122				TS	A		1664	374	58	20	1676	377	59	21	1670	375
13A 0123				TS	B		1668	375	58	20	1681	378	60	21	1674	376
13A 0124				AS	A		1658	373	58	20	1679	377	59	21	1668	375
13A 0125				AS	B		1654	372	58	20	1683	378	59	21	1669	375
13A 0126				AT	A		1631	367	60	21	1625	365	62	22	1628	366
13A 0127				AT	B		1649	371	59	20	1665	374	60	21	1657	372
13A 0128				AA	A		1653	372	58	20	1669	375	60	21	1661	373
13A 0129				AA	B		1738	391	51	18	1701	382	58	20	1719	386
13A 0130				SA	A		1657	373	58	20	1669	375	60	21	1663	374
13A 0131				SA	B		1712	385	53	18	1699	382	57	20	1706	383
13A 0132				SS	A		1663	374	58	20	1643	369	62	22	1653	372
13A 0133				SS	B		1658	373	58	20	1641	369	62	22	1650	371
13A 0134				ST	A		1661	373	58	20	1657	373	61	21	1659	373
13A 0135				ST	B		1658	373	58	20	1660	373	60	21	1659	373

Table A1.2 Continued

Test Serial Number	Date	Condition	Configuration Per Table 1.2	Orientation (I,A)	Replication	Modes Used for Analysis	Set 1 Estimated Tension (Uncorrected)		Set 1 Stiffness		Set 2 Estimated Tension (Uncorrected)		Set 2 Stiffness		Set 1-2 Average Tension (Uncorrected)	
							kN	klbf	kN-m^2	Mlbf-in^2	kN	klbf	kN-m^2	Mlbf-in^2	kN	klbf
13A 0136	4/7/2006	After first cut, Sloping End	13A 1	TT	A	2-4	1498	337	69	24	1490	335	77	27	1494	336
13A 0137				TT	B		1495	336	69	24	1490	335	77	27	1493	336
13A 0138				TA	A		1496	336	70	24					1496	336
13A 0139				TA	B		1494	336	70	24	1520	342	70	25	1507	339
13A 0140				TS	A		1500	337	73	26	1480	333	72	25	1490	335
13A 0141				TS	B						1476	332	73	25	1476	332
13A 0142				AS	A		1496	336	74	26	1442	324	76	26	1469	330
13A 0143				AS	B		1504	338	73	25	1442	324	76	26	1473	331
13A 0144				AT	A		1491	335	70	24					1491	335
13A 0145				AT	B		1533	345	62	22					1533	345
13A 0146				AA	A						1490	335	71	25	1490	335
13A 0147				AA	B		1491	335	70	25	1524	343	70	24	1507	339
13A 0148				SA	A		1489	335	70	24	1481	333	77	27	1485	334
13A 0149				SA	B		1442	324	76	26	1483	333	78	27	1463	329
13A 0150				SS	A		1477	332	77	27					1477	332
13A 0151				SS	B		1478	332	77	27	1427	321	80	28	1452	326
13A 0152				ST	A		1491	335	70	24	1530	344	70	24	1510	340
13A 0153				ST	B		1495	336	70	24					1495	336

Table A1.2 Continued

Test Serial Number	Date	Condition	Configuration Per Table 1.2	Orientation (I,A)	Replication	Modes Used for Analysis	Set 1 Estimated Tension (Uncorrected)		Set 1 Stiffness		Set 2 Estimated Tension (Uncorrected)		Set 2 Stiffness		Set 1-2 Average Tension (Uncorrected)	
							kN	klbf	kN-m^2	Mlbf-in^2	kN	klbf	kN-m^2	Mlbf-in^2	kN	klbf
13A 0154	4/7/2006	After first cut, Horizontal End	13A 4	TT	A	2-4	1642	369	59	21	1655	372	63	22	1648	371
13A 0155				TT	B		1642	369	59	21	1657	372	63	22	1649	371
13A 0156				TA	A		1649	371	59	21					1649	371
13A 0157				TA	B		1651	371	59	21	1682	378	59	21	1666	375
13A 0158				TS	A		1660	373	58	20					1660	373
13A 0159				TS	B		1541	347	65	23	1636	368	62	22	1589	357
13A 0160				AS	A		1653	372	59	21					1653	372
13A 0161				AS	B		1653	372	59	20					1653	372
13A 0162				AT	A		1645	370	59	21	1680	378	59	21	1662	374
13A 0163				AT	B		1647	370	59	21	1658	373	60	21	1652	371
13A 0164				AA	A		1649	371	59	20					1649	371
13A 0165				AA	B		1652	371	59	21					1652	371
13A 0166				SA	A		1651	371	59	21					1651	371
13A 0167				SA	B		1652	371	59	20					1652	371
13A 0168				SS	A		1647	370	62	22	1663	374	59	20	1655	372
13A 0169				SS	B		1647	370	62	22	1663	374	59	20	1655	372
13A 0170				ST	A		1653	372	59	21	1655	372	62	21	1654	372
13A 0171				ST	B		1656	372	59	21	1654	372	61	21	1655	372

Table A1.2 Continued

Test Serial Number	Date	Condition	Configuration Per Table 1.2	Orientation (I,A)	Replication	Modes Used for Analysis	Set 1 Estimated Tension (Uncorrected)		Set 1 Stiffness		Set 2 Estimated Tension (Uncorrected)		Set 2 Stiffness		Set 1-2 Average Tension (Uncorrected)	
							kN	klbf	kN-m^2	Mlbf-in^2	kN	klbf	kN-m^2	Mlbf-in^2	kN	klbf
13A 0172	4/7/2006	Before second cut, Sloping End	13A 1	TT	C	2-4	1491	335	70	24					1491	335
13A 0173				TT	D		1490	335	70	24					1490	335
13A 0174				AA	C		1491	335	70	24					1491	335
13A 0175				AA	D		1491	335	70	24					1491	335
13A 0176				SS	C		1490	335	74	26					1490	335
13A 0177				SS	D		1489	335	74	26					1489	335
13A 0178	4/7/2006	Before second cut, Horizontal End	13A 4	TT	C	2-4	1643	369	59	21	1650	371	63	22	1647	370
13A 0179				TT	D		1643	369	59	21	1650	371	63	22	1647	370
13A 0180				AA	C		1650	371	59	20	1696	381	59	20	1673	376
13A 0181				AA	D		1734	390	51	18	1696	381	58	20	1715	386
13A 0182				SS	C		1682	378	61	21	1679	377	58	20	1680	378
13A 0183				SS	D		1675	377	61	21	1661	373	58	20	1668	375

Table A1.2 Continued

Test Serial Number	Date	Condition	Configuration Per Table 1.2	Orientation (I,A)	Replication	Modes Used for Analysis	Set 1 Estimated Tension (Uncorrected)		Set 1 Stiffness		Set 2 Estimated Tension (Uncorrected)		Set 2 Stiffness		Set 1-2 Average Tension (Uncorrected)	
							kN	klbf	kN-m²	Mlbf-in²	kN	klbf	kN-m²	Mlbf-in²	kN	klbf
13A 0184	4/7/2006	After second cut, Sloping End	13A 1	TT	A	2-4	1450	326	78	27	1457	328	82	28	1454	327
13A 0185				TT	B		1451	326	78	27	1456	327	82	28	1453	327
13A 0186				TA	A		1406	316	83	29					1406	316
13A 0187				TA	B		1453	327	78	27					1453	327
13A 0188				TS	A		1433	322	80	28	1437	323	83	29	1435	323
13A 0189				TS	B		1434	322	80	28	1434	322	83	29	1434	322
13A 0190				AS	A		1398	314	84	29	1444	325	81	28	1421	319
13A 0191				AS	B		1447	325	81	28	1405	316	83	29	1426	321
13A 0192				AT	A		1443	324	79	27					1443	324
13A 0193				AT	B		1440	324	79	28					1440	324
13A 0194				AA	A		1430	321	83	29	1398	314	84	29	1414	318
13A 0195				AA	B		1432	322	83	29	1408	317	83	29	1420	319
13A 0196				SA	A		1402	315	83	29	1458	328	80	28	1430	322
13A 0197				SA	B		1425	320	83	29	1403	315	84	29	1414	318
13A 0198				SS	A		1402	315	83	29	1443	324	81	28	1422	320
13A 0199				SS	B		1402	315	83	29	1443	324	81	28	1423	320
13A 0200				ST	A		1408	317	83	29					1408	317
13A 0201				ST	B		1413	318	82	29					1413	318

Table A1.2 Continued

Test Serial Number	Date	Condition	Configuration Per Table 1.2	Orientation (I,A)	Replication	Modes Used for Analysis	Set 1 Estimated Tension (Uncorrected)		Set 1 Stiffness		Set 2 Estimated Tension (Uncorrected)		Set 2 Stiffness		Set 1-2 Average Tension (Uncorrected)	
							kN	klbf	kN-m^2	Mlbf-in^2	kN	klbf	kN-m^2	Mlbf-in^2	kN	klbf
13A 0202	4/7/2006	After second cut, Horizontal End	13A 4	TT	A	2-4	1648	370	60	21	1643	369	65	23	1646	370
13A 0203				TT	B		1646	370	60	21	1641	369	66	23	1643	369
13A 0204				TA	A		1649	371	60	21					1649	371
13A 0205				TA	B		1650	371	60	21					1650	371
13A 0206				TS	A		1657	373	60	21	1672	376	63	22	1664	374
13A 0207				TS	B		1596	359	68	24	1541	346	66	23	1568	353
13A 0208				AS	A						1657	373	60	21	1657	373
13A 0209				AS	B		1656	372	61	21	1666	375	62	22	1661	373
13A 0210				AT	A		1643	369	60	21					1643	369
13A 0211				AT	B		1644	370	60	21					1644	370
13A 0212				AA	A		1647	370	60	21					1647	370
13A 0213				AA	B						1646	370	60	21	1646	370
13A 0214				SA	A						1657	373	60	21	1657	373
13A 0215				SA	B		1643	369	60	21	1628	366	65	23	1636	368
13A 0216				SS	A		1640	369	64	22	1664	374	60	21	1652	371
13A 0217				SS	B		1639	369	64	22	1670	376	60	21	1655	372
13A 0218				ST	A		1675	376	62	22	1652	371	60	21	1663	374
13A 0219				ST	B		1552	349	65	23	1624	365	65	23	1588	357

Table A1.2 Continued

Test Serial Number	Date	Condition	Configuration Per Table 1.2	Orientation (I,A)	Replication	Modes Used for Analysis	Set 1 Estimated Tension (Uncorrected)		Set 1 Stiffness		Set 2 Estimated Tension (Uncorrected)		Set 2 Stiffness		Set 1-2 Average Tension (Uncorrected)	
							kN	klbf	kN-m^2	Mlbf-in^2	kN	klbf	kN-m^2	Mlbf-in^2	kN	klbf
13B 0100	5/9/2006	Before first cut, Sloping End	13B 1	TT	E	2-4	1575	354	70	24					1575	354
13B 0101				TT	F		1576	354	70	24					1576	354
13B 0102				TA	E		1577	355	70	24	1601	360	93	32	1589	357
13B 0103				TA	F		1575	354	70	24	1601	360	93	32	1588	357
13B 0104				TS	F		1571	353	71	25	1599	359	93	32	1585	356
13B 0105				TS	G		1576	354	70	25	1599	359	93	32	1587	357
13B 0106				ST	E		1570	353	70	24	1600	360	93	32	1585	356
13B 0107				ST	F						1598	359	93	33	1598	359
13B 0108				SA	E						1599	360	93	32	1599	360
13B 0109				SA	F						1599	360	93	32	1599	360
13B 0110				SS	F						1599	359	93	32	1599	359
13B 0111				SS	G						1599	359	93	32	1599	359

Table A1.2 Continued

Test Serial Number	Date	Condition	Configuration Per Table 1.2	Orientation (I,A)	Replication	Modes Used for Analysis	Set 1 Estimated Tension (Uncorrected)		Set 1 Stiffness		Set 2 Estimated Tension (Uncorrected)		Set 2 Stiffness		Set 1-2 Average Tension (Uncorrected)	
							kN	klbf	kN-m^2	Mlbf-in^2	kN	klbf	kN-m^2	Mlbf-in^2	kN	klbf
13B 0112	5/9/2006	Before first cut, Horizontal End	13B 2	TT	F	2-4	1725	388	43	15					1725	388
13B 0113				TT	G		1725	388	43	15					1725	388
13B 0114				TA	E		1726	388	44	15					1726	388
13B 0115				TA	F		1725	388	44	15					1725	388
13B 0116				TS	E						1750	393	77	27	1750	393
13B 0117				TS	F						1734	390	83	29	1734	390
13B 0118				TS	G		1725	388	44	15	1733	390	82	29	1729	389
13B 0119				TT	H		1727	388	43	15					1727	388
13B 0120				TA	G		1725	388	44	15					1725	388
13B 0121				ST	F		1727	388	43	15	1734	390	83	29	1730	389
13B 0122				ST	G		1726	388	43	15	1735	390	83	29	1730	389
13B 0123				SA	E						1733	390	83	29	1733	390
13B 0124				SA	F						1732	389	83	29	1732	389
13B 0125				SS	E						1734	390	82	29	1734	390
13B 0126				SS	F						1734	390	83	29	1734	390
13B 0127				SS	G						1734	390	83	29	1734	390
13B 0128				ST	H		1730	389	43	15	1736	390	83	29	1733	390
13B 0129				SA	G						1735	390	83	29	1735	390

Table A1.2 Continued

Test Serial Number	Date	Condition	Configuration Per Table 1.2	Orientation (I,A)	Replication	Modes Used for Analysis	Set 1 Estimated Tension (Uncorrected)		Set 1 Stiffness		Set 2 Estimated Tension (Uncorrected)		Set 2 Stiffness		Set 1-2 Average Tension (Uncorrected)	
							kN	klbf	kN-m^2	Mlbf-in^2	kN	klbf	kN-m^2	Mlbf-in^2	kN	klbf
13B 0130	5/9/2006	After first cut, Sloping End	13B 1	TT	A	2-4	1574	354	68	24					1574	354
13B 0131				TT	B		1570	353	69	24					1570	353
13B 0132				TA	A		1568	353	69	24					1568	353
13B 0133				TA	B		1569	353	69	24					1569	353
13B 0134				TS	A		1572	353	69	24	1575	354	92	32	1573	354
13B 0135				TS	B		1571	353	69	24	1574	354	92	32	1573	354
13B 0136				ST	A		1568	352	69	24	1578	355	93	32	1573	354
13B 0137				ST	B		1567	352	69	24	1576	354	93	32	1572	353
13B 0138				SA	A						1575	354	92	32	1575	354
13B 0139				SA	B						1575	354	92	32	1575	354
13B 0140				SS	A						1576	354	92	32	1576	354
13B 0141				SS	B						1575	354	92	32	1575	354

Table A1.2 Continued

Test Serial Number	Date	Condition	Configuration Per Table 1.2	Orientation (I,A)	Replication	Modes Used for Analysis	Set 1 Estimated Tension (Uncorrected)		Set 1 Stiffness		Set 2 Estimated Tension (Uncorrected)		Set 2 Stiffness		Set 1-2 Average Tension (Uncorrected)	
							kN	klbf	$kN\text{-}m^2$	$Mlbf\text{-}in^2$	kN	klbf	$kN\text{-}m^2$	$Mlbf\text{-}in^2$	kN	klbf
13B 0142	5/9/2006	After first cut, Horizontal End	13B 2	TT	A	2-4	1729	389	84	29					1729	389
13B 0143				TT	B		1723	387	43	15					1723	387
13B 0144				TA	A		1722	387	43	15	1730	389	83	29	1726	388
13B 0145				TA	B		1719	386	43	15	1729	389	83	29	1724	388
13B 0146				TS	A		1721	387	43	15	1727	388	82	29	1724	388
13B 0147				TS	B		1718	386	43	15	1728	389	82	29	1723	387
13B 0148				ST	A		1723	387	43	15	1731	389	83	29	1727	388
13B 0149				ST	B		1723	387	43	15	1730	389	83	29	1726	388
13B 0150				SA	A						1729	389	83	29	1729	389
13B 0151				SA	B						1729	389	83	29	1729	389
13B 0152				SS	A						1729	389	83	29	1729	389
13B 0153				SS	B						1729	389	82	29	1729	389

Table A1.2 Continued

Test Serial Number	Date	Condition	Configuration Per Table 1.2	Orientation (I,A)	Replication	Modes Used for Analysis	Set 1 Estimated Tension (Uncorrected)		Set 1 Stiffness		Set 2 Estimated Tension (Uncorrected)		Set 2 Stiffness		Set 1-2 Average Tension (Uncorrected)	
							kN	klbf	kN-m^2	Mlbf-in^2	kN	klbf	kN-m^2	Mlbf-in^2	kN	klbf
13B 0154	5/9/2006	Before second cut, Sloping End	13B 1	TT	C	2-4	1568	353	68	24					1568	353
13B 0155				TT	D		1567	352	68	24					1567	352
13B 0156				TA	C		1568	352	68	24					1568	352
13B 0157				TA	D		1567	352	68	24					1567	352
13B 0158				TS	C		1569	353	68	24	1570	353	92	32	1570	353
13B 0159				TS	D		1560	351	69	24	1570	353	92	32	1565	352
13B 0160				TS	E		1568	352	68	24	1573	354	92	32	1570	353
13B 0161				ST	C		1567	352	68	24	1576	354	92	32	1572	353
13B 0162				ST	D		1564	352	68	24					1564	352
13B 0163				SA	C						1572	353	92	32	1572	353
13B 0164				SA	D						1570	353	92	32	1570	353
13B 0165				SS	C						1570	353	92	32	1570	353
13B 0166				SS	D						1570	353	92	32	1570	353
13B 0167				SS	E						1569	353	92	32	1569	353

Table A1.2 Continued

Test Serial Number	Date	Condition	Configuration Per Table 1.2	Orientation (I,A)	Replication	Modes Used for Analysis	Set 1 Estimated Tension (Uncorrected)		Set 1 Stiffness		Set 2 Estimated Tension (Uncorrected)		Set 2 Stiffness		Set 1-2 Average Tension (Uncorrected)	
							kN	klbf	kN-m²	Mlbf-in²	kN	klbf	kN-m²	Mlbf-in²	kN	klbf
13B 0168	5/9/2006	Before second cut, Horizontal End	13B 2	TT	C	2-4	1721	387	43	15					1721	387
13B 0169				TT	D		1722	387	43	15					1722	387
13B 0170				TA	C		1721	387	43	15					1721	387
13B 0171				TA	D		1721	387	43	15					1721	387
13B 0172				TS	C		1717	386	43	15	1726	388	83	29	1721	387
13B 0173				TS	D		1718	386	43	15	1726	388	83	29	1722	387
13B 0174				ST	C		1722	387	43	15	1728	388	83	29	1725	388
13B 0175				ST	D		1722	387	43	15	1728	389	83	29	1725	388
13B 0176				SA	C						1728	388	83	29	1728	388
13B 0177				SA	D						1728	389	83	29	1728	389
13B 0178				SS	C						1728	389	83	29	1728	389
13B 0179				SS	D						1729	389	83	29	1729	389

Table A1.2 Continued

Test Serial Number	Date	Condition	Configuration Per Table 1.2	Orientation (I,A)	Replication	Modes Used for Analysis	Set 1 Estimated Tension (Uncorrected)		Set 1 Stiffness		Set 2 Estimated Tension (Uncorrected)		Set 2 Stiffness		Set 1-2 Average Tension (Uncorrected)	
							kN	klbf	kN-m^2	Mlbf-in^2	kN	klbf	kN-m^2	Mlbf-in^2	kN	klbf
13B 0180	5/9/2006	After second cut, Sloping End	13B 1	TT	A	2-4	1554	349	66	23					1554	349
13B 0181				TT	B		1555	350	66	23					1555	350
13B 0182				TA	A		1555	350	66	23					1555	350
13B 0183				TA	B		1554	349	66	23					1554	349
13B 0184				TS	A		1554	349	66	23	1545	347	90	31	1550	348
13B 0185				TS	B		1556	350	66	23	1544	347	90	31	1550	348
13B 0186				TS	C		1552	349	66	23	1544	347	90	31	1548	348
13B 0187				ST	A		1554	349	66	23	1546	347	91	32	1550	348
13B 0188				ST	B						1546	348	91	32	1546	348
13B 0189				SA	A		1544	347	91	32					1544	347
13B 0190				SA	B						1545	347	90	31	1545	347
13B 0191				SS	A						1545	347	90	31	1545	347
13B 0192				SS	B						1545	347	90	31	1545	347
13B 0193				SS	C						1544	347	90	31	1544	347

Table A1.2 Continued

Test Serial Number	Date	Condition	Configuration Per Table 1.2	Orientation (I,A)	Replication	Modes Used for Analysis	Set 1 Estimated Tension (Uncorrected)		Set 1 Stiffness		Set 2 Estimated Tension (Uncorrected)		Set 2 Stiffness		Set 1-2 Average Tension (Uncorrected)	
							kN	klbf	kN-m^2	Mlbf-in^2	kN	klbf	kN-m^2	Mlbf-in^2	kN	klbf
13B 0194	5/9/2006	After second cut, Horizontal End	13B 2	TT	A	2-4	1718	386	42	15					1718	386
13B 0195				TT	B		1717	386	43	15					1717	386
13B 0196				TA	A		1716	386	43	15					1716	386
13B 0197				TA	B		1716	386	43	15					1716	386
13B 0198				TS	A		1715	386	43	15					1715	386
13B 0199				TS	B		1716	386	43	15					1716	386
13B 0200				ST	A		1718	386	42	15	1722	387	84	29	1720	387
13B 0201				ST	B		1717	386	42	15	1720	387	84	29	1719	386
13B 0202				SA	A						1721	387	84	29	1721	387
13B 0203				SA	B						1721	387	84	29	1721	387
13B 0204				SS	A						1720	387	84	29	1720	387
13B 0205				SS	B						1719	386	84	29	1719	386

Table A1.3- Analysis results for each reported deflection test.

Deflection Test Serial Number (See Appendix A1.4 for Data Table)	Date	Condition	Configuration Per Table 1.2	Orientation	Replication	δ μm/N (μin/lbf)	R^2
D0A 001	7/18/2005	Lc at center		V	A	1.456 (255.0)	0.9999
D0A 002	7/19/2005	Dial gage 7.5 cm from center and LC at center		V	A	1.443 (252.8)	0.9999
D0A 003	7/19/2005	Lc at center		H	A	1.437 (251.7)	0.9999
D0A 004	7/20/2005			V	A	1.414 (247.7)	0.9997
D0A 005	7/21/2005			H	A	1.456 (254.9)	0.9999
D0A 006	7/21/2005			A	A	1.429 (250.2)	0.9991
D0B 001	9/26/2005	Lc at center		V	A	1.581 (276.8)	0.9997
D0B 002	9/26/2005			H	A	1.587 (277.9)	0.9996
D0B 003	9/26/2005			A	A	1.912 (334.9)	0.9854
D0B 004	9/28/2005			V	A	1.581 (276.8)	0.9999
D0B 005	9/28/2005			H	A	1.580 (276.6)	0.9995
D0B 006	9/28/2005			A	A	1.572 (275.3)	0.9984
D0B 007	9/30/2005	(After first cut)		H	A	1.657 (290.1)	0.9997

Table A1.4- Data table for deflection tests.

D0A 001

Force		Deflection	
N	lbf	mm	in
82.4	18.53	0.127	0.005
188.5	42.38	0.284	0.0112
299.1	67.25	0.447	0.0176
403.4	90.69	0.589	0.0232
525.6	118.16	0.767	0.0302
675.2	151.78	0.993	0.0391
773.2	173.83	1.135	0.0447

D0A 002

Force		Deflection	
N	lbf	mm	in
23.3	5.23	0.034	0.00135
67.4	15.15	0.097	0.0038
151.2	34	0.218	0.0086
215.7	48.49	0.312	0.0123
285.4	64.15	0.419	0.0165
367.8	82.68	0.533	0.021
449.4	101.02	0.649	0.02555
553.8	124.5	0.800	0.0315
625.3	140.57	0.903	0.03555
715.8	160.91	1.036	0.0408
757.0	170.17	1.095	0.0431
798.1	179.43	1.151	0.0453
713.9	160.49	1.036	0.0408
646.7	145.39	0.944	0.03715
550.1	123.67	0.800	0.0315
485.8	109.22	0.706	0.0278
376.4	84.62	0.550	0.02165
281.2	63.22	0.417	0.0164
192.0	43.17	0.287	0.0113
134.7	30.29	0.203	0.008
67.4	15.15	0.099	0.0039
20.8	4.68	0.033	0.0013
-0.4	-0.09	0.003	0.0001

D0A 003

Force		Deflection	
N	lbf	mm	in
45.1	10.14	0.071	0.0028
142.8	32.1	0.203	0.008
205.2	46.13	0.292	0.0115
250.5	56.32	0.356	0.014
311.3	69.99	0.447	0.0176
368.4	82.82	0.531	0.0209
420.3	94.49	0.610	0.024
478.6	107.6	0.692	0.02725
536.7	120.66	0.773	0.03045
627.4	141.04	0.902	0.0355
708.7	159.33	1.016	0.04
649.8	146.09	0.935	0.0368
574.0	129.04	0.832	0.03275
521.5	117.23	0.759	0.0299
459.9	103.38	0.667	0.02625
384.1	86.34	0.556	0.0219
320.8	72.12	0.465	0.0183
229.7	51.64	0.330	0.013
141.3	31.77	0.206	0.0081
72.1	16.21	0.107	0.0042
38.1	8.57	0.061	0.0024
16.9	3.8	0.028	0.0011
1.9	0.42	0.005	0.0002

D0A 004

Force		Deflection	
N	lbf	mm	in
0.0	0	0.000	0
22.9	5.14	0.030	0.0012
103.0	23.16	0.140	0.0055
217.8	48.96	0.325	0.0128
280.6	63.08	0.394	0.0155
369.0	82.96	0.523	0.0206
446.1	100.28	0.635	0.025
468.3	105.28	0.665	0.0262
560.4	125.98	0.790	0.0311
645.5	145.11	0.909	0.0358
734.7	165.17	1.036	0.0408
604.7	135.94	0.864	0.034
511.0	114.87	0.734	0.0289
420.1	94.44	0.607	0.0239
209.3	47.06	0.300	0.0118
103.0	23.16	0.152	0.006
33.4	7.5	0.053	0.0021
0.0	0	0.003	0.0001

Table A1.4 Continued

D0A 005

Force		Deflection	
N	lbf	mm	in
48.6	10.93	0.076	0.003
176.5	39.69	0.264	0.0104
272.8	61.32	0.406	0.016
405.3	91.11	0.597	0.0235
511.6	115.01	0.752	0.0296
644.3	144.84	0.945	0.0372
731.4	164.43	1.072	0.0422
620.2	139.42	0.914	0.036
473.5	106.44	0.701	0.0276
342.8	77.07	0.508	0.02
189.4	42.57	0.290	0.0114
137.0	30.8	0.213	0.0084
50.9	11.44	0.089	0.0035
1.0	0.23	0.003	0.0001

D0A 006

Force		Deflection	
N	lbf	mm	in
41.4	9.31	0.066	0.0026
134.6	30.25	0.193	0.0076
230.8	51.88	0.333	0.0131
350.7	78.83	0.513	0.0202
490.4	110.24	0.721	0.0284
581.0	130.62	0.848	0.0334
694.9	156.23	1.006	0.0396
740.5	166.47	1.077	0.0424
650.9	146.32	0.960	0.0378
409.2	91.99	0.615	0.0242
305.1	68.6	0.462	0.0182
190.6	42.84	0.297	0.0117
134.1	30.15	0.216	0.0085
70.9	15.93	0.132	0.0052
-6.2	-1.39	0.028	0.0011

D0B 001

Force		Deflection	
N	lbf	mm	in
15.4	3.46	0.020	0.0008
63.3	14.24	0.104	0.0041
119.7	26.91	0.188	0.0074
214.0	48.11	0.335	0.0132
289.7	65.12	0.457	0.018
356.7	80.19	0.569	0.0224
426.6	95.9	0.676	0.0266
565.1	127.05	0.889	0.035
678.9	152.63	1.069	0.0421
779.6	175.26	1.227	0.0483
711.5	159.96	1.135	0.0447
615.8	138.44	0.986	0.0388
487.9	109.68	0.782	0.0308
354.0	79.59	0.574	0.0226
218.1	49.03	0.353	0.0139
145.1	32.63	0.231	0.0091
85.9	19.31	0.142	0.0056
35.1	7.88	0.064	0.0025

D0B 002

Force		Deflection	
N	lbf	mm	in
6.1	1.38	0.038	0.0015
125.0	28.11	0.239	0.0094
226.7	50.97	0.399	0.0157
343.0	77.1	0.582	0.0229
471.3	105.95	0.787	0.031
555.5	124.89	0.922	0.0363
643.3	144.61	1.064	0.0419
739.8	166.32	1.219	0.048
787.4	177.01	1.298	0.0511
584.0	131.29	0.975	0.0384
495.7	111.43	0.843	0.0332
407.1	91.52	0.704	0.0277
258.3	58.07	0.462	0.0182
156.2	35.12	0.302	0.0119
90.8	20.42	0.198	0.0078
13.3	3	0.076	0.003
-8.0	-1.8	0.038	0.0015

Table A1.4 Continued

D0B 003

Force		Deflection	
N	lbf	mm	in
74.4	16.73	0.137	0.0054
188.8	42.44	0.343	0.0135
268.8	60.42	0.483	0.019
364.9	82.03	0.650	0.0256
465.1	104.56	0.838	0.033
594.5	133.64	1.082	0.0426
667.5	150.05	1.237	0.0487
759.1	170.65	1.412	0.0556
782.7	175.95	1.476	0.0581
691.0	155.35	1.336	0.0526
550.0	123.64	1.115	0.0439
405.9	91.25	0.889	0.035
242.9	54.61	0.630	0.0248
194.5	43.73	0.300	0.0118
126.5	28.43	0.191	0.0075
40.8	9.17	0.046	0.0018
19.9	4.47	0.015	0.0006
-3.1	-0.69	-0.015	-0.0006

D0B 004

Force		Deflection	
N	lbf	mm	in
50.0	11.24	0.074	0.0029
150.0	33.73	0.241	0.0095
254.2	57.14	0.411	0.0162
365.7	82.21	0.582	0.0229
442.0	99.36	0.709	0.0279
534.6	120.19	0.853	0.0336
607.0	136.45	0.965	0.038
668.3	150.23	1.059	0.0417
702.1	157.84	1.113	0.0438
738.4	165.99	1.168	0.046
769.7	173.04	1.217	0.0479
659.4	148.25	1.054	0.0415
510.6	114.79	0.820	0.0323
415.1	93.32	0.668	0.0263
288.2	64.79	0.470	0.0185
192.1	43.18	0.312	0.0123
102.9	23.13	0.168	0.0066
76.1	17.1	0.127	0.005
51.2	11.52	0.089	0.0035
-1.0	-0.23	0.003	0.0001

D0B 005

Force		Deflection	
N	lbf	mm	in
39.1	8.8	0.064	0.0025
91.4	20.55	0.150	0.0059
125.0	28.11	0.201	0.0079
168.1	37.79	0.269	0.0106
232.1	52.17	0.373	0.0147
352.0	79.13	0.572	0.0225
436.8	98.2	0.709	0.0279
524.8	117.97	0.848	0.0334
613.3	137.88	0.986	0.0388
669.3	150.46	1.072	0.0422
732.8	164.75	1.176	0.0463
767.5	172.54	1.229	0.0484
687.3	154.52	1.102	0.0434
591.8	133.04	0.953	0.0375
432.5	97.24	0.709	0.0279
338.9	76.18	0.564	0.0222
226.5	50.92	0.381	0.015
166.1	37.33	0.287	0.0113
109.9	24.7	0.201	0.0079
62.7	14.1	0.127	0.005
23.4	5.25	0.064	0.0025
-1.4	-0.32	0.028	0.0011

D0B 006

Force		Deflection	
N	lbf	mm	in
19.5	4.38	0.041	0.0016
60.7	13.64	0.112	0.0044
160.7	36.13	0.277	0.0109
252.5	56.77	0.429	0.0169
303.4	68.2	0.516	0.0203
397.5	89.36	0.668	0.0263
508.6	114.33	0.843	0.0332
649.0	145.9	1.067	0.042
733.2	164.84	1.201	0.0473
767.9	172.63	1.260	0.0496
637.5	143.32	1.049	0.0413
515.5	115.9	0.861	0.0339
371.4	83.5	0.648	0.0255
226.5	50.92	0.417	0.0164
190.8	42.9	0.358	0.0141
147.2	33.09	0.290	0.0114
132.8	29.86	0.269	0.0106
87.3	19.63	0.193	0.0076
48.8	10.97	0.137	0.0054
31.1	7	0.112	0.0044
10.5	2.35	0.081	0.0032
-0.4	-0.09	0.064	0.0025

Table A1.4 Continued

D0B 007

Force		Deflection	
N	lbf	mm	in
50.2	11.29	0.079	0.0031
121.6	27.33	0.196	0.0077
229.6	51.61	0.376	0.0148
289.4	65.07	0.470	0.0185
376.0	84.52	0.615	0.0242
445.2	100.09	0.726	0.0286
583.4	131.15	0.953	0.0375
632.8	142.26	1.026	0.0404
785.1	176.5	1.278	0.0503
680.4	152.95	1.113	0.0438
565.8	127.19	0.922	0.0363
371.0	83.41	0.602	0.0237
318.5	71.61	0.516	0.0203
230.4	51.8	0.371	0.0146
135.5	30.46	0.211	0.0083
112.5	25.3	0.163	0.0064
58.6	13.18	0.074	0.0029
35.9	8.06	0.038	0.0015
9.8	2.21	-0.008	-0.0003
0.0	0	-0.023	-0.0009

Table A1.5- Data Table for Load Cell Measurements and Calculated Tensions

Tendon	Date	Approximate Test Period Start	Approximate Test Period End	Conditions	Test Serial Number Start	Test Serial Number End	Test Period Average Load Cell Measurement kN (klbf)											Test Period Average Force Calculated kN (klbf)		Force Balance/%		
							North Block Horizontal Reactions				Deviation Block Vertical Reactions				Deviation Block Horizontal Reactions		South Block Anchor					
							NB	NB	NB	NB	DB	DB	DB	DB	DBN	DBN	TSB		Free Segment TF	SB Anchor-Free		
0A	7/8/2005	1 PM	-	***Grouting***	-	-	450 (101.2)	527 (118.5)	453 (101.8)	33 (7.4)	NA	NA	NA	NA	NA	NA	1453 (326.6)		1464 (329.1)	***-0.8***		
0A	8/2/2005	1:12 PM	2:01 PM	0A 1- BC1	0A 0100	0A 0117	433 (97.3)	541 (121.6)	450 (101.2)	43 (9.7)	NA	NA	NA	NA	NA	NA	1435 (322.6)		1467 (329.8)	-2.3		
0A	8/4/2005	9:06 AM	9:42 AM	0A 11 - BC1	0A 0118	0A 0135	442 (99.4)	512 (115.1)	474 (106.6)	33 (7.4)	NA	NA	NA	NA	NA	NA	-		1462 (328.7)	-		
0A	8/4/2005	9:55 AM	10:25 AM	AC1	0A 0136	0A 0153	443 (99.6)	511 (114.9)	475 (106.8)	32 (7.2)	NA	NA	NA	NA	NA	NA	1335 (300.1)		1461 (328.4)	-9.5		
0A	8/4/2005	1:50 PM	3:08 PM	0A 11- AC2	0A 0154	0A 0171	410 (92.2)	554 (124.5)	442 (99.4)	66 (14.8)	NA	NA	NA	NA	NA	NA	1256 (282.4)		1472 (330.9)	-17.2		
0A	8/3/2005	3:20 PM	3:51 PM	0A 9 - BC1-SF	0A 172	0A 189	441 (99.1)	515 (115.8)	476 (107.0)	34 (7.6)	NA	NA	NA	NA	NA	NA	1435 (322.6)		1466 (329.6)	-2.1		
0A	8/3/2005	4:42 PM	5:11 PM	BC1 - TF	0A 190	0A 207	441 (99.1)	515 (115.8)	476 (107.0)	34 (7.6)	NA	NA	NA	NA	NA	NA	1435 (322.6)		1466 (329.6)	-2.1		

BC1: Before First Cut
AC1: After First Cut
AC2: After Second Cut
SF: Short Frets
TF: Tall Frets

Table A1.5 Continued

Tendon	Date	Approximate Test Period Start	Approximate Test Period End	Conditions	Test Serial Number Start	Test Serial Number End	Test Period Average Load Cell Measurement kN (klbf)											Test Period Average Force Calculated kN (klbf)		Force Balance/%		
							North Block Horizontal Reactions				Deviation Block Vertical Reactions				Deviation Block Horizontal Reactions		South Block Anchor					
							NB	NB	NB	NB	DB	DB	DB	DB	DBN	DBN	TSB		Free Segment TF	SB Anchor-Free		
0B	9/15/2005	4:30 PM	-	***Grouting***	-	-	142 (31.9)	299 (67.3)	271 (60.9)	629 (141.4)	NA	NA	NA	NA	NA	NA	1320 (296.7)		1341 (301.5)	***-1.6***		
0B	9/27/2005	9:03 AM	10:16 AM	0B 1-BC1	0B 0100	0B 0124	149 (33.5)	299 (67.2)	289 (65.0)	620 (139.4)	NA	NA	NA	NA	NA	NA	1312 (294.9)		1358 (305.3)	-3.5		
0B	9/27/2005	10:29 AM	11:19 AM	0B 3-BC1	0B 0125	0B 0148	149 (33.5)	299 (67.2)	290 (65.2)	620 (139.4)	NA	NA	NA	NA	NA	NA	1312 (294.9)		1358 (305.3)	-3.5		
0B	9/27/2005	3:32 PM	4:17 PM	0B 5-BC1	0B 0149	0B 0170	149 (33.5)	299 (67.2)	289 (65.0)	620 (139.4)	NA	NA	NA	NA	NA	NA	1312 (294.9)		1358 (305.3)	-3.6		
0B	9/30/2005	9:31 AM	10:12 AM	0B 5-AC1	0B 0171	0B 0194	143 (32.1)	286 (64.3)	274 (61.6)	605 (136.0)	NA	NA	NA	NA	NA	NA	1223 (274.9)		1307 (293.8)	-6.9		
0B	9/30/2005	2:12 PM	3:05 PM	0B 5-AC2	0B 0195	0B 0212	132 (29.7)	270 (60.7)	249 (56.0)	588 (132.2)	NA	NA	NA	NA	NA	NA	1127 (253.4)		1239 (278.5)	-10.0		
0B	9/29/2005	3:49 PM	4:09 PM	0B 9-BC1-SF	0B 0213	0B 0230	149 (33.5)	299 (67.2)	284 (63.8)	624 (140.3)	NA	NA	NA	NA	NA	NA	1313 (295.2)		1356 (304.8)	-3.3		
0B	9/29/2005	5:29 PM	5:51 PM	0B 10-BC2-TF	0B 0231	0B 0251	149 (33.5)	299 (67.2)	282 (63.4)	625 (140.5)	NA	NA	NA	NA	NA	NA	1320 (296.7)		1355 (304.6)	-3.2		

BC1: Before First Cut
AC1: After First Cut
AC2: After Second Cut
SF: Short Frets
TF: Tall Frets

Table A1.5 Continued

Tendon	Date	Approximate Test Period Start	Approximate Test Period End	Conditions	Test Serial Number Start	Test Serial Number End	Test Period Average Load Cell Measurement kN (klbf)											Test Period Average Force Calculated kN (klbf)		Force Balance/%		
							North Block Horizontal Reactions				Deviation Block Vertical Reactions				Deviation Block Horizontal Reactions		South Block Anchor	Sloping Segment TS	Horizontal Segment TH	SB Anchor-Sloping	Vertical	Horizontal
							NB	NB	NB	NB	DB	DB	DB	DB	DBNE	DBNW	TSB					
13A	1/6/2006	11 AM	-	***Grouting***	-	-	578 (129.9)	404 (90.8)	6 (1.3)	440 (98.9)	82 (18.4)	2 (0.4)	142 (31.9)	73 (16.4)	0 (0.0)	8 (1.8)	1493 (335.6)	1456 (327.3)	1428 (321.0)	***2.5***	2.6	-0.1
13A	4/7/2006	9:18 AM	9:39 AM	13A 1-BC1-S	13A 0100	13A 0117	565 (127.0)	440 (98.9)	5 (1.1)	470 (105.7)	74 (16.6)	4 (0.9)	140 (31.5)	72 (16.2)	68 (15.3)	59 (13.3)	1464 (329.1)	1388 (312.0)	1479 (332.5)	5.2	4.7	-0.2
13A	4/7/2006	9:46 AM	10:09 AM	13A 4-BC1-H	13A 0118	13A 0135	565 (127.0)	440 (98.9)	5 (1.1)	470 (105.7)	74 (16.6)	4 (0.9)	140 (31.5)	72 (16.2)	68 (15.3)	60 (13.5)	1464 (329.1)	1387 (311.8)	1479 (332.5)	5.2	4.7	-0.2
13A	4/7/2006	11:49 AM	12:12 PM	13A 1-AC1-S	13A 0136	13A 0153	565 (127.0)	438 (98.5)	5 (1.1)	470 (105.7)	73 (16.4)	4 (0.9)	137 (30.8)	71 (16.0)	78 (17.5)	67 (15.1)	1364 (306.6)	1367 (307.3)	1476 (331.8)	-0.3	4.9	-0.2
13A	4/7/2006	12:17 PM	12:36 PM	13A 4-AC1-H	13A 0154	13A 0171	565 (127.0)	437 (98.2)	5 (1.1)	470 (105.7)	73 (16.4)	4 (0.9)	137 (30.8)	71 (16.0)	79 (17.8)	68 (15.3)	1364 (306.6)	1365 (306.9)	1476 (331.8)	-0.1	5.0	-0.2
13A	4/7/2006	1:47 PM	1:55 PM	13A 1-BC2-S	13A 0172	13A 0177	566 (127.2)	435 (97.8)	4 (0.9)	470 (105.7)	73 (16.4)	4 (0.9)	137 (30.8)	72 (16.2)	80 (18.0)	69 (15.5)	1364 (306.6)	1363 (306.4)	1476 (331.8)	0.1	5.2	-0.3
13A	4/7/2006	1:57 PM	2:02 PM	13A 4-BC2-H	13A 0178	13A 0183	566 (127.2)	435 (97.8)	4 (0.9)	470 (105.7)	73 (16.4)	4 (0.9)	137 (30.8)	72 (16.2)	80 (18.0)	69 (15.5)	1363 (306.4)	1362 (306.2)	1476 (331.8)	0.1	5.2	-0.3
13A	4/7/2006	14:58:00	15:34:00	13A 1-AC2-S	13A 0184	13A 0201	564 (126.8)	434 (97.6)	4 (0.9)	469 (105.4)	73 (16.4)	4 (0.9)	133 (29.9)	70 (15.7)	95 (21.4)	78 (17.5)	1259 (283.0)	1332 (299.4)	1470 (330.5)	-5.9	5.9	-0.3
13A	4/7/2006	15:36:00	15:55:00	13A 4-AC2-H	13A 0202	13A 0219	564 (126.8)	433 (97.3)	4 (0.9)	469 (105.4)	73 (16.4)	4 (0.9)	133 (29.9)	70 (15.7)	96 (21.6)	79 (17.8)	1259 (283.0)	1330 (299.0)	1470 (330.5)	-5.6	5.9	-0.3

BC1: Before First Cut
AC1: After First Cut
AC2: After Second Cut
S: Sloping
H: Horizontal

Table A1.5 Continued

	Date	Approximate Test Period Start	Approximate Test Period End	Conditions	Test Serial Number Start	Test Serial Number End	Test Period Average Load Cell Measurement kN (klbf)											Test Period Average Force Calculated kN (klbf)		Force Balance/%		
							North Block Horizontal Reactions				Deviation Block Vertical Reactions				Deviation Block Horizontal Reactions		South Block Anchor	Sloping Segment TS	Horizontal Segment TH	SB Anchor-Sloping	Vertical	Horizontal
							NB	NB	NB	NB	DB	DB	DB	DB	DBNE	DBNW	TSB					
13B	4/28/2006	12 PM	-	***Grouting***	-	-	436 (98.0)	345 (77.6)	415 (93.3)	443 (99.6)	52 (11.7)	4 (0.9)	89 (20.0)	141 (31.7)	11 (2.5)	-7 (-1.6)	1570 (353.0)	1665 (374.3)	1639 (368.5)	***-6.1***	-17.3	0.6
13B	5/9/2006	9:24 AM	9:35 AM	13B 1- BC1-S	13B 0100	13B 0111	448 (100.7)	358 (80.5)	427 (96.0)	457 (102.7)	49 (11.0)	5 (1.1)	87 (19.6)	140 (31.5)	21 (4.7)	51 (11.5)	1544 (347.1)	1647 (370.3)	1690 (379.9)	-6.7	-18.6	0.7
13B	5/9/2006	9:45 AM	10:18 AM	13B 2-BC1-H	13B 0112	13B 0129	448 (100.7)	358 (80.5)	427 (96.0)	457 (102.7)	49 (11.0)	5 (1.1)	87 (19.6)	140 (31.5)	21 (4.7)	50 (11.2)	1544 (347.1)	1647 (370.3)	1690 (379.9)	-6.7	-18.6	0.7
13B	5/9/2006	2:42 PM	2:55 PM	13B 1-AC1-S	13B 0130	13B 0141	449 (100.9)	355 (79.8)	422 (94.9)	461 (103.6)	48 (10.8)	4 (0.9)	86 (19.3)	139 (31.2)	26 (5.8)	63 (14.2)	1433 (322.2)	1626 (365.5)	1687 (379.3)	-13.5	-18.0	0.6
13B	5/9/2006	2:59 PM	3:06 PM	13B 2-AC1-H	13B 0142	13B 0153	449 (100.9)	355 (79.8)	421 (94.6)	460 (103.4)	48 (10.8)	4 (0.9)	86 (19.3)	139 (31.2)	26 (5.8)	63 (14.2)	1432 (321.9)	1625 (365.3)	1686 (379.0)	-13.4	-18.1	0.6
13B	5/9/2006	3:47 PM	3:54 PM	13B 1-BC2-S	13B 0154	13B 0167	449 (100.9)	355 (79.8)	421 (94.6)	461 (103.6)	48 (10.8)	4 (0.9)	86 (19.3)	139 (31.2)	27 (6.1)	65 (14.6)	1432 (321.9)	1622 (364.6)	1686 (379.0)	-13.3	-18.2	0.6
13B	5/9/2006	3:34 PM	3:42 PM	13B 2-BC2-H	13B 0168	13B 0179	449 (100.9)	355 (79.8)	421 (94.6)	461 (103.6)	48 (10.8)	4 (0.9)	86 (19.3)	139 (31.2)	27 (6.1)	64 (14.4)	1432 (321.9)	1623 (364.9)	1686 (379.0)	-13.3	-18.2	0.6
13B	5/9/2006	4:14 PM	4:19 PM	13B 1-AC2-S	13B 0180	13B 0193	446 (100.3)	355 (79.8)	421 (94.6)	457 (102.7)	45 (10.1)	3 (0.7)	85 (19.1)	136 (30.6)	36 (8.1)	88 (19.8)	1316 (295.8)	1583 (355.9)	1680 (377.7)	-20.2	-18.2	0.6
13B	5/9/2006	4:25 PM	4:29 PM	13B 2-AC2-H	13B 0194	13B 0205	446 (100.3)	355 (79.8)	421 (94.6)	457 (102.7)	45 (10.1)	3 (0.7)	85 (19.1)	135 (30.3)	37 (8.3)	89 (20.0)	1317 (296.1)	1580 (355.2)	1679 (377.5)	-20.0	-18.3	0.6

BC1: Before First Cut
AC1: After First Cut
AC2: After Second Cut
S: Sloping
H: Horizontal

APPENDIX 2

SIMPLIFIED TESTING AND ANALYSIS METHOD

TENDON VIBRATIONAL TESTING STEP-BY-STEP PROCEDURE

A. EQUIPMENT AND SETUP FOR ANALYZER-M
B. SYSTEM STARTUP AND PRE-TEST STEPS
C. TEST EXECUTION STEPS

ADDENDUM 1 - Preparations
ADDENDUM 2 - Notice and Disclaimer
ADDENDUM 3 - Log Form (Generic)
ADDENDUM 4 – Tension spreadsheet

Note: this step by step guide and the analysis software described were prepared for field use. Measurement, display and calculation units were chosen per prior successful experience and convenience. For brevity, no unit conversions are embedded in the text.

TENDON VIBRATIONAL TESTING STEP-BY-STEP PROCEDURE

Prepared by University of South Florida - All Rights Reserved - See Addendum 2 for Notice and Disclaimer

A. EQUIPMENT AND SETUP FOR ANALYZER-M

Minimum items required:

1. Laptop **DELL** LATITUDE 840 computer with ***Analyzer-M*** software
2. Memory stick with at least 1GB of empty space for “drag and drop” operation.
3. 110 V 60Hz AC Power Source adequate for computer
4. Thermometer to record ambient temperature
5. Long (100 ft) and accurate measuring tape
6. Log Form binder/clipboard/ballpoint pens.
7. Accelerometer Kit Box containing
   - 7a. Accelerometer (PCB 338B34)
   - 7b. Accelerometer Extension Cable
   - 7c. Sensor Signal Conditioner (ICP – Model 480E09)
   - 7d. Stereo Adapter Cable
   - 7e. Spare 9V Alkaline Batteries (bag of 3)
8. BNC Black Extension Cable (2 50-ft sections with 2 Female-Female couplers)
9. Rubber hammer
10. Tuning Fork
11. Wireless presentation remote (Targus, model PAUM30).
12. Card Table and Stool - essential for accurate work.
13. Adequate lighting

Note: Items 1,7 and 8 must be on site in duplicate to provide full spare backup.

Physical arrangement (see Figure 1):

a) Set up Card Table centrally in the Test Station area chosen, so the computer screen is within easy view from the impact position (see **ADDENDUM 1**).

b) Set up power source outlet next to Card Table.

c) Ensure that accelerometer wiring can run unobstructed to each of the accelerometer locations in the Test Station. *Ensure that operator movement does not result in tripping over wires or equipment falling down.*

d) Place DELL Computer and Log Form on Card Table. Leave space also for tuning fork. A comfortable working space is essential for reliable operation and record keeping.

e) Make sure that cooling fan in computer is not obstructed.

Equipment is now ready for operation. Proceed To Part B, System Startup and Pre-Test Steps.

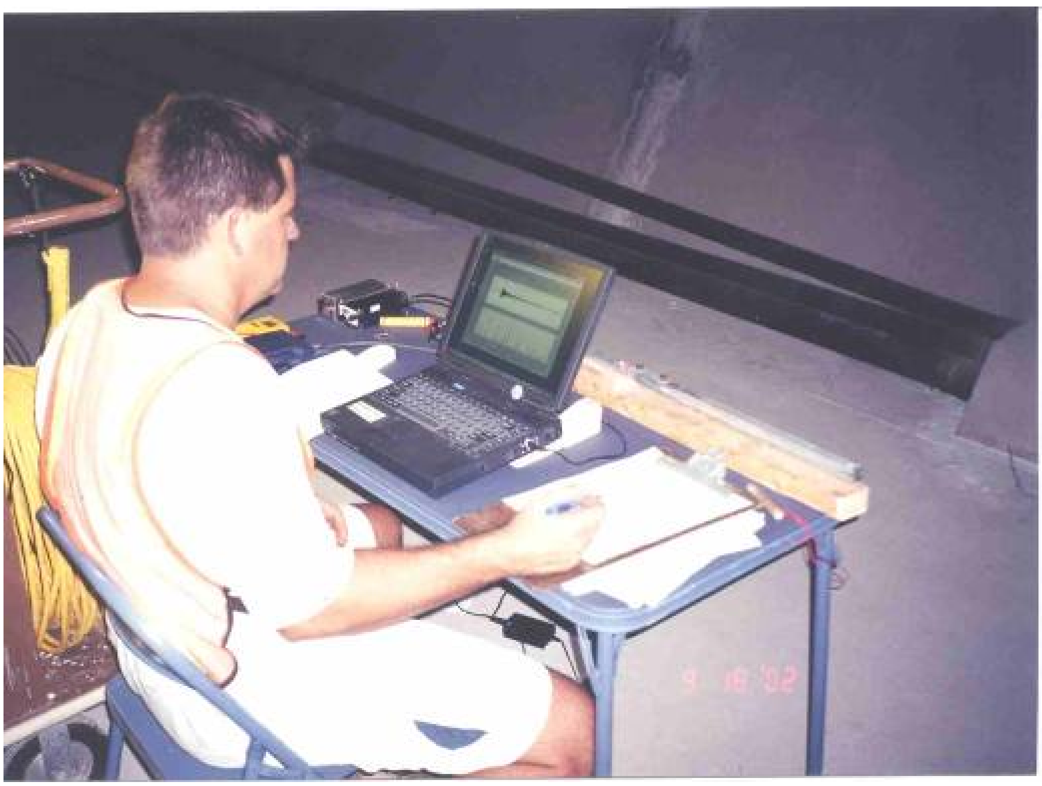

Figure 1. Example of efficient on-site test layout.

B. SYSTEM STARTUP AND PRE-TEST STEPS

READ EACH STEP COMPLETELY BEFORE ACTING

Step 0. Span and tendon segment ID and preparatory measurements

See **ADDENDUM 1** for ID procedures and preparatory work.

Step 1. Set up computer:

1.1 Write down Test Station number (for example 07) on Log Form.

1.2 Power up and boot up computer. Record on Log Form designation of computer being used.

1.3 Perform audio input setup check:

Perform once at beginning of shift. Perform also if machine was operated by others during shift or if abnormal test results are observed.

On desktop, double click Volume Control icon
Ensure Mute All is selected.
Ensure Line In Volume is all the way up and not muted.
Click Options, Properties.
Click Recording, then OK.
Ensure Stereo Mix Volume is all the way up.
Ensure Stereo Mix Select is clicked.
Ensure nothing else is selected.
Close window.

1.4 Double-click ***ANALYZER-M*** icon on desktop. After Logo appears, press F2 and choose OK or Cancel conditions. If OK is chosen, the operating panel shows up on screen. Turn Caps Lock on.

Step 2. Wire accelerometer, Sensor Signal Conditioner, and connection to computer. Check/replace Sensor Signal Conditioner batteries:

2.1 Remove from Accelerometer Kit Box #1 the Accelerometer. [Use parts in spare Kit Box #2 only if parts in #1 fail]. Record on Log Form Serial Number (SN) of accelerometer being used. The Accelerometer is a precision instrument. Handle it gently and do not drop.

Connect Accelerometer to white Accelerometer Extension Cable . Turn “floating clamp nut”, never the accelerometer as that may damage connector pin. Do not kink or stress Accelerometer Extension Cable.

Connect Accelerometer Extension Cable to BNC Black Extension Cable with provided adaptor. If only one 50-ft length is sufficient, store away the other 50-ft length. ***Do not use cables to pull on or hold equipment!***

2.2 Connect other end of BNC Black Extension Cable to **XDCR** jack on Sensor Signal Conditioner. Verify that Sensor Signal Conditioner controls are as follows:

Gain:	10
Red Rocker:	Press right side (ON) and let go.

2.3 Connect Stereo Adapter Cable to **SCOPE** on Sensor Signal Conditioner #1.

2.4 Connect other end of Stereo Adapter Cable to **LINE INPUT** of computer. *MAKE SURE NOT TO USE THE MICROPHONE INPUT*. For easier identification, the **LINE INPUT** has been marked by a white ring.

2.5 Check batteries by momentarily pressing right side Red Rocker in Sensor Signal Conditioner all the way down. Meter should point to the "BATT OK" region. If it doesn't, replace all three batteries (open box by loosening Phillips-head screw on back).

2.6 After verifying the batteries are OK, check that needle in Sensor Signal Conditioner is in green region. If it isn't, check cables, accelerometer and connectors and reconnect/replace until condition is remedied.

Step 3. Place accelerometer on Tuning Fork 3:

Attach accelerometer with wax securely and precisely between scribe marks on Tuning Fork 3. Route Accelerometer Extension Cable loosely through the back of the tuning fork so cable does not touch vibrating beams or interferes with accelerometer motion.

Step 4. Run Tendon Test program section and acquire Tuning Fork vibration data. Examine response:

4.1 Press **(CTRL+R)**. Press **F3**. A File Save window appears on screen. Type XX**T** (where XX is the Test Station designation, for example 07 and the letter **T** indicates Tuning Fork test). DO NOT ENTER ANY FILE EXTENSIONS OR ALTER THIS PROCEDURE IN ANY WAY. Press **ENTER**.

Note: this does not cause a file to be saved yet. It only prepares the system to save the result of the test under the file name chosen, if the test is completed successfully.

4.2 Gently place 1/2 inch dowel crosswise just inside Tuning Fork end until dowel touches stop screw.

4.3 Press F3 or use the wireless remote to press the PUSH BUTTON display on the computer screen ("TEST IN PROGRESS" appears on screen). Immediately start counting: one-thousand-one, one-thousand-two, so as to have a 2-second wait. Immediately following, pull dowel straight out (along main axis of tuning fork) in one quick motion and without introducing torque. The data acquisition stops automatically 12 seconds after pressing **F3**.

Do not touch anything while the "TEST IN PROGRESS" message shows.

A short while later the test output will appear on the screen.

4.4 a) The frequency plot should show a clear peak at about 33 Hz (electric noise may also cause another peak near 60 Hz; ignore it).

b) Press TAB repeating as needed to select RANGE box. Pressing the **UP** or **DOWN** keys causes the spectrum to zoom into a 10 Hz wide window that shifts in 5 Hz steps (window cycles to full width after multiple steps). Move the zoom until it includes the peak near 33 Hz. Read the peak frequency as shown in the "Peak" box. Peak frequency for Tuning Fork 3 should be a value from 33.8 Hz to 34.0 Hz.

c) Read the peak height, as indicated in the vertical axis. Height for Tuning Fork should be between 200 to 500 units.

Note 1: The "Peak" box always shows the frequency of the highest point in the window. Read the box only when the near-33 Hz peak is the only one showing in the 10 Hz wide window.

Note 2: Since the windows move only in short steps, the peak near 33 Hz will appear in two consecutive windows. The "Peak" reading in those two windows may differ by 0.1 Hz. That small variation is normal; in such case record only one of those values.

Step 5. If Tuning Fork response is adequate, save data and proceed to Step 7:

If response is as indicated in each of 4.4 (a), (b) and (c), Press **F4**, press E**NTER** (to select "Yes"), and the machine saves the results of the Tuning Fork test under the file name selected earlier. A confirmation message appears (see note after Step 16). The system is now ready for testing the tendons. Write down Peak frequency and Height in Log Form Supplementary Information section and proceed to Step 7.

Otherwise, proceed to Step 6.

Step 6. If Tuning Fork response is inadequate, check all settings and connections, and proceed to Step 4:

If response fails to result in any one of 4.4 (a), (b) or (c), the test response is inadequate, indicating a problem. Press **F4** and then **TAB** (to select "No") and then **ENTER**. This resets the program. Check everything (including that accelerometer is firmly attached to tuning fork, connections, switch positions, etc.) and repeat test starting at Step 4.

Step 7. Record ambient temperature and Span test start time:

Enter operator initials, temperature and date/time information on Log Form.

Always use ball-point pen. If there are any entry errors, strike over and write correct entry on the side - do not attempt to write over old entry.

Testing system is now ready to operate. Proceed to Part C.

C. TEST EXECUTION STEPS

Step 8. Select tendon to test, measure length, mark positions for accelerometer and hammer impact, and place accelerometer:

8.1. Tendon segment designations, segment length measurement and accelerometer placement position: Follow instructions in **ADDENDUM 1**.

8.2 Select tendon segments to be tested in the order indicated in the Log Form for the appropriate Test Station. Special procedures for tendon segments obstructed from free vibration will be provided in a separate document.

8.3 Attaching accelerometer to tendon:

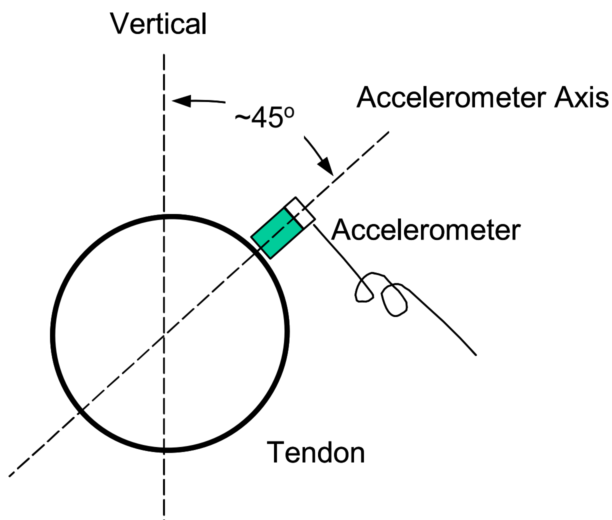

Figure 2. Accelerometer Orientation

The accelerometer is to be placed, with its axis on a plane approximately 45° from vertical, on the plastic duct as shown in Figure 2. Use mounting wax, cleaning any dust first. Avoid dropping accelerometer. If accelerometer is dropped make a note of it on Log Form Supplementary Information section.

Loose accelerometers are major source of rejected data. If necessary, further secure the accelerometer to the duct using adhesive tape or a Velcro strap.

Route Accelerometer Extension Cable so that it does not rattle against tendon during vibration. Cable may be lightly wrapped around the next tendon to avoid accidental yanking and to restrain accelerometer fall.

8.4 Hammer impact is to be always applied on a direction perpendicular to the axis of the tendon, at a point approximately halfway between accelerometer and the deviation saddle end of the tendon. Impact will be applied in two manners: Straight and Side. In **Straight** impact the direction of the blow is contained in a vertical plane. In **Side** impact the direction of the blow is in a horizontal plane.

Step 9. Run Hammer Practice program section and practice to deliver adequate hammer blow strength. SKIP STEP IF ALREADY TRAINED:

9.1 Ensure that Steps 1 through 8 are completed.

9.2 Using the designated hammer, impact (Straight) the tendon. See **ADDENDUM 2** for important Notice and Disclaimer. For this operation screen must be within easy view from impact position.

Hammer hitting:

Adjust impact to obtain desired amplitude as detailed in instructions below.

If duct is not tightly filled with grout at impact point (as indicated by unusual sound), change impact position to a point a few inches to the right or left of initial position)

9.3 Press **(CTRL+R)**. Press **F1** and hit tendon repeatedly, waiting about 3 seconds between hits. Watch signal display. Signal trace at impact should go well beyond inner lines but should not cross the outer lines. Train yourself to adjust Straight impact strength until signal stays within limits. With display still running, switch impact direction to Side and train for it similarly.

Press **F2** when operation within limits is achieved in both directions and stop hitting tendon. The Save Wave File window will appear; do not attempt to close it.

Training is complete. Wait about 20 seconds before next action.

Step 10. Run Tendon Test program section and acquire vibration data:

10.1 Ensure that Steps 1 through 8 are completed and that operator has already been trained to deliver adequate impact strength. Each tendon is tested 2 times with Straight impact (tests 1 and 2) and 2 times with Side impact (tests 3 and 4).

10.2 Press **F3** if the Save Wave File window is not already on screen.

Type the file name (ALL CAPITALS) for the tendon segment to be tested and press **ENTER**. The file name is the same as tendon segment designation (see **ADDENDUM 1**) but with the number 1 appended for the first test performed for the tendon segment, 2 for the second test, etc.

Example: File for 1st test on tendon segment **116209NE** is named **116209NE1** . File for 3rd test is named **116209NE3**. If a test is a repeat of a test that was not acceptable (due to implementation of Step 11), repeat the same file name used in the failed test (the failed test file will be written over). DO NOT ENTER ANY FILE EXTENSIONS OR ALTER THIS PROCEDURE IN ANY WAY.

> Note: this does not cause a file to be saved yet. It only prepares the system to save the result of the test under the file name chosen, if the test is completed successfully.

Have operator standby with hammer ready to hit (Straight for tests 1 and 2, Side for tests 3 and 4) when directed.

10.3 Press F3 or the PUSH BOTTON ("TEST IN PROGRESS" appears on screen). Immediately start counting: one-thousand-one, one-thousand-two, so as to have a 2-second wait. Immediately following, direct operator to hit tendon **only once**. The data acquisition stops automatically 12 seconds after pressing **F3**.

> ***Do not touch the tendon, accelerometer or anything else in the equipment while the "TEST IN PROGRESS" message shows.***

About 20 seconds later the test output appears on the screen. Signal analysis by the computer is now complete.

Step 11.Check to see If data are adequate or not:

a) Examine strip record of top channel. Is signal in top chart within limits described in step 9.3 ?

b) Examine the spectrum record in the lower chart. A distinct peak should appear near the left end of the chart. That is the Mode 1 peak (as a rough guide, the expected approximate value of the frequency for Mode 1 in sound tendons is shown in Table A1 in **ADDENDUM 1**). An overtone peak (Mode 2) should be visible at about twice the frequency of Mode 1. Higher overtones may be visible at about three or four times the frequency of Mode 1. Also, the line between the peaks should be relatively smooth with few jagged regions.

The signal in the top chart should be relatively symmetric and showing a gentle decay. See Figure 3 for examples of "good" and "bad "signals and spectra.

<u>Do signal and spectrum have the "good' appearance shown in Figure 3?</u>

c) If answers to both (a) and (b) are YES, ***go to Step 12****.*

d) If answer to (a) is NO, too low or too high impact has been applied. Press **F4** and then **TAB** (to select "No") and then **ENTER**. Check equipment and ***go to Step 9*** for hammer practice.

e) If answer to (a) is YES but answer to (b) is NO, test needs to be rerun. "Bad" signals and spectra are often due to a loose accelerometer, obstructions in the tendon motion, or abnormal hammer impact. Check for those problems as well as equipment and connections. Correct deficiencies. Press **F4** and then **TAB** (to select "No") and then **ENTER**. Press **(CTRL+R)**. This resets the program. ***Go to Step 10*** to repeat test.

> *Note: If a "bad" spectrum or signal persists after a few tries, complete the tests anyway, make a note of the problem, and proceed to the next tendon. Repeated difficulties in subsequent tendons may indicate equipment malfunction.*

Step 12. Identify and record peak frequencies:

12.1 Press TAB and select RANGE box. Afterwards, pressing the **UP** or **DOWN** keys causes the spectrum to zoom into a 10 Hz wide window that shifts in 5 Hz steps. Shift the window until it includes the Mode 1 peak. Read the peak frequency as shown in the "Peak" box and enter in Log Form. Repeat for Mode 2 peak.

Note 1: The "Peak" box always shows the frequency of the highest point in the window. Read the box only when the desired Mode is the main feature showing in the 10 Hz wide window. Some peaks may be split into two closely spaced peaks; record only the tallest.

Note 2: Since the windows move only in short steps, each desired mode may appear in two consecutive windows. The “Peak” reading in those two windows may differ by 0.1 Hz. That small variation is normal; in such case record only one of those values for the Mode. The approximate Mode 1 frequencies expected are listed in Table 1 (rough estimates - actual behavior may be substantially different).

Step 13. Save file:

Press **F4**, press **ENTER**. The machine saves the results. A confirmation message appears (see note after Step 16). Press **CTRL+R**.

Step 14. Conduct second, third or fourth test of the tendon segment. (Steps 10 - 13):

If the previous test was not the fourth successful test for this tendon segment, repeat Steps (10) through (13). Otherwise, go to Step (15).

Step 15. Proceed to next tendon segment in span starting at step (8):

After the 4th successful test for this tendon segment is concluded, go to Step (8). Continue until all tendon segments in the Test Station are tested. Then go to Step (16).

Step 16. After the last segment in the span is tested, record temperature, copy data to CDRW drive, and prepare for next Span:

Press left side of Red Rocker switch of <u>Sensor Signal Conditioner</u> to the OFF position.

Exit ***Analyzer-M*** program by pressing **(ALT+F4)**.

Read temperature and record temperature and time in Log File.

The files from all tendon tests plus the Tuning Fork test file for this Test Station have been stored in the Folder named ANALYZER FILES in the C drive (folder ANALYZER FILES accumulates all the data from all the Test Stations). Copy all the files for this Test Station to a folder named STATION## (where ## is the Test Station designation) onto the memory stick. Copy into the same folder also any other files that may have originated for this Test Station (for example, from extra tests).

Go through Windows Shut Down sequence and turn off computer.

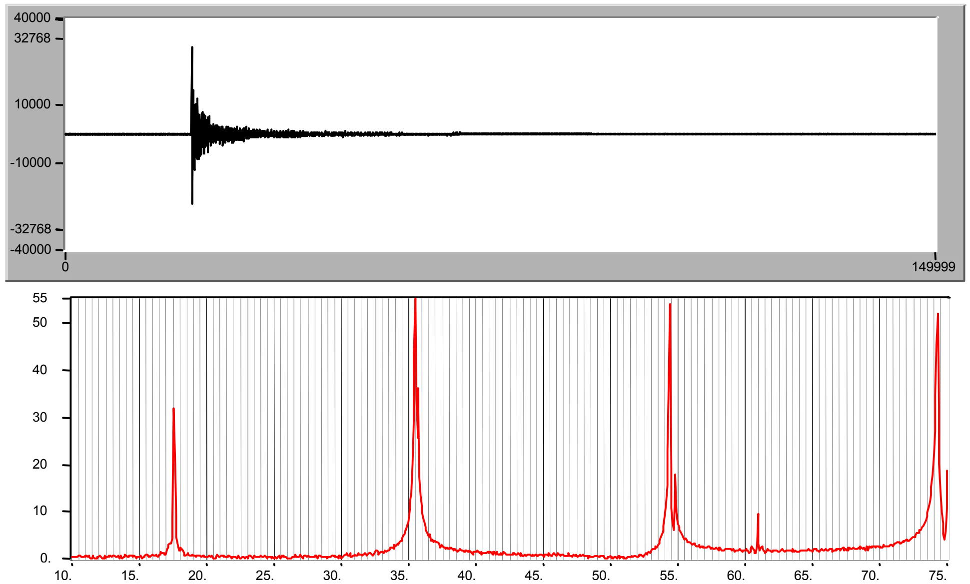

“Good” signal trace and spectrum

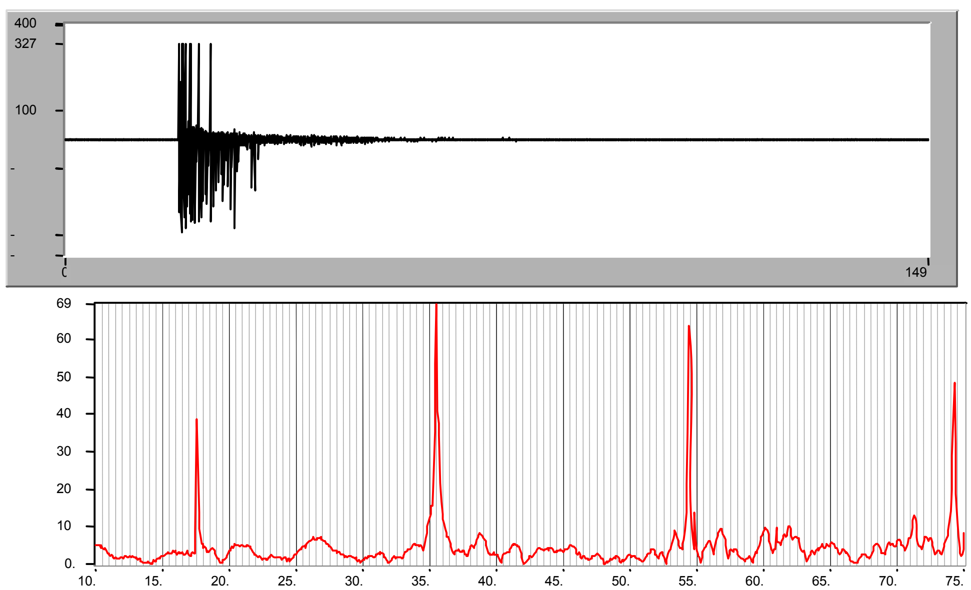

“Bad” signal trace and spectrum

Figure 3. Examples of test spectra.

ADDENDUM 1 - Preparations

Procedure for identifying tendon segments, measuring and recording lengths, and marking for accelerometer and impact location.

1. Tendon segment designations

The following applies to a generic N-S twin, 110-spans in both directions, segmental box construction bridge with three external tendons in each side of each span. Deviation blocks are present so that each tendon has a slopping free segment reaching the diaphragm at the S end of the span, and a segment at the other end reaching the diaphragm at the N end. It is assumed that only the end segments will be tested. In this generic example, the sloping segments of the three tendons in a given side are differentiated by their length. In other cases they may be differentiated by their position e.g. high, medium and low.

Use following order to assign a tendon segment name: Span number, direction, position along span, position across span, length of the sloping segment, creating an eight-character name **FFFGGHIJ**. The values that each of the characters can take are per Table Add.1.1.

Table Add.1.1 - Eight-Character Tendon Segment Designation

FFFGGHIJ

Span Designation		Position Along Span **H**	Position Across Span **I**	Length of Sloping Segment **J**
Span Number **FFF**	Direction **GG**			
001 to **110**	**SB**: Southbound **NB**: Northbound	**S**: South End **N**: North End	**W**: West Side **E**: East Side	**L**: Longest **M**: Medium **S**: Shortest

Example: All tendon segments to be tested in Span 093 North Bound:

West side

South End | North End

093NBSWL	**093NBNWL**
093NBSWM	**093NBNWM**
093NBSWS	**093NBNWS**
093NBSEL	**093NBNEL**
093NBSEM	**093NBNEM**
093NBSES	**093NBNES**

East side

2. Measuring and recording length.

a. For each tendon segment to be tested, clear any obstructions or debris that may prevent tendon from vibrating freely. **Note: If the tendon is obstructed by unremovable obstacles (e.g, contact with walls), frets may be installed but special procedures apply. not coveed in this guide.**

b. On each tendon segment, measure and record in Log Form the clear concrete-to-concrete distance. Make a note of any unusual details such as uneven concrete surface.

If available, use a metric tape and write result with 1 mm precision (if only English-units tape is available, write result in inches with 1/8 inch precision). If any other device [e.g. Laser unit] is used instead of tape, ensure first that device is accurate by making independent tape and device measurements.

- If using tape, ensure that an accurate, stretch-free tape is used. Do not pull on tape excessively. Replace kinked or damaged tape.
- Make sure that any folding tabs at end of tape are properly positioned.
- If concrete face is irregular, refer distance to main plane representing surface.

3. Marking accelerometer and impact positions.

a. Mark with tape or bright marker position where accelerometer is to be placed. See Figure A1 (if end points are not against a bulkhead or a deviation saddle, measure distances from lowest point). Position is at distance L_A from low end, where L_A is ~1/3 of the tendon segment length. The value of this distance is not critical but once chosen it must be recorded.

b. Mark with tape or bright marker position where impact is to be made. See Figure Add.1.1. Position is at distance L_I from low end, where L_I is ~1/6 of the tendon segment length. The value of this distance is not critical but once chosen it must be recorded.

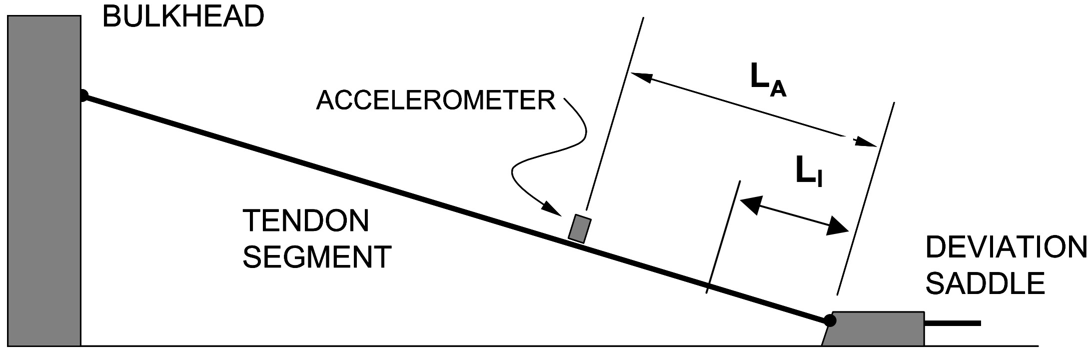

Figure Add.1.1

ADDENDUM 2 - Notice and Disclaimer

Notice and Disclaimer:

This guide is not to be construed as to include safety instruction. All safety issues (including any needed safety instruction) are the responsibility of the Florida Department of Transportation (FDOT), and its other contractors.

Field activities may involve risks to personnel. The test procedures developed by University of South Florida (USF) and instructed to the operators are provided to FDOT for its consideration and decision as to whether they are to be implemented by any party. Implementation in the field is to be conducted under the responsibility only of the FDOT and its other contractors. Neither USF nor its personnel assume any liability for any events that may result from implementing those procedures.

Upon completion of the testing FDOT and its contractors will return to USF the test equipment, software, and copies of the acquired data.

ADDENDUM 3 - Log Form (Generic)

LOG FORM - PAGE 1 OF 2
SOUTH SIDE OF SPAN AND TUNING FORK TESTS

SPAN_____

COMPUTER _____
DATE _________ START TIME T
OPERATOR_DRC END TIME T

SEGMENT	LENGTH (m)	TEST	MODE 1 f(Hz)	MODE 2 f(Hz)	OBSERVATIONS
SWL		1			
		2			
		3			
		4			
SWM		1			
		2			
		3			
		4			
SWS		1			
		2			
		3			
		4			
SEL		1			
		2			
		3			
		4			
SEM		1			
		2			
		3			
		4			
SES		1			
		2			
		3			
		4			

TESTS 1 AND 2 : STRAIGHT IMPACT **TESTS 3 AND 4 : SIDE IMPACT**

TUNING FORK TEST:

ACCELEROMETER:

Enter any additional notes in Supplementary Information box next page.

LOG FORM - PAGE 2 OF 2

NORTH SIDE OF SPAN AND SUPPLEMENTARY INFORMATION

SPAN_____

SEGMENT	LENGTH (m)	TEST	MODE 1 f(Hz)	MODE 2 f(Hz)	OBSERVATIONS
NWL		1			
		2			
		3			
		4			
NWM		1			
		2			
		3			
		4			
NWS		1			
		2			
		3			
		4			
NEL		1			
		2			
		3			
		4			
NEM		1			
		2			
		3			
		4			
NES		1			
		2			
		3			
		4			

TESTS 1 AND 2 : STRAIGHT IMPACT **TESTS 3 AND 4 : SIDE IMPACT**

SUPPLEMENTARY INFORMATION

ADDENDUM 4 - Tension Spreadsheet

a) Tension.xls Spreadsheet Instructions

1 - Open the Excel Workbook called "Tension.xls".

2 - In the Worksheet called "Inputs" enter the following data in their corresponding cells:

-Bridge's name.

-Length L (meters) and Mode Frequencies f (Hz) for each of the tendon segments tested, from the Log Form.

- Number of Strands from bridge construction data.

- Mass mu per unit length (kg/m), and stiffness S of the tendon (N-m^2), from the Estimation Table (Table Add.4.1, see next page) for each tendon segment of being analyzed. The Estimation Table use as input the number and type of strands.

Note: Leave cells empty if data are not available.

3 - The calculated Tension per strand (kN/strand), in each of the bridge segments, appears on the "Results" Worksheet.

Table Add.4.1
Estimation Table

Nominal Strand Size (in)	Number of Strands	Linear Mass (kg/m)	Linear Mass (lb/in)	Stiffness ($kN\text{-}m^2$)	Stiffness ($Mlbf\text{-}in^2$)
0.5	12	17.5	0.98	75	26
	17	20	1.12	95	33
	19	22	1.22	120	42
	24	32	1.77	170	59
	27	33	1.87	225	78
	28	34	1.91	245	85
	29	35	1.94	250	87
0.6	19	33	1.84	260	91
	12	27	1.50	160	56

Notes:

1. This table contains values roughly representative of linear mass and flexural stiffness obtained in prior detailed investigations of tendons in various FDOT segmental bridges, and in the present work, for tendons with the indicated number of strands and strand size. Typically duct diameter is adjusted by design to match number and size of strands so no entry is given for that dimension. Values for conditions not shown in the table can be obtained by interpolation/extrapolation as a first approximation.

2. A more accurate estimate of linear mass may be calculated if reliable data on duct diameter and wall thickness as well as grout density values are available, using standard strand cross section area values, and densities for steel and HDPE duct equal to 7.9 g/cm^3 and 1.0 g/cm^3 respectively.

3. To insert in Tension.xls, convert listed S value to $N\text{-}m^2$ by multiplying by 1,000. Note the spreadsheet is prepared for SI units; the English unit values are provided only for completeness. The nominal strand size is given in English units only to conform to common usage.

b) Example of Spreadsheet application and Input and Output Fields

This example of the simplified test approach includes actual field data from Span 117SB of the High Approaches of the Sunshine Skyway Bridge. This span is also part of the structures that were examined using the full detailed vibrational analysis procedures, reported separately in Appendix 3. Those analyses employed the entire vibration file and spectral information of seven vibration modes. The simplified procedure illustrated here uses only the data displayed at the time of the test on the computer screen for the first two modes, and recorded in a log form.

The input data fields from the log form for each of the tendons in this span are shown next page in Illustration A2A41. The values for mass per unit length (abbreviated as mu in this spreadsheet) and S deviate somewhat from those in the Estimation Table as they were custom-chosen for this application based on additional available data.

Using Segment SWL as an illustration, the Mode 1 frequency results for the four tests were 8.8, 8.7, 8.8 and 8.8 Hz. Mode 2 yielded 17.6, 17.4, 17.5 and 17.6 Hz. The spreadsheet calculated the averages for each mode (8.775 and 17.525 Hz respectively). Application of Equation 2.14 in the Section Task : Simplified Testing and Analysis Method produced T estimates equal to 116.1 kN/strand (26.1 klbf/strand) and 115.1 kN/strand (25.9 klbf/strand) respectively. The average is 115.6 kN/strand (26.0 klbf/strand), and the Quality descriptor (percent difference between both estimates) is 0.85%. The sheet where those calculations are made is normally hidden from the user to avoid accidental cell corruption, but it can be displayed if desired using the Microsoft Excel Format/Sheet/Unhide command.

The result is displayed in the Output Field Listing of Illustration A2A41. It is noted that the full detailed calculations for tendon segment 117SB SWL (see Table 6, Appendix 3) returned a tension value of 115.4 kN/strand (26.0 klbf), remarkable close to that obtained by the simplified method used here. The other tendon segments in the group returned values by both methods that were typically within ~2% of each other.

Illustration A2A41: Example of Input and Output Fields
Input Field:

Segment	L meters	Strands	mu	S	Test	Mode 1	Mode 2
SWL	18.65	19	21.72	127275	1	8.8	17.6
					2	8.7	17.4
					3	8.8	17.5
					4	8.8	17.6
SWM	13.24	24	31.69	165700	1	12	24.1
					2	12.1	24.1
					3	12.1	24.2
					4	12.1	24.3
SWS	7.852	28	34.04	246875	1	20.7	42.3
					2	20.7	42.3
					3	20.8	42.5
					4	20.8	42.5
SEL	18.641	19	21.72	127275	1	8.8	17.5
					2	8.8	17.4
					3	8.8	17.5
					4	8.8	17.5
SEM	13.258	24	31.69	165700	1	12.1	24.3
					2	12.1	24.3
					3	12	24.5
					4	12.1	24.5
SES	7.879	28	34.04	246875	1	20.6	42.2
					2	20.6	42.2
					3	20.9	43
					4	20.9	43
NWL	18.581	19	21.72	127275	1	8.7	17.4
					2	8.6	17.4
					3	8.7	17.4
					4	8.7	17.5
NWM	13.215	24	31.69	165700	1	12	24
					2	12	24
					3	12	24
					4	12	24
NWS	7.911	28	34.04	246875	1	20	40.9
					2	20.2	40.9
					3	20.2	41.4
					4	20.2	41.4
NEL	18.554	19	21.72	127275	1	8.9	17.7
					2	8.9	17.7
					3	8.9	17.7
					4	8.9	17.7
NEM	13.23	24	31.69	165700	1	12	24
					2	12	24
					3	12.1	24.2
					4	12.1	24.2
NES	7.901	28	34.04	246875	1	20.3	41.6
					2	20.3	41.6
					3	20.5	41.9
					4	20.5	41.9

Output Field - Listing

Results		
Segment	Avg Tension (kN/strand)	Quality%
SWL	115.60	0.79
SWM	124.77	0.72
SWS	110.39	0.87
SEL	115.48	1.97
SEM	126.37	1.23
SES	111.92	2.00
NWL	112.68	0.38
NWM	122.52	0.96
NWS	105.24	0.62
NEL	117.22	1.65
NEM	123.90	0.95
NES	108.11	1.19

Output Field - Graphic:

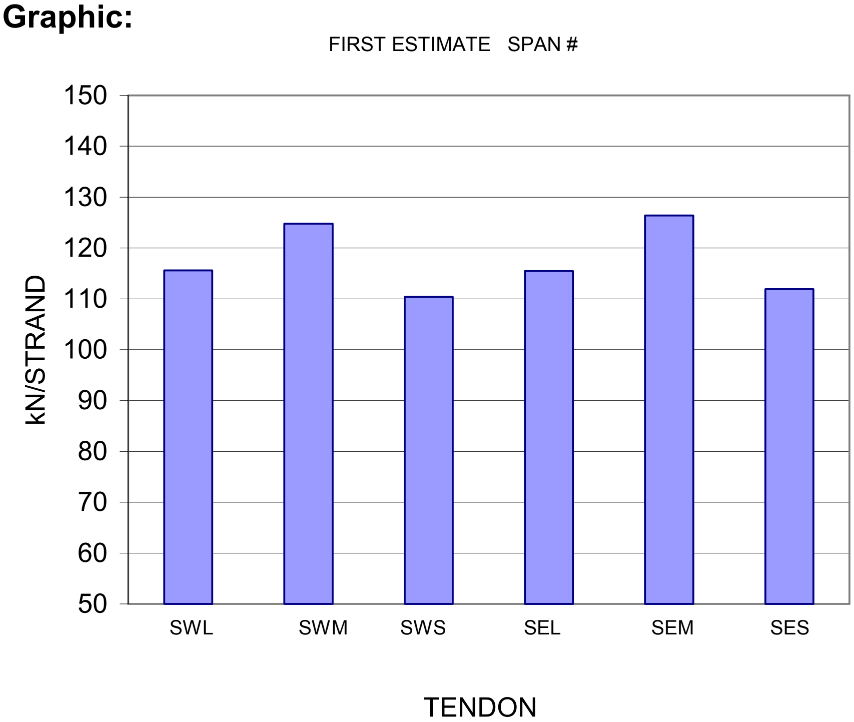

APPENDIX 3

TESTING AT THE SUNSHINE SKYWAY BRIDGE

Reproduction of the December 22, 2003 Task 4 Final Report.

RESULTS OF DETAILED ANALYSIS OF VIBRATION TESTING OF EXTERNAL TENDONS IN THE HIGH APPROACHES OF THE SUNSHINE SKYWAY BRIDGE

FINAL REPORT ON TASK 4 OF PROJECT

"VALIDATION AND PRACTICAL PROCEDURE FOR VIBRATIONAL EVALUATION OF TENDONS" BC353, RPWO #44

Alberto A. Sagüés, P.I.
Department of Civil and Environmental Engineering

Thomas G. Eason III, Co. P.I.
Department of Mechanical Engineering

University of South Florida
4202 E. Fowler Ave.
Tampa, FL 33620

Report Prepared by
A.A. Sagüés, T.G. Eason, C. Cotrim and A. Saradhi

Submitted for review October 14, 2003
Submitted as final December 22, 2003.

Scope of this report

Results of detailed analysis of vibrational tests of the external tendons in the segmental box spans of the high approaches of the Sunshine Skyway bridge are presented. The results were interpreted to identify tendons with symptoms of tension loss possibly indicative of corrosion damage. No instance of dramatic loss of tension became apparent, but tendons showing the greatest negative deviations from typical behavior of their peer group were flagged for special attention during upcoming inspections.

The detailed calculation procedures used in this report became recently available as developed under the other tasks of this contract. This report supersedes previous Draft reports based on earlier simplified analysis of the vibrational data.

Tendons tested and nomenclature

All tendons in the high approaches were tested. The span identifications were:

South High Approach:

Span 88 Northbound (NB) to 105 NB
Span 88 Southbound (SB) to 105 SB

North High Approach:

Span 117 NB to 134 NB
Span 117 SB to 134 SB

The spans are aligned in an approximately North-South direction. Each span contains six tendons, three on the West side and three on the East side. The longest external portions (hereafter called segments) of each tendon slope down from the diaphragm wall to the closest deviation block and were used for vibration testing. The tendons on each side of the span were named according to the length of their sloping sections: "Long" (L); "Medium" (M) and "Short" (S).

Two values of estimated tension were obtained for each tendon: one for the segment at the North end of the tendon, and one for the segment at the South end. The testing involved 432 tendons in 72 spans, yielding useful tension estimates for all but one of the 864 tendon segments.

Segments and the corresponding tension estimates were identified as in the following example: 97 NB NWM, meaning segment at the North end of the Medium tendon in the West side of Span 97 NB.

Tendons were identified as exemplified by 97 NB WM, meaning Medium tendon, West side of Span 97 NB.

Test procedure and data analysis

Tests were started September 18, 2002 and completed October 30, 2002.

The tests were conducted generally in the manner described in the report "Initial Development of Methods for Assessing Condition of Post-Tensioned Tendons of Segmental Bridges" [1], except that each tendon segment was subject to four test impacts; two in the vertical direction and two horizontally, yielding four data files and four manual records of test results. Each manual result record consisted of Mode 1 and Mode 2 frequencies, read by the operator from the computer screen; precise tendon segment length and air temperature measured by operator, and supplementary information such as observations of tendon vibration obstructions or presence of post-tensioning bars in the span. Manual records and data files were conveyed regularly to USF for analysis.

The results were initially analyzed using a simplified procedure based on the manual result records, and subsequently using the detailed analysis procedure based on the electronic data files. The simplified procedure results served as an approximate check of the detailed calculations, with which there was general agreement. This report describes only the findings from the detailed analysis.

For each tendon segment tested, the detailed analysis procedure combined the data from the four impact tests and produced a single estimate of the tendon segment tension. A peak identification algorithm identified the first seven vibration modes of the tendon segment. The mathematical procedure to estimate tension used an automated version of the methods described in Reference [1], assumed clamped conditions at each tendon segment end, and used the concrete-to-concrete distance as the vibrating length with no corrections for protruding steel collars or short concrete rings at the ends. The estimate was divided by the number of strands in the tendon (expressed as kN/strand), thus providing a value that allowed direct comparison of results from tendons with different numbers of strands.

Global tendon properties and parameters used for calculating tension with the detailed procedure

The parameters and properties are presented in Tables 1A and 1B. Number of strands and mass per unit length were obtained from design information and assumed steel, grout and polymer duct densities. Based on initial evidence from grout analyses under the other tasks of this contract, an effective value of 1,850 Kg/m^3 was adopted for the effective density of the grout. This value supersedes that used for estimates communicated in earlier draft reports. Precise tendon segment lengths used for the tension calculations varied slightly from tendon to tendon. Approximate lengths for the L, M and S designations are 18.5 m, 13.2 m and 7.9 m respectively. A number of tendon segments mainly at Expansion Joint or at End spans (See Table 2) had physical obstructions that reduced the effective vibration length, and the reduced vibration length was used for the tension calculations in all but one case. The vibrating length of segment 134 NB NEM was deemed to be too poorly defined for meaningful tension evaluation; tension data for that segment were not used in subsequent analyses.

Results

Vibration spectra were well defined and suitable for detailed analysis in the vast majority of the segments tested. Exceptions were all the tendon segments listed in Table 2 section A, which had major obstructions to vibration. Tendon segment 124NBNEL showed somewhat high scatter in its frequency response but analysis yielded no highly unusual estimated tension value.

Tables 3-4 (NB spans) and 5-6 (SB spans) display all the estimated tension results. For each span the results are listed for the L, M and S tendons indicating whether the tendon segment for which the tension is given was located on the SW, NW, SE or NE corner of the span. Tensions are reported as both KN/Strand and KLBF/Strand. The corresponding unit conversions are 1KN=0.22481 KLBF and 1KLBF=4.4482 KN.

The tension values are typically in the neighborhood of ~110 kN/strand or ~24.8 KLBF/Strand. This value corresponds to the force on regular ½ inch strand stressed to 60% of the nominal strength (1.86 Gpa or 270 ksi), a common expectation for the terminal condition of tendons initially stressed to 75% of nominal strength.

Each listing shows also how much the estimated tension of the N end of each tendon differed from that of the S end. Designating tension of N and S ends by TN and TS respectively, the N-S disparity is defined (in percents) by

$$\text{N-S Disparity\%} = 100\,[TN - TS] / [(TN+TS) / 2]$$

The disparity would ideally be zero if no friction had existed at the deviation blocks, but the results typically show appreciable values instead. In Regular spans the N-S disparity is on average about 5% , 9% and 12% for L, M and S tendons respectively which corresponds to the increasing number of intermediate deviation blocks. The sign of the disparity reflects the direction of erection, which was S to N in the S approach and N to S in N approach. Thus, for Regular spans on the S approach (where the tendons were stretched from the N end), the observed disparity is typically positive while for the N approach the disparity is typically negative. The extent of disparity tended to be less at the end or expansion joint spans, presumably due to differences in the way these spans were stressed.

An W-E disparity was also calculated by

W-E Disparity% = 100 [TW – TE] / [(TW+TE) / 2]

and displayed in Tables 3-6 together with the N-S disparity. The W-E disparity should average zero if the tensioning practice on each side of the span had been similar (e.g. balanced tensioning sequences, similarly calibrated and operated hydraulic jacks). The absolute value of this disparity was small (typical absolute value ~3%) and there seems to little if any global bias in either direction.

Examination of possible indications of tendon distress

Severe corrosion distress in a tendon could cause breakage of one or more strands and still not be apparent from external visual observation. However, such failure would result in significant reduction of overall tendon tension if force transfer to the remaining strands (by force development at the steel-grout interface, or by inter-strand friction) is not efficiently accomplished in a short distance. In such case, tension reduction is detectable by the vibration test as a diagnostic of distress.

Two main potential indicators of distress were sought by comparing tendon results with those of their peer group: (i) significantly low overall tendon tension, suggestive of a failure that caused force relaxation along the entire length and (ii) unusual end-to-end tension disparity, suggesting that corrosion was affecting one of the tendon ends but friction at the deviation blocks limited relaxation at the other end. The E-W disparity was used as a potential confirming indicator by looking for unusual deviation from the behavior of the twin tendon on the other side of the span.

Figures 1-12 were constructed to reveal possible instances of indicators (i) and (ii) by plotting TN as a function of TS for each sizable peer group of tendons. Thus each tendon is represented by one point that, if TN and TS were identical, would fall exactly on the ideal 1:1 diagonal line. The extent of deviation from the diagonal represents N-S disparity. The further the point is from the origin, the greater the average tension of the tendon.

Figures 1-6 examine results for tendons in the Regular spans, which constituted the largest uniform span population, grouped by L, M and S tendons. Because many tendons are available in this category, separate graphs were made for the NB and SB spans to avoid possible obscuring bias from any differences in construction practice of the NB and SB spans. The data for tendons in the N and S approaches, as well as for tendons on the E and W side of each span, are labeled with different symbols. The graphs show little systematic differentiation between tendons in the E and W sides of a given set of spans. However, the points for tendons from the N approach are clustered below the 1:1 line while those for the S approach are clustered above, because of the opposite directions of erection as discussed above. As expected, the separation between data clusters increased from L to M to S tendons reflecting increasing deviation block friction. The spread of points along the horizontal or the vertical direction is indicative of variability of estimated tension of the South or North tendon ends respectively. That variability was quantified by calculating the standard deviation of the South and North tension data of each group, yielding an average standard deviation of only 2.4%. No tendon segment had estimated tension lower than 9% below the average of its peer group. This spread is small considering that the typical tolerance expected from tendon tensioning procedures in construction is in the order of 5%, and that the precision of the vibration tension estimates presented here is expected to be in the order of 3%. Thus the largest majority of tendons in this category do not seem to have symptoms of distress per indicator (i). Attention was given to the few tendons for which the data appear to be conspicuously away from their peer group cluster. Based on the tolerance/uncertainty values indicated above, it was decided to flag any tendons having estimated tensions lower than ~7% below the average of their North-end or South-end peer group. Those tendons are noted in Figures 1-6 and listed in Table 7.

Figures 6-12 examine the behavior of the tendons in the Expansion Joint spans and the End spans. In these categories the peer groups are much smaller that in the Regular spans so deviations from "usual" behavior are more difficult to establish. Therefore, the data for W and E tendons of NB or SB spans were treated together to address a larger population (keeping in mind that some obscuring may result from bias of individual subgroups). The same overall trends observed for the Regular span tendons are apparent in these groups. The average standard deviation within peer groups was 3.4% and no tensions were found lower than 15% below peer group average (11% if tendon 134SBNEM is excluded). Thus as for the Regular spans, tendons with estimated tensions lower than ~7% below their group average are noted and listed in Table 7 as well.

Variations in N-S disparity per indicator (ii) were examined by means of the cumulative distribution curves shown in Figures 13-18. These curves are produced by plotting for each group in the Y axis the fraction of tendons having N-S disparity equal to or less than the indicated value in the X axis. Tables below each figure rank the tendons in each series from highest to lowest N-S disparity. The data series for the Regular spans (Figures 13-16) show that the not only the average N-S disparity, but also its spread, increases from L to M to S tendons. The increase in spread is not surprising as friction variability is expected to increase with its magnitude. The N-S disparity distributions were S-shaped curves resembling a Normal statistical distribution but the relatively small number of elements in each series precludes detailed statistical analysis. Similar graphs were made in Figures 17-18 for the Expansion Joint and End spans, but . the presence of some vibration obstructions in these spans further obscures interpretation. Due to these uncertainties, only one tendon (94 SB WM, Figure 14) was deemed to show unusual enough deviation from the overall trends to merit identification by indicator (ii).

Tendons Proposed For Special Attention During Inspection (see Table 8)

Based on the above analyses, the vibration tests did not reveal any indications of dramatically reduced tension in any of the tendons examined. However, tension in a few tendon segments deviated enough (after accounting for expected actual variability and uncertainty in estimates) from that of their peer groups to merit further attention. Those tendons segments were identified in Table 7 and are prioritized in Table 8 for receiving special attention during upcoming bridge inspections. Of that group, only two tendons are not associated with either the presence of PT rods in the span, or vibration obstructions that needed the use of corrected vibration lengths for the calculations. Those two tendons are therefore given the highest priority. It is emphasized that there could be tendons affected by corrosion having not enough tension loss to be revealed by the vibration test, which should be considered only as a complement to other forms of inspection.

Conclusions

1) Tension estimates from vibration testing were successfully conducted using the detailed analysis in all but one of the 864 tendon segments tested.

2) Estimated tension patterns were in agreement with the presence of friction at deviation blocks. The end-to-end tension disparity increased with the number of intermediate deviation blocks.

3) Vibration testing did not reveal any indications of dramatically reduced tension in any of the tendons segments evaluated. The average estimated tension standard deviation within tendon segment peer groups was on the order of 3%. No estimated tension (with one exception where vibration was obstructed) was lower than 11% below the average of its tendon segment peer group.

4) Tendon segments having estimated tensions lower than ~7% below their peer group average, and a tendon with unusual end-to-end tension disparity, were flagged for proposed special attention during upcoming inspections.

References.

[1] A. A. Sagues, S.C. Kranc and R.H. Hoehne, “Initial Development of Methods for Assessing Condition of Post-Tensioned Tendons of Segmental Bridges” , Final Report to Florida Department of Transportation, Contract # BC374, May 17, 2000.

Table 1A. PARAMETERS USED FOR ANALYSIS – TENDON TYPES.

Span Type and Number (both NB and SB)	Tendon Designation per Plans	Tendon Name for Testing	Number of Strands
End Span (88,105,117,134)	12	Long	19
	13	Medium	24
	14	Short	28
Expansion Joint Span (95,96,126,127)	1,9	Long	19
	2,10	Medium	29
	3,11	Short	28
Regular Span (89-95, 97-104, 118-125,128-133)	4	Long	24
	5	Medium	19
	6	Short	27

Table 1B. PARAMETERS USED FOR ANALYSIS – DUCT DIMENSIONS AND MASS.

# Strands	Sheath Outer Diameter (in)	Sheath Thickness (in)	Tendon Unit Length Mass (kg/m)*	%Grout Mass*
19	3.509	0.17	21.72	27%
24	4.511	0.199	31.69	36%
27	4.511	0.199	33.45	33%
28	4.511	0.199	34.04	32%
29	4.511	0.199	34.63	31%

*Assumed effective grout, steel and duct polymer densities of 1,850 Kg/m^3, 7,800 Kg/m^3 and 1,000 Kg/m^3 respectively. Assumed regular 0.5 in strand (0.153 in^2 per strand). The percent grout mass is the resulting fraction of the tendon mass per unit length corresponding to the grout. Estimated force is directly proportional to value of mass per unit length used for calculations. Tension estimates can be updated accordingly by simple proportion if revised input parameter values (especially for grout density) become available.

Table 2 - TENDON SEGMENTS WITH PHYSICAL OBSTRUCTIONS REDUCING EFFECTIVE VIBRATION LENGTH.

A. Tendon segments with obstructions acting as a fret and causing substantial reduction (typ. ~5 m) in effective vibration length:

105 SB NEM
105 SB NWM
134 SB NEM
134 NB NEL
134 NB NWL
134 NB NEM*

*Length deemed too poorly defined for analysis.

B. Tendon segments with obstructions, typically due to grout spills, causing modest reduction (typ. 0.1 m to 0.4 m) in effective vibration length.

89 NB NEL	123 NB SWM	134 NB NWS
117 SB NEL	126 SB SEL	134 NB SWM
123 NB NWL	132 NB NWL	134 NB SWS
123 NB NWM	132 NB SEL	134 NB SEM
123 NB NWS	134 NB NES	134 NB SES
123 NB SWL	134 NB NWM	

Table 3 –HIGH APPROACH SOUTH SIDE. NORTHBOUND SPANS 88 TO 105

Span	Tendon	Tension (KN/Strand)				Tension (KLBF/Strand)				N-S Disparity		W-E Disparity		
		SW	NW	SE	NE	SW	NW	SE	NE	W	E	N	S	
88NB	L	106.7	111.1	105.5	109.7	24.0	25.0	23.7	24.7	4%	4%	1%	1%	End Span
	M	113.5	117.2	111.4	117.1	25.5	26.3	25.1	26.3	3%	5%	0%	2%	
	S	103.3	110.0	102.4	108.5	23.2	24.7	23.0	24.4	6%	6%	1%	1%	
89NB	L	109.1	111.0	106.0	106.8	24.5	25.0	23.8	24.0	2%	1%	4%	3%	
	M	102.4	112.9	97.1	105.9	23.0	25.4	21.8	23.8	10%	9%	6%	5%	
	S	95.5	103.8	95.0	104.6	21.5	23.3	21.4	23.5	8%	10%	-1%	1%	
90NB	L	101.5	105.4	100.9	107.3	22.8	23.7	22.7	24.1	4%	6%	-2%	1%	
	M	94.2	102.0	95.5	105.5	21.2	22.9	21.5	23.7	8%	10%	-3%	-1%	
	S	91.0	99.0	94.8	104.1	20.5	22.3	21.3	23.4	8%	9%	-5%	-4%	
91NB	L	110.8	111.6	101.3	105.3	24.9	25.1	22.8	23.7	1%	4%	6%	9%	
	M	103.4	112.2	98.7	109.9	23.2	25.2	22.2	24.7	8%	11%	2%	5%	
	S	87.9	95.4	90.8	99.9	19.8	21.4	20.4	22.5	8%	10%	-5%	-3%	
92NB	L	98.6	104.8	103.5	107.6	22.2	23.6	23.3	24.2	6%	4%	-3%	-5%	
	M	101.0	110.8	101.6	109.2	22.7	24.9	22.8	24.5	9%	7%	1%	-1%	
	S	97.0	104.2	95.8	106.6	21.8	23.4	21.5	24.0	7%	11%	-2%	1%	
93NB	L	104.9	107.3	103.8	110.5	23.6	24.1	23.3	24.8	2%	6%	-3%	1%	
	M	101.7	112.1	100.9	110.7	22.9	25.2	22.7	24.9	10%	9%	1%	1%	
	S	94.4	105.1	90.9	103.7	21.2	23.6	20.4	23.3	11%	13%	1%	4%	
94NB	L	107.3	108.5	108.1	112.9	24.1	24.4	24.3	25.4	1%	4%	-4%	-1%	
	M	99.0	109.2	106.0	113.8	22.3	24.6	23.8	25.6	10%	7%	-4%	-7%	
	S	95.9	102.7	93.7	108.0	21.6	23.1	21.1	24.3	7%	14%	-5%	2%	
95NB	L	109.9	110.5	108.2	109.9	24.7	24.9	24.3	24.7	1%	2%	1%	2%	
	M	101.3	107.2	105.6	108.3	22.8	24.1	23.7	24.4	6%	3%	-1%	-4%	
	S	102.3	105.8	108.0	108.5	23.0	23.8	24.3	24.4	3%	0%	-3%	-5%	Expansion Joint
96NB	L	110.3	115.9	109.8	113.8	24.8	26.1	24.7	25.6	5%	4%	2%	1%	
	M	105.2	111.9	106.0	109.0	23.7	25.2	23.8	24.5	6%	3%	3%	-1%	
	S	105.2	115.4	100.2	109.0	23.6	25.9	22.5	24.5	9%	8%	6%	5%	
97NB	L	106.1	112.0	107.7	113.9	23.9	25.2	24.2	25.6	5%	6%	-2%	-1%	
	M	102.9	112.6	106.3	114.0	23.1	25.3	23.9	25.6	9%	7%	-1%	-3%	
	S	96.5	110.6	99.6	107.5	21.7	24.9	22.4	24.2	14%	8%	3%	-3%	
98NB	L	102.7	107.0	104.6	108.7	23.1	24.1	23.5	24.4	4%	4%	-2%	-2%	
	M	97.7	110.0	102.2	112.8	22.0	24.7	23.0	25.4	12%	10%	-3%	-5%	
	S	97.0	106.1	97.7	107.6	21.8	23.9	22.0	24.2	9%	10%	-1%	-1%	
99NB	L	110.2	113.8	110.8	117.1	24.8	25.6	24.9	26.3	3%	6%	-3%	-1%	
	M	102.0	114.0	102.7	113.6	22.9	25.6	23.1	25.5	11%	10%	0%	-1%	
	S	92.6	108.8	93.1	108.5	20.8	24.5	20.9	24.4	16%	15%	0%	-1%	
100NB	L	107.9	112.1	106.7	113.5	24.2	25.2	24.0	25.5	4%	6%	-1%	1%	
	M	106.7	114.1	104.3	115.1	24.0	25.7	23.4	25.9	7%	10%	-1%	2%	
	S	95.2	106.4	96.3	109.9	21.4	23.9	21.6	24.7	11%	13%	-3%	-1%	
101NB	L	106.2	114.8	107.1	114.0	23.9	25.8	24.1	25.6	8%	6%	1%	-1%	
	M	102.5	111.5	103.3	113.7	23.0	25.1	23.2	25.6	8%	10%	-2%	-1%	
	S	93.8	103.8	95.8	110.0	21.1	23.3	21.5	24.7	10%	14%	-6%	-2%	
102NB	L	106.8	113.1	106.1	112.8	24.0	25.4	23.9	25.4	6%	6%	0%	1%	
	M	104.6	115.7	102.5	114.4	23.5	26.0	23.1	25.7	10%	11%	1%	2%	
	S	95.0	108.3	94.5	102.0	21.4	24.3	21.2	22.9	13%	8%	6%	1%	
103NB	L	105.6	111.1	107.6	112.6	23.7	25.0	24.2	25.3	5%	5%	-1%	-2%	
	M	105.9	110.0	102.7	113.6	23.8	24.7	23.1	25.5	4%	10%	-3%	3%	
	S	100.2	106.4	93.6	103.8	22.5	23.9	21.1	23.3	6%	10%	2%	7%	
104NB	L	104.1	111.2	103.4	108.1	23.4	25.0	23.3	24.3	7%	4%	3%	1%	
	M	101.8	112.3	102.8	114.9	22.9	25.2	23.1	25.8	10%	11%	-2%	-1%	
	S	93.9	104.2	93.2	107.3	21.1	23.4	20.9	24.1	10%	14%	-3%	1%	
105 NB	L	110.1	113.3	110.3	112.4	24.7	25.5	24.8	25.3	3%	2%	1%	0%	
	M	108.3	114.8	114.7	119.6	24.3	25.8	25.8	26.9	6%	4%	-4%	-6%	End Span
	S	98.6	106.1	101.0	108.8	22.2	23.9	22.7	24.5	7%	7%	-3%	-2%	

Table 4 –HIGH APPROACH NORTH SIDE. NORTHBOUND SPANS 117 TO 134

Span	Tendon	Tension (KN/Strand)				Tension (KLBF/Strand)				N-S Disparity		W-E Disparity		
		SW	NW	SE	NE	SW	NW	SE	NE	W	E	N	S	
117NB	L	113.5	107.4	114.4	110.0	25.5	24.2	25.7	24.7	-5%	-4%	-2%	-1%	End Span
	M	121.2	113.9	120.4	112.6	27.3	25.6	27.1	25.3	-6%	-7%	1%	1%	
	S	104.8	102.7	105.3	99.8	23.6	23.1	23.7	22.4	-2%	-5%	3%	-1%	
118NB	L	108.5	101.3	108.5	103.3	24.4	22.8	24.4	23.2	-7%	-5%	-2%	0%	
	M	103.2	96.0	109.5	101.1	23.2	21.6	24.6	22.7	-7%	-8%	-5%	-6%	
	S	103.7	91.4	106.6	95.3	23.3	20.5	24.0	21.4	-13%	-11%	-4%	-3%	
119NB	L	107.7	103.5	107.8	106.1	24.2	23.3	24.2	23.9	-4%	-2%	-3%	0%	
	M	103.8	98.5	108.8	98.7	23.3	22.1	24.5	22.2	-5%	-10%	0%	-5%	
	S	105.5	94.1	110.1	93.4	23.7	21.2	24.7	21.0	-11%	-16%	1%	-4%	
120NB	L	105.4	103.5	110.9	106.6	23.7	23.3	24.9	24.0	-2%	-4%	-3%	-5%	
	M	102.0	94.0	108.9	102.2	22.9	21.1	24.5	23.0	-8%	-6%	-8%	-7%	
	S	105.3	97.6	106.5	94.8	23.7	21.9	23.9	21.3	-8%	-12%	3%	-1%	
121NB	L	107.2	104.7	109.0	103.0	24.1	23.5	24.5	23.2	-2%	-6%	2%	-2%	
	M	104.3	94.2	105.2	93.7	23.4	21.2	23.7	21.1	-10%	-12%	1%	-1%	
	S	103.0	94.4	107.0	96.3	23.2	21.2	24.1	21.7	-9%	-11%	-2%	-4%	
122NB	L	107.3	103.4	107.9	103.6	24.1	23.2	24.3	23.3	-4%	-4%	0%	-1%	
	M	101.4	92.0	101.1	93.5	22.8	20.7	22.7	21.0	-10%	-8%	-2%	0%	
	S	102.8	95.9	102.0	96.0	23.1	21.5	22.9	21.6	-7%	-6%	0%	1%	
123NB	L	104.9	101.2	106.3	102.0	23.6	22.7	23.9	22.9	-4%	-4%	-1%	-1%	
	M	102.3	93.1	105.3	98.0	23.0	20.9	23.7	22.0	-9%	-7%	-5%	-3%	
	S	110.7	98.9	103.8	95.2	24.9	22.2	23.3	21.4	-11%	-9%	4%	6%	
124NB	L	105.6	102.3	108.9	102.8	23.7	23.0	24.5	23.1	-3%	-6%	-1%	-3%	
	M	98.9	90.7	105.4	94.5	22.2	20.4	23.7	21.3	-9%	-11%	-4%	-6%	
	S	99.8	94.9	99.9	90.2	22.4	21.3	22.5	20.3	-5%	-10%	5%	0%	
125NB	L	99.9	95.9	106.9	103.3	22.5	21.6	24.0	23.2	-4%	-3%	-7%	-7%	
	M	105.6	96.6	104.3	97.3	23.7	21.7	23.4	21.9	-9%	-7%	-1%	1%	
	S	107.4	97.6	98.3	94.9	24.1	22.0	22.1	21.3	-10%	-3%	3%	9%	
126NB	L	106.3	101.1	116.2	105.6	23.9	22.7	26.1	23.7	-5%	-10%	-4%	-9%	
	M	103.2	101.4	100.7	101.1	23.2	22.8	22.6	22.7	-2%	0%	0%	2%	
	S	101.7	98.7	109.0	106.0	22.9	22.2	24.5	23.8	-3%	-3%	-7%	-7%	Expansion Joint
127NB	L	109.3	104.7	109.2	106.0	24.6	23.5	24.5	23.8	-4%	-3%	-1%	0%	
	M	106.9	100.7	106.9	102.1	24.0	22.6	24.0	23.0	-6%	-5%	-1%	0%	
	S	104.2	98.2	105.0	103.0	23.4	22.1	23.6	23.2	-6%	-2%	-5%	-1%	
128NB	L	108.1	103.1	109.0	106.7	24.3	23.2	24.5	24.0	-5%	-2%	-3%	-1%	
	M	104.8	97.9	107.9	105.0	23.6	22.0	24.3	23.6	-7%	-3%	-7%	-3%	
	S	108.9	100.1	106.8	101.0	24.5	22.5	24.0	22.7	-8%	-6%	-1%	2%	
129NB	L	107.0	99.9	110.6	107.2	24.1	22.5	24.9	24.1	-7%	-3%	-7%	-3%	
	M	104.3	93.7	107.4	100.7	23.4	21.1	24.1	22.6	-11%	-6%	-7%	-3%	
	S	104.9	93.4	109.1	100.9	23.6	21.0	24.5	22.7	-12%	-8%	-8%	-4%	
130NB	L	107.5	106.9	111.0	105.2	24.2	24.0	25.0	23.6	-1%	-5%	2%	-3%	
	M	102.7	92.3	109.3	100.9	23.1	20.7	24.6	22.7	-11%	-8%	-9%	-6%	
	S	104.2	91.4	106.8	98.8	23.4	20.5	24.0	22.2	-13%	-8%	-8%	-2%	
131NB	L	108.8	103.5	107.7	104.9	24.5	23.3	24.2	23.6	-5%	-3%	-1%	1%	
	M	108.8	98.2	111.2	102.7	24.5	22.1	25.0	23.1	-10%	-8%	-4%	-2%	
	S	103.0	91.5	105.9	102.1	23.2	20.6	23.8	23.0	-12%	-4%	-11%	-3%	
132NB	L	106.4	97.2	104.2	103.2	23.9	21.9	23.4	23.2	-9%	-1%	-6%	2%	
	M	103.8	95.0	106.2	98.2	23.3	21.4	23.9	22.1	-9%	-8%	-3%	-2%	
	S	99.1	91.9	102.6	93.4	22.3	20.7	23.1	21.0	-8%	-9%	-2%	-3%	
133NB	L	108.8	102.8	111.2	108.1	24.5	23.1	25.0	24.3	-6%	-3%	-5%	-2%	
	M	102.8	95.5	110.8	100.4	23.1	21.5	24.9	22.6	-7%	-10%	-5%	-7%	
	S	110.3	99.9	108.6	97.6	24.8	22.5	24.4	22.0	-10%	-11%	2%	2%	
134NB	L	103.0	96.5	112.0	105.1	23.2	21.7	25.2	23.6	-7%	-6%	-9%	-8%	
	M	115.2	117.0	116.1	-	25.9	26.3	26.1	-	1%	-	-	-1%	
	S	98.2	100.0	98.8	97.6	22.1	22.5	22.2	21.9	2%	-1%	2%	-1%	End Span

Table 5 –HIGH APPROACH SOUTH SIDE. SOUTHBOUND SPANS 88 TO 105

Span	Tendon	Tension (KN/Strand)				Tension (KLBF/Strand)				N-S Disparity		W-E Disparity		
		SW	NW	SE	NE	SW	NW	SE	NE	W	E	N	S	
88SB	L	110.0	117.5	109.1	114.7	24.7	26.4	24.5	25.8	7%	5%	2%	1%	End Span
	M	113.3	118.5	108.6	115.9	25.5	26.7	24.4	26.1	5%	7%	2%	4%	
	S	99.5	108.6	104.6	111.4	22.4	24.4	23.5	25.0	9%	6%	-3%	-5%	
89SB	L	108.1	115.1	108.5	114.5	24.3	25.9	24.4	25.8	6%	5%	1%	0%	
	M	109.0	115.9	100.8	112.7	24.5	26.1	22.7	25.3	6%	11%	3%	8%	
	S	94.3	109.7	96.5	109.1	21.2	24.7	21.7	24.5	15%	12%	1%	-2%	
90SB	L	107.6	114.0	106.0	112.9	24.2	25.6	23.8	25.4	6%	6%	1%	2%	
	M	104.4	115.3	106.4	114.6	23.5	25.9	23.9	25.8	10%	7%	1%	-2%	
	S	95.9	111.3	92.1	106.6	21.6	25.0	20.7	24.0	15%	15%	4%	4%	
91SB	L	106.0	113.5	106.4	111.0	23.8	25.5	23.9	25.0	7%	4%	2%	0%	
	M	106.9	116.7	105.0	115.3	24.0	26.2	23.6	25.9	9%	9%	1%	2%	
	S	96.1	109.1	95.9	108.0	21.6	24.5	21.6	24.3	13%	12%	1%	0%	
92SB	L	108.4	116.1	104.7	110.5	24.4	26.1	23.5	24.8	7%	5%	5%	3%	
	M	110.1	118.3	103.7	112.0	24.7	26.6	23.3	25.2	7%	8%	5%	6%	
	S	94.1	108.1	90.3	108.4	21.2	24.3	20.3	24.4	14%	18%	0%	4%	
93SB	L	108.2	113.5	103.9	108.4	24.3	25.5	23.4	24.4	5%	4%	5%	4%	
	M	104.9	115.7	101.3	110.9	23.6	26.0	22.8	24.9	10%	9%	4%	3%	
	S	94.0	109.7	90.5	106.2	21.1	24.7	20.4	23.9	15%	16%	3%	4%	
94SB	L	108.0	107.3	104.6	109.1	24.3	24.1	23.5	24.5	-1%	4%	-2%	3%	
	M	109.5	105.3	99.2	110.8	24.6	23.7	22.3	24.9	-4%	11%	-5%	10%	
	S	98.7	107.2	90.6	103.7	22.2	24.1	20.4	23.3	8%	13%	3%	9%	
95SB	L	106.7	109.9	104.6	108.8	24.0	24.7	23.5	24.5	3%	4%	1%	2%	
	M	101.6	107.2	101.4	104.1	22.8	24.1	22.8	23.4	5%	3%	3%	0%	
	S	96.2	103.9	95.5	103.0	21.6	23.4	21.5	23.2	8%	8%	1%	1%	Expansion Joint
96SB	L	108.3	109.0	109.3	113.4	24.3	24.5	24.6	25.5	1%	4%	-4%	-1%	
	M	102.9	108.9	98.3	101.7	23.1	24.5	22.1	22.9	6%	3%	7%	5%	
	S	102.5	108.6	97.3	105.0	23.1	24.4	21.9	23.6	6%	8%	3%	5%	
97SB	L	107.2	114.8	106.7	112.2	24.1	25.8	24.0	25.2	7%	5%	2%	0%	
	M	107.0	114.8	107.8	115.4	24.0	25.8	24.2	25.9	7%	7%	-1%	-1%	
	S	97.2	107.3	94.5	107.3	21.9	24.1	21.2	24.1	10%	13%	0%	3%	
98SB	L	104.0	113.2	103.6	109.7	23.4	25.5	23.3	24.7	9%	6%	3%	0%	
	M	102.4	114.7	100.9	112.7	23.0	25.8	22.7	25.3	11%	11%	2%	1%	
	S	94.9	103.8	89.4	103.9	21.3	23.3	20.1	23.4	9%	15%	0%	6%	
99SB	L	108.3	113.3	103.5	108.3	24.3	25.5	23.3	24.3	5%	5%	5%	5%	
	M	109.9	117.7	103.4	111.4	24.7	26.5	23.2	25.0	7%	7%	6%	6%	
	S	93.0	107.0	95.8	109.1	20.9	24.1	21.5	24.5	14%	13%	-2%	-3%	
100SB	L	108.2	113.9	104.1	110.5	24.3	25.6	23.4	24.8	5%	6%	3%	4%	
	M	106.2	115.2	103.2	112.8	23.9	25.9	23.2	25.4	8%	9%	2%	3%	
	S	98.0	108.6	94.3	107.6	22.0	24.4	21.2	24.2	10%	13%	1%	4%	
101SB	L	109.4	110.6	105.2	110.8	24.6	24.9	23.6	24.9	1%	5%	0%	4%	
	M	104.7	114.2	103.1	112.8	23.5	25.7	23.2	25.4	9%	9%	1%	2%	
	S	93.1	109.1	95.9	107.0	20.9	24.5	21.6	24.1	16%	11%	2%	-3%	
102SB	L	111.3	113.8	107.5	112.2	25.0	25.6	24.2	25.2	2%	4%	1%	3%	
	M	104.3	114.6	104.0	114.1	23.4	25.8	23.4	25.6	9%	9%	1%	0%	
	S	95.9	106.2	95.9	109.1	21.6	23.9	21.6	24.5	10%	13%	-3%	0%	
103SB	L	112.9	118.6	107.5	110.9	25.4	26.7	24.2	24.9	5%	3%	7%	5%	
	M	112.8	115.6	103.4	114.6	25.4	26.0	23.2	25.8	3%	10%	1%	9%	
	S	95.0	109.9	96.4	110.4	21.4	24.7	21.7	24.8	15%	14%	-1%	-1%	
104SB	L	104.9	112.2	106.6	112.3	23.6	25.2	24.0	25.3	7%	5%	0%	-2%	
	M	108.2	118.1	103.0	110.9	24.3	26.5	23.2	24.9	9%	7%	6%	5%	
	S	98.3	111.2	98.6	108.3	22.1	25.0	22.2	24.3	12%	9%	3%	0%	
105SB	L	108.2	113.3	108.8	112.1	24.3	25.5	24.5	25.2	5%	3%	1%	-1%	
	M	113.2	115.5	110.0	106.2	25.4	26.0	24.7	23.9	2%	-4%	8%	3%	
	S	102.7	111.1	96.2	106.3	23.1	25.0	21.6	23.9	8%	10%	4%	7%	End Span

Table 6 –HIGH APPROACH NORTH SIDE. SOUTHBOUND SPANS 117 TO 134

Span	Tendon	Tension (KN/Strand)				Tension (KLBF/Strand)				N-S Disparity		W-E Disparity		
		SW	NW	SE	NE	SW	NW	SE	NE	W	E	N	S	
117SB	L	115.4	113.0	115.5	116.5	26.0	25.4	26.0	26.2	-2%	1%	-3%	0%	End Span
	M	121.8	119.7	124.1	120.4	27.4	26.9	27.9	27.1	-2%	-3%	-1%	-2%	
	S	108.7	103.6	108.9	106.6	24.4	23.3	24.5	24.0	-5%	-2%	-3%	0%	
118SB	L	113.9	108.6	113.5	110.5	25.6	24.4	25.5	24.8	-5%	-3%	-2%	0%	
	M	112.3	102.3	114.9	102.8	25.2	23.0	25.8	23.1	-9%	-11%	-1%	-2%	
	S	111.4	97.9	110.5	101.5	25.0	22.0	24.8	22.8	-13%	-8%	-4%	1%	
119SB	L	115.5	107.7	115.8	109.0	26.0	24.2	26.0	24.5	-7%	-6%	-1%	0%	
	M	114.4	109.0	115.6	108.9	25.7	24.5	26.0	24.5	-5%	-6%	0%	-1%	
	S	112.0	101.5	108.2	97.8	25.2	22.8	24.3	22.0	-10%	-10%	4%	3%	
120SB	L	113.7	109.2	114.4	108.7	25.6	24.6	25.7	24.4	-4%	-5%	0%	-1%	
	M	114.7	106.3	115.1	106.9	25.8	23.9	25.9	24.0	-8%	-7%	-1%	0%	
	S	111.2	98.2	109.4	97.8	25.0	22.1	24.6	22.0	-12%	-11%	0%	2%	
121SB	L	113.3	108.4	112.5	109.1	25.5	24.4	25.3	24.5	-4%	-3%	-1%	1%	
	M	112.7	104.4	113.6	106.1	25.3	23.5	25.5	23.9	-8%	-7%	-2%	-1%	
	S	110.9	98.6	111.9	95.8	24.9	22.2	25.2	21.5	-12%	-16%	3%	-1%	
122SB	L	113.2	109.0	113.6	108.2	25.4	24.5	25.5	24.3	-4%	-5%	1%	0%	
	M	114.0	104.7	117.1	106.0	25.6	23.5	26.3	23.8	-8%	-10%	-1%	-3%	
	S	113.1	101.3	110.4	101.5	25.4	22.8	24.8	22.8	-11%	-8%	0%	2%	
123SB	L	114.2	111.6	113.1	107.4	25.7	25.1	25.4	24.1	-2%	-5%	4%	1%	
	M	114.0	107.8	115.0	104.2	25.6	24.2	25.9	23.4	-6%	-10%	3%	-1%	
	S	105.6	96.2	110.7	95.7	23.7	21.6	24.9	21.5	-9%	-15%	1%	-5%	
124SB	L	112.9	109.5	110.7	105.5	25.4	24.6	24.9	23.7	-3%	-5%	4%	2%	
	M	114.4	106.2	114.2	105.0	25.7	23.9	25.7	23.6	-7%	-8%	1%	0%	
	S	108.5	95.6	106.5	97.5	24.4	21.5	23.9	21.9	-13%	-9%	-2%	2%	
125SB	L	115.2	110.5	112.2	107.9	25.9	24.8	25.2	24.2	-4%	-4%	2%	3%	
	M	115.6	103.3	114.7	107.0	26.0	23.2	25.8	24.1	-11%	-7%	-4%	1%	
	S	109.4	97.9	107.9	98.3	24.6	22.0	24.3	22.1	-11%	-9%	0%	1%	
126SB	L	117.0	111.6	109.6	108.3	26.3	25.1	24.6	24.4	-5%	-1%	3%	7%	
	M	108.8	103.0	106.8	100.6	24.5	23.2	24.0	22.6	-5%	-6%	2%	2%	
	S	110.9	101.4	109.2	106.0	24.9	22.8	24.6	23.8	-9%	-3%	-4%	1%	Expansion Joint
127SB	L	117.4	111.6	111.9	110.9	26.4	25.1	25.2	24.9	-5%	-1%	1%	5%	
	M	114.5	107.1	112.9	106.4	25.7	24.1	25.4	23.9	-7%	-6%	1%	1%	
	S	112.1	105.4	109.3	104.9	25.2	23.7	24.6	23.6	-6%	-4%	0%	3%	
128SB	L	113.6	108.9	112.3	106.8	25.5	24.5	25.2	24.0	-4%	-5%	2%	1%	
	M	115.8	104.9	113.8	101.1	26.0	23.6	25.6	22.7	-10%	-12%	4%	2%	
	S	111.1	97.7	109.5	99.8	25.0	22.0	24.6	22.4	-13%	-9%	-2%	1%	
129SB	L	115.5	110.8	111.1	104.8	26.0	24.9	25.0	23.6	-4%	-6%	6%	4%	
	M	116.8	105.4	111.0	99.6	26.3	23.7	25.0	22.4	-10%	-11%	6%	5%	
	S	109.9	101.5	108.2	94.4	24.7	22.8	24.3	21.2	-8%	-14%	7%	2%	
130SB	L	113.8	110.2	112.5	105.0	25.6	24.8	25.3	23.6	-3%	-7%	5%	1%	
	M	115.9	106.0	111.4	103.4	26.0	23.8	25.0	23.2	-9%	-7%	2%	4%	
	S	112.5	102.0	112.0	98.2	25.3	22.9	25.2	22.1	-10%	-13%	4%	0%	
131SB	L	113.9	107.7	113.5	103.9	25.6	24.2	25.5	23.4	-6%	-9%	4%	0%	
	M	116.9	106.5	112.2	105.1	26.3	23.9	25.2	23.6	-9%	-7%	1%	4%	
	S	113.6	96.2	107.3	94.7	25.5	21.6	24.1	21.3	-17%	-12%	2%	6%	
132SB	L	110.6	106.0	111.6	104.9	24.9	23.8	25.1	23.6	-4%	-6%	1%	-1%	
	M	114.9	104.3	110.8	100.9	25.8	23.4	24.9	22.7	-10%	-9%	3%	4%	
	S	105.2	93.0	104.4	94.6	23.7	20.9	23.5	21.3	-12%	-10%	-2%	1%	
133SB	L	110.9	106.5	110.5	105.6	24.9	23.9	24.8	23.7	-4%	-4%	1%	0%	
	M	114.5	105.5	111.7	104.4	25.7	23.7	25.1	23.5	-8%	-7%	1%	3%	
	S	109.7	97.5	107.0	97.7	24.7	21.9	24.1	22.0	-12%	-9%	0%	2%	
134SB	L	112.2	105.4	111.0	104.8	25.2	23.7	25.0	23.6	-6%	-6%	1%	1%	
	M	117.3	112.3	115.2	99.0	26.4	25.3	25.9	22.3	-4%	-15%	13%	2%	
	S	108.9	101.4	110.5	105.3	24.5	22.8	24.8	23.7	-7%	-5%	-4%	-1%	End Span

Table 7 – Tendons showing notable vibration test response

Span	Tendon	**X** : Tension < ~93% of peer group average **U** : Unusual N-S disparity; end with possible deficiency		Notes
		N end	S end	
Regular	90 NB WM	**X**	**X**	-
	91 NB WS	**X**	**X**	-
	94 SB WM	**X,U**		PT Rod
End	105 SB EM	**X**		Severe Obstruction at North End
	134 NB WL	**X**	**X**	Severe Obstruction at North End
	134 SB EM	**X**		Severe Obstruction at North End

Table 8 – Tendons Proposed for Special Attention During Inspection

Priority	Tendon	Tendon End of Greater Interest	Possible Source of False Indication
1 (Highest)	90 NB WM	Both	None identified
	91 NB WS	Both	
2	94 SB WM	N	Presence of PT bar altering stress pattern
3	134 NB WL	Both	Uncertain vibration length
	134 SB EM	N	
	105 SB EM	N	

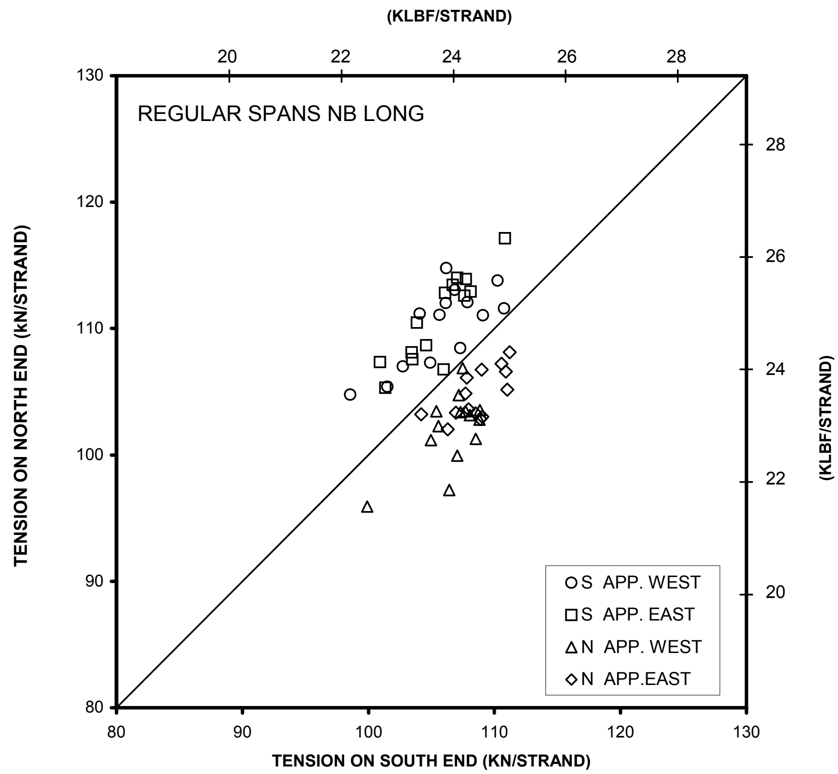

FIGURE 1:Tension on N end as function of tension on S end of each Long tendon (W and E side) in Regular NB spans, S and N approaches.

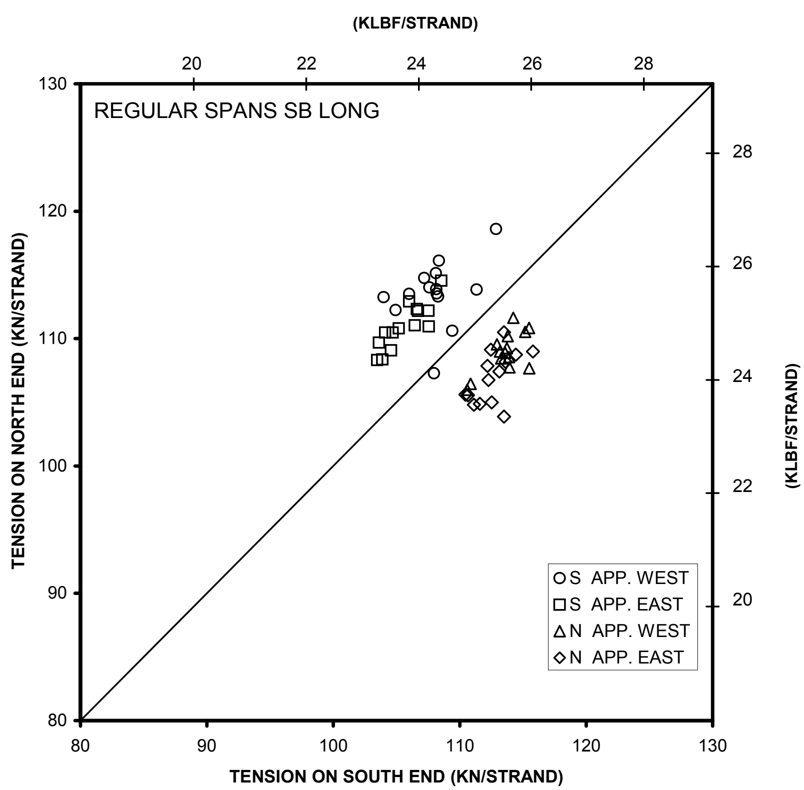

FIGURE 2: Tension on N end as function of tension on S end of each Long tendon (W and E side) in Regular SB spans, S and N approaches.

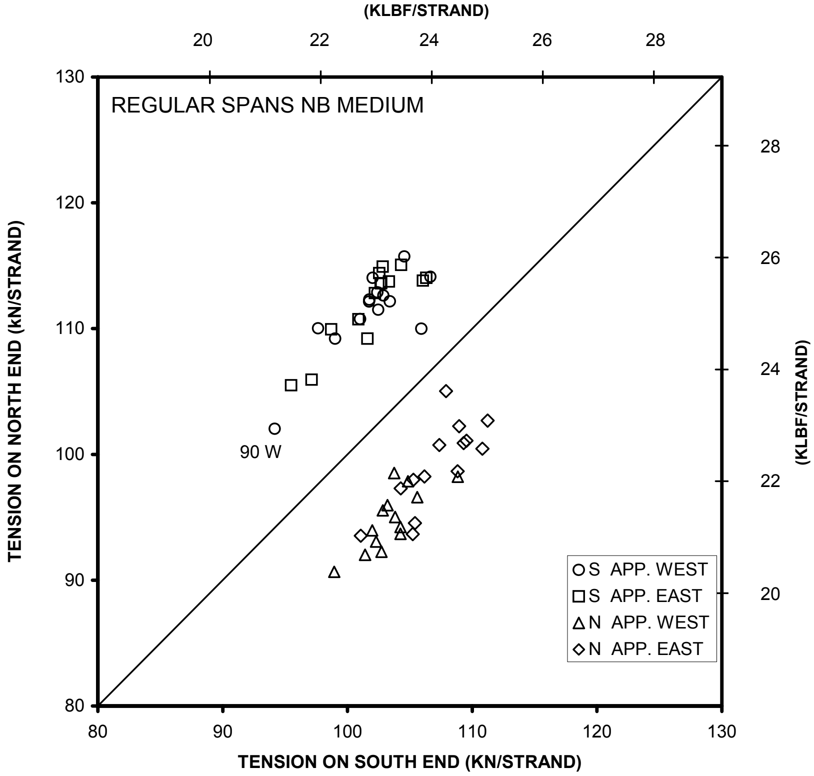

FIGURE 3: Tension on N end as function of tension on S end of each Medium tendon (W and E side) in Regular NB spans, S and N approaches.

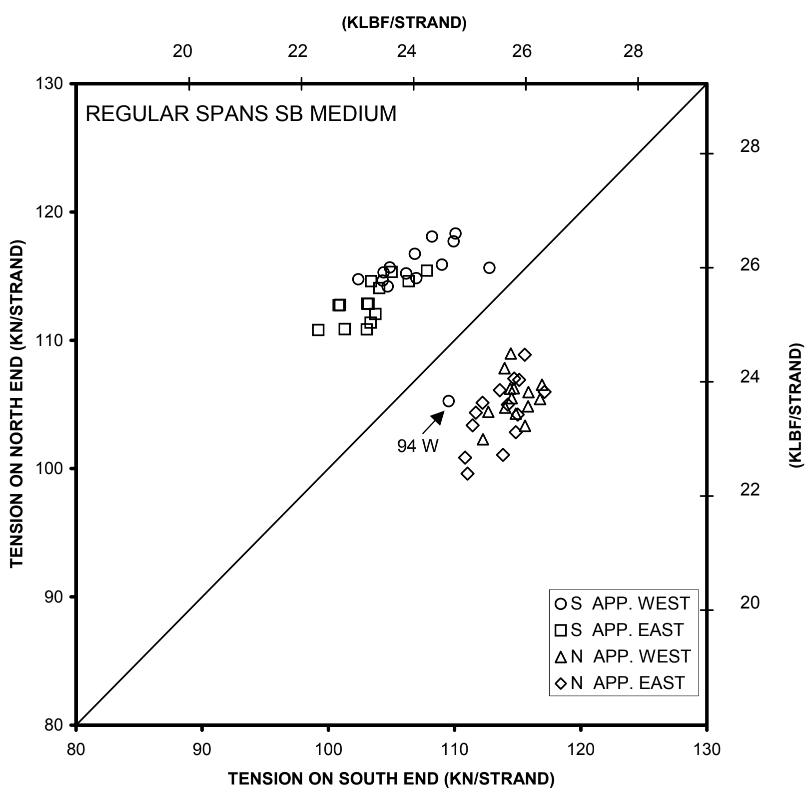

FIGURE 4: Tension on N end as function of tension on S end of each Medium tendon (W and E side) in Regular SB spans, S and N approaches.

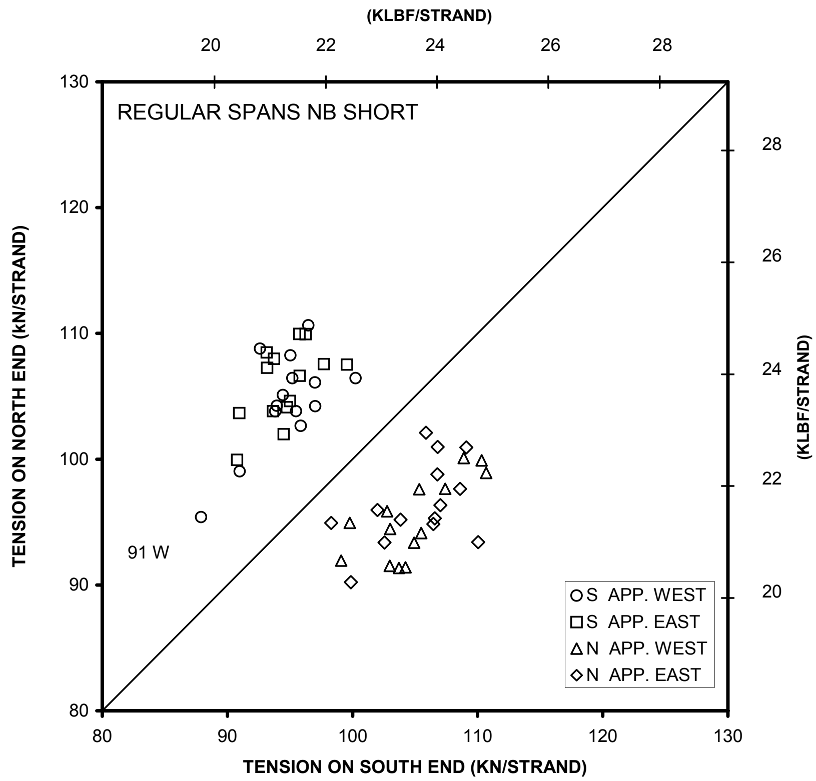

FIGURE 5: Tension on N end as function of tension on S end of each Short tendon (W and E side) in Regular NB spans, S and N approaches.

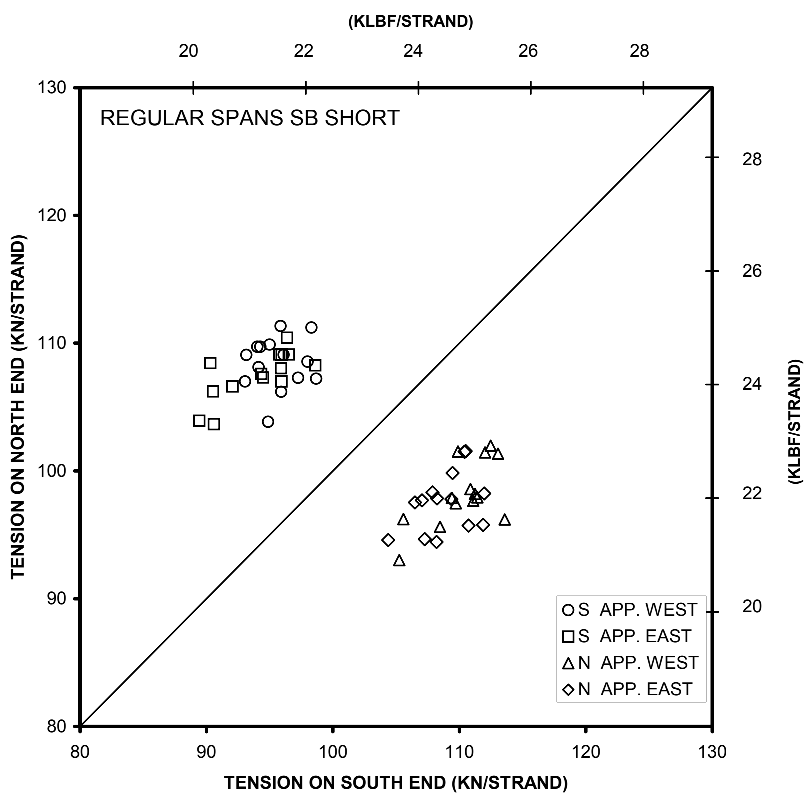

FIGURE 6: Tension on N end as function of tension on S end of each Short tendon (W and E side) in Regular SB spans, S and N approaches.

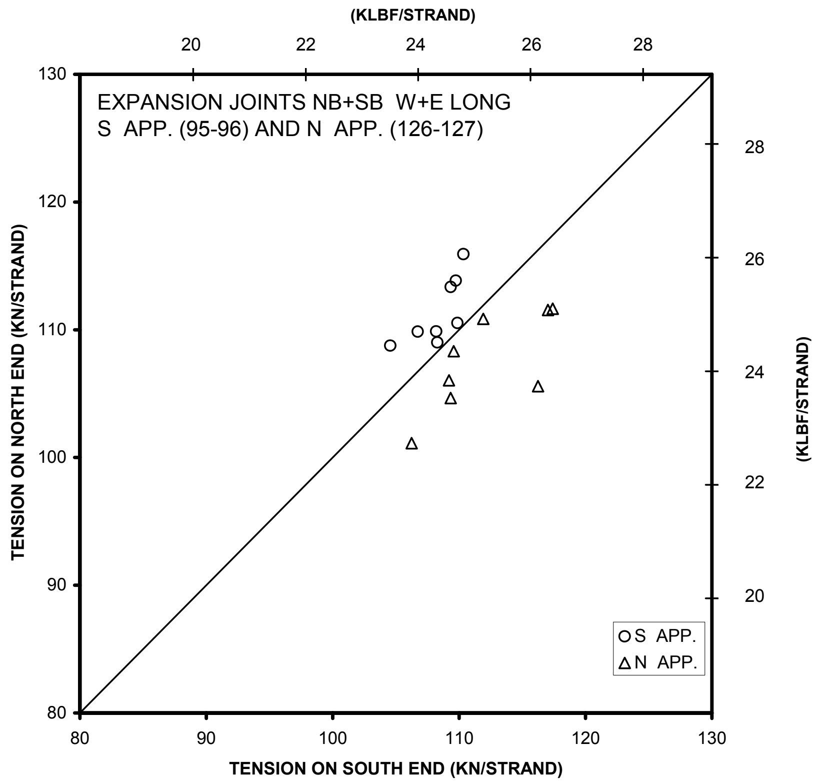

FIGURE 7: Tension on N end as function of tension on S end of each Long tendon (W and E side) in Expansion Joints NB and SB spans, S and N approaches.

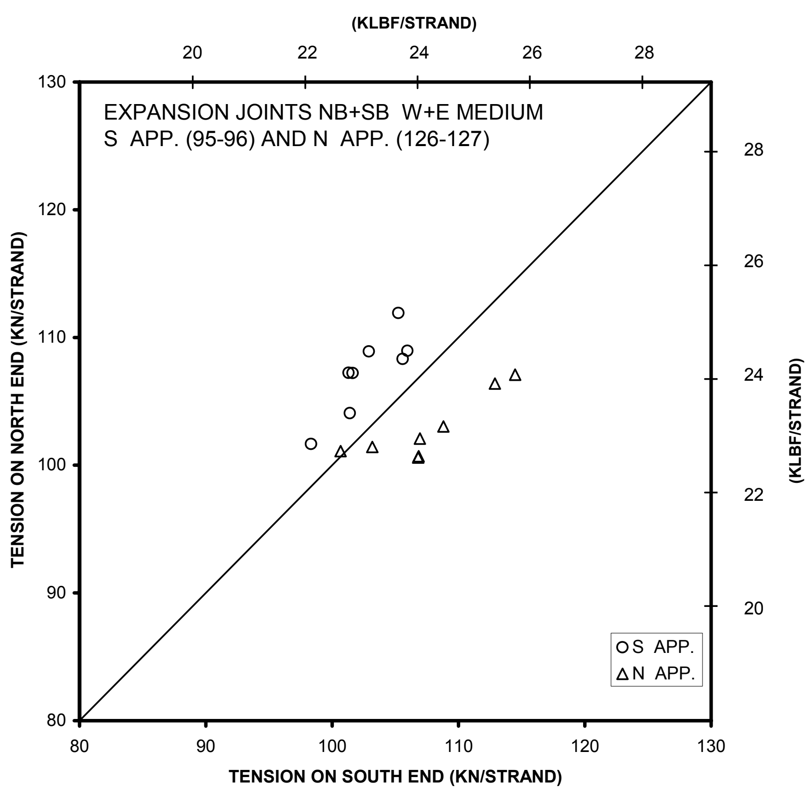

FIGURE 8: Tension on N end as function of tension on S end of each Medium tendon (W and E side) in Expansion Joints NB and SB spans, S and N approaches.

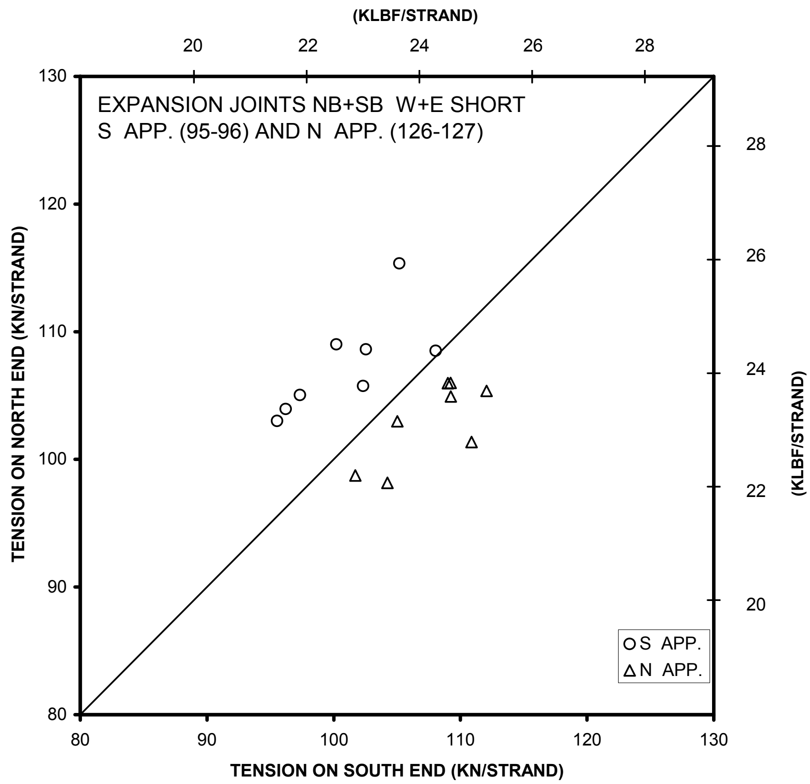

FIGURE 9: Tension on N end as function of tension on S end of each Short tendon (W and E side) in Expansion Joints NB and SB spans, S and N approaches.

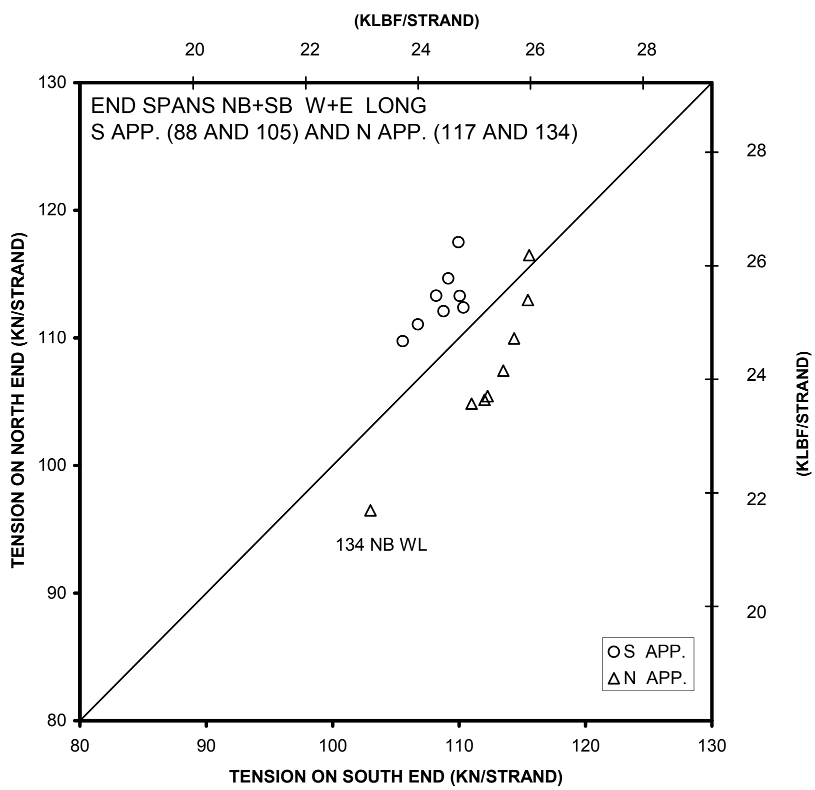

FIGURE 10: Tension on N end as function of tension on S end of each Long tendon (W and E side) in End NB and SB spans, S and N approaches.

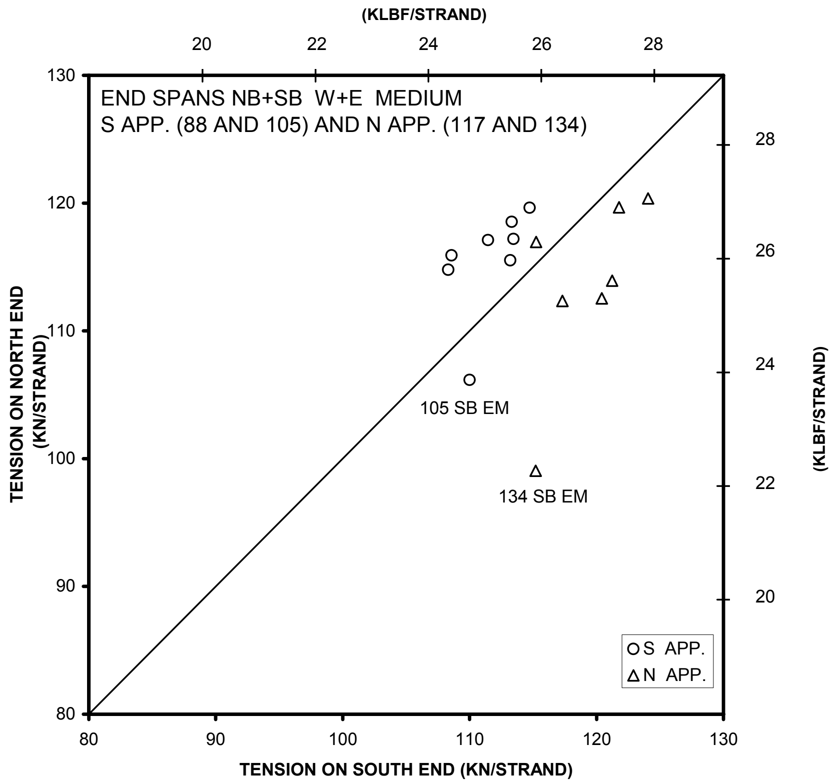

FIGURE 11: Tension on N end as function of tension on S end of each Medium tendon (W and E side) in End NB and SB spans, S and N approaches.

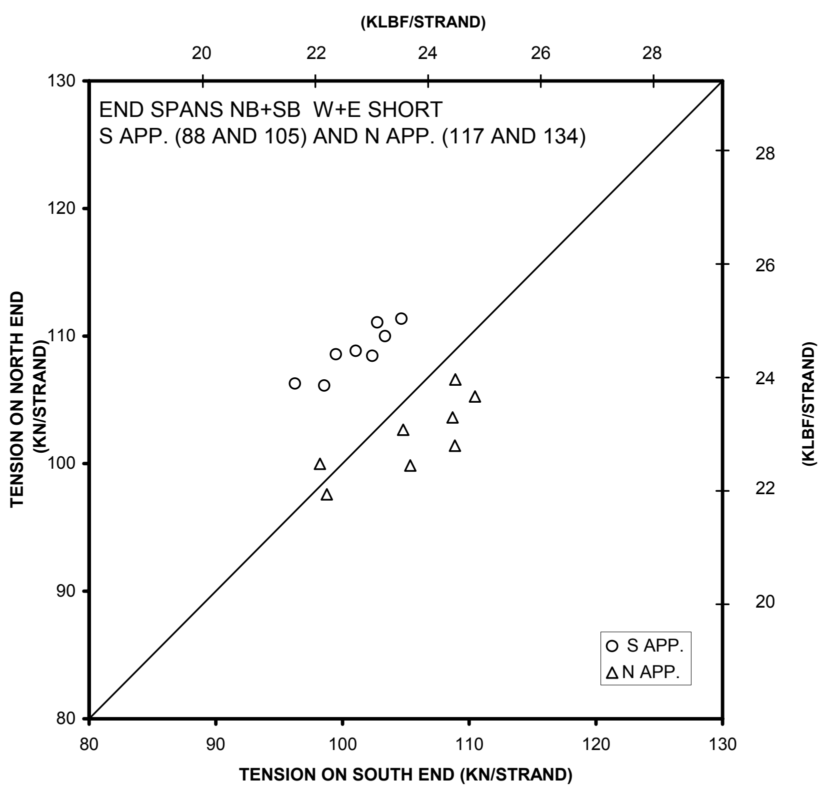

FIGURE 12: Tension on N end as function of tension on S end of each Short tendon (W and E side) in End NB and SB spans, S and N approaches.

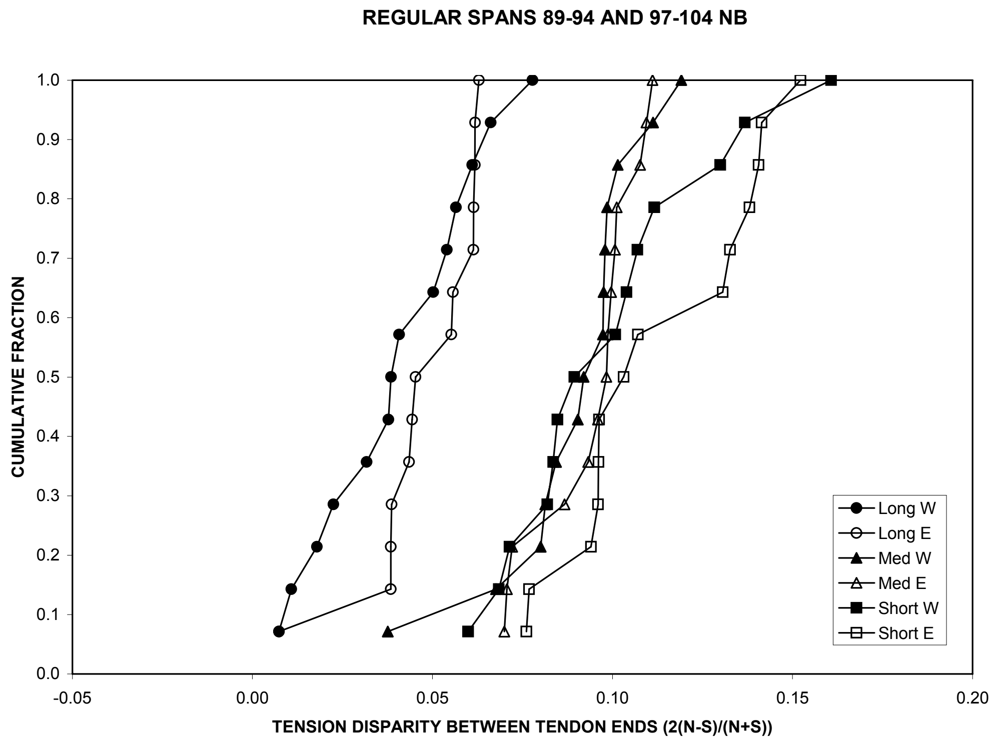

Figure 13:Cumulative Distribution of Estimated Tension Disparity for Regular Spans in the Northbound Elevated Approaches, South of the Main Span.
Ranking indicated below.

Long W	Long E	Med W	Med E	Short W	Short E
101	101	98	104	99	99
104	93	99	102	97	94
92	90	102	91	102	104
102	102	104	99	100	101
97	100	94	103	93	100
103	97	89	90	104	93
98	99	93	98	101	92
100	103	92	100	98	103
90	104	97	101	90	89
99	94	101	93	89	91
93	92	91	89	91	98
89	91	90	92	92	90
94	98	100	94	94	97
91	89	103	97	103	102

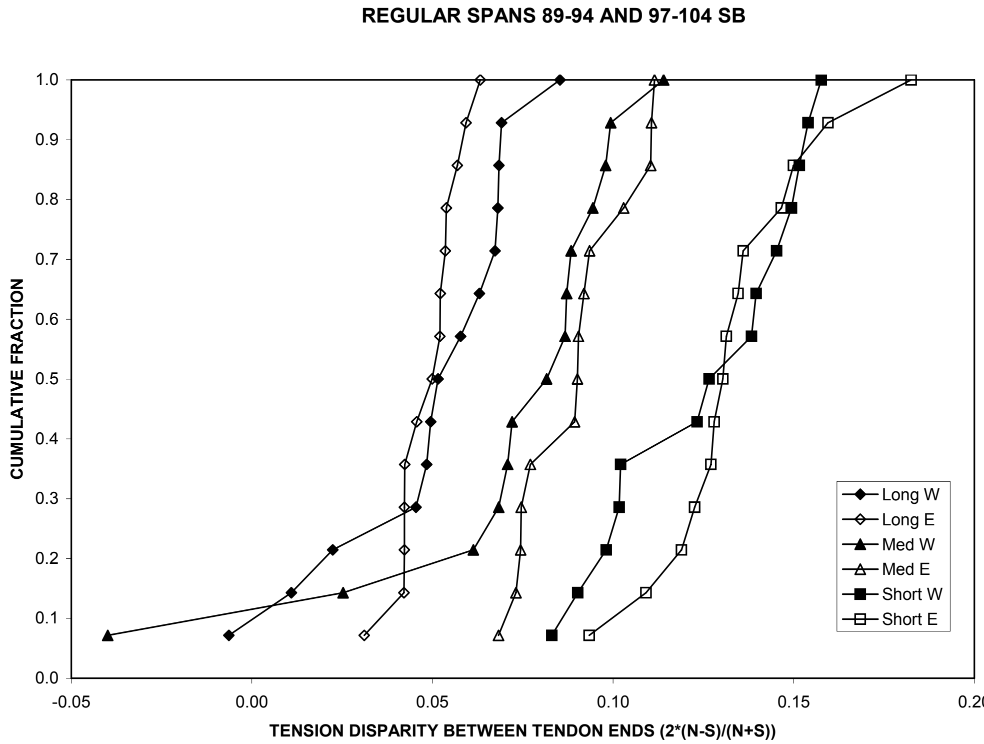

Figure 14: Cumulative Distribution of Estimated Tension Disparity for Regular Spans in the Southbound Elevated Approaches, South of the Main Span.
Ranking indicated below.

Long W	Long E	Med W	Med E	Short W	Short E
98	90	98	89	101	92
92	100	90	98	93	93
91	98	93	94	89	98
97	89	102	103	90	90
104	92	91	91	103	103
89	104	104	102	99	94
90	101	101	101	92	100
100	97	100	93	91	99
103	99	92	100	104	102
93	102	97	92	100	97
99	91	99	99	102	89
102	94	89	90	97	91
101	93	103	104	98	101
94	103	94	97	94	104

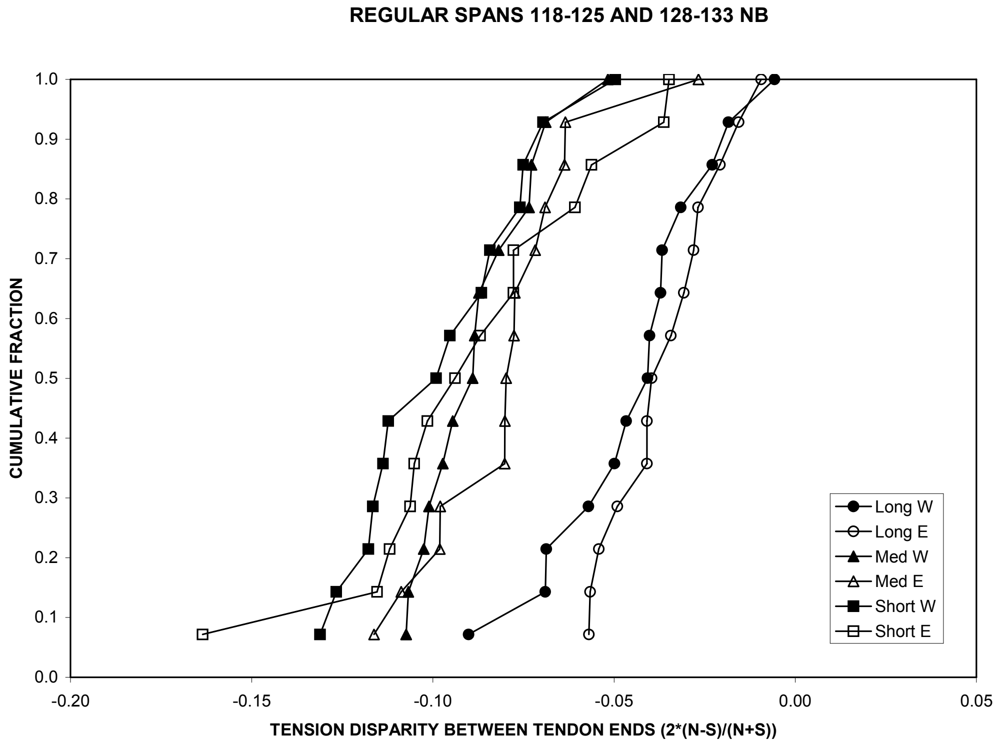

Figure 15: Cumulative Distribution of Estimated Tension Disparity for Regular Spans in the Northbound Elevated Approaches, North of the Main Span.
Ranking indicated below.

Long W	Long E	Med W	Med E	Short W	Short E
130	132	119	128	124	125
120	119	128	120	122	131
121	128	118	129	132	128
124	131	133	125	120	122
123	133	120	123	128	129
122	129	124	122	121	130
119	125	132	132	125	123
125	120	125	131	133	132
128	123	123	130	123	124
131	122	122	118	119	121
133	118	121	119	129	133
129	130	131	133	131	118
118	121	129	124	118	120
132	124	130	121	130	119

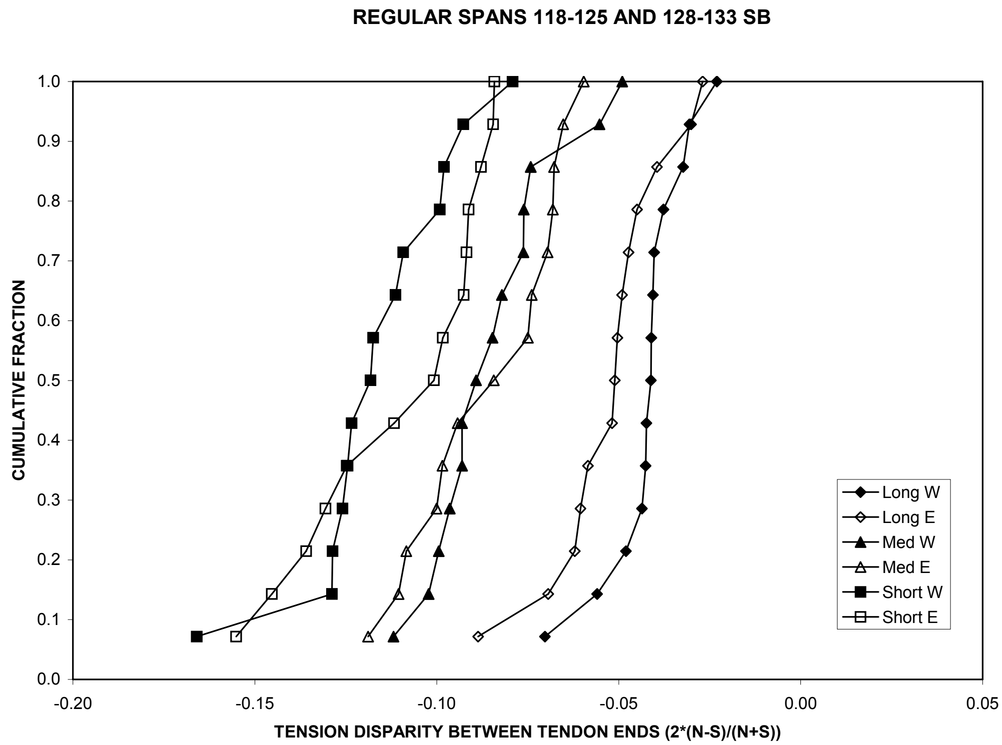

Figure 16: Cumulative Distribution of Estimated Tension Disparity for Regular Spans in the Southbound Elevated Approaches, North of the Main Span.
Ranking indicated below.

Long W	Long E	Med W	Med E	Short W	Short E
123	118	119	119	129	122
124	121	123	131	123	118
130	125	124	133	130	124
122	133	121	121	119	133
120	124	120	125	122	128
133	122	133	120	125	125
129	128	122	130	121	132
125	120	130	124	133	119
128	123	118	132	132	120
132	129	131	123	120	131
121	119	132	122	124	130
118	132	128	129	128	129
131	130	129	118	118	123
119	131	125	128	131	121

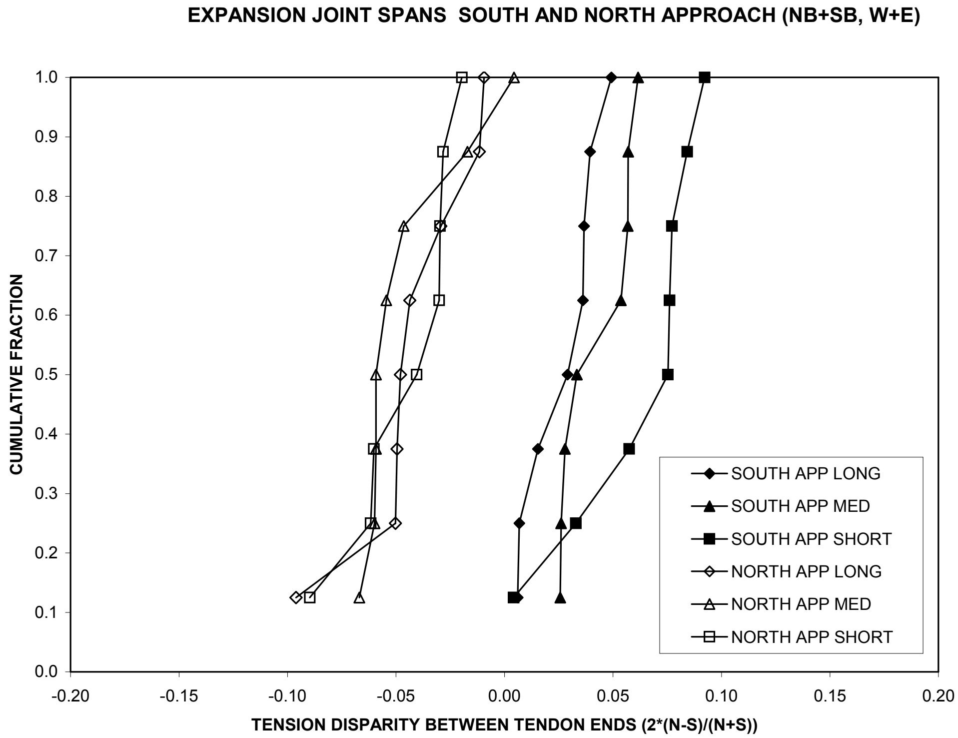

Figure 17: Cumulative Distribution of Estimated Tension Disparity for Expansion Joints in the Southbound and Northbound Elevated Approaches, North and South of the Main Span. Ranking indicated below.

S APP. Long W+E	**S APP. Med W+E**	**S APP. Short W+E**	**N APP. Long W+E**	**N APP. Med W+E**	**N APP. Short W+E**
96 NB W	96 NB W	96 NB W	127 SB E	126 NB E	127 NB E
95 SB E	95 NB W	96 SB E	126 SB E	126 NB W	126 NB E
96 SB E	96 SB W	95 SB W	127 NB E	127 NB E	126 NB W
96 SB E	95 SB W	96 SB E	127 NB W	126 SB W	126 SB E
95 SB W	96 SB E	95 SB E	126 SB W	127 SB E	127 SB E
95 NB E	96 SB E	96 SB W	126 NB W	127 NB W	127 NB W
96 SB W	95 SB E	95 NB W	127 SB W	126 SB E	127 SB W
95 NB W	95 NB E	95 NB E	126 NB E	127 SB W	126 SB W

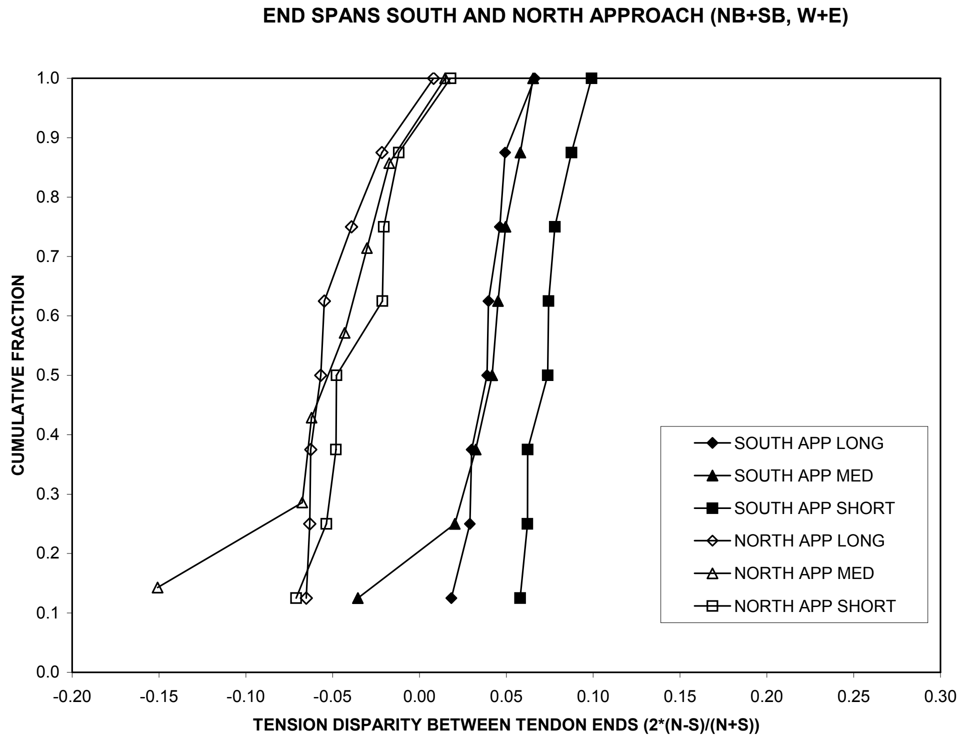

Figure 18: Cumulative Distribution of Estimated Tension Disparity for End Spans in the Southbound and Northbound Elevated Approaches, North and South of the Main Span. Ranking indicated below.

S APP. Long W+E	**S APP. Med W+E**	**S APP. Short W+E**	**N APP. Long W+E**	**N APP. Med W+E**	**N APP. Short W+E**
88 SB W	88 SB E	105 SB E	117 SB E	134 NB W	134 NB W
88 SB E	105 NB W	88 SB W	117 SB W	117 SB W	134 NB E
105 SB W	88 NB E	105 SB W	117 NB E	117 SB E	117 NB W
88 NB W	88 SB W	105 NB E	117 NB W	134 SB W	117 SB E
88 NB E	105 NB E	105 NB W	134 SB E	117 NB W	117 SB W
105 SB E	88 NB W	88 NB W	134 SB W	117 NB E	134 SB E
105 NB W	105 SB W	88 SB E	134 NB E	134 SB E	117 NB E
105 NB E	105 SB E	88 NB E	134 NB W		134 SB W

APPENDIX 4

USER-ORIENTED SUMMARY OF PRINCIPLES AND FINDINGS

A4.1 Scope

The Task 1 and 2 sections of the main body of this report are an in-depth treatment of specific issues that had been identified in previous work as needing resolution. Thus, the overall introduction and the findings in those sections of the main body of the report serve readers with specialized knowledge in those topics. However, that report structure is not oriented toward a potential user of those findings who is being introduced to the vibration method for the first time, and who seeks to go beyond the "black box" approach used in the Simplified Test Method described in the Task 3 section. This Summary is intended for such user, typified by an FDOT engineer or contractor working in the near future.

Because data acquisition equipment and processing software evolve rapidly, the target user is assumed to have access to computerized equipment that can acquire vibration spectra and identify mode frequencies, as well as obtaining force-deflection information if desired. The following summary therefore focuses on interpretation of those data to obtain tendon tension estimates.

The following section, Principles, addresses fundamental aspects and approaches to solve the problem of finding tendon tension from vibrational measurements (supplemented by static deflection tests if available). Some of those approaches are the result of the research conducted in this project and are so identified.

A subsequent section, Application, contains brief itemized guides to the interpretation of vibration data for obtaining tendon tension using the techniques and formulas detailed under Principles.

A4.2 Principles

A4.2.1 Vibration modes

A stretched string fixed at both ends (e.g. dashed line between points A and B in Figure A4.1) vibrates laterally after being excited by a lateral impact. In its simplest manifestation, a snapshot of that vibrating string could look like curve 1 in Figure A4.1, where the vibration amplitude is exaggerated for clarity. Snapshots taken at other times will show the same shape as curve 1 but oscillating in amplitude between equal extreme deflections above and below AB. This shape corresponds to the lowest possible vibration frequency of the string, named the fundamental or Mode 1 frequency. Often the string vibrates simultaneously at higher frequencies too, with shapes as in curve 2 (Mode 2) or 3 (Mode 3) as well as for higher Modes. The shape of the string at a given moment (thick Sum curve) corresponds to the sum, for all active modes, of the vibration amplitudes at every point of the string at that moment. That shape is more complex than that of a single mode, and changes appearance with time in a periodic fashion.

A4.2.2 The simple vibrating string

If the string is uniform and has negligible flexural stiffness, the ruling differential equation is (Morse 1948)

$$T\, \partial^2 y / \partial x^2 = m\, \partial^2 y / \partial t^2 \qquad \text{(Eq. A4.1)}$$

where T is the tension, L is the string length and m is the string mass per unit length (also called the linear mass). Solution of that equation shows that the mode shapes are simple sine functions of position along the string (the case illustrated in Figure A4.1), and the frequencies for each mode are given by

$$f_n = (n / 2L)\, (T/m)^{1/2} \qquad \text{(Eq. A4.2)}$$

where n is the mode number. For this string the frequencies of the higher modes are exact multiples ("harmonics") of the Mode 1 frequency. If the excitation is in the form of a sharp lateral impact exactly on the center of the string, the resulting vibration is mostly in the form of Mode 1, with lesser manifestations of odd-numbered modes (3, 5, 7...) of decreasing amplitude as n increases. As indicated by Eq. A4.2, for a given linear mass the higher the tension in the string, the higher the frequency of all modes. For a given tension, the heavier the string the lower the frequencies are.

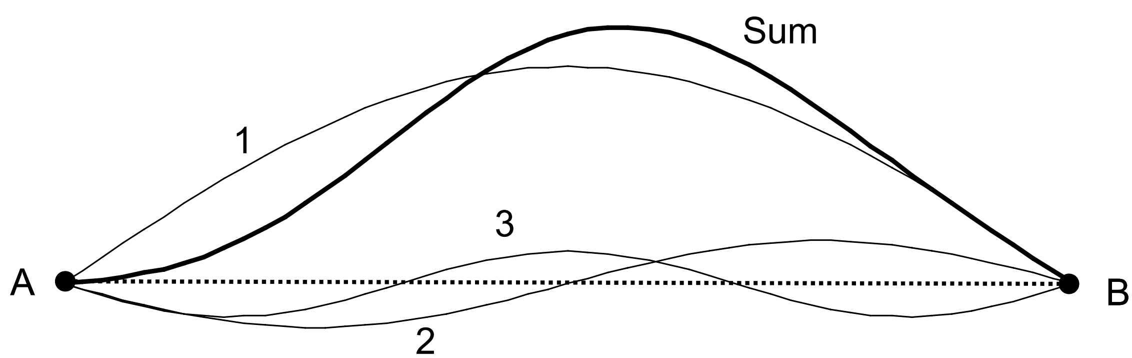

Figure A4.1 - Lateral vibration of a linear body.

The above results are called the solution of the direct problem (given the conditions, find the mode frequencies). The actual interest is the inverse problem, which is to obtain an estimate of the value of T given the Mode frequencies as determined by testing. This can be achieved if the linear mass of the string is known beforehand, as the value of T can be calculated from a measurement of the vibrating frequency of any mode if the mode number is know. If a vibration detection device is used (for example an accelerometer placed at a point in the string away from the ends), Fourier transform analysis of the data can then readily indicate which modes are present, along with their frequencies and amplitudes (maximum lateral deflection for a given mode) at the test point. Mode 1 can be easily identified as having the lowest of all frequencies detected. Thus, the tension is simply given by

$$T = 4\ f_1^2\ L^2\ m \qquad \text{(Eq. A4.3)}$$

where f_1 is the frequency for Mode 1. Additional independently calculated values of the same tension can be obtained from the other modes, if detected by the test equipment, by substituting f_n^2/n^2 for f_1^2 in Eq. S3. Given the presence of experimental scatter in the measurements, an improved estimate of the value of T can thus be obtained by averaging the values obtained by using data from the various vibration modes. Further sophistication can be introduced by use of weighted averaging favoring the best defined modes.

The above treatment is presented for introductory purposes, but vibration of tendons in actual structures involves more complex behavior. Estimation of the tendon tension then requires additional information, as indicated in the next sections.

A4.2.3 The vibrating string with finite stiffness

The freely vibrating portions of tendons in typical segmental box post-tensioned bridges exhibit appreciable flexural stiffness, so vibration behavior deviates significantly from that of a simple string. Treating the tendon as a stretched string with finite flexural stiffness S. the ruling equation is (Morse 1948)

$$T\ \partial^2 y / \partial x^2\ - S\ \partial^4 y / \partial \chi^4\ =\ m\ \partial^2 y / \partial t^2 \qquad \text{(Eq. A4.3)}$$

The presence of stiffness also requires considering the end condition of the string. As tendons are grouted and usually emerge nearly straight from solid reinforced concrete surfaces, the ends may be approximated as being fully clamped so the end conditions are

$$\partial y / \partial x = 0 \quad \text{at}\ \ x=0,\ L \qquad \text{(Eq. A4.4)}$$

Such end conditions imply that the mode shapes are no longer simple sinusoids, as near the ends the slope must be zero even when the deflection elsewhere is finite. Moreover, the frequencies of Modes 2 and greater are no longer simple multiples of that of Mode 1

The direct problem for Eqs. A4.3 and A4.4 is to find the Mode frequencies given T, S and m (and of course L which is always considered to be known since it can be measured directly). It is noted that such the exact solution cannot be expressed in mathematically closed form for these equations. A close form expression is possible however for approximate solutions as shown below.

In the inverse problem an estimate of the value of T may be obtained from the Mode frequencies determined by testing, if one or both of the other parameters (m, S) in addition to L are known. Approaches of increasing sophistication for the direct and inverse problem solutions are presented below.

A4.2.4 Approximate solution to obtain tension given known linear mass and stiffness

For low mode numbers (e.g. n<5) and small stiffness values relative to tension and length (e.g. $S/TL^2 < 10^{-3}$) the direct problem solution for the mode frequencies can be approximated by (Morse 1948)

$$f_n = (n/2L)(T/m)^{1/2}\,(1+2(S/(TL^2))^{1/2} + (4+n^2\pi^2/2)S/(TL^2)) \qquad \text{(Eq. A4.5)}$$

For the inverse problem, if vibration measurements provide values of mode frequencies f_n for one of the modes, a fairly precise estimate of the tension can be obtained by solving Eq. A4.5 for T provided the values of m and S are known beforehand. Sources for those two parameters will be discussed later on. As indicated in the Task 4 section of the main body of the report, solution for T of the approximate solution Eq. A4.5 can be obtained in closed form and is given by

$$T = \left[L^2 \frac{f_n}{n} - \sqrt{\frac{S}{m}} + \frac{1}{n\sqrt{2}} \cdot \left(\frac{2f_n^2 \cdot L^4 \cdot m \cdot \sqrt{\frac{S}{m}} - 6S \cdot n^2 \cdot \sqrt{\frac{S}{m}} - n^4 \cdot \sqrt{\frac{S}{m}} \cdot \pi^2 \cdot S - 4L^2 \cdot f_n \cdot S \cdot n}{m \cdot \sqrt{\frac{S}{m}}} \right)^{\frac{1}{2}} \right]^2 \cdot \frac{m}{L^2}$$

(Eq. A4.6)

Frequency data from more than one Mode provides independent estimates of T that can then be averaged (with appropriate weighing if warranted) to obtain a better overall estimate.

A4.2.5 Precise solution to obtain tension and stiffness given known linear mass

In the direct problem Eqs. A4.3 and A4.4 can be solved for the mode frequencies with arbitrary precision by means of numerical methods, which means the results need to be presented with the aid of a table of values. Per the findings of this project (Task 2, Items 2.1 and 2.2 of the main body of the report) the solution has the form

$$f_n = (n/L)(T/m)^{1/2}\,\nu_n(\sigma) \qquad \text{(Eq. A4.7)}$$

where

$$\sigma = S/(TL^2) \qquad \text{(Eq. A4.8)}$$

The value of $\nu_n(\sigma)$ is tabulated as function of n and σ in Table A5.1 (Appendix 5), which lists numerically calculated solutions for Modes 1 to 7 and σ values between 10^{-4} and 10^{-2}. That Mode number and σ range has been found to cover adequately most cases encountered in field tendons in Florida bridges. Table A5.1 uses a fine step between consecutive σ values, suitable for simple interpolation to cover intermediate cases with greater precision is desired.

For the inverse problem the values in Table A5.1 permit using measured frequency data from multiple Modes to reverse the process by numerical fitting, and obtain precise estimates of not only the value of T but also of S. A solution method was developed in the present project and is detailed in Task 2, Item 2.2.1 in the main body of the report. A summary of that method follows.

The solution is achieved by noting first that for a given tendon, per Eq. A4.7, the ratio $R_n = f_n/ (n\ \nu_n)$ is always the same value R regardless of the Mode number:

$R = R_n = f_n/ (n\ \nu_n) = L^{-1} (T/m)^{1/2}$ (Eq. A4.9)

The value of σ for the tendon being tested can be found by taking the measured f_n^m values and calculating $R_n (\sigma_i)= f_n^m/ \nu_n (\sigma_i)$ for each of modes in each of the σ_i entries in Table A5.1 (the index i indicates the ith entry in the table) . Ideally the values of $R_n(\sigma_i)$ would be the same (equal to R), regardless of n, only for the σ entry that exactly matched that of the tendon being tested.

A convenient procedure was used to determine the σ entry for which the $R_n(\sigma_i)$ values are (most nearly) the same across the nodes evaluated. The procedure is to first calculate, for each σ_i in Table A5.1, the average of the $R_n (\sigma_i)$ values of all the modes tested. The relative difference of each individual $R_n (\sigma_i)$ value from the average of those for the same σ_i is then calculated and squared, the squared differences added, and tallied in another column. The column is then searched, and the value of σ for which the sum of the squares is the lowest is declared as the value corresponding to the tendon and named σ_e, the estimated non dimensional stiffness for the tendon. Further precision in the value of σ_e for minimum deviation can be achieved, if desired, by interpolating between adjacent table entries. This procedure also yields an estimated value of R, given by R_{avm}, the average of the values of $R_n (\sigma_e)$.

Once the estimate values σ_e and R_{avm} are obtained, an estimate of the tendon tension is given by

$T_e = R_{avm}{}^2 L^2 m$ (Eq. A4.10)

After Te is determined, an estimate of the tendon stiffness is calculated by

$S_e = R_{avm} T_e L^2$ (Eq. A4.11)

A4.2.6 Precise solution to obtain tension, stiffness and linear mass from combined vibration and static deflection measurements

The above approaches required prior knowledge of the linear mass of the tendon. That parameter can be estimated from construction data (number and type of strands, duct dimensions and tabulated steel and grout properties). However, the result is often subject to considerable uncertainty since the density of grout, which contributes about 25% of the linear mass, can vary significantly depending on the extent of expansion agent used and the possibility of linear voids along the top of the tendon. The nature of Eq. A4.3 prevents obtaining an estimate of m solely from mode frequencies obtained in vibration measurements. However, data from supplemental measurements of static lateral deflection of the tendon upon application of a known lateral force can be used to complete the information needed to precisely estimate T without prior knowledge of m and S. Indeed, the values of m and S are obtained as a result of the measurements and data processing. The method to achieve this was developed in the present project and presented in the Task1 section, Item 1.4.4. A summary follows.

The vibration measurements are conducted in the usual manner, yielding the values of f_n for the Modes chosen for evaluation. Those results are processed as shown above to obtain the values of R and σ.

The deflection test is conducted by applying a lateral force F at the center of the tendon, and measuring the resulting lateral deflection d. A deflection compliance δ is then calculated as

$$\delta = d/F \qquad \text{(Eq. A4.12)}$$

Standard solutions for the problem of lateral deflection of a stiff stretched beam show that when $\sigma = S/(TL^2) < 10^{-2}$ (a situation encountered commonly in tendons in post tensioned bridges) the relationship between d and the other parameters is well approximated by

$$\delta = L\,(1/4 - \sigma^{1/2}) / T \qquad \text{(Eq. A4.13)}$$

and therefore the tension is obtained from the value of σ (from the vibration test) and the value of δ (from the deflection test) by

$$T = \delta^{-1} L\,(1/4-\sigma^{1/2}) \qquad \text{(Eq. A4.14)}$$

From that calculated value of T and the values of σ and R already available, the stiffness S and linear mass m can then be calculated by

$$S = \sigma\, T\, L^2 \qquad \text{(Eq. A4.15)}$$

$$m = T\, R^{-2}\, L^{-2} \qquad \text{(Eq. A4.16)}$$

A4.27 Complicating Factors

The above approaches to obtain tendon tension with various degrees of precision and reliance in prior knowledge of tendon parameters can be applied successfully in many instances. However, some complicating factors can introduce uncertainty and two of those merit special attention. The first concerns the presence of dual modes with closely spaced frequencies where only one was expected. The second concerns uncertainty in the value of the vibrating tendon length, since the ends of the vibrating portion of the tendon are usually encased for a short distance in a highly stiff steel pipe that protrudes from the concrete surface. Procedures to deal with those two complicating factors are described below.

A4.2.7.1 Dual Modes

In an ideal tensioned stiff string the mode frequencies follow a series such as that approximated by Eq. A4.5. However, in tendon tests it is often seen that instead of only just one Mode at each frequency f_n there are instead two Modes with closely spaced frequencies f_{nH} and f_{nL} (for the high and low frequency component of the pair respectively). In a frequency spectrum display this is manifested by the presence of peaks doublets, instead of single peaks, centered on the frequencies expected for each Mode. The resulting spectrum is as exemplified in Figure A4.2.

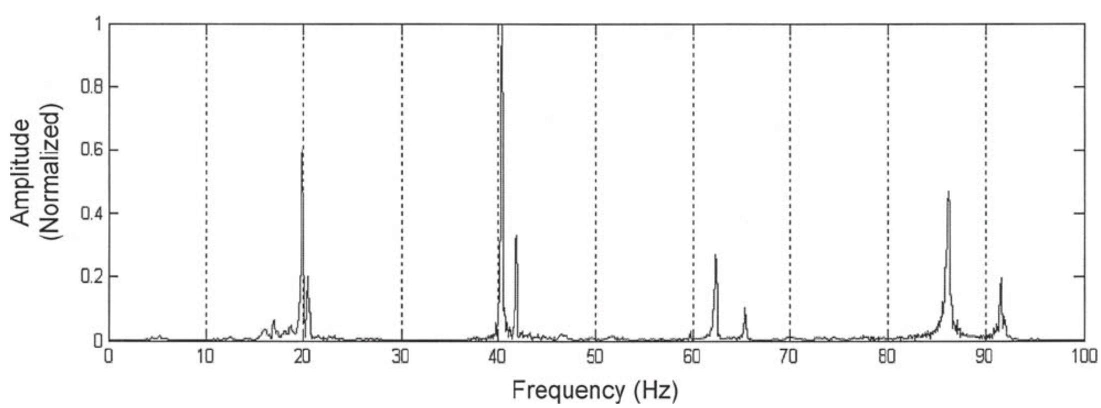

Figure A4.2 - Dual Modes in the frequency spectrum of a 27-strand tendon in a post tensioned segmental bridge.

As confirmed by findings from the present project (Task 1 section, Item 1.4.3) the presence of dual peaks is associated with asymmetry in the placement of strands in the tendon cross section. The asymmetry often results from strands crowding against the top or bottom of the duct in deviation blocks or bulkheads. As a result, the stiffness for up-down flexion can be significantly less than for side-to-side flexion. Consequently the tendon displays vibration modes that have in common the same tension and linear mass, but that are slightly different in frequency depending on whether the displacement is aligned with one or the other principal axes of the moment of inertia of the tendon cross section.

On first approximation those double modes may be treated as if they were occurring independently, so the series of frequencies f_{1H}, f_{2H} ... f_{3H}... can be processed in the manner indicated in Item A4.2.5 above (assuming that m is known) to obtain a tension estimate T_H. Likewise, the series f_{1L}, f_{2L} ... f_{3L}... can be processed to obtain a tension estimate T_L. Extensive experience with Florida segmental bridge tendons as well as the findings from this project (Task 1 section, Item 1.4.3) have shown that the resulting values of T_L and T_H are typically very close to each other (e.g. within 1%), indicating that the assumption of nearly independent behavior is justified. Thus the presence of dual peaks is addressed by performing independent calculations of T_L and T_H and reporting tendon tension as the average of both.

A4.2.7.2 End pipe effects

If the steel pipes were infinitely stiff and the tendon behaved as a homogeneous string, then the vibration length L would be simply equal to the distance between the concrete walls at each end of the tendon (L_C) , minus the sum of the lengths of both protruding steel pipes (L_P). However, the pipe stiffness is finite so the effective length is expected to be somewhere between L_C and L_C-L_P. Item 1.4.4 in the Task 1 section of the main report details development of a method to account for the presence of the end pipes and thus refine tension estimates. It is noted that this procedure as developed to date is only approximate and limited to selected applications, so that further investigation is needed for additional refinement.

The correction factor was evaluated by theoretical finite element calculations of the mode frequencies of a tendon having end segments stiffer than in the main section, given the corresponding lengths L_C and L_P, stiffness of the end and main section (Sp, Sm respectively), linear mass, and tension T. The resulting frequencies were then processed, using the procedure indicated in Item A4.2.5, as if they were the results of a tendon of length L_C, thus obtaining an estimated tension Te. The ratio k=T/Te was calculated for a range of conditions relevant to those in commonly encountered actual tendons. That ratio serves a correction factor that, when multiplied by Te, provides the value of the actual tension T for the specific cases analyzed. It is noted that to date these calculations have been developed only for cases in which the frequencies for either modes 2 and 3, or 2, 3 and 4 are used for tension calculations. Application of the resulting k factors to data involving a different selection of mode frequencies is expected to produce still useful, but less accurate results.

For general application, the results were processed by a multiple regression method to obtain a master formula they gives an approximation of k as a function of any L_C, L_P, Sp, Sm and T combination in the range of interest. The master formula is

$$k=1- k_0 P^q \qquad \text{(Eq. A4.17)}$$

where

$$P= (1-k_{INF}) (1-Sm/Sp)^{1.5} (\sigma_m/(1+\sigma_m))^{0.25} \qquad \text{(Eq. A4.18)}$$

k_{INF}= $((L-Lp)/L)^2$ (Eq. A4.19)

σ_m = Sm/ T L^2 (Eq. A4.20)

and k_0 and q are non-dimensional parameters that depend on whether Modes 2-3 or 2-4 are used for the calculations, per Table A4.1

Table A4.1 - Power law parameters for estimating k

Modes Used	k_0	q
2-3	2.0815	0.7843
2-4	2.0848	0.767

The present investigation (Task 1 section, Items 1.2.7 and 1.4.2) showed that the effective value of Sp is subject to significant uncertainty. The experimental evidence suggests that coupling between pipe and tendon core may be quite weak, so that instead of Sp being simply the sum of Sm and the steel pipe stiffness Spp, it may be better calculated by

Sp= Sm + βSpp (Eq. A4.21)

where β is ~0.25, significantly less than 1.

Moreover, analysis of the results (Task 1 section, Item 1.4.2) suggests that for relatively long tendons (e.g. when L_P ~<0.02 L_C) any increases in effective stiffness from the presence of the pipe segment may be approximately canceled by less than ideal fixity at the concrete-tendon junction. Thus, corrections for end pipe effects appear to be useful only for relatively long pipes compared with the tendon length, as would be the case in the tests conducted with tendons 13A and 13B.

For applicable cases, a practical procedure is to first ignore the presence of the steel pipes, and calculate an estimate of Te and Se from the f_n^mdata using the procedure in A4.2.5. Those values are then used in lieu of T and Sm respectively and input together with Spp (calculated from pipe dimensions) into Eqs. A4.18-21 to obtain an approximate value of k, named k_{APPR}. That factor is then used to calculate the improved estimate of the tension:

T_{IMPR} = k_{APPR} Te (Eq. A4.21)

Considering the uncertainties noted above, that the corrections usually involve only a small fraction of the value of T, and that the value of P is weakly dependent of Sm or T, the above procedure is deemed to be sufficient without further iterations.

A4.3 Application

A4.3.1 Cases covered

This section contains step-by-step guides on processing vibration test data for tension estimation of a typical external tendon configuration as it may be encountered in segmental post tensioned bridge. The guides refer to advanced methods and formulas described in section A4.2, as well as occasional reference to material contained in the main body of the report and appendices.

The guides do not address specific data acquisition equipment or software. For an equipment- and software-specific approach oriented to technical assistance personnel, the reader is referred to the Task 3 section and Appendix 3 of the main report, which address the simplified test and analysis procedure developed under the present project.

The first guide covers analysis of data that assuming that the linear mass of the tendon is known either by direct weighing of tendon segments removed from the bridge and assumed to be nearly identical to the one tested, or calculated from construction and materials properties data, or estimated by lookup to Table Add.4.1, in Appendix 3 of the main body of the report. The second guide addresses the use of additional static deflection tests to obtain the tension without prior information on the tendon linear mass. The third guide is for correction of the tension to account for end pipe effects in the case of relatively short tendons.

A4.3.2 Guide for cases where the linear mass is assumed to be known.

Prior information needed:

a. Values of the overall tendon linear mass m and the vibrating length L (distance between the points at which the tendon centerline intersects the concrete walls at each end of the tendon).

b. Acquired vibration spectrum with reliable identification of mode frequencies.

Step 1: By examination of the measured spectrum and mode frequencies, determine if either a series of single frequencies (f_1^m, f_2^m ... f_n^m...) or a series of double mode frequencies (f_{1H}^m, f_{1L}^m; f_{2H}^m, f_{2L}^m... f_{nH}^m,f_{nL}^m.......) is present. If a single series is present, treat it as in the following steps. If a double series is present, treat the high and the low frequency components series separately as if each were a single series.

Step 2: For mode numbers n=1 to n_{max} (with n_{max} =<7), and for each σ_i entry in Table A5.1, calculate the ratio $R_n(\sigma_i)= f_n^m/ \nu_n(\sigma_i)$. This and subsequent steps can be easily laid out in a spreadsheet.

Step 3: For each σ_i entry calculate $R_{avg}(\sigma_i)$ = Average $(R_1(\sigma_i)....R_{nmax}(\sigma_i))$

Step 4: For each σ_i entry calculate $Er(\sigma_i) = \sum_{n=1}^{n=n_{max}} (((R_n(\sigma_i) - R_{avg}(\sigma_i))/R_{avg}(\sigma_i))^2$

Step 4: Identify the entry among all σ_i values that yields the smallest value of $Er(\sigma_i)$. Name that entry σ_e, the estimated non-dimensional stiffness of the tendon. Name $R_{avm} = R_{avg}(\sigma_e)$.

Step 5: Calculate the estimated tendon tension $T_e = R_{avm}^2 L^2 m$

Step 6: Calculate the estimated tendon flexural stiffness $S_e = \sigma_e T_e L^2$

Step 7: If the tendon exhibited dual modes, average the values of Te obtained for the H and L series and report that average as the estimated tendon tension. As a descriptor of the quality of the estimate, calculate and report the percentage difference between the H and L estimates. Experience indicates that differences of 2% or less typical. Differences greater than 4% may be indicative of possible irregularities in the determination of one or both of the mode frequency series measured. While the Te values are usually very close, the values of Se for both series may differ markedly (see Task 1 section item 1.4.3) as they reflect normal asymmetric positioning of strands in the tendon cross section.

Notes:

a) An illustration of calculations per the above procedure is presented in the Task 2 section, Item 2.2.4.

b) This procedure assumes that spectral analysis and mode frequency identification is performed by the user or by software which may be obtained from market sources in the future. Thus, no itemized procedure is included above to deal with possible mode frequency misidentification. The reader is referred to the Task 2 section, Item 2.2.2 for an approach developed under this project based on currently available computational software.

c) If desired, more precise identification of σ_e can be made by creating linearly interpolated values of $\nu_n(\sigma)$ for finely spaced values of σ one Table step above and another below the initially identified value of σ_e. Steps 2 to 4 are then repeated for the narrow σ interval thus created, resulting in a refined estimate of σ_e. This or equivalent procedures have been successfully used in the present project, implemented with common macro procedures in a spreadsheet.

A4.3.3 Guide for processing supplemental deflection test results to obtain tension without prior information on linear mass.

Notice: this procedure has been successfully used in the present project in the Tendon Test Facility, but has not been deployed in the field. Static deflection tests in the field are expected to be time consuming. Therefore, this approach may be best limited to a small selection of tendons representative of a larger peer group. As the procedure yields not only tension but also the value of the linear mass, an average of that value can then be used for the rest of the tendons in the peer group using the procedure in Item A4.3.2.

Prior information needed

a. Values of the overall vibrating length L (distance between the points at which the tendon centerline intersects the concrete walls at each end of the tendon).

b. Acquired vibration spectrum with reliable identification of Mode frequencies.

c. Static deflection test data (e.g. performed as in the Task 1section Items 1.2.2, 1.32 and 1.4.4) for center point of tendon, yielding ratio δ = lateral displacement / applied lateral force. For better results, test should be performed along two lateral directions 90^o apart and the ratio δ reported as the average of the two tests.

Steps 1-4: Same as in Item A4.3.2 (but note Step 8 below if dual Modes are observed)

Step 5: Calculate the estimated tendon tension:

$$T_D = \delta^{-1} L (1/4-\sigma_e^{1/2})$$

(subscript "D" indicates the combined vibration-deflection approach).

Step 6: If desired, calculate the estimated tendon flexural stiffness

$$S_D = \sigma_e T_D L^2$$

Step 7: If desired for application to a larger tendon peer group to be evaluated by the method in Item A4.3.1, calculate the estimated tendon linear mass m_D as shown below and use it in lieu of m in the A4.3.1 steps.

$$m_D= T_D R_{avm}^{-2} L^{-2}$$

Step 8: If the tendon exhibited dual Modes, average the values of σ_e obtained for the H and L series and use that average for estimating tendon tension in Step 5. Apply Step 6 with σ_e from each series to obtain, if desired, estimates of stiffness along the effective principal cross section axes.

Notes:

a) An illustration of results obtained per the above procedure is presented in the Task 1 section, Item 1.4.4.

b) Notes (b) and (c) of Item A4.3.2 apply here as well.

c) Values of m_D and S_D recovered by this method should be checked against the range of values expected from independent estimates, or reported elsewhere for comparable tendons, to ascertain that results are plausible or to reveal possible procedural errors or data deficiencies.

A4.3.4 Guide for correcting for end pipe effects in short tendons.

Notice: This procedure yields an incremental accuracy improvement and is expected to be superseded by results from future investigations. This procedure is recommended only for tendons having a ratio L_P /L>0.02 (see definitions under (a) below).

Prior information needed

a. Value of the overall vibrating length L (distance between the points at which the tendon centerline intersects the concrete walls at each end of the tendon), and the sum of steel pipe ends protruding from the concrete at each end (L_P).

b. Value of tendon linear mass m, or static deflection data, according to whether the initial phase of this procedure proceeds as in Item A4.3.2 or A4.3.3 respectively.

b. Acquired vibration spectrum with reliable identification of Mode frequencies.

Steps 1-7: Same as in Items A4.3.2 or A4.3.3 according to choice in (b) above.

Step 8: Same as in Item A4.3.2 if that procedure is followed, otherwise proceed to next step.

Step 9: Call Sm = Se or S_D according to choice in (b).

Step 10: Call σ_m = Sm/ (Te L^2) [or Sm/ (T_D L^2)] according to choice in (b).

Step 11: Based on pipe cross section dimensions calculate

$Spp = I\ E$

with I = flexural moment of inertia of pipe cross section ($I = \pi((D+d)^4 - D^4)/64$ where D, d = inner diameter and wall thickness respectively)

E= steel elastic modulus (202.0 GPa ($2.93\ 10^7$ psi))

Step 12: Calculate $Sp = Sm + \beta Spp$ with $\beta=0.25$.

Step 13: Calculate k per equations A4.17 to A4.19 in Item A4.2.7.2 and Table A4.1. Use entry for Modes 2-3 if only those were used in calculating tension and stiffness, otherwise use entry for Modes 2-4 in all other cases. Name the result k_{APPR}.

Step 14: Calculate improved estimate of tendon tension with $T_{IMPR} = k_{APPR}\ Te$ [or $k_{APPR}\ T_D$] according to choice in (b).

APPENDIX 5

DETAILED TABLE OF NONDIMENSIONAL MODE FREQUENCIES AS FUNCTION OF NONDIMENSIONAL STIFFNESS

A numeric image of this table suitable for use in a spreadsheet can be exported by text selection from .pdf electronic versions of this document, if optical character recognition (OCR) is enabled. Otherwise, the document can be processed first by the user through OCR processing software such as Adobe Acrobat ™.

Table A5.1 - Master table of non-dimensional frequencies as function of non-dimensional stiffness σ for Modes 1-7. Values of σ range from 10^{-4} to 10^{-2}.

σ	ν_1	ν_2	ν_3	ν_4	ν_5	ν_6	ν_7
0.0001	0.510457	1.022432	1.537433	2.056954	2.582463	3.1154	3.65716529
0.00012	0.511494	1.02481	1.541758	2.064123	2.593658	3.132071	3.68101784
0.00014	0.512456	1.027039	1.545859	2.070995	2.604479	3.148284	3.7043096
0.000159	0.513359	1.02915	1.549785	2.077633	2.615004	3.164128	3.72714516
0.000179	0.514212	1.031164	1.553566	2.084079	2.625284	3.179666	3.74959698
0.000199	0.515025	1.033097	1.557227	2.090364	2.635358	3.194945	3.77171771
0.000219	0.515803	1.034961	1.560785	2.09651	2.645256	3.209997	3.79354702
0.000239	0.516551	1.036765	1.564254	2.102538	2.654999	3.224851	3.81511571
0.000258	0.517273	1.038516	1.567645	2.10846	2.664605	3.239526	3.83644825
0.000278	0.517971	1.040222	1.570967	2.114289	2.674089	3.254041	3.85756451
0.000298	0.518648	1.041886	1.574226	2.120034	2.683462	3.268408	3.87848088
0.000318	0.519306	1.043512	1.57743	2.125703	2.692735	3.28264	3.8992111
0.000338	0.519947	1.045104	1.580584	2.131303	2.701915	3.296746	3.91976683
0.000357	0.520572	1.046666	1.583691	2.13684	2.71101	3.310736	3.94015808
0.000377	0.521183	1.048199	1.586755	2.142319	2.720026	3.324615	3.96039354
0.000397	0.521781	1.049706	1.589781	2.147744	2.728968	3.338392	3.98048082
0.000417	0.522366	1.051189	1.59277	2.153118	2.737841	3.35207	4.00042663
0.000437	0.52294	1.052649	1.595726	2.158446	2.746649	3.365656	4.02023695
0.000456	0.523504	1.054089	1.59865	2.16373	2.755395	3.379153	4.03991713
0.000476	0.524057	1.055509	1.601544	2.168972	2.764083	3.392565	4.05947201
0.000496	0.524601	1.05691	1.604411	2.174176	2.772715	3.405896	4.07890596
0.000516	0.525137	1.058294	1.607252	2.179342	2.781295	3.419149	4.09822296
0.000536	0.525664	1.059662	1.610069	2.184474	2.789824	3.432327	4.11742667
0.000555	0.526184	1.061015	1.612862	2.189573	2.798305	3.445433	4.13652045
0.000575	0.526696	1.062353	1.615633	2.194639	2.80674	3.458469	4.1555074
0.000595	0.527201	1.063677	1.618383	2.199676	2.81513	3.471437	4.17439042
0.000615	0.527699	1.064989	1.621113	2.204684	2.823477	3.484339	4.19317218
0.000635	0.528191	1.066288	1.623825	2.209664	2.831782	3.497177	4.21185518
0.000654	0.528677	1.067574	1.626518	2.214617	2.840048	3.509953	4.23044177
0.000674	0.529158	1.06885	1.629194	2.219545	2.848274	3.522669	4.24893416
0.000694	0.529633	1.070115	1.631853	2.224448	2.856463	3.535325	4.26733442
0.000714	0.530102	1.071369	1.634496	2.229328	2.864616	3.547924	4.28564452
0.000734	0.530567	1.072614	1.637124	2.234184	2.872733	3.560467	4.30386631
0.000753	0.531027	1.073849	1.639737	2.239019	2.880816	3.572955	4.32200156
0.000773	0.531482	1.075075	1.642336	2.243832	2.888865	3.58539	4.34005195
0.000793	0.531932	1.076292	1.644922	2.248624	2.896881	3.597772	4.35801906
0.000813	0.532379	1.0775	1.647494	2.253396	2.904866	3.610102	4.37590442
0.000833	0.532821	1.0787	1.650054	2.258149	2.912819	3.622382	4.39370949
0.000852	0.533259	1.079893	1.652601	2.262882	2.920742	3.634612	4.41143566
0.000872	0.533694	1.081078	1.655136	2.267598	2.928635	3.646794	4.42908427
0.000892	0.534124	1.082255	1.65766	2.272295	2.936499	3.658928	4.4466566
0.000912	0.534551	1.083426	1.660172	2.276974	2.944334	3.671015	4.46415389
0.000932	0.534975	1.08459	1.662674	2.281637	2.952142	3.683055	4.48157732
0.000951	0.535395	1.085747	1.665165	2.286283	2.959922	3.695051	4.49892805
0.000971	0.535812	1.086897	1.667646	2.290912	2.967675	3.707002	4.51620716
0.000991	0.536226	1.088041	1.670118	2.295526	2.975401	3.718909	4.53341574
0.001011	0.536637	1.08918	1.672579	2.300124	2.983102	3.730773	4.55055481
0.001031	0.537045	1.090312	1.675031	2.304707	2.990777	3.742594	4.56762537
0.00105	0.53745	1.091439	1.677474	2.309275	2.998427	3.754373	4.58462838
0.00107	0.537852	1.09256	1.679908	2.313829	3.006053	3.766111	4.60156479
0.00109	0.538251	1.093676	1.682333	2.318368	3.013654	3.777808	4.6184355
0.00111	0.538648	1.094786	1.684749	2.322893	3.021231	3.789465	4.63524139

σ	ν_1	ν_2	ν_3	ν_4	ν_5	ν_6	ν_7
0.00113	0.539042	1.095891	1.687158	2.327405	3.028785	3.801082	4.65198333
0.001149	0.539434	1.096992	1.689558	2.331902	3.036315	3.81266	4.66866213
0.001169	0.539823	1.098087	1.69195	2.336387	3.043823	3.824199	4.68527863
0.001189	0.54021	1.099178	1.694335	2.340859	3.051309	3.8357	4.70183359
0.001209	0.540595	1.100264	1.696712	2.345318	3.058772	3.847164	4.7183278
0.001229	0.540977	1.101346	1.699081	2.349764	3.066213	3.85859	4.73476199
0.001248	0.541357	1.102423	1.701444	2.354198	3.073633	3.86998	4.75113691
0.001268	0.541735	1.103496	1.703799	2.35862	3.081031	3.881333	4.76745325
0.001288	0.542111	1.104565	1.706147	2.36303	3.088409	3.892651	4.78371172
0.001308	0.542485	1.10563	1.708488	2.367428	3.095765	3.903933	4.79991299
0.001328	0.542857	1.106691	1.710823	2.371814	3.103101	3.91518	4.81605772
0.001347	0.543226	1.107748	1.713151	2.376189	3.110417	3.926392	4.83214657
0.001367	0.543594	1.108801	1.715472	2.380553	3.117713	3.93757	4.84818015
0.001387	0.54396	1.10985	1.717788	2.384906	3.124989	3.948714	4.8641591
0.001407	0.544325	1.110895	1.720097	2.389247	3.132246	3.959825	4.88008402
0.001427	0.544687	1.111937	1.722399	2.393578	3.139483	3.970902	4.89595549
0.001446	0.545048	1.112976	1.724696	2.397899	3.146701	3.981947	4.9117741
0.001466	0.545407	1.114011	1.726987	2.402208	3.153901	3.992959	4.92754042
0.001486	0.545764	1.115042	1.729272	2.406508	3.161081	4.003939	4.943255
0.001506	0.54612	1.116071	1.731552	2.410797	3.168243	4.014887	4.95891838
0.001526	0.546474	1.117096	1.733825	2.415076	3.175387	4.025804	4.9745311
0.001545	0.546826	1.118117	1.736094	2.419345	3.182513	4.036689	4.99009367
0.001565	0.547177	1.119136	1.738356	2.423604	3.189621	4.047544	5.00560663
0.001585	0.547526	1.120152	1.740614	2.427853	3.196711	4.058368	5.02107046
0.001605	0.547874	1.121164	1.742866	2.432093	3.203783	4.069162	5.03648566
0.001625	0.548221	1.122174	1.745113	2.436323	3.210838	4.079926	5.05185271
0.001644	0.548566	1.123181	1.747355	2.440544	3.217876	4.09066	5.06717209
0.001664	0.548909	1.124185	1.749591	2.444755	3.224897	4.101364	5.08244427
0.001684	0.549251	1.125186	1.751823	2.448958	3.231901	4.11204	5.0976697
0.001704	0.549592	1.126184	1.75405	2.453151	3.238888	4.122686	5.11284884
0.001724	0.549932	1.127179	1.756272	2.457335	3.245858	4.133304	5.12798213
0.001743	0.55027	1.128172	1.758489	2.46151	3.252813	4.143894	5.14306999
0.001763	0.550607	1.129162	1.760701	2.465676	3.25975	4.154455	5.15811286
0.001783	0.550942	1.13015	1.762909	2.469834	3.266672	4.164989	5.17311116
0.001803	0.551277	1.131135	1.765112	2.473983	3.273578	4.175494	5.1880653
0.001823	0.55161	1.132118	1.76731	2.478123	3.280468	4.185973	5.20297568
0.001842	0.551942	1.133098	1.769505	2.482255	3.287342	4.196424	5.21784271
0.001862	0.552273	1.134075	1.771694	2.486378	3.2942	4.206849	5.23266677
0.001882	0.552602	1.135051	1.773879	2.490494	3.301043	4.217246	5.24744825
0.001902	0.552931	1.136024	1.77606	2.4946	3.307871	4.227617	5.26218754
0.001922	0.553258	1.136994	1.778237	2.498699	3.314683	4.237962	5.276885
0.001941	0.553584	1.137963	1.780409	2.50279	3.32148	4.248281	5.29154101
0.001961	0.553909	1.138929	1.782578	2.506872	3.328263	4.258574	5.30615592
0.001981	0.554233	1.139892	1.784742	2.510947	3.33503	4.268842	5.32073009
0.002001	0.554556	1.140854	1.786902	2.515013	3.341783	4.279084	5.33526387
0.002021	0.554878	1.141813	1.789058	2.519072	3.348521	4.289301	5.34975761
0.00204	0.555199	1.142771	1.79121	2.523123	3.355245	4.299492	5.36421165
0.00206	0.555519	1.143726	1.793358	2.527166	3.361954	4.309659	5.37862632
0.00208	0.555838	1.144679	1.795502	2.531202	3.368649	4.319802	5.39300196
0.0021	0.556156	1.14563	1.797642	2.53523	3.37533	4.32992	5.40733889
0.00212	0.556473	1.146579	1.799778	2.539251	3.381997	4.340013	5.42163742
0.002139	0.556789	1.147526	1.801911	2.543264	3.388649	4.350083	5.43589788
0.002159	0.557104	1.148471	1.804039	2.54727	3.395288	4.360129	5.45012058
0.002179	0.557418	1.149414	1.806165	2.551269	3.401913	4.370151	5.46430582
0.002199	0.557731	1.150355	1.808286	2.55526	3.408525	4.380149	5.4784539
0.002219	0.558043	1.151295	1.810404	2.559244	3.415123	4.390124	5.49256513
0.002238	0.558355	1.152232	1.812518	2.563221	3.421707	4.400077	5.5066398

σ	ν_1	ν_2	ν_3	ν_4	ν_5	ν_6	ν_7
0.002258	0.558665	1.153168	1.814628	2.56719	3.428278	4.410006	5.5206782
0.002278	0.558975	1.154101	1.816735	2.571153	3.434836	4.419912	5.53468061
0.002298	0.559284	1.155033	1.818839	2.575108	3.44138	4.429795	5.54864732
0.002318	0.559591	1.155963	1.820939	2.579057	3.447912	4.439656	5.5625786
0.002337	0.559899	1.156892	1.823035	2.582999	3.45443	4.449495	5.57647473
0.002357	0.560205	1.157818	1.825128	2.586934	3.460935	4.459311	5.59033598
0.002377	0.56051	1.158743	1.827218	2.590862	3.467428	4.469106	5.60416262
0.002397	0.560815	1.159667	1.829304	2.594783	3.473908	4.478879	5.61795491
0.002417	0.561119	1.160588	1.831387	2.598698	3.480375	4.48863	5.63171311
0.002436	0.561422	1.161508	1.833467	2.602606	3.48683	4.498359	5.64543748
0.002456	0.561724	1.162426	1.835544	2.606507	3.493272	4.508067	5.65912827
0.002476	0.562026	1.163343	1.837617	2.610402	3.499702	4.517753	5.67278573
0.002496	0.562326	1.164257	1.839687	2.61429	3.506119	4.527419	5.68641011
0.002516	0.562627	1.165171	1.841753	2.618172	3.512524	4.537064	5.70000165
0.002535	0.562926	1.166083	1.843817	2.622047	3.518917	4.546687	5.7135606
0.002555	0.563224	1.166993	1.845877	2.625916	3.525298	4.55629	5.72708718
0.002575	0.563522	1.167901	1.847935	2.629779	3.531667	4.565873	5.74058164
0.002595	0.563819	1.168808	1.849989	2.633635	3.538023	4.575435	5.75404421
0.002615	0.564116	1.169714	1.85204	2.637485	3.544368	4.584977	5.76747512
0.002634	0.564412	1.170618	1.854088	2.641328	3.550701	4.594498	5.78087458
0.002654	0.564707	1.171521	1.856133	2.645166	3.557023	4.604	5.79424284
0.002674	0.565001	1.172422	1.858175	2.648997	3.563333	4.613482	5.8075801
0.002694	0.565295	1.173321	1.860214	2.652822	3.569631	4.622944	5.82088658
0.002714	0.565588	1.17422	1.86225	2.656641	3.575917	4.632386	5.8341625
0.002733	0.56588	1.175116	1.864283	2.660454	3.582193	4.641809	5.84740808
0.002753	0.566172	1.176012	1.866314	2.664261	3.588456	4.651212	5.86062352
0.002773	0.566463	1.176906	1.868341	2.668062	3.594709	4.660596	5.87380903
0.002793	0.566754	1.177798	1.870365	2.671857	3.60095	4.669962	5.88696481
0.002813	0.567043	1.178689	1.872387	2.675646	3.60718	4.679308	5.90009107
0.002832	0.567333	1.179579	1.874406	2.67943	3.613399	4.688635	5.91318802
0.002852	0.567621	1.180468	1.876422	2.683207	3.619607	4.697943	5.92625584
0.002872	0.567909	1.181355	1.878435	2.686979	3.625804	4.707233	5.93929473
0.002892	0.568197	1.182241	1.880445	2.690745	3.63199	4.716504	5.9523049
0.002912	0.568483	1.183125	1.882453	2.694505	3.638165	4.725757	5.96528652
0.002931	0.56877	1.184008	1.884457	2.698259	3.644329	4.734991	5.97823979
0.002951	0.569055	1.18489	1.88646	2.702008	3.650483	4.744207	5.99116489
0.002971	0.56934	1.185771	1.888459	2.705751	3.656625	4.753406	6.00406202
0.002991	0.569625	1.18665	1.890456	2.709488	3.662758	4.762586	6.01693135
0.003011	0.569909	1.187528	1.89245	2.71322	3.668879	4.771748	6.02977306
0.00303	0.570192	1.188405	1.894441	2.716946	3.67499	4.780893	6.04258734
0.00305	0.570475	1.189281	1.89643	2.720667	3.681091	4.790019	6.05537436
0.00307	0.570757	1.190155	1.898416	2.724382	3.687182	4.799129	6.0681343
0.00309	0.571039	1.191028	1.900399	2.728092	3.693261	4.80822	6.08086732
0.00311	0.57132	1.1919	1.90238	2.731796	3.699331	4.817295	6.09357361
0.003129	0.571601	1.192771	1.904359	2.735495	3.705391	4.826352	6.10625332
0.003149	0.571881	1.193641	1.906334	2.739189	3.71144	4.835392	6.11890664
0.003169	0.57216	1.194509	1.908307	2.742877	3.717479	4.844415	6.13153372
0.003189	0.572439	1.195376	1.910278	2.74656	3.723508	4.853421	6.14413472
0.003209	0.572718	1.196242	1.912246	2.750237	3.729528	4.86241	6.15670982
0.003228	0.572996	1.197107	1.914212	2.753909	3.735537	4.871383	6.16925917
0.003248	0.573274	1.197971	1.916175	2.757576	3.741536	4.880339	6.18178292
0.003268	0.573551	1.198833	1.918136	2.761238	3.747525	4.889278	6.19428125
0.003288	0.573827	1.199695	1.920094	2.764895	3.753505	4.898201	6.2067543
0.003308	0.574103	1.200555	1.92205	2.768546	3.759475	4.907107	6.21920223
0.003327	0.574379	1.201415	1.924003	2.772192	3.765435	4.915997	6.23162518
0.003347	0.574654	1.202273	1.925954	2.775834	3.771386	4.924871	6.24402332
0.003367	0.574928	1.20313	1.927903	2.77947	3.777327	4.933729	6.25639679

σ	ν_1	ν_2	ν_3	ν_4	ν_5	ν_6	ν_7
0.003387	0.575203	1.203986	1.929849	2.783101	3.783258	4.94257	6.26874573
0.003407	0.575476	1.204841	1.931792	2.786727	3.78918	4.951396	6.2810703
0.003426	0.57575	1.205695	1.933734	2.790347	3.795092	4.960206	6.29337064
0.003446	0.576022	1.206547	1.935673	2.793963	3.800996	4.969	6.3056469
0.003466	0.576295	1.207399	1.93761	2.797574	3.806889	4.977779	6.3178992
0.003486	0.576566	1.20825	1.939544	2.80118	3.812774	4.986542	6.33012771
0.003506	0.576838	1.209099	1.941476	2.804782	3.818649	4.995289	6.34233255
0.003525	0.577109	1.209948	1.943406	2.808378	3.824515	5.004021	6.35451386
0.003545	0.577379	1.210795	1.945333	2.811969	3.830371	5.012738	6.36667178
0.003565	0.577649	1.211642	1.947258	2.815556	3.836219	5.021439	6.37880645
0.003585	0.577919	1.212488	1.949181	2.819137	3.842057	5.030125	6.390918
0.003605	0.578188	1.213332	1.951102	2.822714	3.847887	5.038796	6.40300655
0.003624	0.578457	1.214176	1.95302	2.826286	3.853707	5.047453	6.41507225
0.003644	0.578725	1.215018	1.954936	2.829853	3.859519	5.056094	6.42711522
0.003664	0.578993	1.21586	1.95685	2.833416	3.865322	5.06472	6.4391356
0.003684	0.579261	1.2167	1.958762	2.836974	3.871115	5.073332	6.4511335
0.003704	0.579528	1.21754	1.960671	2.840527	3.8769	5.081929	6.46310906
0.003723	0.579795	1.218379	1.962579	2.844075	3.882676	5.090511	6.4750624
0.003743	0.580061	1.219216	1.964484	2.847619	3.888444	5.099078	6.48699364
0.003763	0.580327	1.220053	1.966387	2.851158	3.894203	5.107632	6.49890291
0.003783	0.580592	1.220889	1.968288	2.854693	3.899953	5.11617	6.51079033
0.003803	0.580857	1.221724	1.970186	2.858222	3.905694	5.124695	6.52265602
0.003822	0.581122	1.222558	1.972083	2.861748	3.911427	5.133205	6.5345001
0.003842	0.581386	1.223391	1.973977	2.865269	3.917151	5.141701	6.54632269
0.003862	0.58165	1.224223	1.975869	2.868785	3.922867	5.150183	6.5581239
0.003882	0.581914	1.225054	1.97776	2.872297	3.928574	5.158651	6.56990386
0.003902	0.582177	1.225884	1.979648	2.875804	3.934273	5.167105	6.58166267
0.003921	0.58244	1.226713	1.981534	2.879306	3.939964	5.175545	6.59340045
0.003941	0.582702	1.227542	1.983417	2.882805	3.945646	5.183971	6.60511731
0.003961	0.582964	1.228369	1.985299	2.886299	3.95132	5.192384	6.61681337
0.003981	0.583226	1.229196	1.987179	2.889788	3.956986	5.200782	6.62848873
0.004001	0.583487	1.230022	1.989057	2.893273	3.962643	5.209167	6.64014351
0.00402	0.583748	1.230847	1.990932	2.896754	3.968292	5.217539	6.65177782
0.00404	0.584009	1.231671	1.992806	2.90023	3.973933	5.225897	6.66339176
0.00406	0.584269	1.232494	1.994677	2.903702	3.979566	5.234242	6.67498544
0.00408	0.584529	1.233316	1.996547	2.907169	3.985191	5.242573	6.68655897
0.0041	0.584788	1.234137	1.998415	2.910633	3.990808	5.250891	6.69811245
0.004119	0.585047	1.234958	2.00028	2.914092	3.996417	5.259196	6.70964598
0.004139	0.585306	1.235778	2.002144	2.917546	4.002018	5.267487	6.72115968
0.004159	0.585565	1.236596	2.004005	2.920997	4.007611	5.275766	6.73265364
0.004179	0.585823	1.237414	2.005865	2.924443	4.013196	5.284031	6.74412796
0.004199	0.586081	1.238232	2.007722	2.927885	4.018773	5.292284	6.75558275
0.004218	0.586338	1.239048	2.009578	2.931323	4.024342	5.300523	6.7670181
0.004238	0.586595	1.239863	2.011432	2.934756	4.029904	5.30875	6.77843412
0.004258	0.586852	1.240678	2.013283	2.938185	4.035457	5.316964	6.7898309
0.004278	0.587108	1.241492	2.015133	2.941611	4.041003	5.325165	6.80120853
0.004298	0.587364	1.242305	2.016981	2.945032	4.046541	5.333353	6.81256713
0.004317	0.58762	1.243117	2.018827	2.948449	4.052072	5.341529	6.82390677
0.004337	0.587876	1.243929	2.020671	2.951862	4.057595	5.349693	6.83522756
0.004357	0.588131	1.244739	2.022513	2.95527	4.06311	5.357843	6.84652959
0.004377	0.588386	1.245549	2.024354	2.958675	4.068618	5.365982	6.85781296
0.004397	0.58864	1.246358	2.026192	2.962076	4.074118	5.374108	6.86907775
0.004416	0.588894	1.247167	2.028029	2.965472	4.079611	5.382221	6.88032406
0.004436	0.589148	1.247974	2.029863	2.968865	4.085096	5.390323	6.89155198
0.004456	0.589402	1.248781	2.031696	2.972253	4.090574	5.398412	6.9027616
0.004476	0.589655	1.249587	2.033527	2.975638	4.096044	5.406489	6.91395301
0.004496	0.589908	1.250392	2.035356	2.979018	4.101507	5.414554	6.9251263

σ	ν_1	ν_2	ν_3	ν_4	ν_5	ν_6	ν_7
0.004515	0.59016	1.251196	2.037183	2.982395	4.106963	5.422607	6.93628155
0.004535	0.590413	1.252	2.039009	2.985767	4.112411	5.430647	6.94741886
0.004555	0.590665	1.252802	2.040832	2.989136	4.117852	5.438676	6.9585383
0.004575	0.590916	1.253605	2.042654	2.992501	4.123286	5.446693	6.96963998
0.004595	0.591168	1.254406	2.044474	2.995862	4.128713	5.454699	6.98072396
0.004614	0.591419	1.255206	2.046292	2.999219	4.134132	5.462692	6.99179034
0.004634	0.59167	1.256006	2.048108	3.002572	4.139544	5.470674	7.0028392
0.004654	0.59192	1.256805	2.049923	3.005921	4.144949	5.478644	7.01387062
0.004674	0.592171	1.257604	2.051735	3.009266	4.150347	5.486602	7.02488469
0.004694	0.59242	1.258401	2.053546	3.012608	4.155738	5.494549	7.03588149
0.004713	0.59267	1.259198	2.055355	3.015946	4.161122	5.502484	7.04686109
0.004733	0.592919	1.259994	2.057163	3.019279	4.166498	5.510408	7.05782358
0.004753	0.593169	1.26079	2.058968	3.02261	4.171868	5.51832	7.06876905
0.004773	0.593417	1.261584	2.060772	3.025936	4.177231	5.526221	7.07969756
0.004793	0.593666	1.262378	2.062574	3.029258	4.182587	5.534111	7.0906092
0.004812	0.593914	1.263172	2.064375	3.032577	4.187935	5.541989	7.10150405
0.004832	0.594162	1.263964	2.066173	3.035892	4.193277	5.549856	7.11238217
0.004852	0.59441	1.264756	2.06797	3.039204	4.198613	5.557712	7.12324366
0.004872	0.594657	1.265547	2.069765	3.042511	4.203941	5.565557	7.13408859
0.004892	0.594904	1.266338	2.071559	3.045815	4.209262	5.573391	7.14491703
0.004911	0.595151	1.267127	2.073351	3.049115	4.214577	5.581214	7.15572905
0.004931	0.595398	1.267916	2.075141	3.052412	4.219885	5.589025	7.16652474
0.004951	0.595644	1.268705	2.076929	3.055705	4.225186	5.596826	7.17730417
0.004971	0.59589	1.269492	2.078716	3.058994	4.230481	5.604616	7.1880674
0.004991	0.596136	1.270279	2.080501	3.06228	4.235768	5.612395	7.19881452
0.00501	0.596382	1.271065	2.082284	3.065562	4.241049	5.620163	7.20954559
0.00503	0.596627	1.271851	2.084066	3.06884	4.246324	5.627921	7.22026069
0.00505	0.596872	1.272636	2.085845	3.072115	4.251592	5.635668	7.23095989
0.00507	0.597117	1.27342	2.087624	3.075386	4.256853	5.643404	7.24164326
0.00509	0.597361	1.274204	2.0894	3.078654	4.262108	5.651129	7.25231086
0.005109	0.597605	1.274987	2.091175	3.081918	4.267356	5.658844	7.26296278
0.005129	0.597849	1.275769	2.092949	3.085178	4.272598	5.666548	7.27359907
0.005149	0.598093	1.27655	2.09472	3.088435	4.277833	5.674242	7.28421981
0.005169	0.598337	1.277331	2.09649	3.091689	4.283062	5.681926	7.29482507
0.005189	0.59858	1.278111	2.098259	3.094939	4.288284	5.689599	7.30541491
0.005208	0.598823	1.278891	2.100025	3.098185	4.2935	5.697261	7.3159894
0.005228	0.599066	1.27967	2.101791	3.101428	4.29871	5.704914	7.3265486
0.005248	0.599308	1.280448	2.103554	3.104668	4.303913	5.712556	7.33709259
0.005268	0.599551	1.281226	2.105316	3.107904	4.30911	5.720187	7.34762143
0.005288	0.599793	1.282003	2.107076	3.111136	4.314301	5.727809	7.35813518
0.005307	0.600034	1.282779	2.108835	3.114366	4.319485	5.73542	7.36863391
0.005327	0.600276	1.283555	2.110592	3.117591	4.324663	5.743022	7.37911769
0.005347	0.600517	1.28433	2.112348	3.120814	4.329835	5.750613	7.38958657
0.005367	0.600758	1.285104	2.114102	3.124033	4.335	5.758194	7.40004062
0.005387	0.600999	1.285878	2.115854	3.127248	4.34016	5.765765	7.41047991
0.005406	0.60124	1.286651	2.117605	3.13046	4.345313	5.773326	7.42090449
0.005426	0.60148	1.287424	2.119354	3.133669	4.35046	5.780878	7.43131443
0.005446	0.60172	1.288195	2.121102	3.136874	4.355601	5.788419	7.44170979
0.005466	0.60196	1.288967	2.122848	3.140076	4.360736	5.795951	7.45209063
0.005486	0.6022	1.289737	2.124592	3.143275	4.365864	5.803472	7.46245702
0.005505	0.602439	1.290507	2.126335	3.146471	4.370987	5.810984	7.472809
0.005525	0.602678	1.291277	2.128077	3.149663	4.376104	5.818487	7.48314665
0.005545	0.602917	1.292045	2.129817	3.152851	4.381214	5.825979	7.49347002
0.005565	0.603156	1.292814	2.131555	3.156037	4.386319	5.833462	7.50377917
0.005585	0.603395	1.293581	2.133292	3.159219	4.391417	5.840936	7.51407416
0.005604	0.603633	1.294348	2.135027	3.162398	4.39651	5.848399	7.52435505
0.005624	0.603871	1.295115	2.136761	3.165574	4.401597	5.855854	7.5346219

σ	ν_1	ν_2	ν_3	ν_4	ν_5	ν_6	ν_7
0.005644	0.604109	1.29588	2.138493	3.168746	4.406678	5.863298	7.54487475
0.005664	0.604347	1.296645	2.140224	3.171915	4.411752	5.870734	7.55511368
0.005684	0.604584	1.29741	2.141954	3.175081	4.416822	5.878159	7.56533874
0.005703	0.604821	1.298174	2.143681	3.178244	4.421885	5.885576	7.57554998
0.005723	0.605058	1.298937	2.145408	3.181404	4.426942	5.892983	7.58574746
0.005743	0.605295	1.2997	2.147132	3.18456	4.431994	5.900381	7.59593123
0.005763	0.605531	1.300462	2.148856	3.187713	4.437039	5.907769	7.60610136
0.005783	0.605768	1.301224	2.150578	3.190863	4.442079	5.915148	7.61625789
0.005802	0.606004	1.301985	2.152298	3.19401	4.447114	5.922518	7.62640088
0.005822	0.60624	1.302745	2.154017	3.197153	4.452142	5.929879	7.63653038
0.005842	0.606476	1.303505	2.155734	3.200294	4.457165	5.937231	7.64664645
0.005862	0.606711	1.304264	2.15745	3.203431	4.462182	5.944573	7.65674914
0.005882	0.606946	1.305023	2.159165	3.206565	4.467194	5.951907	7.66683851
0.005901	0.607182	1.305781	2.160878	3.209696	4.472199	5.959231	7.6769146
0.005921	0.607416	1.306539	2.162589	3.212824	4.4772	5.966547	7.68697747
0.005941	0.607651	1.307296	2.164299	3.215949	4.482194	5.973853	7.69702718
0.005961	0.607886	1.308052	2.166008	3.219071	4.487183	5.981151	7.70706376
0.005981	0.60812	1.308808	2.167715	3.22219	4.492166	5.988439	7.71708728
0.006	0.608354	1.309563	2.169421	3.225305	4.497144	5.995719	7.72709779
0.00602	0.608588	1.310318	2.171125	3.228418	4.502117	6.00299	7.73709533
0.00604	0.608821	1.311072	2.172828	3.231527	4.507083	6.010252	7.74707996
0.00606	0.609055	1.311826	2.17453	3.234634	4.512045	6.017505	7.75705172
0.00608	0.609288	1.312579	2.17623	3.237737	4.517	6.024749	7.76701067
0.006099	0.609521	1.313331	2.177929	3.240838	4.521951	6.031985	7.77695685
0.006119	0.609754	1.314083	2.179626	3.243935	4.526896	6.039212	7.78689032
0.006139	0.609987	1.314834	2.181322	3.247029	4.531835	6.046431	7.79681112
0.006159	0.610219	1.315585	2.183016	3.250121	4.536769	6.05364	7.8067193
0.006179	0.610452	1.316335	2.184709	3.253209	4.541698	6.060842	7.81661491
0.006198	0.610684	1.317085	2.186401	3.256295	4.546621	6.068034	7.826498
0.006218	0.610916	1.317834	2.188091	3.259377	4.551539	6.075218	7.83636861
0.006238	0.611147	1.318583	2.18978	3.262457	4.556452	6.082394	7.84622679
0.006258	0.611379	1.319331	2.191467	3.265533	4.561359	6.089561	7.8560726
0.006278	0.61161	1.320078	2.193154	3.268607	4.566261	6.09672	7.86590606
0.006297	0.611841	1.320825	2.194838	3.271677	4.571158	6.10387	7.87572724
0.006317	0.612072	1.321572	2.196522	3.274745	4.576049	6.111012	7.88553618
0.006337	0.612303	1.322318	2.198204	3.27781	4.580935	6.118146	7.89533292
0.006357	0.612534	1.323063	2.199884	3.280872	4.585816	6.125271	7.90511751
0.006377	0.612764	1.323808	2.201564	3.283931	4.590692	6.132388	7.91488999
0.006396	0.612994	1.324552	2.203242	3.286987	4.595562	6.139496	7.92465042
0.006416	0.613224	1.325296	2.204918	3.29004	4.600428	6.146597	7.93439882
0.006436	0.613454	1.32604	2.206593	3.29309	4.605288	6.153689	7.94413526
0.006456	0.613684	1.326782	2.208267	3.296138	4.610143	6.160773	7.95385976
0.006476	0.613913	1.327525	2.20994	3.299182	4.614993	6.167849	7.96357238
0.006495	0.614143	1.328266	2.211611	3.302224	4.619837	6.174917	7.97327317
0.006515	0.614372	1.329007	2.213281	3.305263	4.624677	6.181976	7.98296215
0.006535	0.614601	1.329748	2.214949	3.308299	4.629512	6.189028	7.99263938
0.006555	0.614829	1.330488	2.216617	3.311332	4.634341	6.196071	8.00230489
0.006575	0.615058	1.331228	2.218283	3.314363	4.639166	6.203107	8.01195874
0.006594	0.615286	1.331967	2.219947	3.31739	4.643985	6.210135	8.02160096
0.006614	0.615515	1.332706	2.22161	3.320415	4.6488	6.217154	8.0312316
0.006634	0.615743	1.333444	2.223272	3.323437	4.653609	6.224166	8.04085069
0.006654	0.615971	1.334181	2.224933	3.326457	4.658413	6.23117	8.05045828
0.006674	0.616198	1.334918	2.226592	3.329473	4.663213	6.238165	8.06005441
0.006693	0.616426	1.335655	2.22825	3.332487	4.668007	6.245153	8.06963912
0.006713	0.616653	1.336391	2.229907	3.335498	4.672797	6.252134	8.07921245
0.006733	0.61688	1.337127	2.231562	3.338506	4.677581	6.259106	8.08877444
0.006753	0.617107	1.337862	2.233216	3.341511	4.682361	6.266071	8.09832513

σ	ν_1	ν_2	ν_3	ν_4	ν_5	ν_6	ν_7
0.006773	0.617334	1.338596	2.234869	3.344514	4.687136	6.273028	8.10786457
0.006792	0.617561	1.33933	2.236521	3.347514	4.691906	6.279977	8.11739279
0.006812	0.617787	1.340064	2.238171	3.350511	4.696671	6.286918	8.12690982
0.006832	0.618014	1.340797	2.23982	3.353506	4.701431	6.293852	8.13641572
0.006852	0.61824	1.34153	2.241468	3.356497	4.706186	6.300778	8.14591052
0.006872	0.618466	1.342262	2.243114	3.359487	4.710937	6.307697	8.15539426
0.006891	0.618692	1.342993	2.244759	3.362473	4.715683	6.314608	8.16486697
0.006911	0.618917	1.343725	2.246403	3.365457	4.720424	6.321511	8.1743287
0.006931	0.619143	1.344455	2.248046	3.368438	4.72516	6.328407	8.18377948
0.006951	0.619368	1.345185	2.249687	3.371416	4.729891	6.335295	8.19321935
0.006971	0.619593	1.345915	2.251328	3.374392	4.734618	6.342176	8.20264835
0.00699	0.619818	1.346644	2.252966	3.377365	4.73934	6.34905	8.21206652
0.00701	0.620043	1.347373	2.254604	3.380335	4.744057	6.355915	8.22147389
0.00703	0.620268	1.348101	2.25624	3.383303	4.74877	6.362774	8.23087051
0.00705	0.620493	1.348829	2.257876	3.386268	4.753477	6.369625	8.2402564
0.00707	0.620717	1.349556	2.259509	3.389231	4.75818	6.376469	8.2496316
0.007089	0.620941	1.350283	2.261142	3.392191	4.762879	6.383305	8.25899616
0.007109	0.621165	1.351009	2.262774	3.395148	4.767573	6.390134	8.2683501
0.007129	0.621389	1.351735	2.264404	3.398103	4.772262	6.396956	8.27769347
0.007149	0.621613	1.35246	2.266033	3.401055	4.776946	6.40377	8.28702629
0.007169	0.621836	1.353185	2.26766	3.404004	4.781626	6.410578	8.29634862
0.007188	0.62206	1.35391	2.269287	3.406951	4.786302	6.417378	8.30566047
0.007208	0.622283	1.354633	2.270912	3.409895	4.790973	6.42417	8.31496188
0.007228	0.622506	1.355357	2.272536	3.412837	4.795639	6.430956	8.3242529
0.007248	0.622729	1.35608	2.274159	3.415776	4.8003	6.437735	8.33353355
0.007268	0.622952	1.356802	2.275781	3.418713	4.804958	6.444506	8.34280387
0.007287	0.623175	1.357525	2.277401	3.421647	4.80961	6.45127	8.3520639
0.007307	0.623397	1.358246	2.279021	3.424578	4.814258	6.458027	8.36131366
0.007327	0.623619	1.358967	2.280639	3.427507	4.818902	6.464777	8.3705532
0.007347	0.623842	1.359688	2.282255	3.430434	4.823541	6.47152	8.37978255
0.007367	0.624064	1.360408	2.283871	3.433358	4.828176	6.478256	8.38900173
0.007386	0.624285	1.361128	2.285486	3.436279	4.832806	6.484985	8.39821079
0.007406	0.624507	1.361847	2.287099	3.439198	4.837431	6.491707	8.40740975
0.007426	0.624729	1.362566	2.288711	3.442115	4.842053	6.498422	8.41659866
0.007446	0.62495	1.363285	2.290322	3.445028	4.846669	6.50513	8.42577754
0.007466	0.625171	1.364002	2.291932	3.44794	4.851282	6.511831	8.43494642
0.007485	0.625393	1.36472	2.29354	3.450849	4.85589	6.518525	8.44410535
0.007505	0.625614	1.365437	2.295147	3.453755	4.860494	6.525213	8.45325434
0.007525	0.625834	1.366154	2.296754	3.456659	4.865093	6.531893	8.46239344
0.007545	0.626055	1.36687	2.298359	3.459561	4.869688	6.538567	8.47152267
0.007565	0.626276	1.367585	2.299962	3.46246	4.874278	6.545234	8.48064207
0.007584	0.626496	1.368301	2.301565	3.465356	4.878865	6.551894	8.48975167
0.007604	0.626716	1.369015	2.303167	3.468251	4.883447	6.558547	8.4988515
0.007624	0.626936	1.36973	2.304767	3.471142	4.888024	6.565193	8.50794159
0.007644	0.627156	1.370444	2.306366	3.474032	4.892598	6.571833	8.51702198
0.007664	0.627376	1.371157	2.307964	3.476918	4.897167	6.578466	8.52609269
0.007683	0.627596	1.37187	2.309561	3.479803	4.901731	6.585093	8.53515375
0.007703	0.627815	1.372583	2.311157	3.482685	4.906292	6.591712	8.5442052
0.007723	0.628035	1.373295	2.312752	3.485565	4.910848	6.598326	8.55324707
0.007743	0.628254	1.374007	2.314345	3.488442	4.9154	6.604932	8.56227938
0.007763	0.628473	1.374718	2.315937	3.491317	4.919948	6.611532	8.57130217
0.007782	0.628692	1.375429	2.317529	3.494189	4.924491	6.618125	8.58031547
0.007802	0.628911	1.376139	2.319119	3.497059	4.929031	6.624712	8.5893193
0.007822	0.629129	1.376849	2.320708	3.499927	4.933566	6.631292	8.5983137
0.007842	0.629348	1.377559	2.322295	3.502792	4.938097	6.637866	8.6072987
0.007862	0.629566	1.378268	2.323882	3.505655	4.942624	6.644433	8.61627433
0.007881	0.629785	1.378977	2.325468	3.508516	4.947147	6.650993	8.6252406

σ	ν_1	ν_2	ν_3	ν_4	ν_5	ν_6	ν_7
0.007901	0.630003	1.379685	2.327052	3.511374	4.951665	6.657547	8.63419757
0.007921	0.630221	1.380393	2.328635	3.51423	4.956179	6.664095	8.64314524
0.007941	0.630439	1.3811	2.330218	3.517083	4.96069	6.670636	8.65208366
0.007961	0.630656	1.381807	2.331799	3.519934	4.965196	6.677171	8.66101285
0.00798	0.630874	1.382513	2.333379	3.522783	4.969698	6.683699	8.66993284
0.008	0.631091	1.38322	2.334958	3.52563	4.974196	6.690222	8.67884366
0.00802	0.631309	1.383925	2.336535	3.528474	4.97869	6.696737	8.68774533
0.00804	0.631526	1.384631	2.338112	3.531316	4.98318	6.703247	8.69663789
0.00806	0.631743	1.385335	2.339688	3.534156	4.987666	6.70975	8.70552136
0.008079	0.63196	1.38604	2.341262	3.536993	4.992147	6.716246	8.71439577
0.008099	0.632176	1.386744	2.342835	3.539828	4.996625	6.722737	8.72326115
0.008119	0.632393	1.387447	2.344408	3.542661	5.001099	6.729221	8.73211752
0.008139	0.63261	1.388151	2.345979	3.545491	5.005568	6.735699	8.74096491
0.008159	0.632826	1.388853	2.347549	3.548319	5.010034	6.742171	8.74980336
0.008178	0.633042	1.389556	2.349118	3.551145	5.014496	6.748636	8.75863288
0.008198	0.633258	1.390258	2.350686	3.553969	5.018953	6.755095	8.76745351
0.008218	0.633474	1.390959	2.352253	3.55679	5.023407	6.761548	8.77626527
0.008238	0.63369	1.39166	2.353818	3.559609	5.027857	6.767995	8.78506818
0.008258	0.633906	1.392361	2.355383	3.562426	5.032303	6.774436	8.79386228
0.008277	0.634121	1.393061	2.356947	3.565241	5.036745	6.780871	8.80264759
0.008297	0.634337	1.393761	2.358509	3.568053	5.041183	6.787299	8.81142414
0.008317	0.634552	1.394461	2.360071	3.570863	5.045617	6.793722	8.82019195
0.008337	0.634767	1.39516	2.361631	3.573671	5.050047	6.800138	8.82895104
0.008357	0.634982	1.395858	2.36319	3.576477	5.054473	6.806549	8.83770146
0.008376	0.635197	1.396557	2.364749	3.57928	5.058896	6.812953	8.84644321
0.008396	0.635412	1.397254	2.366306	3.582081	5.063314	6.819351	8.85517634
0.008416	0.635627	1.397952	2.367862	3.58488	5.067729	6.825744	8.86390085
0.008436	0.635841	1.398649	2.369417	3.587677	5.07214	6.83213	8.87261678
0.008456	0.636056	1.399346	2.370971	3.590472	5.076547	6.83851	8.88132416
0.008475	0.63627	1.400042	2.372524	3.593264	5.08095	6.844885	8.890023
0.008495	0.636484	1.400738	2.374076	3.596055	5.085349	6.851253	8.89871333
0.008515	0.636698	1.401433	2.375627	3.598843	5.089745	6.857616	8.90739519
0.008535	0.636912	1.402128	2.377177	3.601628	5.094136	6.863972	8.91606858
0.008555	0.637126	1.402823	2.378726	3.604412	5.098524	6.870323	8.92473355
0.008574	0.63734	1.403517	2.380273	3.607194	5.102908	6.876668	8.9333901
0.008594	0.637553	1.404211	2.38182	3.609973	5.107289	6.883007	8.94203828
0.008614	0.637767	1.404904	2.383366	3.61275	5.111665	6.88934	8.95067809
0.008634	0.63798	1.405597	2.38491	3.615526	5.116038	6.895667	8.95930957
0.008654	0.638193	1.40629	2.386454	3.618298	5.120407	6.901989	8.96793274
0.008673	0.638406	1.406982	2.387997	3.621069	5.124773	6.908305	8.97654762
0.008693	0.638619	1.407674	2.389538	3.623838	5.129134	6.914615	8.98515423
0.008713	0.638832	1.408366	2.391079	3.626605	5.133492	6.920919	8.99375261
0.008733	0.639045	1.409057	2.392618	3.629369	5.137846	6.927217	9.00234278
0.008753	0.639257	1.409747	2.394157	3.632131	5.142197	6.93351	9.01092475
0.008772	0.63947	1.410438	2.395694	3.634891	5.146544	6.939797	9.01949855
0.008792	0.639682	1.411128	2.397231	3.637649	5.150887	6.946079	9.0280642
0.008812	0.639894	1.411817	2.398766	3.640405	5.155226	6.952354	9.03662174
0.008832	0.640106	1.412506	2.400301	3.643159	5.159562	6.958624	9.04517117
0.008852	0.640318	1.413195	2.401834	3.645911	5.163894	6.964889	9.05371253
0.008871	0.64053	1.413884	2.403366	3.648661	5.168223	6.971147	9.06224584
0.008891	0.640742	1.414572	2.404898	3.651408	5.172548	6.9774	9.07077111
0.008911	0.640954	1.415259	2.406428	3.654154	5.176869	6.983648	9.07928838
0.008931	0.641165	1.415946	2.407958	3.656897	5.181187	6.98989	9.08779766
0.008951	0.641376	1.416633	2.409486	3.659639	5.185501	6.996126	9.09629898
0.00897	0.641588	1.41732	2.411014	3.662378	5.189811	7.002357	9.10479236
0.00899	0.641799	1.418006	2.41254	3.665115	5.194118	7.008582	9.11327782
0.00901	0.64201	1.418692	2.414065	3.66785	5.198421	7.014802	9.12175538

σ	ν_1	ν_2	ν_3	ν_4	ν_5	ν_6	ν_7
0.00903	0.642221	1.419377	2.41559	3.670583	5.202721	7.021016	9.13022507
0.00905	0.642432	1.420062	2.417113	3.673315	5.207017	7.027225	9.13868691
0.009069	0.642642	1.420746	2.418636	3.676044	5.21131	7.033428	9.14714091
0.009089	0.642853	1.421431	2.420157	3.678771	5.215599	7.039626	9.15558711
0.009109	0.643063	1.422115	2.421678	3.681496	5.219885	7.045818	9.16402552
0.009129	0.643274	1.422798	2.423197	3.684218	5.224167	7.052005	9.17245617
0.009149	0.643484	1.423481	2.424716	3.686939	5.228445	7.058186	9.18087907
0.009168	0.643694	1.424164	2.426233	3.689658	5.23272	7.064362	9.18929424
0.009188	0.643904	1.424846	2.42775	3.692375	5.236992	7.070533	9.19770172
0.009208	0.644114	1.425528	2.429266	3.69509	5.24126	7.076698	9.20610151
0.009228	0.644324	1.42621	2.43078	3.697803	5.245524	7.082858	9.21449365
0.009248	0.644533	1.426891	2.432294	3.700514	5.249785	7.089012	9.22287814
0.009267	0.644743	1.427572	2.433807	3.703223	5.254043	7.095162	9.23125502
0.009287	0.644952	1.428252	2.435318	3.705929	5.258297	7.101305	9.2396243
0.009307	0.645162	1.428933	2.436829	3.708634	5.262548	7.107444	9.24798601
0.009327	0.645371	1.429612	2.438339	3.711337	5.266795	7.113577	9.25634016
0.009347	0.64558	1.430292	2.439848	3.714038	5.271039	7.119705	9.26468677
0.009366	0.645789	1.430971	2.441356	3.716737	5.275279	7.125828	9.27302587
0.009386	0.645998	1.43165	2.442863	3.719434	5.279516	7.131945	9.28135747
0.009406	0.646207	1.432328	2.444369	3.722129	5.28375	7.138057	9.2896816
0.009426	0.646415	1.433006	2.445874	3.724822	5.28798	7.144164	9.29799827
0.009446	0.646624	1.433683	2.447378	3.727513	5.292207	7.150266	9.30630751
0.009465	0.646832	1.434361	2.448881	3.730202	5.29643	7.156362	9.31460934
0.009485	0.647041	1.435038	2.450383	3.732889	5.300651	7.162453	9.32290377
0.009505	0.647249	1.435714	2.451885	3.735574	5.304867	7.16854	9.33119082
0.009525	0.647457	1.43639	2.453385	3.738258	5.309081	7.17462	9.33947052
0.009545	0.647665	1.437066	2.454884	3.740939	5.313291	7.180696	9.34774288
0.009564	0.647873	1.437741	2.456383	3.743618	5.317497	7.186767	9.35600793
0.009584	0.648081	1.438417	2.45788	3.746296	5.321701	7.192832	9.36426568
0.009604	0.648288	1.439091	2.459377	3.748971	5.325901	7.198893	9.37251615
0.009624	0.648496	1.439766	2.460872	3.751645	5.330097	7.204948	9.38075937
0.009644	0.648703	1.44044	2.462367	3.754317	5.334291	7.210998	9.38899534
0.009663	0.648911	1.441113	2.463861	3.756987	5.338481	7.217043	9.39722409
0.009683	0.649118	1.441787	2.465354	3.759655	5.342668	7.223084	9.40544565
0.009703	0.649325	1.44246	2.466846	3.762321	5.346851	7.229119	9.41366002
0.009723	0.649532	1.443132	2.468337	3.764985	5.351031	7.235149	9.42186722
0.009743	0.649739	1.443805	2.469827	3.767647	5.355208	7.241173	9.43006728
0.009762	0.649946	1.444476	2.471316	3.770307	5.359382	7.247193	9.43826022
0.009782	0.650153	1.445148	2.472804	3.772966	5.363552	7.253208	9.44644605
0.009802	0.650359	1.445819	2.474292	3.775622	5.36772	7.259218	9.45462478
0.009822	0.650566	1.44649	2.475778	3.778277	5.371884	7.265223	9.46279645
0.009842	0.650772	1.447161	2.477263	3.78093	5.376044	7.271223	9.47096107
0.009861	0.650979	1.447831	2.478748	3.78358	5.380202	7.277218	9.47911865
0.009881	0.651185	1.448501	2.480232	3.786229	5.384356	7.283209	9.48726921
0.009901	0.651391	1.44917	2.481715	3.788877	5.388507	7.289194	9.49541278
0.009921	0.651597	1.449839	2.483196	3.791522	5.392655	7.295174	9.50354936
0.009941	0.651803	1.450508	2.484677	3.794165	5.3968	7.301149	9.51167898
0.00996	0.652009	1.451176	2.486157	3.796807	5.400941	7.30712	9.51980166
0.00998	0.652214	1.451844	2.487637	3.799447	5.40508	7.313086	9.52791742
0.01	0.65242	1.452512	2.489115	3.802085	5.409215	7.319046	9.53602626